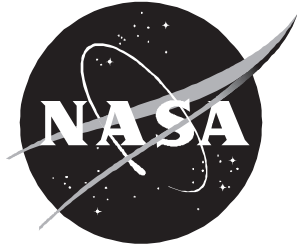


NASA/CR-2000-209337



Integral Airframe Structures (IAS)— Validated Feasibility Study of Integrally Stiffened Metallic Fuselage Panels for Reducing Manufacturing Costs

*J. Munroe, K. Wilkins, and M. Gruber
Boeing Commercial Airplane Group, Seattle, Washington*

May 2000

The NASA STI Program Office . . . in Profile

Since its founding, NASA has been dedicated to the advancement of aeronautics and space science. The NASA Scientific and Technical Information (STI) Program Office plays a key part in helping NASA maintain this important role.

The NASA STI Program Office is operated by Langley Research Center, the lead center for NASA's scientific and technical information. The NASA STI Program Office provides access to the NASA STI Database, the largest collection of aeronautical and space science STI in the world. The Program Office is also NASA's institutional mechanism for disseminating the results of its research and development activities. These results are published by NASA in the NASA STI Report Series, which includes the following report types:

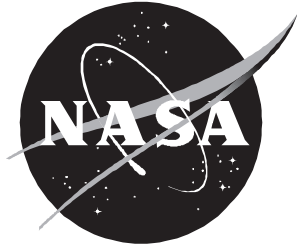
- **TECHNICAL PUBLICATION.** Reports of completed research or a major significant phase of research that present the results of NASA programs and include extensive data or theoretical analysis. Includes compilations of significant scientific and technical data and information deemed to be of continuing reference value. NASA counterpart of peer-reviewed formal professional papers, but having less stringent limitations on manuscript length and extent of graphic presentations.
- **TECHNICAL MEMORANDUM.** Scientific and technical findings that are preliminary or of specialized interest, e.g., quick release reports, working papers, and bibliographies that contain minimal annotation. Does not contain extensive analysis.
- **CONTRACTOR REPORT.** Scientific and technical findings by NASA-sponsored contractors and grantees.
- **CONFERENCE PUBLICATION.** Collected papers from scientific and technical conferences, symposia, seminars, or other meetings sponsored or co-sponsored by NASA.
- **SPECIAL PUBLICATION.** Scientific, technical, or historical information from NASA programs, projects, and missions, often concerned with subjects having substantial public interest.
- **TECHNICAL TRANSLATION.** English-language translations of foreign scientific and technical material pertinent to NASA's mission.

Specialized services that complement the STI Program Office's diverse offerings include creating custom thesauri, building customized databases, organizing and publishing research results . . . even providing videos.

For more information about the NASA STI Program Office, see the following:

- Access the NASA STI Program Home Page at <http://www.sti.nasa.gov>
- Email your question via the Internet to help@sti.nasa.gov
- Fax your question to the NASA STI Help Desk at (301) 621-0134
- Telephone the NASA STI Help Desk at (301) 621-0390
- Write to:
NASA STI Help Desk
NASA Center for AeroSpace Information
7121 Standard Drive
Hanover, MD 21076-1320

NASA/CR-2000-209337



Integral Airframe Structures (IAS)— Validated Feasibility Study of Integrally Stiffened Metallic Fuselage Panels for Reducing Manufacturing Costs

*J. Munroe, K. Wilkins, and M. Gruber
Boeing Commercial Airplane Group, Seattle, Washington*

National Aeronautics and
Space Administration

Langley Research Center
Hampton, Virginia 23681-2199

Prepared for Langley Research Center
under Contracts NAS1-20014 and NAS1-20267

May 2000

The use of trademarks or names of manufacturers in this report is for accurate reporting and does not constitute an official endorsement, either expressed or implied, of such products or manufacturers by the National Aeronautics and Space Administration.

Available from:

NASA Center for AeroSpace Information (CASI)
7121 Standard Drive
Hanover, MD 21076-1320
(301) 621-0390

National Technical Information Service (NTIS)
5285 Port Royal Road
Springfield, VA 22161-2171
(703) 605-6000

Table of Contents

Executive Summary	ix
1 Introduction	1
1.1 About the IAS Program.....	1
1.2 Background—The ADAM Technology Development Road Map.....	3
1.3 IAS Program Kick-Off and Concept Part Selection.....	10
1.4 About the Rest of This Report.....	13
2 Technology Assessment	15
2.1 Overview	15
2.2 Identifying the Options—The IAS White Paper	16
2.3 The Down Selection Process.....	19
2.4 Down Selection Results	20
2.5 Outstanding Issues.....	31
2.6 Conclusions and Recommendations.....	32
3 Fabricated Test Coupons and Subcomponents	33
3.1 Overview	33
3.2 Background	34
3.3 Hardware Fabrication at Boeing Seattle.....	36
3.4 Fabrication of the Alcoa Extrusion Panels.....	48
3.5 Outstanding Issues.....	53
3.6 Conclusions and Recommendations.....	53

4 Test Hardware Design Parameters	55
4.1 Overview	55
4.2 Test Specimen Design Methods.....	56
4.3 Outstanding Issues.....	59
5 Two-Bay Longitudinal Crack Test and Results	61
5.1 Overview	61
5.2 Pressure Test Facility	61
5.3 Test Panel	64
5.4 Test Results	68
5.5 Conclusions and Recommendations.....	85
6 Longitudinal Two-Bay Analysis and Correlation	87
6.1 Summary	87
6.2 Preliminary Analysis and Panel Design Modifications.....	89
6.3 Modeling Assumptions	90
6.4 Analysis Results	96
6.5 Test and Analysis Correlation	101
6.6 Outstanding Issues.....	117
6.7 Conclusions	117
7 Inspection, Maintenance, and Repair Considerations	119
7.1 Overview	119
7.2 A Review of Typical Airline Inspection and Maintenance Practices.....	120
7.3 Inspection, Maintenance, and Repair Expectations for IAS.....	122
7.4 Outstanding Issues.....	128
7.5 Conclusions and Recommendations.....	128

8 Long-Range Plan	129
8.1 Overview	129
8.2 Basis For This Long-Range Plan.....	130
8.3 Recommended Long-Range Activities.....	132
8.4 Outstanding issues.....	143
8.5 Conclusions and Recommendations.....	144
9 Full-Scale Validation Plan	145
9.1 Overview	145
9.2 Implementing New Airplane Technologies.....	146
9.3 Implementing IAS Technology	148
9.4 Overview of Testing and Validation Criteria	150
9.5 Theoretical Scenario for Crown Panel	152
9.6 “Big Hitter” Testing Requirements for Various Structures.....	157
9.7 Conclusions and Recommendations.....	158
10 References	159
Appendix A Forming Technology Assessment for Integral Airframe Structures	A-1
Appendix B IAS Program Test Matrix	B-1
Appendix C Integral Airframe Structures Test Panel Fabrication	C-1
Appendix D IAS Material Characterization Test Plan	D-1
Appendix E Extruded Panel Measurements	E-1
Appendix F Strain Gage Readings and Gage Locations	F-1
Appendix G Northrop Grumman Analytical Task 1 and Task 2	G-1
Appendix H Integral Tear Strap Crack Arrest Evaluation	H-1

List of Figures

Figure 1-1. Fuselage Assembly Methodology.....	5
Figure 1-2. Precision Assembly Methodology.....	6
Figure 1-3. Strong Effect of Fuselage Panel Size on Cost	7
Figure 1-4. Impact of Fuselage Cost	8
Figure 1-5. The IAS Vision.....	8
Figure 1-6. IAS Program Schedule	10
Figure 2-1. Part Consolidation With IAS.....	29
Figure 3-1. Three-Axis, Five-Facing, 3000-rpm Milling Machine	37
Figure 3-2. Panel B (Bump Formed).....	39
Figure 3-3. Lower Panel of Two-Bay Longitudinal Crack Panel After Machining	40
Figure 3-4. Panel 2 Before Bump Forming.....	41
Figure 3-5. Milling Fixture for 7050 Frames	42
Figure 3-6. Rough Stock and Machined Frame.....	43
Figure 3-7. IAS Panel in the Assembly Fixture	44
Figure 3-8. Boeing 747 (Built-Up) Fuselage Panel.....	44
Figure 3-9. IAS Repair Panel—Inside View	46
Figure 3-10. IAS Repair Panel—Outside View	46
Figure 3-11. Extrusion Exiting the Press	50
Figure 3-12. Extrusion Cut Into Lengths.....	50
Figure 3-13. Variations in Center of Panel.....	51
Figure 3-14. Panel 1—Origin End	52
Figure 3-15. Panel 2—Origin End	52
Figure 5-1. Wide-Body Pressure Test Fixture.....	62

Figure 5-2. Wide-Body Fixture	62
Figure 5-3. Standard-Body Fixture.....	63
Figure 5-4. Structural Details	65
Figure 5-5. Structural Dimensions of Panel	66
Figure 5-6. Frame and Stringer Dimensions	67
Figure 5-7. Structural Configuration and Test Locations.....	69
Figure 5-8. Initial Sawcut Details for Test 1	70
Figure 5-9. Crack Growth History of Test 1	72
Figure 5-10. Crack Growth Trajectory of Test 1.....	73
Figure 5-11. IAS Panel, Test 1, Crack at 10,333 Cycles.....	74
Figure 5-12. Residual Strength Crack Configuration of Test 2.....	76
Figure 5-13. Panel Repair of Test 1 Location	77
Figure 5-14. IAS Panel, Repair of Test 1 Location at 10,355 Cycles	78
Figure 5-15. Initial Sawcut Details for Test 2	79
Figure 5-16. IAS Panel, 10-Inch Sawcut at Test 2 Location.....	80
Figure 5-17. Crack Growth History of Test 2	81
Figure 5-18. Crack Growth Trajectory of Test 2.....	82
Figure 5-19. Residual Strength Crack Configuration of Test 2.....	84
Figure 5-20. Dynamic Panel Failure—Test 2.....	85
Figure 6-1. Panel Structural Configuration	90
Figure 6-2. Skin, Stringer, and Frame Dimensions	91
Figure 6-3. Skin Mesh.....	92
Figure 6-4. Frame and Stringer Mesh.....	92
Figure 6-5. Schematic for Non-linear Rivet Elements and Shear Deflection Properties	95

Figure 6-6. Displaced Intact Skin Mesh, Internal Pressure = 8.6 psi, Magnification Factor = 100x	96
Figure 6-7. Displaced Mesh with a 38-inch crack, Internal Pressure = 8.6 psi, Magnification Factor = 10x.....	97
Figure 6-8. Stress Intensity Factors for a Longitudinal Crack Centered on a Broken Frame	98
Figure 6-9. Rivet Shear Loads at Adjacent Frame Location versus Crack Length, Applied Pressure = 9.4psi.....	99
Figure 6-10. Test/Analysis Strain Gage Correlation for an Intact Panel at 8.6 psi	102
Figure 6-11. Skin Stress Correlation Midway Between Stringer S-1 and S-2L for an Intact Panel at 8.6 psi	104
Figure 6-12. Skin Stress Correlation at Station 130 for an Intact Panel at 8.6 psi.....	105
Figure 6-13. Skin Stress Correlation at Station 140 for an Intact Panel at 8.6 psi.....	106
Figure 6-14. Skin Stress Correlation Midway Between Stringer S-1 and S-2L for a Panel Containing a 38-Inch Crack Centered on a Broken Frame.....	108
Figure 6-15. Skin Stress Correlation at Station 130 for a Panel Containing a 38-Inch Crack Centered on a Broken Frame	109
Figure 6-16. Skin Stress Correlation at Station 140 for a Panel Containing a 38-Inch Crack Centered on a Broken Frame	110
Figure 6-17. Crack Growth Rate Data for $R = 0.0$	113
Figure 6-18. Crack Growth Predictions and Test Results for Test 1	114
Figure 6-19. Residual Strength Prediction Using K_c	116
Figure 7-1. IAS Repair Panel—Inside View	125
Figure 7-2. IAS Repair Panel—Outside View	125
Figure 8-1. Vee-Shaped Extrusion	134
Figure 8-2. Strength Versus Toughness of Candidate Airframe Materials	136
Figure 8-3. The IAS Vision.....	138
Figure 8-4. Incorporating a Butt Joint Weld Into Traditional Fuselage Structure.....	139

Figure 8-5. Future Integrated Design 142

Figure 9-1. Extensive Testing Required for Full-Scale Validation..... 152

List of Tables

Table 1-1. Advances in Manufacturing Processes	3
Table 1-2. Candidate Application/Technology Combinations Example.....	12
Table 2-1. Manufacturing Processes/Design Concepts	18
Table 2-2. Summary—Option A	21
Table 2-3. Summary—Option B	22
Table 2-4. Summary—Option C	23
Table 2-5. Summary—Option D	24
Table 2-6. Summary—Option E	25
Table 2-7. Summary—Option F.....	26
Table 2-8. Down Selection Priority Rankings.....	27
Table 2-9. Comparison of Baseline and IAS Panels	29
Table 5-1. Test Record of Crack Length Measurements From Test 1	75
Table 5-2. Test Record of Crack Length Measurements From Test 2	83
Table 6-1. Material Elastic Parameters	94
Table 6-2. 7050-T7451 Stress-Strain Curve	94
Table 7-1. Types of Aircraft Inspections	120
Table 7-2. Example: Airline Inspection Schedule.....	121
Table 7-3. Fatigue and Skin Thickness for Panel Materials.....	127
Table 8-1. Installed Fastener Cost—Boeing 747 Fuselage, Sections 42–46.....	138
Table 9-1. Summary of Safety Criteria in Nine Structural Areas	151
Table 9-2. Requirements for Various Types of Integally Stiffened Fuselage Structures.....	157

Executive Summary

The NASA Integral Airframe Structures (IAS) program investigated, and gained significant experience toward validating, the feasibility of using “integrally stiffened” construction for commercial transport aircraft fuselage structure. The objectives of the program were to build and test structure that was less expensive than current “built-up” structure, yet equal in structural performance and weight. The IAS program has shown significant results toward the advancement and application of integrally stiffened fuselage structure. Testing performed as part of this program provided valuable data and experience for designing integral fuselage structure.

The fabrication, analysis, and testing of a large pressure panel at Boeing yielded results that are very promising for IAS-type structure. Fabrication and assembly were fast and efficient. To manufacture the test panels, skin-stringer panels and frames were machined from aluminum plate. Mechanical bend forming (bump forming) was used to form the panels to contour.

The cost study results indicated that, as compared to conventional built-up fabrication methods, high-speed machining of structure from aluminum plate would yield a recurring cost savings of 61%. Part count dropped from 78 individual parts on a baseline panel to just 7 parts for machined IAS structure, so a significant reduction in part count is clearly achieved. Additional experience was gained in near-net-shaped extrusions for fuselage panels. Though not yet fully mature, near-net-shaped extrusions have high potential for fuselage application and manufacturing savings.

Structural performance testing culminated at Boeing Seattle with a large pressure test that included the arrest of a two-bay longitudinal crack, and a measure of residual strength for a two-bay crack centered on a broken frame. The design of the panel arrested a dynamically running two-bay crack at the frame pad-ups at 8.17 psi; this shows very promising results for the design. The residual strength testing of the panel indicated that the panel could hold 9.7 to 9.89 psi. Significantly, twice as much test data was obtained from this panel, because the panel did not fail during the first residual strength test. During the first test, crack extension was stopped by the advance of both crack tips into fastener holes at frame locations. Also, test results showed that the panel machined from 7475-T7351 had superior slow crack growth. Although panel design was not fully optimized and was not detailed to meet all structural requirements, the panel crack arrest performance was very promising.

Calculated panel weight for the baseline configuration was 2.45 pounds per bay and, for the IAS configuration, 2.52 lbs. per bay. The baseline panel was never physically weighed. The actual IAS panel was weighed while it was suspended from a scale at the test site. The weight was 186 pounds. Design optimization is anticipated to achieve weight-neutral structure.

Several other test panels were fabricated for testing. Two circumferential and one compression panel were fabricated by Northrop Grumman. An excellent report on the fabrication details is included as Appendix C of this document. Also, Boeing Seattle fabricated a mechanical repair panel designed by Boeing Long Beach. This panel will be tested in fatigue at NASA Langley. During testing of the two-bay longitudinal crack panel, a mechanical repair was used on the first test site so additional testing could be done on the second test site.

Analysis predictions for the two-bay longitudinal crack panel correlated well with the test results. Analysis activity conducted by the IAS team strongly indicates that current analysis tools predict integral structural behavior as accurately as built-up structure, and analysis should be used along with testing to further investigate integral structure.

The initial design called for the use of 7050 aluminum plate to be used for fabrication of the panel. Analysis predictions indicated that this material would not be satisfactory for arresting a two-bay longitudinal crack, due to low toughness properties for that material orientation (T-L). To improve residual strength capability, 7475-T7351 was selected as an available material with adequate arresting qualities. Analysis predictions validated that 7475-T7351 would be capable of holding a two-bay longitudinal crack.

The IAS program has shown significant progress toward the advancement and application of integrally stiffened fuselage structure. From Boeing's perspective, before existing fuselage structure can be safely replaced, more testing is needed to gain full confidence in integrally stiffened structure. Continued effort should be focused on technology improvements such as near-net extrusions and welding.

1 Introduction

To help maintain its leadership and competitiveness in the global market, the United States aerospace industry is exploring new technologies that have the potential to improve aircraft design and manufacturing processes. The National Aeronautics and Space Administration (NASA) has promoted aircraft technology development by conducting joint industry initiatives on specific projects. Integral airframe structure (IAS) is one technology of interest. This report documents work performed by Boeing Seattle as part of the IAS program NASA launched in 1996.

1.1 About the IAS Program

1.1.1 An Introduction to IAS

Airframes of commercial aircraft are primarily of riveted aluminum skin and stringer construction—that is, complete parts are built up from individually fabricated detail components. IAS is an alternative approach in which the complete part is “integrally stiffened”—that is, skin and stringers are integrated into a single piece of structure.

The general perception is that, if design challenges can be overcome, integral structures could be less expensive to manufacture than built-up structures. For example, there is the potential for significant cost savings associated with assembly labor. In the past, the limitations of existing manufacturing technology made IAS prohibitive on a large scale. However, recent advances in manufacturing technology and the need to find innovative ways to reduce manufacturing costs are bringing increased attention to IAS.

1.1.2 IAS Program Goals

The overall goal of the IAS program was to demonstrate a feasible design concept for producing integral structure that would:

- Weigh the same or less than built-up structure
- Cost less than built-up structure
- Meet performance standards with acceptable damage tolerance and fail-safe behavior

To meet this goal, the IAS program was to include:

- The development of a new and effective design approach for integral structures, along with manufacturing technologies for implementing that approach. The design approach/manufacturing technologies pursued would be selected from various possible concepts based on cost and performance criteria.
- The development of validated analysis methodology for testing the durability and damage tolerance of integral structures. The intent was to demonstrate that integral structures can perform equal to or better than more conventional structures.

1.1.3 IAS Program Participants

NASA selected Boeing Seattle and Boeing Long Beach (formerly McDonnell-Douglas) to lead the industry portion of the IAS program. Boeing Seattle subcontracted with Northrop Grumman, Lockheed Martin, and Alcoa for select work. Boeing Long Beach is submitting a separate report.

1.1.4 Value of the IAS Program

The IAS team recognized early on that this program was an integrated development effort in the areas of design, manufacturing, and analysis methodology. Even though a large portion of the technology assessment for the program had a manufacturing focus, the team felt that a much larger benefit would result from the program's development work on analysis methodology for durability and damage tolerance.

To this end, the IAS program provided an opportunity to both develop and use analysis tools to model the performance of the structure. The side-by-side comparison between built-up structure and integrally stiffened panels would prove to be extremely important in validating the analysis tools and confirming the performance of the structure.

1.2 Background—The ADAM Technology Development Road Map

In May 1996, NASA published the report *Affordable Design and Manufacturing (ADAM) for Commercial Transport Aircraft and Engines*. This document provided a “road map” for the development of affordable commercial transport fuselage and engine technology. According to the ADAM document, “The planned technology will provide major breakthroughs in engine and fuselage structure technology through focused high-risk, high-payoff airframe structural component design, development, test, and implementation, and through engine manufacturing process refinement.” The ADAM vision can only be realized through advances in metallic integral construction.

1.2.1 Key Manufacturing Technologies

The ADAM document included an outline of key manufacturing technologies and their status at the time (see Table 1-1).

TABLE 1-1. ADVANCES IN MANUFACTURING PROCESSES

Technology	Status
High-speed machining	<ul style="list-style-type: none"> • Established basic technology, rapidly evolving new capabilities • High buy/fly ratio requires economic/application evaluation • Thick plate material property advances promise new application viability
Precision assembly	<ul style="list-style-type: none"> • High accuracy at the detail part level • High next-assembly savings • Exploits capability of enhanced accuracy machines • Requires people/equipment investment
Ductile, thin-wall castings	<ul style="list-style-type: none"> • Under continual material property improvement • 12-15% ductility now available • Automotive application leverage and experience are available
Large-scale extrusions	<ul style="list-style-type: none"> • Low-cost/low part count for large components • Emerging experience base being developed • Large, monolithic skins possible to replace complex built-up assemblies
Advance joining	<ul style="list-style-type: none"> • Laser welding, friction stir welding emerging technologies • Large-scale adhesive bonding to minimize fastener installation

Source: *Affordable Design and Manufacturing (ADAM) for Commercial Transport Aircraft and Engines*, May 1996, Table 1-1, page 1-3

These technologies have enjoyed very limited usage even though the cost savings and benefits potential appears very high. These technologies have been developed and applied for discrete, typically military, applications, but, at this time, none of them are close to the design readiness level necessary for commercial transports. High-speed machining and thin-walled castings have had applications in recent products, but use has still been very limited.

1.2.2 Fuselage Assembly Methodology Roadmap

The ADAM proposal projected a roadmap of advance fuselage assembly methodology (see Figure 1-1). This vision added focus to the IAS program, even though, at the beginning, all candidate structures and technologies were still being considered, and no specific part selections had been made. This vision over time could be described as:

- Diligent investigation into materials properties and machining larger and larger parts
- Analysis methods coupled with an optimistic design
- Testing for validation of performance in progressively larger parts
- Application of manufacturing technology to produce cost-effective structure

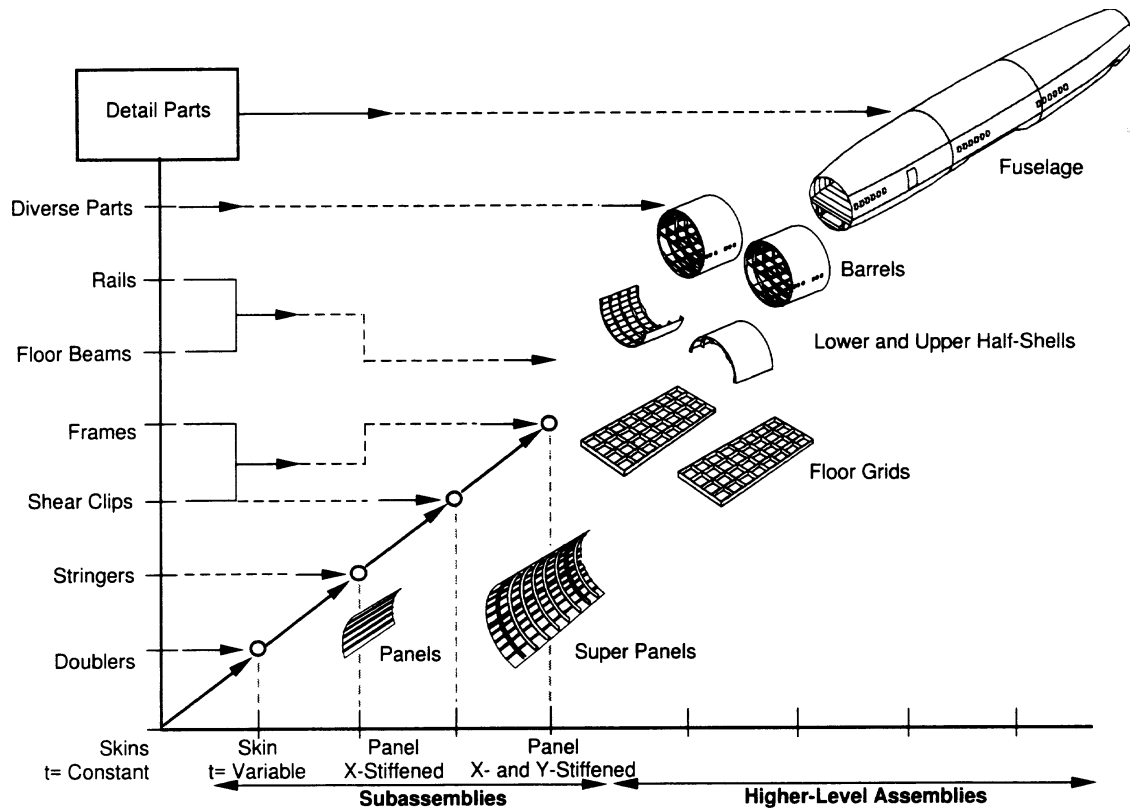


FIGURE 1-1. FUSELAGE ASSEMBLY METHODOLOGY

Source: *Affordable Design and Manufacturing (ADAM) for Commercial Transport Aircraft and Engines*, May 1996, Figure 3-10

Employment of the innovative manufacturing and design concepts necessary to attain this vision would make many attractive benefits available. For example, these advanced and highly innovative production ideas would:

- Take detail parts directly to fuselage assembly areas
- Eliminate many detailed part build-ups
- Reduce labor to assemble
- Reduce inspection
- Minimize inventory
- Reduce tooling costs

1.2.3 Precision Assembly Possibilities

One especially attractive benefit of integral structure is “self-tooling” (see Figure 1-2). Self-tooling implies the elimination of the extremely expensive major assembly tools that are used in today’s manufacturing environment. If primary structural parts are designed to provide locating and fixturing capability, assemblies can be put together accurately with inexpensive holders or simple tools.

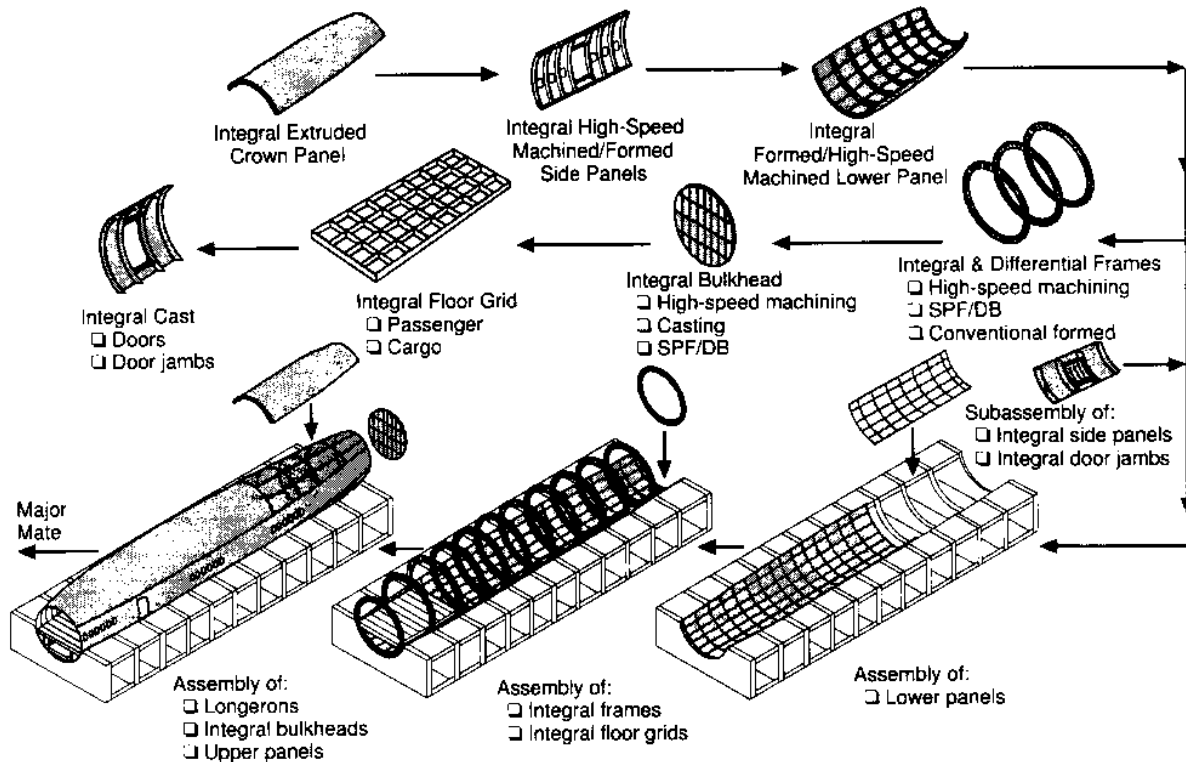


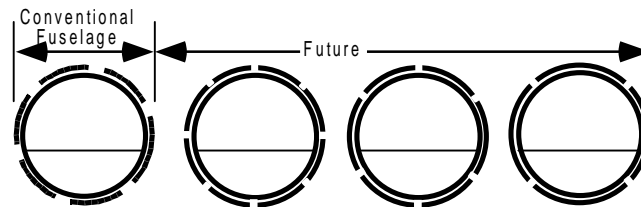
FIGURE 1-2. PRECISION ASSEMBLY METHODOLOGY

Source: *Affordable Design and Manufacturing (ADAM) for Commercial Transport Aircraft and Engines*, May 1996, Figure 2-2

From the outside, the fuselage in Figure 1-2 looks very much like a fuselage made with built-up structure. However, this picture points toward a fabrication environment where the fuselage is assembled from very large parts. Accurate large parts allow major assemblies to fit together without shimming and with the potential for parts to be interchanged. Additional payoffs include reduced tool development costs, faster assembly time, less rework, and more flexible assembly lines. Synergistic thinking between design and manufacturing is needed to apply these innovative structures to commercial airplanes.

1.2.4 Fuselage Barrel Part Consolidation

In general, consolidating parts seems to make sense, and there is a strong indication that making fewer, larger fuselage panels would have a very strong, positive effect on cost drivers. The overall trend of longitudinal joint effects on fuselage barrel assembly costs is shown in Figure 1-3. These percentages are nominal and will change depending on the type of aircraft and airline operator. This figure shows that reducing the radial panel count can reduce numerous manufacturing cost components by significant margins—up to 50%. The high impact of fuselage cost on airplane direct operating cost is illustrated in Figure 1-4. These percentages are nominal and will change for type of aircraft and airline operator. For fuselage panels, a comparison of built-up to advanced construction might look something like Figure 1-5.



Assumption : Integral skin/doubler/stringer panels

No. of Panels/Superpanels	10 (Basis)	8	6	4
Engineering Cost	0	-10%	-20%	-30%
Material Cost	0	-5%	-10%	-15%
Part Fabrication Cost	0	-20%	-35%	-50%
Assembly Cost	0	-15%	-30%	-50%
Weight	0	-2%	-4%	-6%

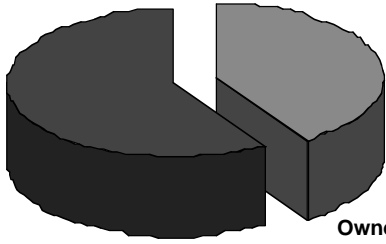
Note: These percentages are nominal and will change depending on the type of aircraft and airline operator. These are an example of direct operator cost and interest.

FIGURE 1-3. STRONG EFFECT OF FUSELAGE PANEL SIZE ON COST

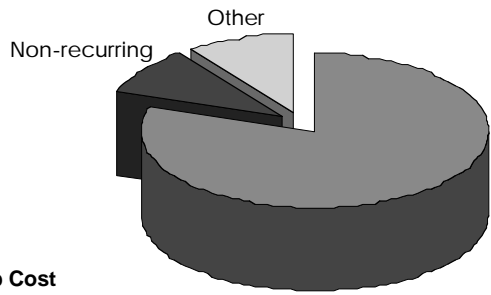
Source: *Affordable Design and Manufacturing (ADAM) for Commercial Transport Aircraft and Engines*, May 1996, Figure 2-3

Cash DOC 50-60%

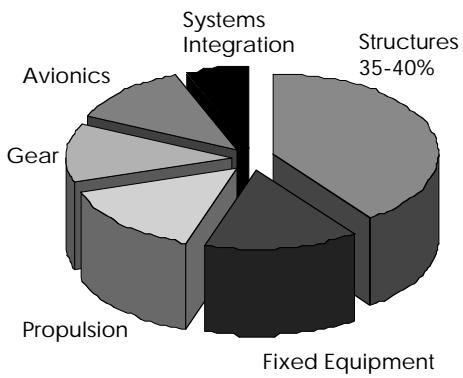
(fuel, crew cost, maintenance,
landing fees, others)



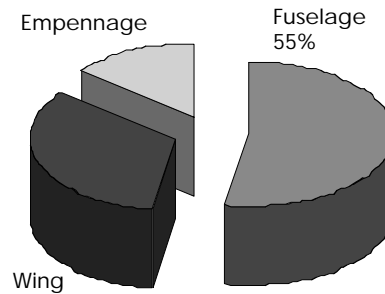
Direct Operating Cost (DOC)



Ownership Cost



Recurring Production Cost



Structures Cost

FIGURE 1-4. IMPACT OF FUSELAGE COST

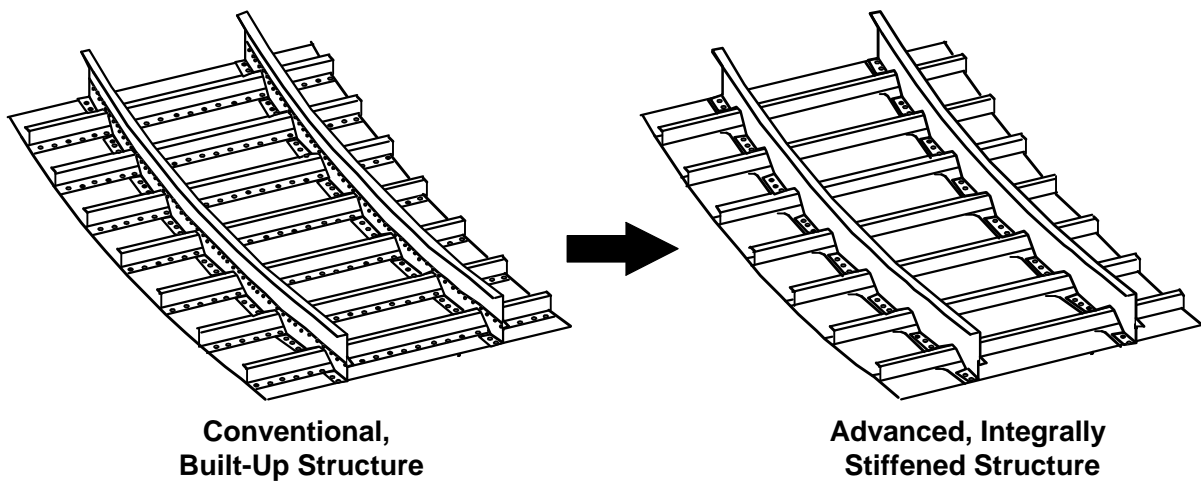


FIGURE 1-5. THE IAS VISION

Part consolidation significantly affects cost, but it also leads to some very high risks and potentially limiting situations. For example, supplier and factory infrastructures may be challenged by:

- Raw material size
- Material availability
- Part transportation
- Fabrication capability limits
- Tooling
- Structural durability
- Part handling
- Shipping

This type of structure also deviates from the traditional engineering knowledge concerning commercial transport structural requirements, because it does not address redundant members and built-up structure.

1.2.5 Application to IAS

The trend illustrated in Figure 1-3 is enticing—the potential for manufacturing and design cost reduction is a major driver, if the challenges can be overcome. These percentages are nominal and will change depending on the type of aircraft and airline operator. These are an example of direct operator cost and interest. When untried fabrication technologies are combined with large integral structures, the technology risk is very high, but the payoff is perceived to be equally high. The promise of advanced computing technology, modeling, and analysis, in combination with advanced assembly approaches and new fabrication technologies, promises substantial manufacturing cost savings.

In order to proceed with the ADAM vision, engineering and analysis challenges needed to be addressed. NASA hoped that a breakthrough program like the IAS program could provide validation that large integral structure can perform equal to or better than built-up structure, and thus demonstrate its engineering and design benefits. Because of performance concerns, establishing an analysis methodology for durability and damage tolerance was an important objective of the IAS program.

1.3 IAS Program Kick-Off and Concept Part Selection

The IAS program began with a kick-off meeting on May 14, 1996. Attendants included representatives of each organization on the team. The main accomplishment of the meeting was the selection, from among the fuselage candidates, a single combination application/technology concept for the program. The kick-off meeting also provided the opportunity to discuss NASA's task-based program schedule (Figure 1-6).

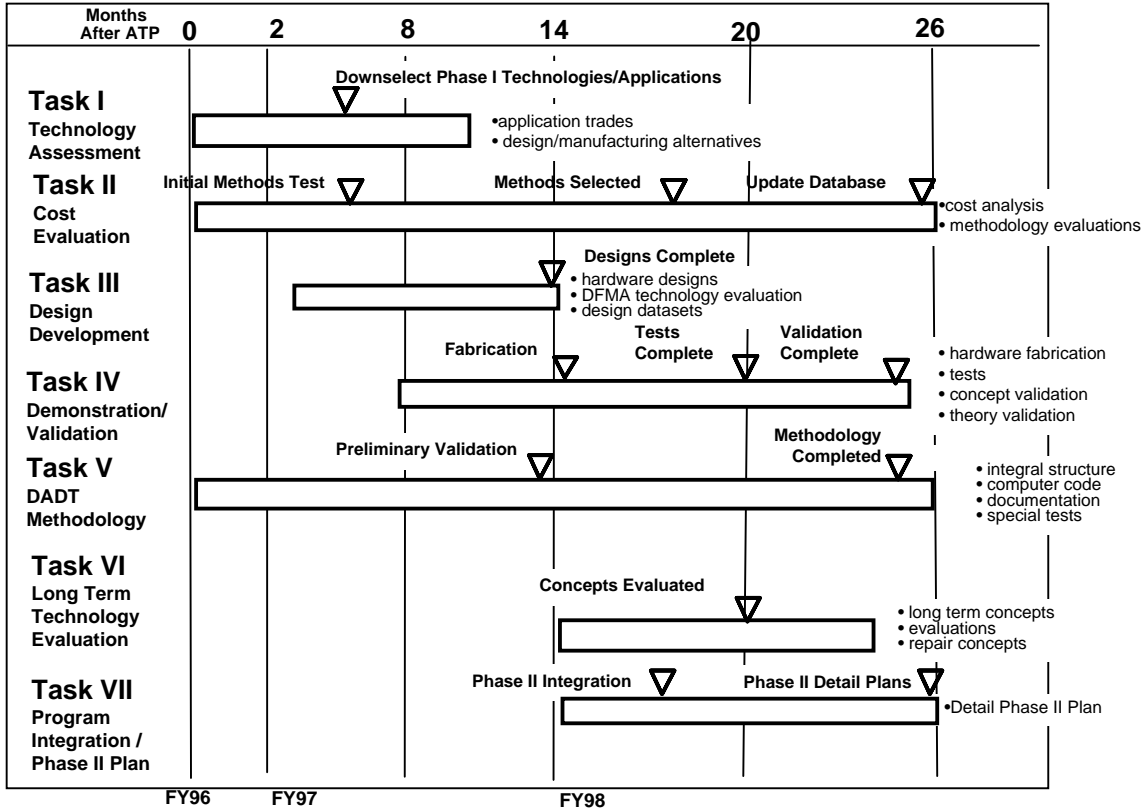


FIGURE 1-6. IAS PROGRAM SCHEDULE

Task 1 is the technology assessment. This task leads into the need for concept part selection with application of technology.

1.3.1 Identification of Concept Part Candidates

The technologies identified in Table 1-1 are easily applied to primary fuselage structure. Doing so indicates some direction for the IAS program. For example, one can visualize part consolidation occurring through the use of techniques such as:

- High-speed machining
- Part self-tooling
- Large-scale extrusions coupled with advanced joining techniques

Each of these is an enabling technology that would allow for part consolidation and large scale-up of integrally stiffened parts.

Figure 1-2 identifies several fuselage parts that could be candidates for combination design/manufacturing development projects for integral structure:

- Integral extruded crown panel
- Integral high-speed machined/formed side panels
- Integral formed/high-speed machined lower panel
- Integral cast doors
- Integral floor grid
- Integral bulkhead
- Integral and differential frames

The ADAM proposal evaluated several combination application/technology candidates for fuselage development (see Table 1-2). Each was initially considered to be a possible candidate for the IAS program.

TABLE 1-2. CANDIDATE APPLICATION/TECHNOLOGY COMBINATIONS EXAMPLE

Rating Criteria	Weight	Extruded Belly Panel Lower Lobe		Extruded, Machined Frame		Machined Side Panel		Machined Door Frame		Machined Bulkheads		Cast Doors	
		Value	Score	Value	Score	Value	Score	Value	Score	Value	Score	Value	Score
Cost Reduction Potential	10	5	50	9	90	5	50	4	40	7	70	10	100
Technical Achievability	10	4	40	8	80	7	70	8	80	10	100	8	80
Implementation Opportunities	8	2	16	6	48	5	40	3	24	6	48	10	80
Development Output Date	8	5	40	10	80	10	80	10	80	10	80	8	64
Spin-Off Potential	6	5	30	3	18	8	48	4	24	8	48	10	60
		Total	176	Total	316	Total	288	Total	248	Total	346	Total	384

Source: *Affordable Design and Manufacturing (ADAM) for Commercial Transport Aircraft and Engines*, May 1996, Table 3-3, page 3-36

Note that Table 1-2 shows the weighted ranking of six potential candidates. ADAM was extremely successful in screening candidates for development. In fact, private industry (Boeing, Northrop Grumman, Alcoa, etc.) began development work on the three highest-ranking items (which are shaded in Table 1-2), because they were attractive from a business sense. Removing these three from consideration realistically left three highly probable and prioritized project candidates that were high-payoff, yet high-risk, and as such required government sponsorship as an incentive for development.

1.3.2 The Concept Part Selection Process

The concept part was selected largely through discussions among the team members during the kick-off meeting.

Dr. Dave Bowles of NASA Langley brought up safety, education, and environmental interests as possible links for a follow-on program. Dr. Bowles thought it was important to keep a constant thread running through the program, from the existing roadmap to the end, by linking the project hardware and activities to damage tolerance and durability. He also felt that making the program more breakthrough and revolutionary and giving it a longer range view were essential for a successful program.

Dave then led a discussion involving all IAS team members, with the goal of choosing a reasonable structure to be the primary focus for the IAS program. The team was aware that, of the three available application/technology combinations (the three not shaded in Table 1-2), the highest-ranking project at the time was machined side panels. This candidate was attractive to a majority of team members; it collected large support during discussion.

The outcome of the discussion was that the team selected the integrally stiffened fuselage panel as the candidate part for the IAS program.

1.3.3 Concept Part Selection Justification

This concept part selection, while somewhat subjective, can be justified on many levels. For example, it:

- Involved an acceptable level of technical risk
- Had the ability to meet required schedule
- Would meet the objective of investigating crack turning
- Would provide the opportunity to establish some analysis for durability and damage tolerance for integrally stiffened structure
- Required collaborative effort and NASA support (that is, industry would not have pursued it without NASA sponsorship)

Integrally stiffened fuselage panels appeared to have the potential to realistically satisfy the scope for this program, and the potential to provide direction and learning for a follow-on program of a broader scale. All team members viewed this selection as an agreeable, yet stretch, concept candidate part and program starting point. It flavored the follow-on technology assessment vision with ideas of large barrel sections and large fuselage projects.

1.4 About the Rest of This Report

The concept part selection allowed the IAS program team to begin conducting other program activities. This work began with a technology assessment intended to identify potential manufacturing processes/design concepts, continued with a comprehensive test and analysis program, and concluded with a look at longer-range technology vision.

The remainder of this report documents the results of the Boeing Seattle work on the IAS program. Each of Sections 2 through 9 addresses some portion of the nine deliverables identified in the statement of work. Additional attachments convey supporting information.

2 Technology Assessment

2.1 Overview

2.1.1 Deliverables

Two deliverables are associated with the technology assessment portion of the Integral Airframe Structure (IAS) program:

1. A set of manufacturing processes/design concepts for integrally stiffened fuselage panels, and evaluations of each concept with respect to cost and to performance (structural integrity and weight). (This work is associated with NASA SOW deliverable 3.2.)
2. A down selection of the most promising manufacturing process/design concept for an integrally stiffened fuselage panel. (This work is associated with NASA SOW deliverable 3.3.)

2.1.2 Purpose

The purpose of the technology assessment was to gain insight into how integral structure might most efficiently be made, what technologies would be needed, and what types of technologies might be addressed during the test hardware and feasibility study portion of the IAS program. The down selection process would provide an opportunity to choose the technologies for further development that would be most appropriate for meeting the remaining program goals.

This work also provided an opportunity for the team to establish agreement that some of the advanced manufacturing technologies, while unavailable, could be represented by alternatives for fabrication, provided they yielded structurally equivalent test hardware. For example, in test hardware fabrication, conventional machine speeds and equipment produced parts equivalent to high-speed machining. This was necessary because access to high-speed machining equipment was not available for the IAS program.

2.1.3 Summary of Results

The technology assessment identified six plausible manufacturing processes/design concepts for integrally stiffened fuselage panels:

- A. Machine isogrid (bi-directionally stiffened) panel from plate, then form to contour.
- B. **Machine orthogonal integral channel from thick plate, then form to contour.**
- C. Machine orthogonal integral channel from comb-shaped extrusion, then form to contour.
- D. Form thick plate to contour, then machine to either isogrid or orthogonal pattern.
- E. Cast the largest possible panels, then join by riveting or welding.
- F. **Extrude skin/channel stiffener in one piece (near-net-shaped) extrusion, touch up using three-axis machine, then join by riveting or welding.**

The down selection process singled out two of these options, B and F (which are shown bold above), for follow-on program activities. Cost studies showed that the panel made from machined plate offers a cost savings of 61% as compared to the baseline built-up panel; the extruded panel was not available for cost comparison. (For more details, see the IAS program “Cost Assessment of Manufacturing/Design Concepts,” October 19, 1998.)

2.2 Identifying the Options—The IAS White Paper

2.2.1 Goals of the IAS White Paper

The Metals Forming Group, part of the Manufacturing Research and Development arm of Boeing Commercial Airplane Group, Seattle, began its work on the IAS program by conducting a preliminary assessment of possible breakthrough technologies for forming, fabricating, and manufacturing integrally stiffened panels. The goal was to develop a list of realistic, yet novel, ideas that would significantly reduce manufacturing cost without compromising the structural performance or weight typical of built-up structure. The results of this work are documented in the report “Forming Technology Assessment for Integral Airframe Structures (IAS),” also referred to as the “IAS White Paper,” dated December 12, 1996 (see Appendix A).

2.2.2 Assessment Method

To begin this assessment, the Metals Forming Group established some simple ground rules:

- Material: aluminum, 7XXX extrusion or plate (with 7050 as a candidate)
- Thickness: raw stock would be 2 to 2.5 inches thick and machined to final skin thickness
- Panel size of hardware: approximately 10 feet by 15 feet
- Contour: simple contour would be considered for test parts, although compound contour may be necessary for production parts

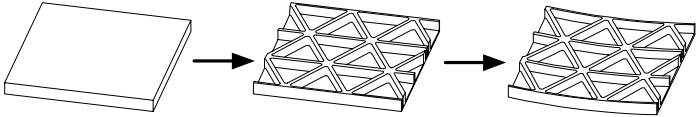
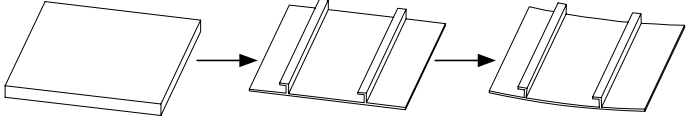
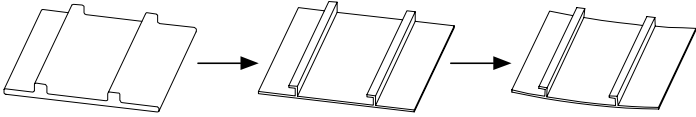
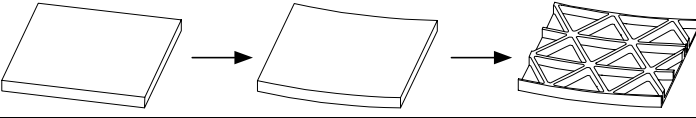
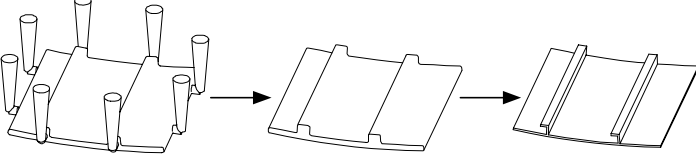
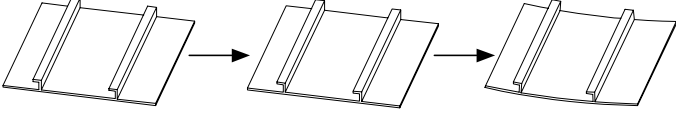
The Metals Forming Group began by brainstorming. The brainstorming activity produced several topic lists, including capability, forming, machining, methods, and risks. These lists were filled with ideas that could be applied for integral structure development. Using the ground rules identified above, the group progressively shaped these lists and ideas into concepts that combined design and manufacturing methodologies.

During this time frame, Boeing Seattle conducted preliminary hardware trials for machining plate. Note that the isogrid design used to demonstrate options A and D was taken from a 1970s McDonnell Douglas isogrid handbook (“Analytical Investigation of Medium STOL Transportation Structural Concepts Volume II, Isogrid Fuselage Study,” by R. E. Adkisson, G. E. Deneff, July 1974, Report #MDC-J6625A).

2.2.3 Six Concepts Identified

During the activity documented in the IAS White Paper, the Metals Forming Group identified six concepts for continued assessment and evaluation (see Table 2-1). The IAS White Paper describes the advantages and disadvantages of each concept the group identified. It also includes an evaluation of various forming technologies (because Group felt that forming would be very difficult). Boeing Seattle forwarded a preliminary copy of the IAS White Paper to each team member for review, comment, and addition of ideas. None of the team members had major comments or changes to the White Paper.

TABLE 2-1. MANUFACTURING PROCESSES/DESIGN CONCEPTS

Option	Description
A	<p>Machine isogrid (bi-directionally stiffened) panel from plate, then form to contour.</p> 
B	<p>Machine orthogonal integral channel from thick plate, then form to contour.</p> 
C	<p>Machine orthogonal integral channel from comb-shaped extrusion, then form to contour.</p> 
D	<p>Form thick plate to contour, then machine to either isogrid or orthogonal pattern.</p> 
E	<p>Cast the largest possible panels, then join by riveting or welding.</p> 
F	<p>Extrude skin and channel stiffener in one-piece (near-net-shaped) extrusion, touch up using three-axis machine, then join by riveting or welding.</p> 

2.3 The Down Selection Process

The method used for a manufacturing technology assessment was driven by several different factors:

- Guidance and direction of the *Affordable Design and Manufacturing (ADAM) for Commercial Transport Aircraft and Engines* proposal
- Concept/design thought for fuselage structure
- The IAS White Paper (discussed above)
- IAS team discussion during the technology assessment workshop at NASA Langley (discussed below)

2.3.1 Technology Assessment Workshop

The IAS program team met April 15 and 16, 1997, at NASA Langley for a status meeting and technology assessment workshop. Attending were: Dr. Dave Bowles, Keith Bird, and Bill Cazier of NASA; Rick Pettit and Chin Hsu of McDonnell Douglas; Keith Wilkins and John Munroe of Boeing; Ed Nichols, Jerry Griffith, and Aubre Howell of Northrop Grumman; Skip Konish and Rich Bentley from Alcoa; and Dave Chellman and Dave Ledbetter of Lockheed Martin.

One purpose of the meeting was a status update, in which each industry team member and NASA shared information. Boeing reported on progress to date regarding delivery of test specimens and test plans to NASA, cost model selection, and technology assessment for forming.

The main emphasis of the meeting, however, was to prioritize the integrally stiffened fuselage panel forming and processing options, and to down select the most promising options for further study.

2.3.2 Down Selection Limitations

During the workshop, team members had the opportunity to comment and prioritize the options presented in the IAS White Paper. Each team member presented their own ideas. A lengthy review of the White Paper and preliminary hardware trials, along with open discussion, lead the team members to make decisions regarding a down selection. These decisions were based on some practical limitations and scope changes:

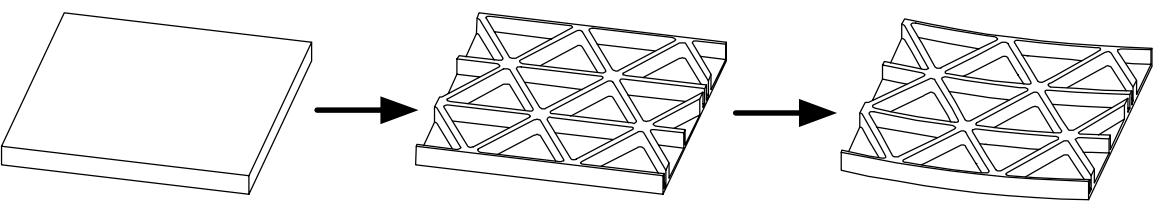
- Forming issues
- Material availability
- Manufacturing processing issues to fit into the development timeline of the IAS program
- At the beginning of the review, NASA stated that a follow-on Phase II program would not occur. This reduced the total funds available to the program, the portion of the funds available to industry, and the ultimate program scope.
- At that time, approximately 17 months of development time remained for the program (April 16, 1997 to September 30, 1998). This necessitated a very tight scope and schedule for hardware fabrication and testing.
- Testing cost, development schedule, and production machinery access limited the test matrix and therefore helped give a practical direction to what the team could accomplish.

2.4 Down Selection Results

2.4.1 Concept Evaluation Summaries

The following tables summarize key information about each option, along with conclusions reached by the IAS team during the technology assessment workshop.

TABLE 2-2. SUMMARY—OPTION A



<p>General Description</p>	<p>Machine isogrid (bi-directionally stiffened) panel from plate, then form to contour.</p>
<p>Demonstration Method Summary</p>	<p>Boeing Seattle demonstrated this concept prior to the technology assessment workshop, by starting with 7075, 1-inch thick plate, machining an isogrid design in flat contour with a three-axis machine, and roll forming into a single-contour radius.</p>
<p>Positives</p>	<ul style="list-style-type: none"> • Machining is with a three-axis (rather than five-axis) machine.
<p>Negatives</p>	<ul style="list-style-type: none"> • Roll forming capability was limited and caused large variation in the part contour. • Part size is limited for roll forming. • Isogrid internal stiffeners distorted during forming because of compressive stress buildup in thin-wall design. • Extensive mark-off on external skin surface degraded appearance. • This structure was not optimized for weight.
<p>Alternative Processes</p>	<p>The team considered but ruled out other forming methods: stretch forming (overall plate size and thickness exceeds machinery capability); bump forming (like roll forming, stiffeners were distorted by the forming process); age creep forming (buckling distortion of the stiffeners was considered a significant risk); shot peen forming (there was high risk of distortion in thin skin areas surrounded by stiffeners, and it did not appear to be cost-effective for large structures.).</p>
<p>Additional Comments</p>	<p>Stretch forming a part with internal stiffeners is extremely difficult, so development of a process appears very high-risk; nonetheless, this would be an ideal long-range development technology.</p>
<p>Team Ranking</p>	<p>Low. This structure did not appear competitive compared to other concepts. It was so different from existing technology that a tremendous design effort would be required. Extensive machining, expensive age creep tools, and long autoclave cycle time requirements did not appear to produce cost-effective results.</p>

TABLE 2-3. SUMMARY—OPTION B

General Description	Machine orthogonal integral channel from thick plate, then form to contour.
Demonstration Method Summary	Boeing Seattle demonstrated this concept shortly after the technology assessment workshop, by starting with 7050, 1.5-inch thick plate, machining the channel with a three-axis machine, and bump forming to contour. This simplified the forming requirements and could be accomplished in time to support the test phase of the IAS program. Variation in test parts was anticipated to be manageable.
Positives	<ul style="list-style-type: none"> • Fabrication techniques that are proven and simulate high speed machining. • The forming process is relatively straightforward and cost-effective. • Machining is with a three-axis (rather than five-axis) machine.
Negatives	<ul style="list-style-type: none"> • Compound contour cannot be done. • The bump forming process is operator dependent.
Alternative Processes	<ul style="list-style-type: none"> • Roll forming does not appear to support forming this structure.
Additional Comments	Stretch forming, shot peening, and age creep forming did not appear applicable for the program time available.
Team Ranking	High, to produce test parts representative in both structure and manufacturing.

TABLE 2-4. SUMMARY—OPTION C

General Description	Machine orthogonal integral channel from comb-shaped extrusion, then form to contour.
Demonstration Method Summary	This is the concept that Lockheed uses for C-130 wing skin planks. The extrusions are very large dimensional parts that accommodate the full range in dimension changes as the planks taper.
Positives	<ul style="list-style-type: none"> • Extrusion material has good material properties.
Negatives	<ul style="list-style-type: none"> • Raw stock is more expensive than plate. It requires less machining than plate, but the machining is still significant, so the buy-to-fly ratio is still very high. • Because this extrusion is non-net-shaped, it must be machined down to the gages required for fuselage optimization. Because it does not lend itself to fuselage optimization, this concept is lower in priority than a near-net-shaped extrusion concept; if it can be achieved, a near-net-shaped extrusion will save machining time. • Forming is difficult. Forming as a wrought extrusion is unlikely, and the processes after machining are either bump forming or age creep forming. Age creep forming would require special backing molds to accommodate stringers. Flexibility in design suffers and is not as readily able to support design changes.
Alternative Processes	Shot peening, roll forming, and stretch forming do not appear to be physically possible as forming options.
Team Ranking	Low, because of cost and design limits.

TABLE 2-5. SUMMARY—OPTION D

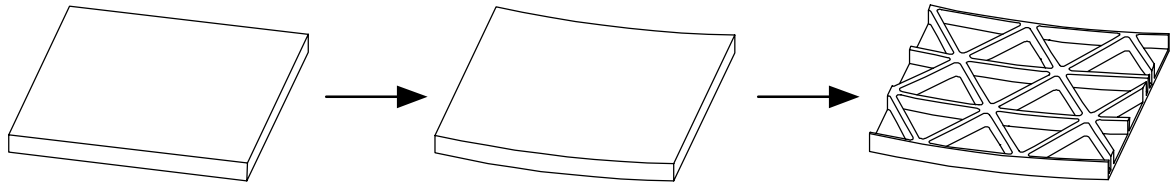
	
General Description	Form thick plate to contour, then machine to either isogrid or orthogonal pattern.
Demonstration Method Summary	Boeing Seattle demonstrated this concept, using an isogrid pattern, prior to the technology assessment workshop, by starting with machined 7075, 1-inch thick plate, roll forming it, and machining an isogrid design using a five-axis machine.
Positives	<ul style="list-style-type: none"> This process was better than concept A, but still varied.
Negatives	<ul style="list-style-type: none"> Variation and stress relieving by the plate caused movement and contour problems during machining. It was less than concept A, but still not good enough. The forming and machining imparted stress relief that caused contour movement in the parts, even though this was stretcher-level plate (plate processed by stretching to impart 7% or more elongation in the material to reduce residual stress). Consistency could not be satisfactorily held in the panels using this method. Variation was well above the 0.005-inch machining tolerance.
Alternative Processes	There do not appear to be any other forming options for this process.
Additional Comments	Compound contour cannot be achieved.
Team Ranking	Low, because of producibility concerns, additional costs associated with five-axis and specially contoured machining beds, and the limitations imposed by roll forming.

TABLE 2-6. SUMMARY—OPTION E

General Description	Cast the largest possible panels, then join by riveting or welding.
Demonstration Method Summary	The IAS schedule did not support a cast part demonstration.
Positives	<ul style="list-style-type: none"> • Castings lend themselves to complex three-dimensional shapes. • Castings do offer advantages in some primary structural applications with significant cost advantages, therefore it is a process that should be investigated for future trade studies. • The size of castings is limited in practice due to quench tank size limitations.
Negatives	<ul style="list-style-type: none"> • Casting is deemed a viable process, but, for the fuselage panel area, issues of weight, material availability, strength and toughness properties lowered the rating. • This cost of the raw material and five-axis machining and schedule of development did not lend itself to this program.
Additional Comments	Casting complex, three-dimensional shapes is a very attractive solution for structure other than fuselage panels.
Team Ranking	Low, but may be applicable for follow-on concepts.

TABLE 2-7. SUMMARY—OPTION F

General Description	Extrude skin and channel stiffener in one-piece (near-net-shaped) extrusion, touch up using three-axis machine, then join by riveting or welding.
Demonstration Method Summary	During the technology assessment workshop, Alcoa described an extrusion concept they are working on with Deutsch Aerospace in 6013 alloy. This extrusion is a 30-inch wide flat panel, with flanged integral stiffeners on 4.9-inch spacing. The panels will be laser welded together. They are identified as potential lower lobe area components. According to Alcoa, the competition is pursuing the vision of a lower barrel section composed of welded extrusions.
Positives	<ul style="list-style-type: none"> • Low buy-to-fly ratio. • Good mechanical properties. • Machining is with a three-axis (rather than five-axis) machine.
Negatives	<ul style="list-style-type: none"> • Material is costly. • This process is not flexible to design needs.
Alternative Processes	Both age creep forming and bump forming are possible.
Additional Comments	Boeing had not directly addressed this concept, because no material was available. However, Alcoa’s presentation at the technology assessment workshop demonstrated their interest in and development of extrusion panels, which stirred considerable interest. Alcoa’s work with thin wall, near-net-shaped extruded panels was so compelling and impressive that the team added this concept to the test matrix for consideration in both 6013-T651X and 7050-T7451 alloys. The thinking was that 6013 should be studied for potential in welding, corrosion, and age creep forming. 7050-T7451 extrusion material properties were of interest to NASA for comparison with 7050-T7451 plate.
Team Ranking	High.

2.4.2 Priority Rankings and Final Down Selected Options

Based on technology assessment workshop discussions, the IAS team prioritized the six concepts from a performance and technical standpoint (see Table 2-8).

TABLE 2-8. DOWN SELECTION PRIORITY RANKINGS

Priority	Option	Description
1	F	Extrude skin and channel stiffener in one-piece (near-net-shaped) extrusion, touch up using three-axis machine, then join by riveting or welding.
2	B	Machine orthogonal integral channel from thick plate, then form to contour
3	C	Machine orthogonal integral channel from comb-shaped extrusion, then form to contour
4	E	Cast the largest possible panels, then join by riveting or welding
5	A	Machine isogrid (bi-directionally stiffened) panel from plate, then form to contour
6	D	Form thick plate to contour, then machine to either isogrid or orthogonal pattern

The IAS team decided to pursue the two highest-priority options, F and B, which are shaded in Table 2-8.

2.4.3 Test Matrix Summary

By selecting these two options, the team agreed that two material forms would be investigated:

- Extrusion
- Machined Plate

The team also agreed that two forming methods would be investigated:

- Bump forming—test parts would be bump formed into simple contour
- Age creep forming—demonstration parts would be age creep formed, if available

The IAS team agreed that age creep forming would be the most viable option for a compound contour in production.

Material selection was driven by engineering performance criteria, and partially by addition of near-net-shaped extrusions in the technology assessment. The original test matrix, as suggested in the IAS White Paper, included 7050 aluminum plate. As a result of discussions after the technology assessment workshop, the test matrix was expanded to include 7475 plate (which the team felt would be better than 7050 for producing a two-bay crack panel), and 6013 and 7050 extrusion material. The final IAS program test matrix is attached as Appendix B.

2.4.4 Cost Assessment

Boeing Seattle screened the two down selected options for cost savings and benefits. This screening was intended to demonstrate whether the selected options are likely to meet the cost objectives for the program. The IAS program “Cost Assessment of Manufacturing/Design Concepts,” dated October 19, 1998, examines program cost issues in detail.

2.4.4.1 Baseline Structure

For cost evaluation purposes, the integral fuselage structure was compared to a C-17 fuselage belly structure. The baseline structure includes generic built-up wide-body panels designed using standard Boeing practices and typical for wide-body fuselage structure.

2.4.4.2 Results for Machined Panel

The machined integral fuselage panel was found to be superior to the baseline structure in terms of part count and cost, and equivalent in terms of weight. These results are summarized in Table 2-9, and discussed in more detail in the Boeing IAS Cost Assessment.

TABLE 2-9. COMPARISON OF BASELINE AND IAS PANELS

Factor	Baseline Panel	IAS Panel	IAS Change From Baseline	Target Savings Over Baseline
Number of Parts	78	7	91% reduction	50%
Weight	179 pounds	186 pounds	4% increase	Neutral
Estimated Cost	\$33,000	\$14,000	58% reduction	25%

Note that, although 78 parts are required for the baseline fuselage panel, 129 parts are required for a 747 fuselage panel. Therefore, the comparison above may actually underestimate the potential parts savings with IAS panels. The potential for part consolidation with IAS is illustrated in Figure 2-1.



FIGURE 2-1. PART CONSOLIDATION WITH IAS

For the IAS structure, the seven parts were machined from plate material. Collectively, the IAS panels and frames took 80 hours to machine and additional hours to assemble. The estimated cost is adjusted to assume high-speed machining. The panel was formed to single contour by using bump forming methods, which took 15 hours. IAS panel performance data is captured in Section 6.

2.4.4.3 Extrusions

Extrusion material was not fully investigated, but cost information indicated that, if the technology is successful, the price of raw extrusions must be \$12 per pound or less to compete with plate material. As of this writing, prices are approximately \$30 per pound.

2.4.5 Notes About the Down Selection Process

The technology assessment workshop down selected the best possible forming and processing options for integrally stiffened fuselage panels for the IAS program. Ultimately, the hardware concept demonstrated may not be the best overall technology development choice. However, it does provide a starting point for analyzing and optimizing a design for integrally stiffened fuselage panels.

Some of the practical considerations that the team applied:

- Cast and extruded panels are limited in size at this time. These processes would be more desirable if friction stir welding or laser welding could be used to join the panels.
- Any process that requires five-axis rather than three-axis machining was downgraded due to capital cost.
- In general, the team felt that isogrid technology is too large a departure from current fuselage panel design for consideration at this time.
- The team did not consider sealing, painting, or other common processes that are necessary and identical for every concept.

Regarding the options available for forming machined plate, the consensus of the team members was that:

- Age creep forming is the best current approach for production volume scenarios and compound contour forming.

- Three-point bend (bump) forming is identified as the current process for simple contour, test panels
- Shot peen forming was identified as a potential candidate, and testing may be warranted to investigate impact of surface finish and forming rates.

2.5 Outstanding Issues

2.5.1 Demonstration Panels

Lockheed Martin and Northrop Grumman were tasked with estimating the cost of fabrication of test panels and demonstration panels. To facilitate development of these estimates, the IAS team outlined the demonstration panel definitions during the technology assessment workshop. The team identified possibilities in age creep forming and compound contour.

Initial cost estimates and timing did not fit within the scope of the IAS program. Therefore, NASA decided during the October 1997 IAS status review to *not* pursue demonstration panels for IAS. A repair panel was modified from a demonstration panel to a test panel. This scope change left the pursuit of compound contour forming and age creep forming technology (and the extent of compound contour that it is possible to attain with age creep forming) for a follow-on or larger technology development program.

2.5.2 Possible Follow-On Activities

Other areas of investigation for follow-on program activities include the following:

- The effect of integral structure on acoustics in the cabin
- Friction stir welding as an alternative to riveting (it was not evaluated during this program because of difficulty arranging the necessary equipment, although small-sized test specimens were produced)
- Optimal process/alloy combinations, since some processes, such as age creep forming and laser welding, are applicable only to certain alloys and tempers

2.6 Conclusions and Recommendations

During the technology assessment, the IAS team recommended that the IAS program focus on integrally stiffened fuselage panels machined from 7050 and 7475 plate. To form these panels, the consensus of the team members was that age creep forming is the best current approach for compound contour forming and production volume scenarios. Bump forming was identified as the process currently available for simple contour forming and producing test hardware. The team also decided to address near-net-shaped extrusions in both 7050 and 6013 alloys.

This recommendation and approach is for the development of fuselage panel concepts that use integrally stiffened panels. It also introduces innovative friction stir welding as a joining technique which could eventually produce superpanels. This approach supports the ADAM vision of eliminating the majority of built-up structure and assembly steps, which leads to a low-cost approach for fuselage structure assembly. Structural performance and weight are equally important criteria that were subsequently addressed by analysis and test during the program.

3 Fabricated Test Coupons and Subcomponents

3.1 Overview

3.1.1 Deliverable

Fabricated test coupons and subcomponent panels, including documented data regarding cost, weight, part count, and manufacturing ease. (This work is associated with NASA SOW deliverable 3.6.)

3.1.2 Purpose

The purpose of this work was to fabricate the coupons and panels for tests intended to evaluate the performance of integrally stiffened fuselage structure. This section documents the fabrication methods and concerns associated with the test hardware that Boeing Seattle was responsible for, as indicated on the Integral Airframe Structure (IAS) program test matrix (see Appendix B).

3.1.3 Summary of Results

Boeing Seattle was responsible for fabricating the following test hardware:

- Test coupons for test groups 1, 2, 3, and 4, which include 7050-T7451 plate, 7050-T74511 extrusions, 6013-T651X extrusions, and 7475-T7351 plate
- Two-bay longitudinal crack panel, group 13
- Repair panel, group 9

Boeing Seattle subcontracted the fabrication of additional panels to Northrop Grumman. The Northrop Grumman report is attached as Appendix C. Original plans for large panels fabricated from extrusion material were abandoned due to poor raw extrusion quality. The raw extrusion panels were subsequently shipped to the National Aeronautics and Space Administration (NASA).

The test hardware design criteria is described in Section 4. The results of the two-bay longitudinal crack panel testing are described in detail in Section 5.

3.2 Background

3.2.1 IAS Program Test Matrix

The IAS team used a test matrix (see Appendix B) to outline the testing that would be conducted, and identify the coupons and panels that would be used, during the IAS program. The test matrix includes team responsibilities and hardware and material details. It proved to be a valuable tool in team discussions.

Boeing Seattle worked with Boeing Long Beach (then McDonnell Douglas) in September 1996 to develop the first draft of the test matrix. The test matrix evolved over time, as the other team members made input and program experience accrued. It grew to include materials that were of interest to the IAS team or were already being tested for performance data.

3.2.2 Boeing Seattle Fabrication Responsibilities

As identified in the test matrix, Boeing Seattle was responsible for the design and fabrication of certain coupons, the longitudinal two-bay crack panel, and the repair panel. Boeing Seattle contracted the fabrication of flat and curved subcomponent panels to Northrop Grumman.

3.2.2.1 Test Coupons

Boeing Seattle was responsible for producing test coupons for test groups 1, 2, 3, and 4, which included the following materials:

- 7050-T7451 plate
- 7050-T74511 extrusions
- 6013-T651X extrusions
- 7475-T7351 plate

The tests specified for these coupons were standard tests used to characterize a material's static behavior, fatigue performance (both unnotched and open hole), crack growth rate, toughness (R-curve), and crack turning parameter (rc). Boeing Seattle coordinated the process necessary to gain NASA approval of each group of specimen designs and testing procedures. Test protocol, specimen identification, and cutting diagrams (diagrams showing the locations where specimens were excised from the parent material) are included in Appendix D.

3.2.2.2 *Two-Bay Longitudinal Crack Panel*

Boeing Seattle was responsible for group 13—the design, fabrication, and test of the two-bay longitudinal crack panel. This panel was to be constructed from 7475-T7351 plate with the integral skin and stringers; 7050-T7451 shear-tied, machined frames were to be riveted to the skin.

3.2.2.3 *Repair Panel*

Boeing Seattle was responsible for fabricating the repair panel called out as test group 9. This panel was to be constructed from 7475-T7451 and include a mechanical repair patch.

3.2.2.4 *Panels Subcontracted to Northrop Grumman*

Boeing Seattle subcontracted to Northrop Grumman the fabrication of panels associated with test groups 11 (flat, unpressurized, circumferential), 12 (curved, pressurized, circumferential), and 14 (curved, unpressurized, compression). All were to be made from 7050-T7451 plate. These panels are described in a separate report prepared by Northrop Grumman. This report is attached as Appendix C.

3.2.2.5 *Extrusion Panels*

Original plans called for the fabrication of large panels in extrusion material. This work was canceled because the raw extrusions were too irregular to be machined. The extrusion panels are discussed in more detail below.

3.3 Hardware Fabrication at Boeing Seattle

3.3.1 Getting Started

3.3.1.1 Test Hardware Material

The majority of IAS program test specimens and panels were machined from plate. Boeing Seattle and Boeing Long Beach initially purchased 7050-T7451 plate for the production of test hardware. An investigation of material properties convinced the team that 7475-T7351 material would be better for producing a two-bay longitudinal crack panel, because it has higher residual strength for longitudinal crack (T-L direction). Therefore, Boeing Seattle purchased 7475-T7351 plate material for the large test panels and some material properties screening tests.

3.3.1.2 Cutting Diagrams

Fabrication began with the coordination of cutting diagrams and drawings developed for communication with the test hardware fabrication shop. Cutting diagrams were supplied for specimen groups 1, 2, 3, and 4. The diagrams called out the type of specimen, material, quantity, location the specimen was taken from the plate or extrusion, type of material, etc. Cutting diagram information for specimen groups 1, 2, 3, and 4 is located in Appendix D.

3.3.1.3 Fabrication Equipment

Fabrication methods for plate and extrusion coupons included rough cutting or sawing to size with a bandsaw, machining on a milling machine, and using a machining lathe for round specimens.

Machining was accomplished on an Okuma three-axis, five-facing-side, vertical-head mill. The machine operates at 0 to 3,000 rpm and is capable of milling 400 inches per minute without errors. Figure 3-1 shows the machine and bed after the 7050 manufacturing trial panel was completed.



FIGURE 3-1. THREE-AXIS, FIVE-FACING, 3000-RPM MILLING MACHINE

Curved panels were formed with a three-point bend machine. Mechanical bending is an economical way to produce parts with a single contour. Three-point mechanical bending of sheet and plate material is a common practice in the metal forming industry. This process is commonly referred to as bump forming or chip forming. It is currently used to form body skins and wing skins for a number of Boeing aircraft.

The trial manufacturing panel and the two-bay longitudinal crack panel were formed to a 127-inch radius using a press brake. The press brake was used to apply a series of small (degree) bends in the panel material along the longitudinal direction, to produce the desired radius in the transverse direction.

Mechanical forming is highly operator-dependent; operator-controlled factors (such as the panel placement in the machine, how many times it is formed in a given area, and the exact sequence of bends) can affect the resulting panel contour. For example, the finish and contour fit may vary depending on whether the operator forms the panel three times or ten times in a foot. Typical physical limitations for using a press brake in this type of application would be the size of the press (width and throat depth) and the size of the part being formed (length, width and thickness). To some degree, the tooling used (punch and die) can also affect the final result.

3.3.2 Coupon Fabrication

Test groups 1, 2, 3, and 4 were produced to drawing definition as shown in the cutting diagrams. Specimens were machined out of designated locations in the specified material in either plate or extrusion. These specimens were very thin, and considerable machine time was required to make them. The extrusion material had warpage problems associated with machining off the stringers, but that was anticipated. However the high degree of variation in the extrusion raw material prevented fabrication of large R-curve panels.

3.3.3 Trial Manufacturing Panel Fabrication

After the IAS team selected machined plate and bump forming to produce test hardware, Boeing Seattle produced a trial manufacturing panel to ensure that fabrication was possible. The panel was machined from 7050-T7451, 2.5-inch thick plate, using the three-axis Okuma machine. No significant warpage occurred in the 7050 part during machining. The operator estimated that 20 hours of machine run time were needed along with part set-up to produce the part. To facilitate ease of machining, machining was primarily done from one side.

The part was then bump formed with a three-point bend machine to a 127-inch radius (see Figure 3-2). Forming went smoothly and required approximately five hours. However, bump forming may be less than robust for the high numbers of parts necessary for production, because it is highly sensitive to operator experience and skill. Consequently, controlling variation for multiple parts in a production run would be a key production issue.



FIGURE 3-2. PANEL B (BUMP FORMED)

3.3.4 Two-Bay Longitudinal Crack Panel Fabrication

For the two-bay longitudinal crack panel, two 7475-T7351 plates were used to machine the skin with stringers. The first plate was used to produce the panel that, after assembly, was the lower portion of the two-bay longitudinal crack panel (Figure 3-3). Fabricating this panel was a learning experience for the machine operator. Different types of cutters were selected for the second plate, and machining was easier.



**FIGURE 3-3. LOWER PANEL OF TWO-BAY LONGITUDINAL CRACK PANEL
AFTER MACHINING**

Each panel took approximately 20 hours to machine and set up. These panels were easy to machine. The first panel was machined with a 3-inch fly-type cutter. The second panel was machined with a 1-inch ball cutter. Because of the difference in cutters, the machining marks on the two panels look different. The machined panels were transported in wooden boxes (see Figure 3-4) to a larger bump forming machine.



FIGURE 3-4. PANEL 2 BEFORE BUMP FORMING

Two experienced operators from Boeing Seattle Developmental Manufacturing successfully bump formed the two panels with a three-point bend machine in about 15 hours. The larger panels were impossible for one operator to manage alone. The curvature was consistent enough and the panels drapable enough for assembly and installation in the test fixture. Skin marring and mark-off or dimpling were insignificant and could be controlled with experience. Overall, the process was effective and economical for the test structure; for full-scale production, this may not be a robust process. After forming, both panels were shipped to Everett for assembly.

While the two panels were being formed, machined frames from 7050-T7451, 1.5-inch plate were produced. The set-up tooling for the frames was produced out of 7050 material (see Figure 3-5, which shows the tooling after the frame has been removed).

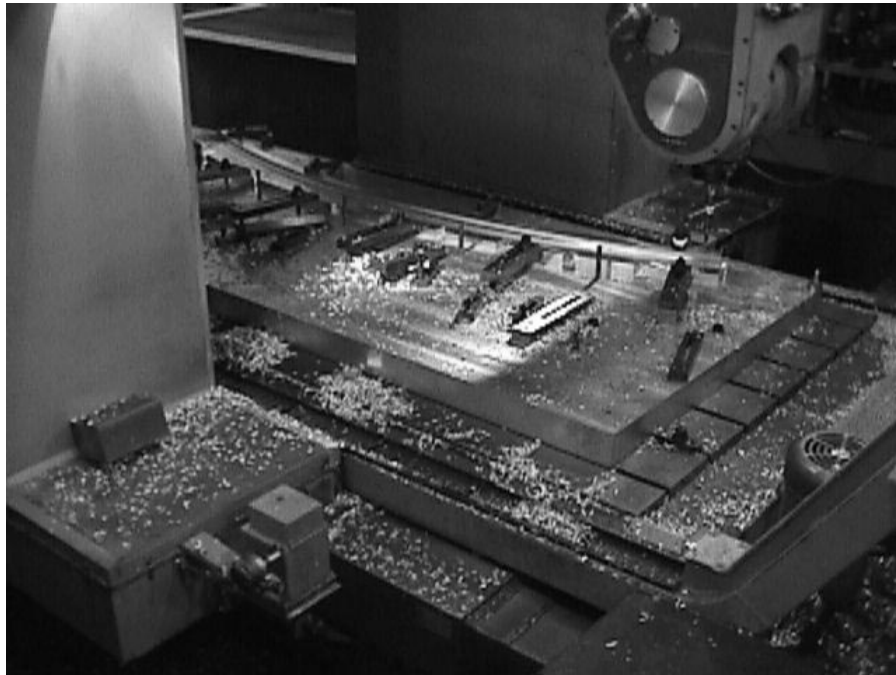


FIGURE 3-5. MILLING FIXTURE FOR 7050 FRAMES

The frames were rough cut and then machined to the specified arch. Some stress relief had to be anticipated and accounted for. To reduce setup time and increase feed through, the frames were produced by machining from one side. A total of seven attempts were required to make the five frames. Two of the frames were scrapped because of warpage and mis-located features. After machining, the frames weighed approximately eight pounds each, and they were within acceptable limits for accuracy. The rough stock and machined frames are shown in Figure 3-6.



FIGURE 3-6. ROUGH STOCK AND MACHINED FRAME

The two-bay longitudinal crack panel was assembled at the Everett test location. First, the two panels were riveted together with a 3-row lap joint, then the frames were attached with rivets. The assembly was then moved into a drill jig and holding fixture to locate the edge fastener holes used for attachment to the test fixture. The assembly mechanics found that the panel went together smoothly and quickly, and commented that this was the easiest panel they had ever assembled at the test site. Alignment was accurate for all parts, and no mismatch was observed between parts.

The assembled two-bay longitudinal crack panel has seven parts (the upper and lower panels and five frames). Compared to built-up structure, this is a radical reduction in the number of parts. For example, the equivalent 747 fuselage panel has 129 individual parts. For a comparison of the IAS versus typical built-up structures, see Figure 3-7 and Figure 3-8. Clearly, the IAS type of construction is much cleaner and has significantly fewer pieces to assemble. Also, the IAS panel weighs 186 pounds, while the built-up panel weighs 179 pounds. IAS can clearly attain the goal of 25% savings on recurring cost, by reductions in production flow time, variation in assembly, and inventory costs.

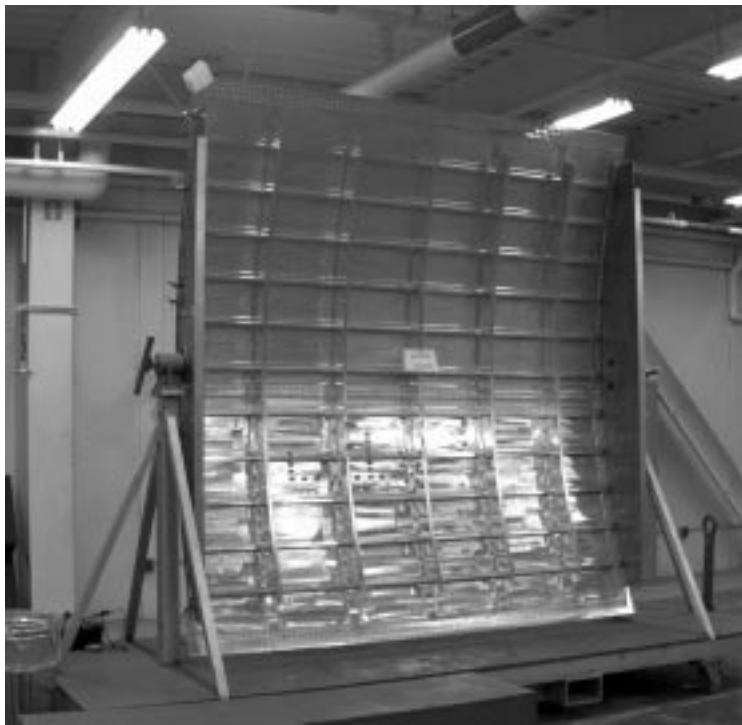


FIGURE 3-7. IAS PANEL IN THE ASSEMBLY FIXTURE



FIGURE 3-8. BOEING 747 (BUILT-UP) FUSELAGE PANEL

3.3.5 Repair Panel Fabrication

The repair panel was fabricated using 7475-T7351, 1.5-inch plate. The repair made use of 5/16-inch rivets, Hi-Lok fasteners, and sealant in the patch area. The inside and outside of the repair panel are shown in Figure 3-9 and Figure 3-10. Machining of the repair panel required 44.8 hours. Assembly and installation of the repair required approximately three 8-hour shifts. Assembly was slow because of the effort required to locate and install all of the fasteners. The final machined panel without the repair patch weighed 58.6 pounds. With the repair riveted in place, the panel weighed 62.8 pounds.

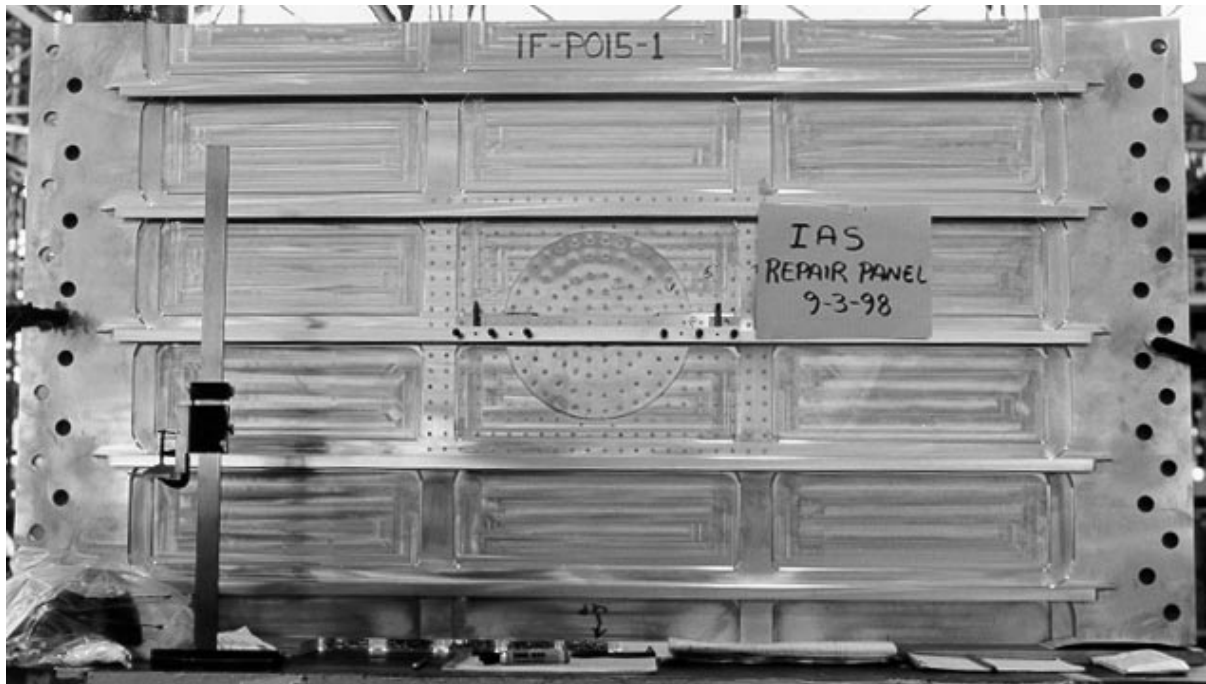


FIGURE 3-9. IAS REPAIR PANEL—INSIDE VIEW

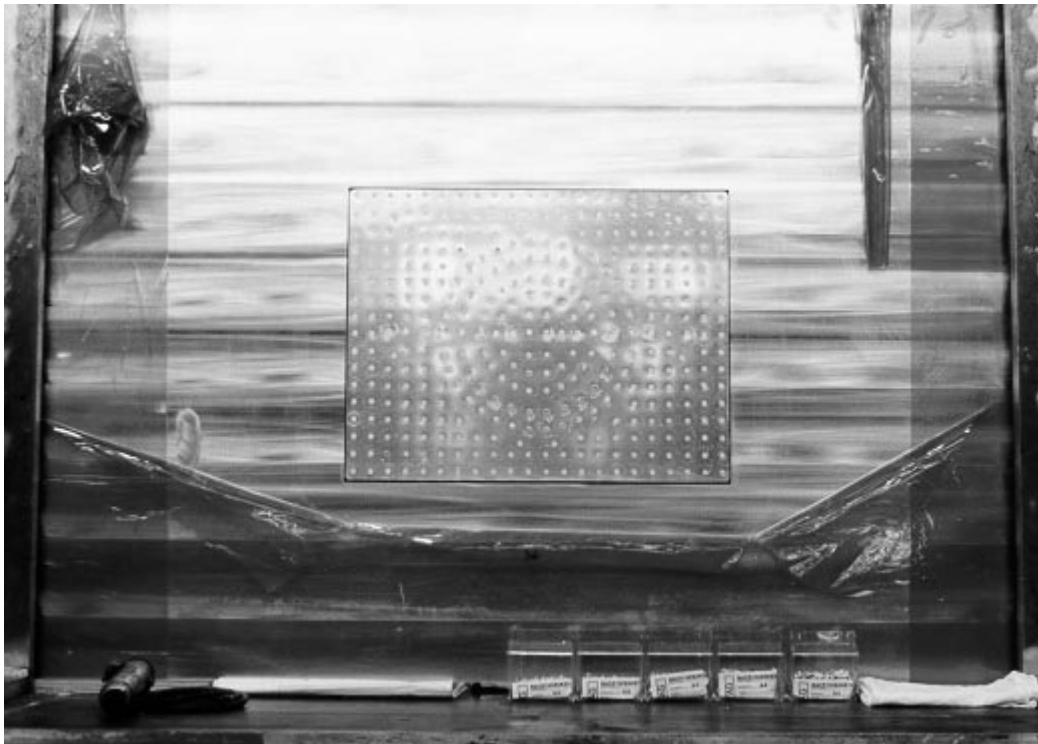


FIGURE 3-10. IAS REPAIR PANEL—OUTSIDE VIEW

3.3.6 A Discussion of Plate Material

As test hardware fabrication progressed, Boeing Seattle learned the following about plate material:

- There were no significant problems with machining items in 7050-T7451 stretcher-level plate, because the majority of machined pieces were quite thin.
- The biggest problem was maintaining vacuum on some of the larger, thin parts.
- 7475-T7451 stretcher-level plate appeared to have more noticeable problems with regard to bow in the raw material versus finished part tolerance. This was a unique occurrence that may have resulted from improper handling, and was specific to these 7475 panels as compared to the 7050 plate used for the manufacturing trial panel.
- Machining of the 7475-T7351 parts was a challenge because the plate was not much thicker than the final part dimensions. Therefore, there was not much excess for making the part. A machinist emphasized the fact that, to reduce the bow and make tolerance, material is usually skimmed on both sides and then vacuumed to the machining bed; the plate was too thin to do so in this case.
- The relative cost of plate material is very attractive, approximately \$1.60 to \$2.50 per pound. The low cost offsets the high buy-to-fly ratios common with most machine hog-outs.

3.3.7 An Analysis of Shot Peen Forming

During the April 1997 IAS technology assessment workshop, the IAS team viewed a test part previously fabricated by Boeing Seattle. This test part convinced the team members that shot peen forming of integrally stiffened fuselage panels was probably not a cost-effective or efficient way to make parts for the IAS program, or to make integrally stiffened fuselage parts in general.

Shot peen forming is a forming process used to contour skins or to enhance fatigue life. For example, it is used to contour 0.25 to 0.75-inch thick aluminum wing skins. In shot peening, wheels are used to throw shot at velocities of approximately 200 feet per second. The wing skin or a candidate integrally stiffened fuselage test part is fed through the shot stream. This creates a compressive layer which causes the plate to grow greater on one surface and results in part curvature. Varying the wheel speeds, part feed rates, and shot flow rates modifies the contour.

Typically, the shot used to form in the chordal direction (width) is 0.054-inch cut wire (CW54), and in the span-wise direction (length) is 0.116-inch cut wire (CW116). For thin specimens representative of fuselage structures, a Z-600 ceramic media (approximately 0.023-inch shot size) is used.

The nature of shot peening is that shot size, roundness, flow rate, and velocity are inconsistent; as a result, parts formed by shot peening may also be inconsistent. Because ceramic shot is smaller and more consistent than cut wire, parts are typically more consistent. Ceramic shot also contains less energy than cut wire, which reduces distortion in thin parts.

The candidate test part was shot peened with ceramic media. Nonetheless, it did not appear that a consistent and repeatable forming process could be developed for integrally stiffened skin sections. The thin skin pocket of the part distorted badly. Note that part programmers use empirical data to help set peening variables to obtain the desired contour; perhaps, in the future, a better means of modeling the process will yield a more consistent part.

3.4 Fabrication of the Alcoa Extrusion Panels

3.4.1 The Addition of Extrusions to the Test Matrix

The initial IAS program test matrix did not include extrusions. Alcoa presented the extrusion concept at the April 1997 technology assessment workshop. They described the stovepipe, vee, and flat panel extrusion shapes, and the methods to process them. The process sequence was described as: anneal, roll form flat, heat treat, stretch, and age. Alcoa described flattening as an area requiring development, and they felt that a roll straightening machine could be used to perform this operation.

Alcoa presented a development drawing of a near-net-shaped thin extrusion panel (a 30-inch wide flat panel, with flanged integral stiffeners on 4.9-inch spacing). The panels were to be laser welded together and were identified as potential lower lobe area components. The extrusions dimensions and development appeared to be an attractive option for the IAS program and fit in with fuselage panel structure.

The IAS team members were enthusiastic about extrusions, and decided to add 6013-T4, 6013-T651X, and 7050-T451 alloy options to the matrix for comparison to plate properties. The option to weld and possibly age form some of the panels was incorporated by ordering the 6013 alloy in both the -T7451 and -T4 heat treats. All of this slightly increased the scope of the program, but it was felt that the concept would be extremely valuable for application of age creep forming, welding, and investigation of structural performance.

3.4.2 Extrusion Fabrication at Alcoa

Alcoa produced the extrusion panels for the IAS program. The extrusion was processed as a vee-shaped extrusion. Figure 3-11 shows the extrusion coming out of the press, and Figure 3-12 shows the extrusion after it was cut into long lengths. After flattening, all of the extrusion panels had extreme variation in the center. Figure 3-13 shows the heavy black marks in the center of a panel that were caused by the rolling process. Note that, at this time, Alcoa can produce a 30-inch wide flat panel. In Russia, the panels are 40 to 45 inches wide. It is possible that a 60-inch wide panel could eventually be produced.



FIGURE 3-11. EXTRUSION EXITING THE PRESS



FIGURE 3-12. EXTRUSION CUT INTO LENGTHS



FIGURE 3-13. VARIATIONS IN CENTER OF PANEL

3.4.3 Extrusion Evaluation at Boeing Seattle

Boeing received the Alcoa extrusion panels in February 1998. Cutting diagrams were coordinated, and fabrication of actual test specimens began in March 1998.

Two of the extrusion panels were inspected by Boeing Manufacturing Research and Development in Seattle, for waviness, stringer angularity, and skin thickness (see Figure 3-14 and Figure 3-15). Inspection revealed that the panels had waviness in excess of ± 0.25 inch in the Y machining axis. The nominal raw material thickness was approximately 0.25 inch. Therefore, these extrusions were unacceptable for machining large panels. The inspection data (see Appendix E) was presented to NASA Langley in April 1998.



FIGURE 3-14. PANEL 1—ORIGIN END

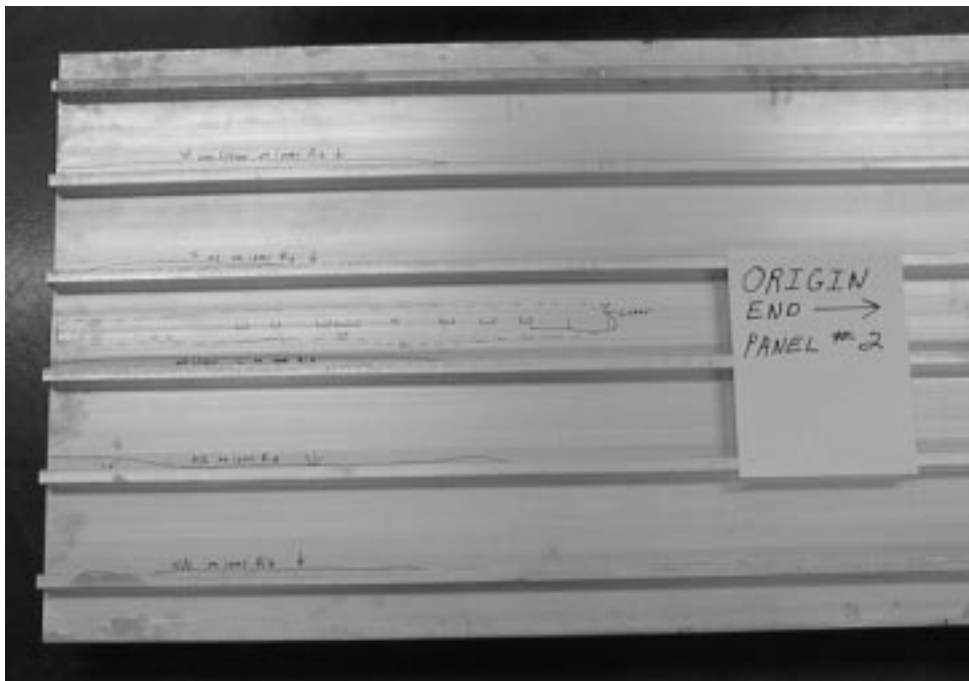


FIGURE 3-15. PANEL 2—ORIGIN END

There was significant processing variation in the panels, up to 0.25 inch in some instances, which greatly increased the difficulty of fabricating parts. Therefore, the planned fabrication of large panels in extrusion material was cancelled.

3.5 Outstanding Issues

Standard Boeing assembly practices, along with the equipment that was available at the time, were used for the fabrication and assembly of these coupons and subcomponents. Fabrication with other equipment would have been preferred if the schedule and equipment availability had allowed it. In some cases, equipment representing currently available technology was used in place of the preferred future technology. For example, conventional machining was used in place of high-speed machining. The structure produced by conventional machining is equivalent to that which would be produced by high speed machining.

Planned fabrication of large panels in extrusion material was cancelled, after it was found they could not be produced due to irregular raw material. Extrusion processing is an area deserving of more work; this is discussed in Section 8.

3.6 Conclusions and Recommendations

Boeing Seattle recommends immediate pursuit of certain follow-on testing and analysis activities:

- Testing to define the difference in residual strength for an integrally stiffened IAS panel versus built-up structure made from the same material. This removes the effect of the material and investigates the differences resulting from the design.
- Fatigue testing in 7475-T7351

Flat panel testing and fatigue testing are logical follow-on testing needs that would support current IAS panel testing. Longer-range activities should include:

- Development of additional welding and welded joints data in 7475-T7351
- Extrusion processing development

Development work in the areas of welding and extrusion would support industry competitiveness and supply needed data for engineering analysis.

4 Test Hardware Design Parameters

4.1 Overview

4.1.1 Deliverable

Test hardware design parameters were required to demonstrate cost and performance (structural integrity and weight). This shall include definition of the material, cost, joint, and substructure requirements for subcomponent panel structures and coupon designs required to support this effort. (This work is associated with NASA SOW deliverable 3.4.)

4.1.2 Purpose

The purpose of this work was to provide an opportunity for Integral Airframe Structure (IAS) program team members to develop and agree on design parameters for the test hardware that would be used to evaluate the performance of integrally stiffened fuselage structure. This section documents the design parameters associated with the test hardware that Boeing Seattle was responsible for, as indicated on the IAS test matrix (see Appendix B).

4.1.3 Summary of Results

Boeing Seattle was responsible for the design of material property specimen groups 1, 2, and 3. (Note that Boeing Seattle was responsible for the fabrication of group 4, but Boeing Long Beach was the designer.) The material property specimens were designed for determining a material's static tensile, fatigue, crack growth rate, and fracture toughness properties. The results obtained from these tests were to be used to predict the larger-scale test results to determine the accuracy of available analysis methods.

The design of the two-bay longitudinal crack panel (group 13) was an evolutionary and joint team activity between Boeing Long Beach and Boeing Seattle. The panel design concept included machined, integral skin and stringers, with riveted-on frames. Parameters affecting the final panel design include static, fail safety (residual strength), repairability, and weight performance. The test fixture and need for comparison to existing built-up structure influenced the panel design. The material selected to fabricate the integral skin and stringers, 7475-T7351 plate, was primarily driven by residual strength criteria.

Note that, although Boeing Seattle was responsible for fabrication, Boeing Long Beach had design responsibility for material property specimen group 4 and the repair panel.

4.2 Test Specimen Design Methods

Boeing Seattle was responsible for, or participated in, the design of the following test specimens:

- Material property specimen groups 1, 2, and 3
- Two-bay longitudinal crack panel, group 13

This section outlines the methods used to design these test specimens.

4.2.1 Material Property Specimens

Boeing Seattle was responsible for the design of three types of material property test specimens:

- **Static tensile** specimens for investigating the elastic-plastic stress-strain properties for all three material orientations—longitudinal (L), longitudinal transverse (LT) and short transverse (ST). These specimens were associated with group 1 of the IAS test matrix.
- **Fatigue** specimens for evaluating the durability performance of an integral structure. To obtain the basic material response to cyclic loading, both smooth and open-hole specimens were tested. Material orientation (L or LT) and the location of the specimen relative to the initial product thickness were also investigated. These specimens were associated with group 2 of the IAS test matrix.
- **Crack growth and fracture toughness** specimens for evaluating the damage tolerance behavior of an integral structure. Parameters investigated with these specimens included material orientation, final specimen thickness, and the location of the specimen with respect to the initial product thickness. These specimens were associated with group 3 of the IAS test matrix.

The material property specimens were designed per American Society for Testing and Materials (ASTM) standards. These ASTM standards outline the steps for determining the static tensile, fatigue, crack growth rate, and fracture toughness properties of a material. Design parameters for each specimen depend on the type of test, material size limitations, and required information.

The results from these tests were to be used to predict the larger-scale test results, and thus to determine the accuracy of available analysis methods.

4.2.2 Two-Bay Longitudinal Crack Panel

Boeing Long Beach was responsible for the overall design task, but design of the two-bay longitudinal crack panel (two-bay panel) was an evolutionary and joint activity between Boeing Long Beach and Boeing Seattle. Boeing Long Beach supplied the original two-bay panel design, but final design was a collaborative effort.

4.2.2.1 Basic Design

The preliminary concept for the two-bay panel consisted of machined stringers integral to a skin with riveted-on frames. Standard test practices and test equipment dictated the global dimensions of the two-bay crack test panel. The 127-inch fixture used to test the panel necessitated that the frame and stringer spacing be 20 inches and 9.25 inches, respectively.

4.2.2.2 Performance Requirements

Initially, the panel's structural members were designed by sizing them from the built-up baseline for the integrally stiffened concept. The local geometric shapes and dimensions were then optimized by considering static, fail safety (residual strength), repairability, and weight performance. The design goal was to make the panel equal to or better than the built-up Federal Aviation Administration panels tested at Boeing in each of these structural criteria. The panel had to:

- Maintain compressive and tensile strength equivalent to the baseline built-up structure
- Hold a two-bay crack at a pressure of 9.4 psi
- Be capable of being easily repaired
- Weigh the same or less than the baseline built-up structure

The two-bay panel design did not consider durability, because this is a bigger issue with joints, which were not part of the two-bay panel test. Nor did it consider crack growth performance, because damage tolerance capability equivalent to the baseline would be achieved by modifying inspection intervals. Section 3 of the Seattle Long Beach IAS program report contains a detailed description of how the panel was designed.

The most critical issue for the two-bay panel turned out to be the residual strength requirement. The static requirements were easily satisfied by the selection of 7050-T7451 plate to fabricate the skin and stringers. However, analysis by Boeing Seattle predicted that this choice of material would be insufficient for holding a two-bay crack at the required pressure. Therefore, 7475-T7351, which has a substantially higher toughness than 7050-T7451, was substituted. Further analysis by Boeing Seattle and Boeing Long Beach showed that this new material selection would enable the two-bay panel to have performance equal or better than the corresponding built-up panel.

4.2.2.3 Fabrication

Once the design features were finalized, a Boeing Seattle drafter drew the panel in CATIA (computer-aided design software) as solid views. Developmental Manufacturing and Test Organizations used this CATIA model to machine and assemble the test panel.

4.3 Outstanding Issues

It should be noted that the design of the two-bay longitudinal crack panel:

- Was created through a joint effort—it does not reflect or necessarily follow Boeing design specifications and procedures; it is instead representative of research screening, which is the function of this program
- Used a traditional approach to sizing and designing structural members—but it is only one possible method
- Was based on material and load data assumptions that will not be verified until 7475 R-curves are tested

5 Two-Bay Longitudinal Crack Test and Results

5.1 Overview

5.1.1 Deliverable

A test plan to demonstrate and validate the cost and performance of the down selected integrally stiffened manufacturing process/design concept. (This work is associated with NASA SOW deliverable 3.5.)

5.1.2 Purpose

The purpose of this testing was to measure the crack growth and residual strength performance of an integrally machined, full-scale, wide-body panel with a crack extending over two bays, when subjected to realistic fuselage pressure loading. The application of this type of testing to a panel fabricated according to the previously down selected manufacturing process/design concept would demonstrate the potential performance of this concept, and of integral structure generally, in full-scale application.

5.1.3 Summary of Results

The two-bay longitudinal crack panel was fabricated for these tests, and the panel was mounted in a wide-body test fixture located in Everett, Washington. Tests were conducted with cracks introduced by sawcutting at two locations on the panel.

5.2 Pressure Test Facility

A wide-body test fixture, located at the Boeing Everett facility, was used to test the Integral Airframe Structure (IAS) program two-bay longitudinal crack panel. This fixture has a 127-inch radius and a 20-foot length (see Figure 5-1). The overall geometry of the fixture is consistent with typical fuselage design, which has frames at a 20-inch pitch and stringers at a 9.25-inch pitch. Photos of Boeing's wide-body and standard-body fixtures are shown in Figure 5-2 and Figure 5-3.

Wide-body Fixture Capabilities:

- 25 seconds/cycle with a 40% polystyrene foam void fill
- 8.6 psi cyclic pressure (100 psi supply air)
- 300-channel data acquisition system

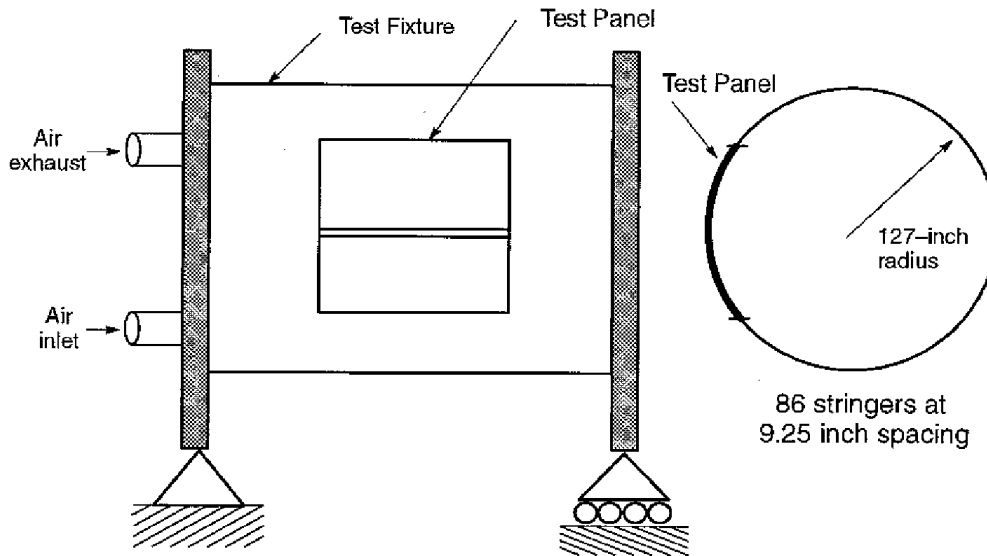


FIGURE 5-1. WIDE-BODY PRESSURE TEST FIXTURE



FIGURE 5-2. WIDE-BODY FIXTURE



FIGURE 5-3. STANDARD-BODY FIXTURE

The test fixture's 2024-T3 clad skin, 7075-T6 frame, and 2024-T3 clad stringer gages are thicker than typical minimum-gage fuselage structure, but have been selected to maintain realistic fixture stiffness and provide adequate longevity. The end bulkheads are steel. One bulkhead is fixed while the other is on rollers, to permit axial expansion during pressurization.

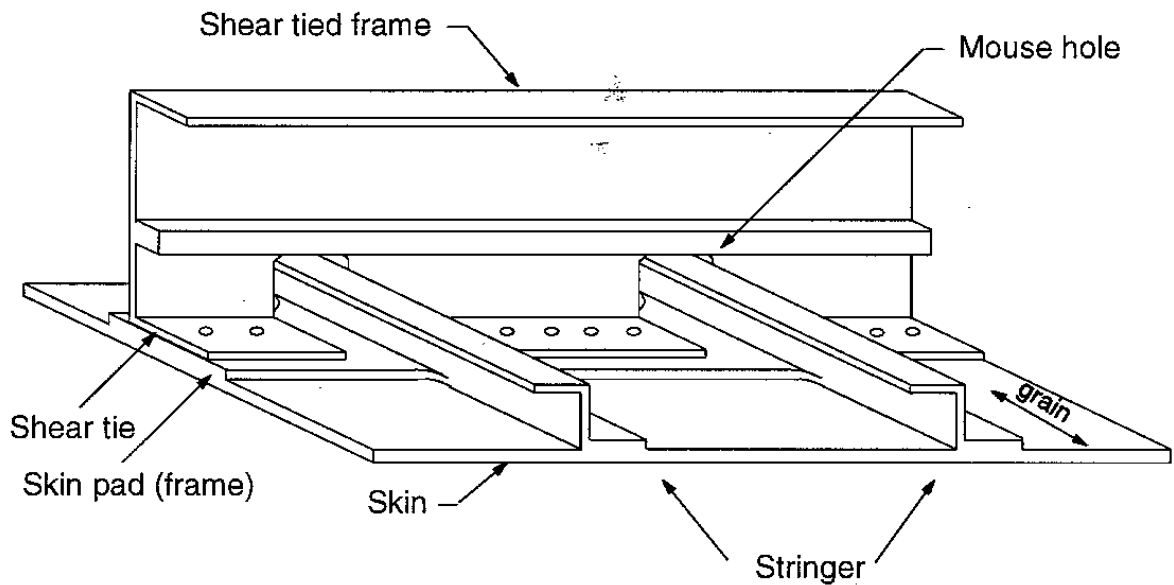
The test fixture has a single rectangular cutout, approximately 10 feet by 10 feet, designed to accept the test panels. Test panels are attached to the fixture at the skin, frames, and stringers by a fusing arrangement that allows the panel to fail at loads below the elastic limit of the fixture components. The stringer and frames splices are designed to allow attachment fasteners to shear during a dynamic panel failure. The test panel skin is allowed to tear circumferentially along the perimeter fasteners, with the help of a sharp notch that is introduced into the panel before it is installed in the fixture. These features make it possible to conduct residual strength tests that result in the test panel failure—without extensive damage to the test fixture.

The pressurizing medium for the test fixture is compressed air. The flow of air into the fixture is regulated with a digitally-controlled valve. During the IAS panel tests, cyclic rates were approximately 25 seconds per cycle. Polystyrene foam blocks are placed within the fixture to reduce the required air volume. To reduce air leakage through the sawcuts and thus improve cycle times, an internal rubber dam was installed after the sawcuts were made. This dam consisted of rubber sheet that was laid up against the skin and clamped to the stringer.

5.3 Test Panel

5.3.1 Configuration

The two-bay longitudinal crack panel (see Figure 5-4) was similar in general configuration to typical wide-body fuselage structure, in that it consisted of shear-tied frames riveted to a local pad on the skin. The integral aspect of the panel was that the skin and stringers were monolithic, having been machined from 1.5-inch thick plate. The panel design concept is discussed in Section 4.



Structural Dimensions	
Radius	127 inches
Stringer spacing	9.25 inches
Frame spacing	20.0 inches
skin thickness (t_{skin})	0.063 inch
skin pad thickness	0.085 inch
total skin thickness under frame	0.148 inch
skin pad width	2.0 inches
R_s = circumferential skin stiffening ratio = Area of skin pad / (Frame spacing x t_{skin}) = 0.13	

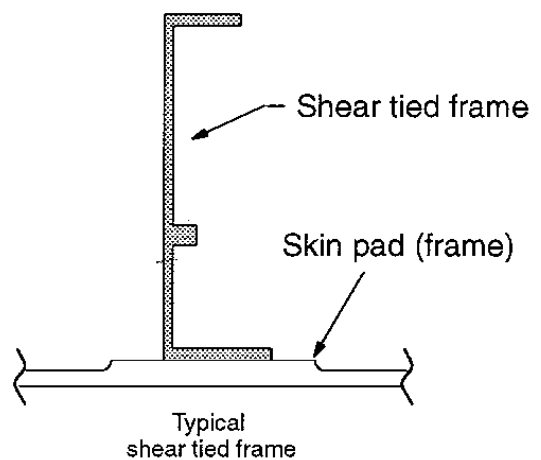
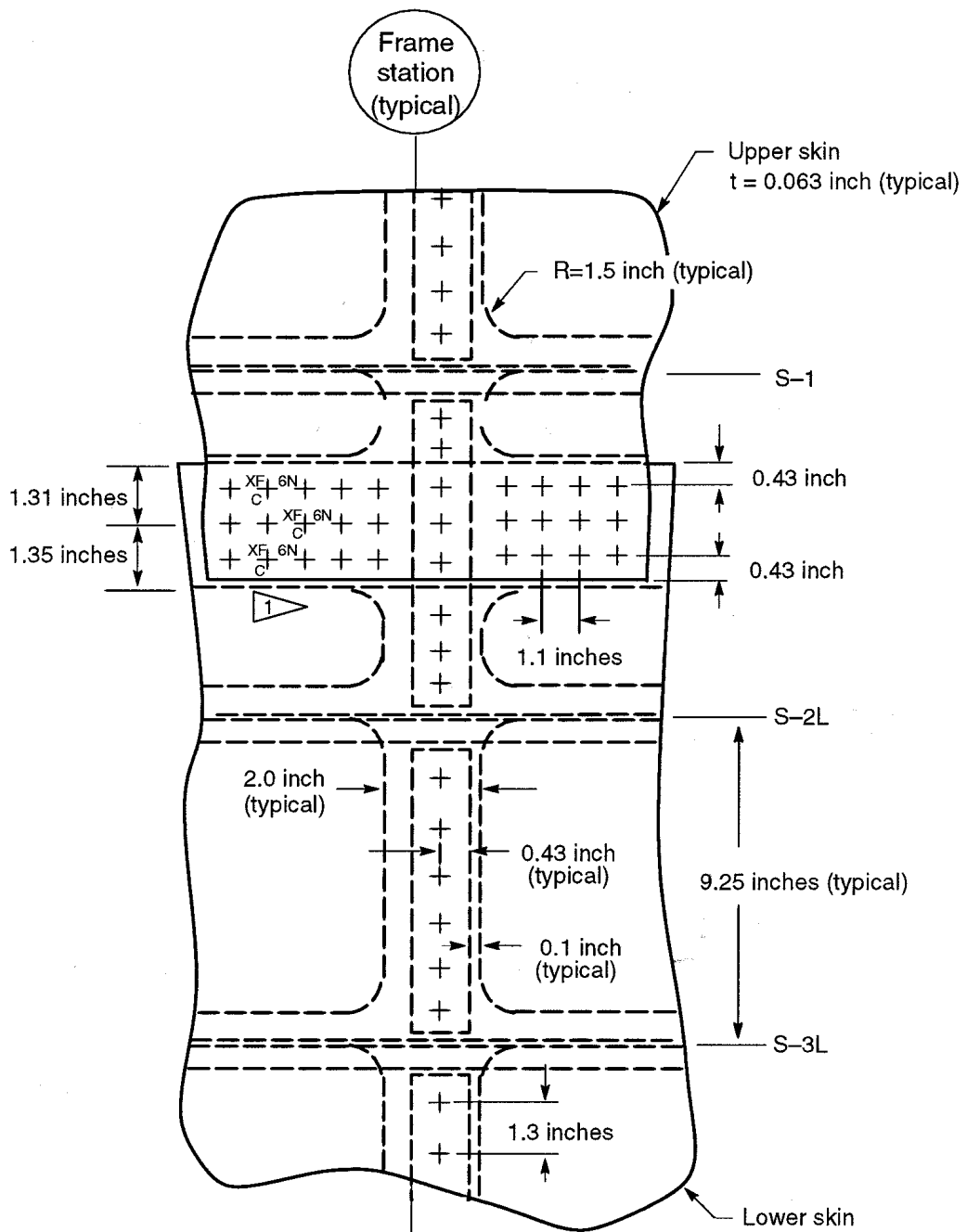


FIGURE 5-4. STRUCTURAL DETAILS

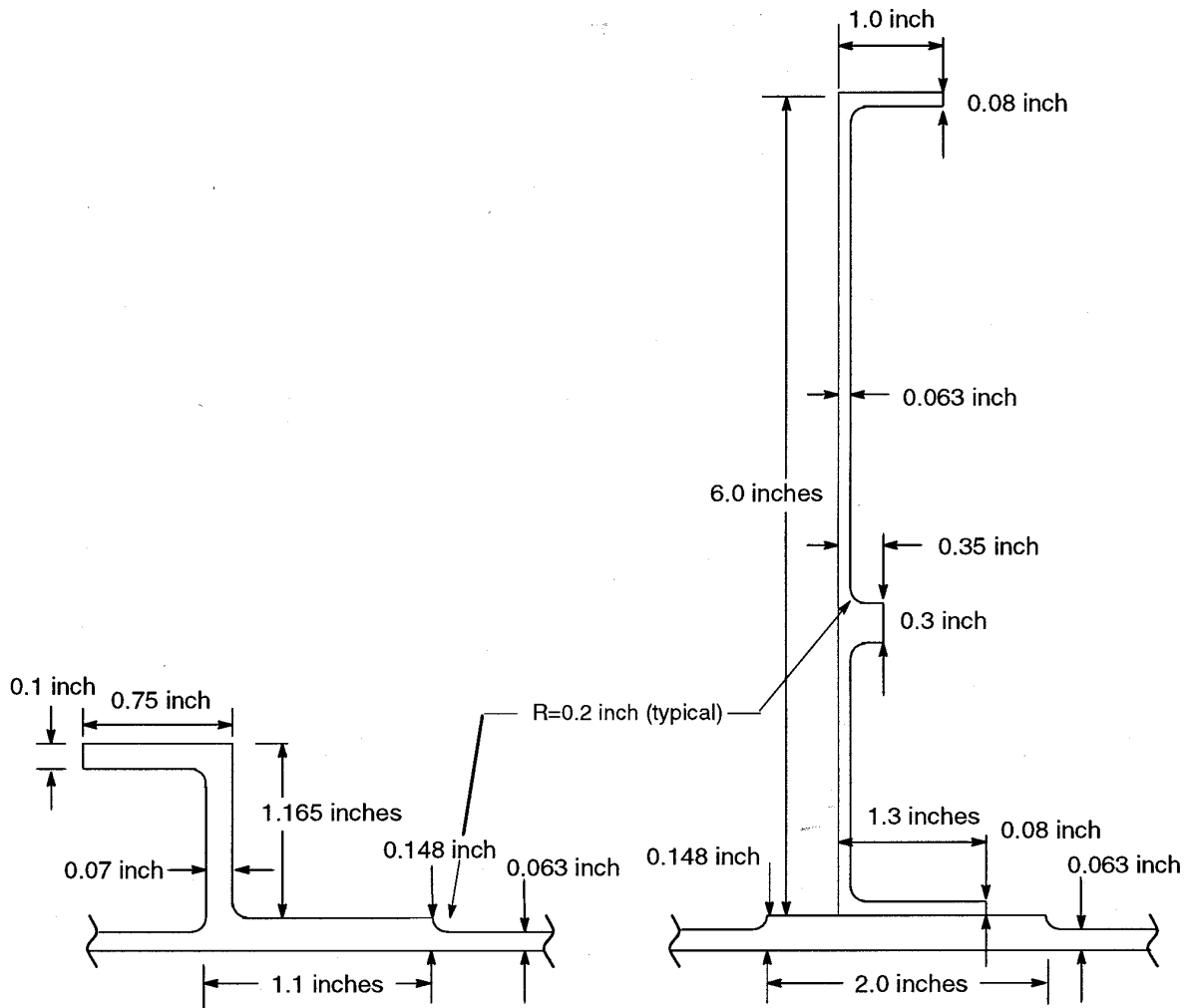
The skin was divided into two sections, upper and lower. These sections were joined together at the longitudinal splice (lap joint) located between stringers 1 and 2 left. The lap joint was a three-row configuration assembled using 3/16-inch diameter 100° countersunk head rivets. The grain in the skin is oriented longitudinally. Typical panel details (such as fastener spacing, lap joint details, and frame and stringer dimensions) are found in Figure 5-4, Figure 5-5, and Figure 5-6.



$\frac{XF}{C} \frac{6N}{C}$

BACR15CE6D (2017-T4 rivet 100° CSK head) 3/16-inch diameter

FIGURE 5-5. STRUCTURAL DIMENSIONS OF PANEL



Stringer

Frame and Skin Pad

FIGURE 5-6. FRAME AND STRINGER DIMENSIONS

Not including the frame cross-sectional area, the two-bay longitudinal crack panel's circumferential skin stiffening ratio, R_s , was 0.13, based on the following equation:

$$R_s = A_{\text{skin pad}} / (B \times t_{\text{skin}})$$

where:

- $A_{\text{skin pad}}$ = skin pad under frame shear tie (see Figure 5-4)
- B = frame spacing = 20 inches
- t_{skin} = basic skin thickness

Designers used the computer-aided design system CATIA to produce the engineering drawings used to build the panel. Panel assembly followed standard Boeing assembly procedures.

5.3.2 Material and Fabrication

The two-bay longitudinal crack panel included integral skin and stringers that were machined from 1.5-inch thick 7475-T7351 plate. This plate was from the same lot used for the material characterization tests described in Section 3. The skin was typical wide-body gage (0.063 inch); 0.085-inch thick circumferential pads were machined into the skin, for a total thickness of 0.148 inch every 20 inches under each frame. The frames were machined from 1.5-inch thick 7050-T7451 plate. Skin and frame fabrication details are covered in Section 3.

5.4 Test Results

Tests were conducted on the two-bay longitudinal crack panel with cracks introduced at two locations (see Figure 5-7).

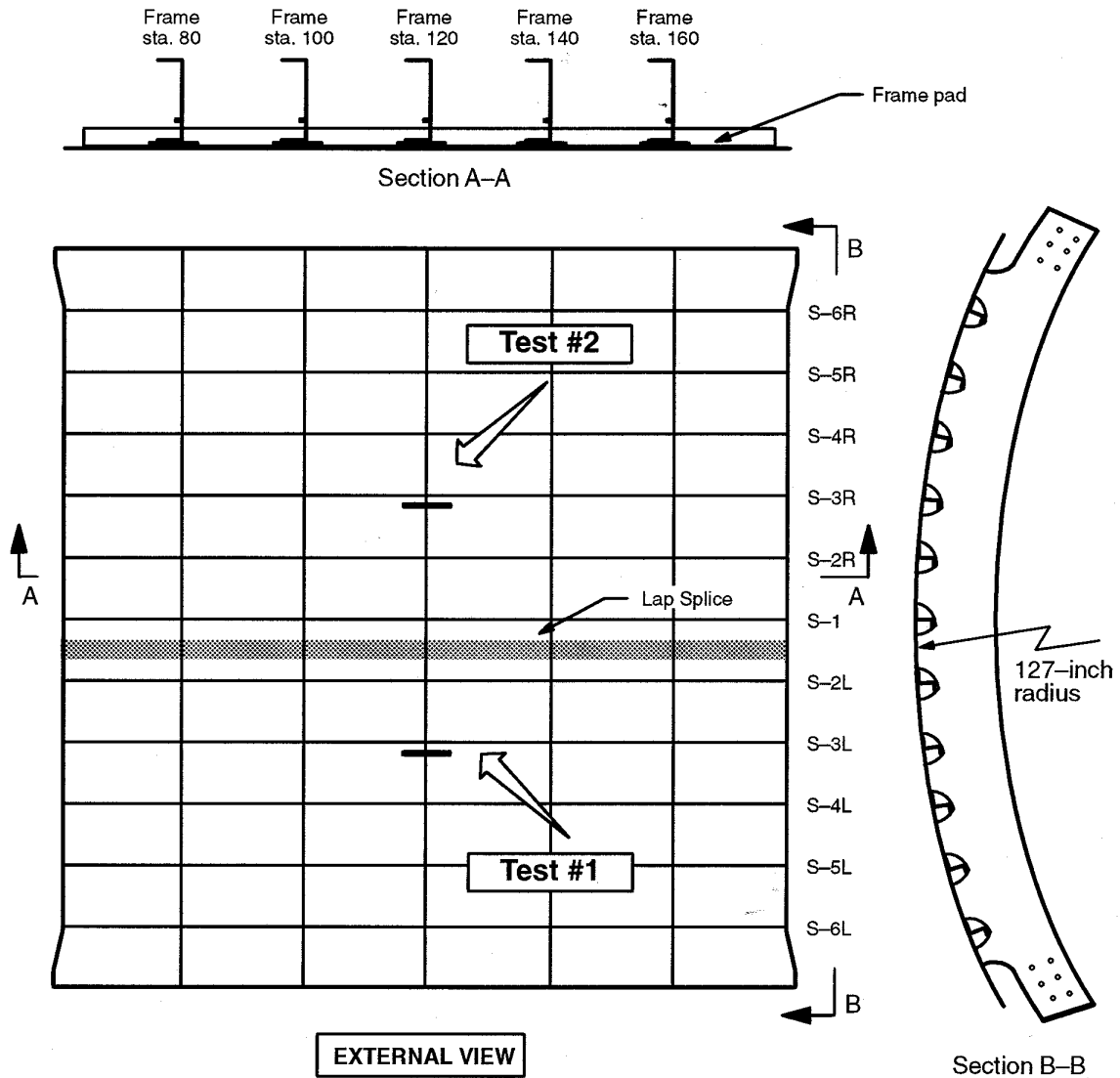


FIGURE 5-7. STRUCTURAL CONFIGURATION AND TEST LOCATIONS

Sawcuts to the skins and frames were installed with an air-driven hand-held abrasive rotary wheel that creates a 0.1-inch sawcut. The resulting sawcut was sharpened with a hand-held X-ACTO saw that creates a sawcut width of approximately 0.012 inch. Instrumentation details and a selection of strain gage readings for both tests are found in Appendix F.

5.4.1 Test 1—Summary

Test 1 consisted of a crack growth test followed by a residual strength test. These tests were conducted at stringer S-3L and centered on the panel, as shown in Figure 5-8. Before the test was started, approximately 20 pressure cycles were applied in order to “seat” the panel in the test fixture. This allows for any permanent settling to occur prior to conducting the initial strain survey.

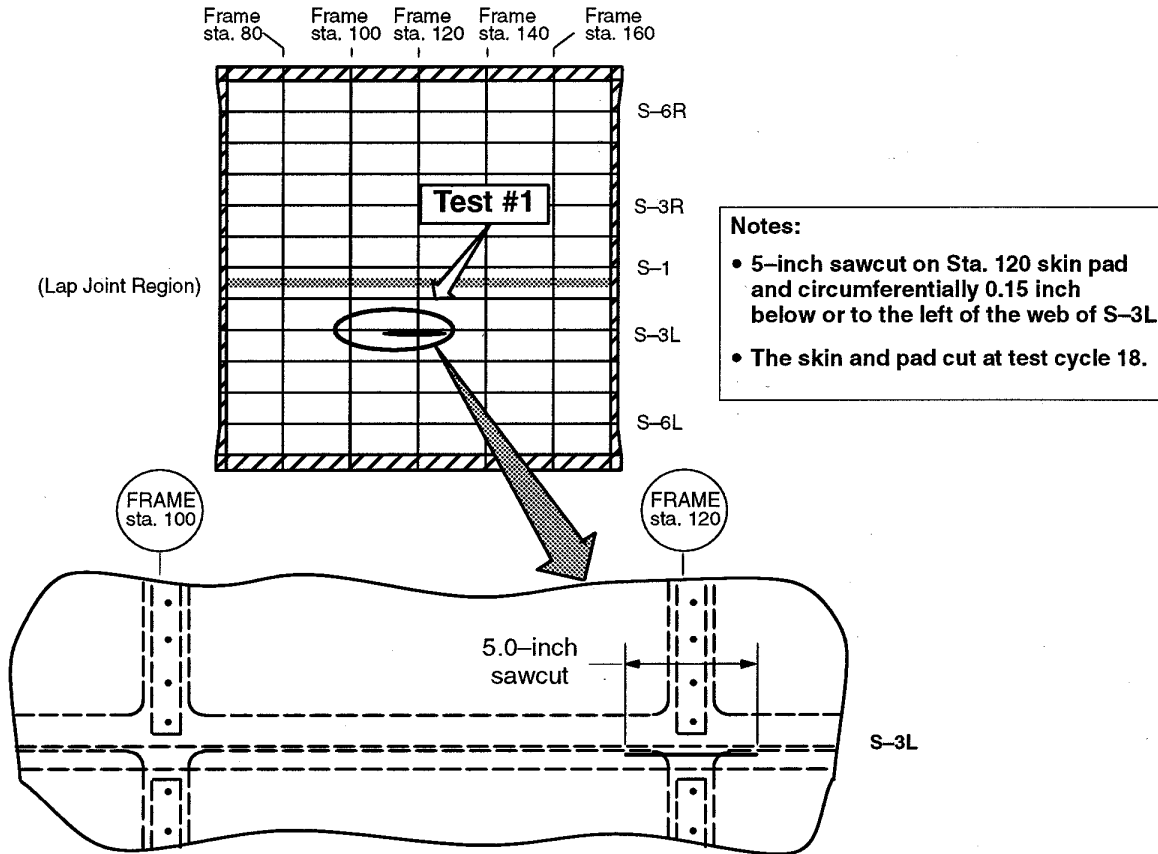


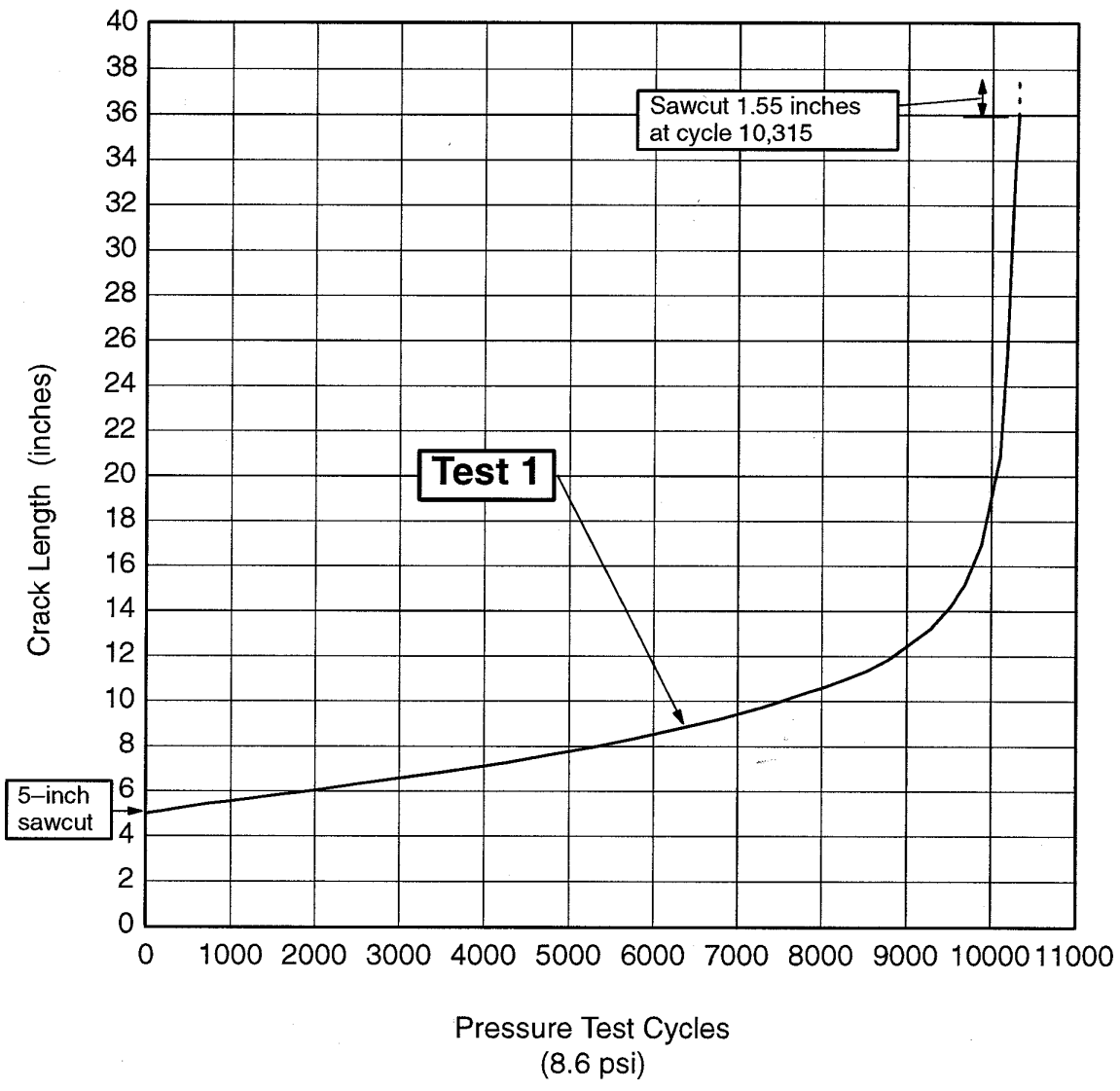
FIGURE 5-8. INITIAL SAWCUT DETAILS FOR TEST 1

The initial 5-inch sawcut was installed in the skin adjacent to stringer S-3L, and centered on frame station 120. The panel was pressure cycled at 8.6 psi, and the crack growth was periodically measured, to a length of 35.9 inches. The crack was then extended by means of a sawcut to 38 inches (skin pad-to-skin pad), and the residual strength test was conducted. During this test, the crack dynamically extended, but it arrested in the shear tie fastener holes at approximately 40 inches. The Test 1 site was repaired in order to conduct Test 2.

The instrumentation details and strain gage readings for Test 1 are included in Appendix F.

5.4.2 Test 1—Crack Growth Results

The initial 5-inch sawcut was made in the skin adjacent to stringer S-3L, at panel cycle 18. No crack initiation out of the sawcut was visible until after 200 cycles at 8.6 psi. However, the crack propagated to a length of 35.90 inches after 10,315 cycles in the longitudinal direction. A plot of crack length versus the number of pressure cycles is shown in Figure 5-9. Once the crack had reached the length of 35.90 inches, the crack had deviated from the longitudinal direction by 1.9 inches at the forward tip and 1.34 inches at the aft tip. The crack trajectory is illustrated in Figure 5-10. A photograph of the crack at 10,333 cycles is shown in Figure 5-11. The recorded crack growth data is shown in Table 5-1.



(after 5-inch sawcut installed)

FIGURE 5-9. CRACK GROWTH HISTORY OF TEST 1

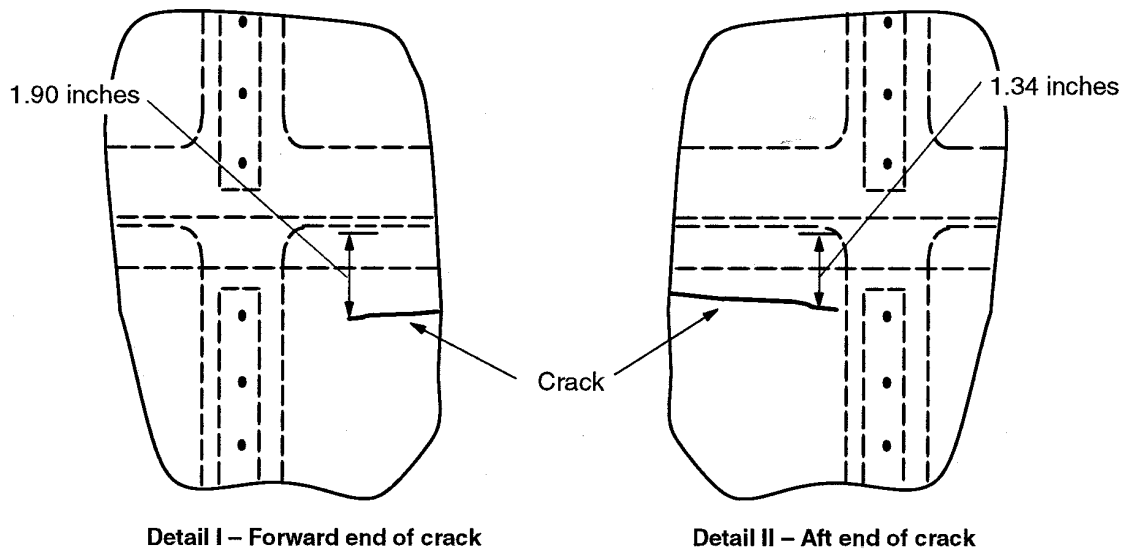
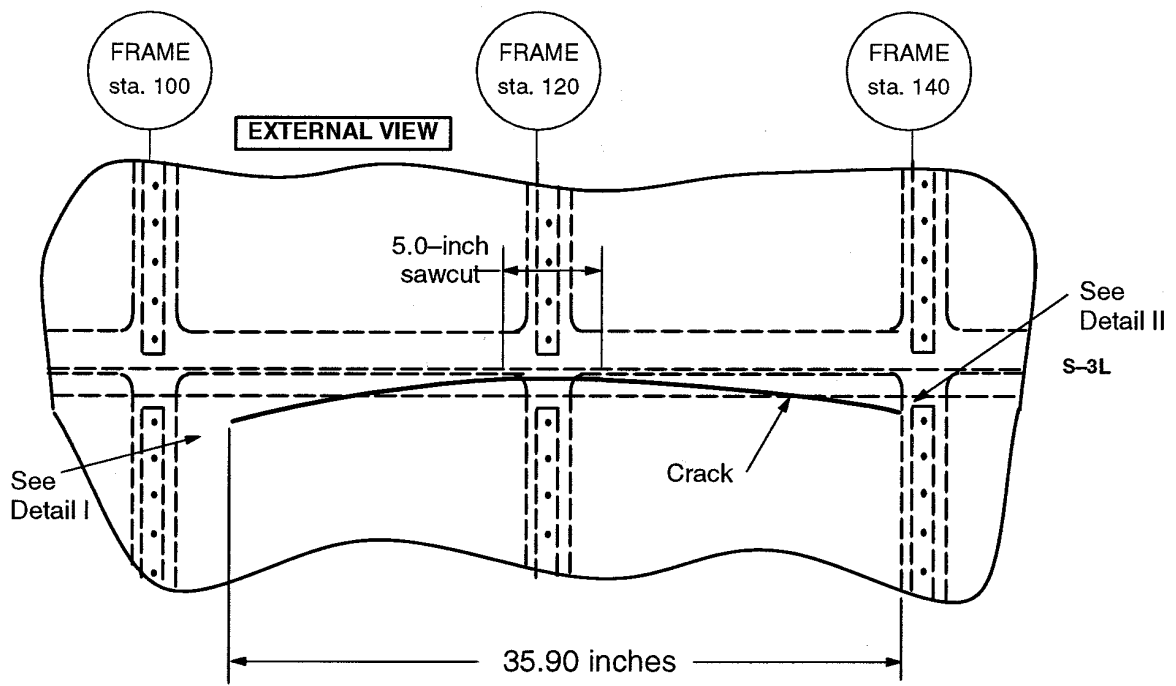


FIGURE 5-10. CRACK GROWTH TRAJECTORY OF TEST 1

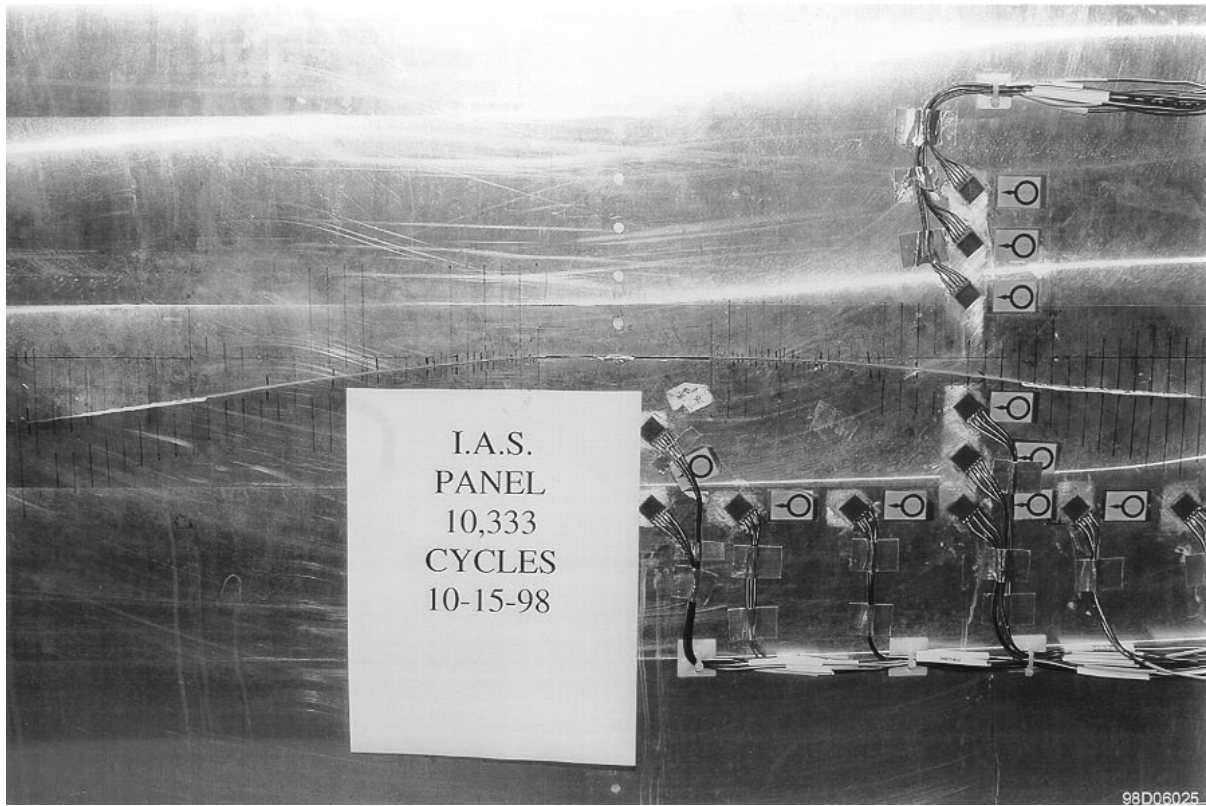


FIGURE 5-11. IAS PANEL, TEST 1, CRACK AT 10,333 CYCLES

TABLE 5-1. TEST RECORD OF CRACK LENGTH MEASUREMENTS FROM TEST 1

Test Cycle Number	Panel Cycle Number	Length of New Growth (inch)	Total (X) Dimension (inch)		Total (Y) Dimension (inch)		Total Crack Length (inch)
			Fwd Tip	Aft Tip	Fwd Tip	Aft Tip	
–	0	Intact	0	0	0	0	0
0	18	Sawcut installed 5.00	–	–	–	–	5.00
200	218	0.11	0.07	0.04	0	0	5.11
400	418	0.13	0.14	0.10	0	0	5.24
732	750	0.20	0.24	0.20	0	0	5.44
932	950	0.07	0.24	0.27	0	0	5.51
1232	1250	0.15	0.34	0.32	0	0	5.66
1562	1580	0.17	0.42	0.41	0	0	5.83
1962	1980	0.18	0.51	0.50	0	0	6.01
2482	2500	0.29	0.65	0.65	0	0	6.30
2982	3000	0.26	0.78	0.78	0.05	0	6.56
3482	3500	0.28	0.91	0.91	0.07	0	6.82
4256	4274	0.45	1.13	1.12	0.07	0	7.25
4756	4774	0.36	1.31	1.30	0.10	0	7.60
5267	5285	0.33	1.48	1.46	0.10	0	7.94
5771	5789	0.39	1.66	1.67	0.13	0	8.33
6282	6300	0.43	1.86	1.90	0.15	0	8.76
6782	6800	0.43	2.06	2.13	0.15	0.05	9.19
7282	7300	0.56	2.32	2.39	0.20	0.07	9.71
7532	7550	0.30	2.47	2.54	0.22	0.07	10.01
7782	7800	0.32	2.63	2.70	0.22	0.08	10.33
8032	8050	0.29	2.78	2.84	0.22	0.10	10.62
8282	8300	0.35	2.98	2.99	0.22	0.10	10.97
8532	8550	0.37	3.18	3.06	0.24	0.12	11.34
8782	8800	0.49	3.43	3.40	0.30	0.12	11.83
9032	9050	0.68	3.81	3.70	0.35	0.13	12.51
9282	9300	0.69	4.12	4.08	0.36	0.17	13.20
9532	9550	1.05	4.64	4.61	0.43	0.21	14.25
9632	9650	0.62	4.97	4.90	0.45	0.23	14.87
9682	9700	0.27	5.07	5.07	0.47	0.23	15.14
9882	9900	1.80	5.92	6.02	0.56	0.35	16.94
10102	10120	3.92	7.82	8.04	0.85	0.53	20.86
10184	10202	4.56	9.97	10.45	1.20	0.90	25.42
10224	10242	3.79	11.26	12.95	1.35	1.05	29.21
10272	10290	4.31	12.91	15.61	1.61	1.26	33.52
10315	10333	2.38	14.66	16.24	1.90	1.34	35.90
10315	10333	1.55 sawcut	16.21	16.24	–	1.34	37.45

5.4.3 Test 1—Residual Strength Results

In preparation for the residual strength test, the crack was extended to the desired 38-inch length (from frame pad to frame pad), by means of a sawcut. Furthermore, the forward tip had to be extended because the crack was not symmetric in length longitudinally or circumferentially. The sawcut extension is illustrated in Figure 5-12.

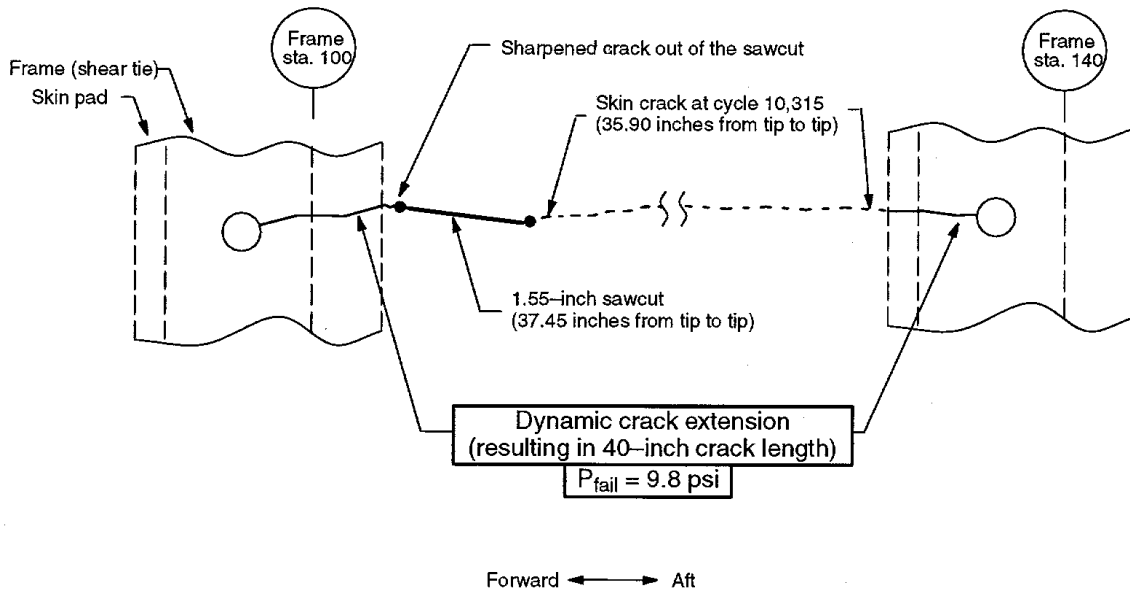


FIGURE 5-12. RESIDUAL STRENGTH CRACK CONFIGURATION OF TEST 1

The residual strength test consisted of increasing the internal pressure until dynamic crack extension occurred. Events during the test were witnessed and recorded on videotape.

Before starting the test, the desired crack configuration was a two-bay skin crack, centered on a severed central frame. Because this condition was not completely achieved by the completion of the crack growth phase of the test, the forward crack tip had to be extended by 1.55 inches to within approximately 0.1 inch of the pad. The panel was then cycled at 5 psi until crack initiation was witnessed emanating from the sawcut at the forward tip. The tips of the crack were then adjacent to the edges of the frame pads as shown in Figure 5-12.

The pressure was then steadily increased at a rate of approximately 0.2 psi per second. As the pressure was increased above 9.8 psi, both the forward and aft crack tip dynamically grew into the first or closest rivet to the stringer at frame stations 100 and 140, respectively (see Figure 5-12). These fastener holes acted as “stop drill” holes by effectively eliminating the crack tips. The pressure continued to be increased from 9.8 to 10.4 psi. At 10.4 psi, the skin crack was 40 inches, and the panel held pressure for approximately 15 seconds. The pressure was then released. After the test, no evidence of crack initiation was visible at either of the shear tie fastener holes.

5.4.4 Test 1—Panel Repair

The Test 1 location was repaired by applying an external doubler (see Figure 5-13 and Figure 5-14). Before installation of the repair, the lower crack face was removed, so it would not be damaged by contact with the mating face. Also, to reduce any influence on the Test 2 location, the circumferential size of the repair was minimized.

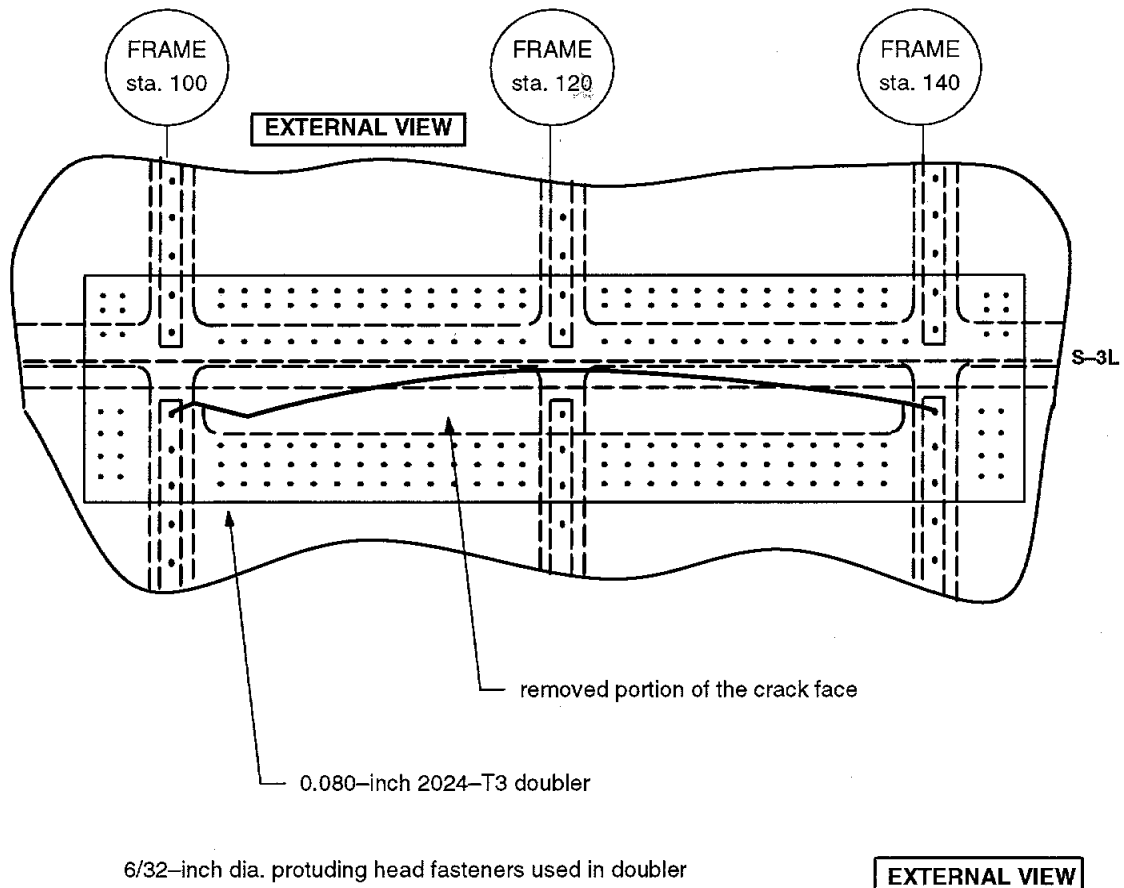


FIGURE 5-13. PANEL REPAIR OF TEST 1 LOCATION

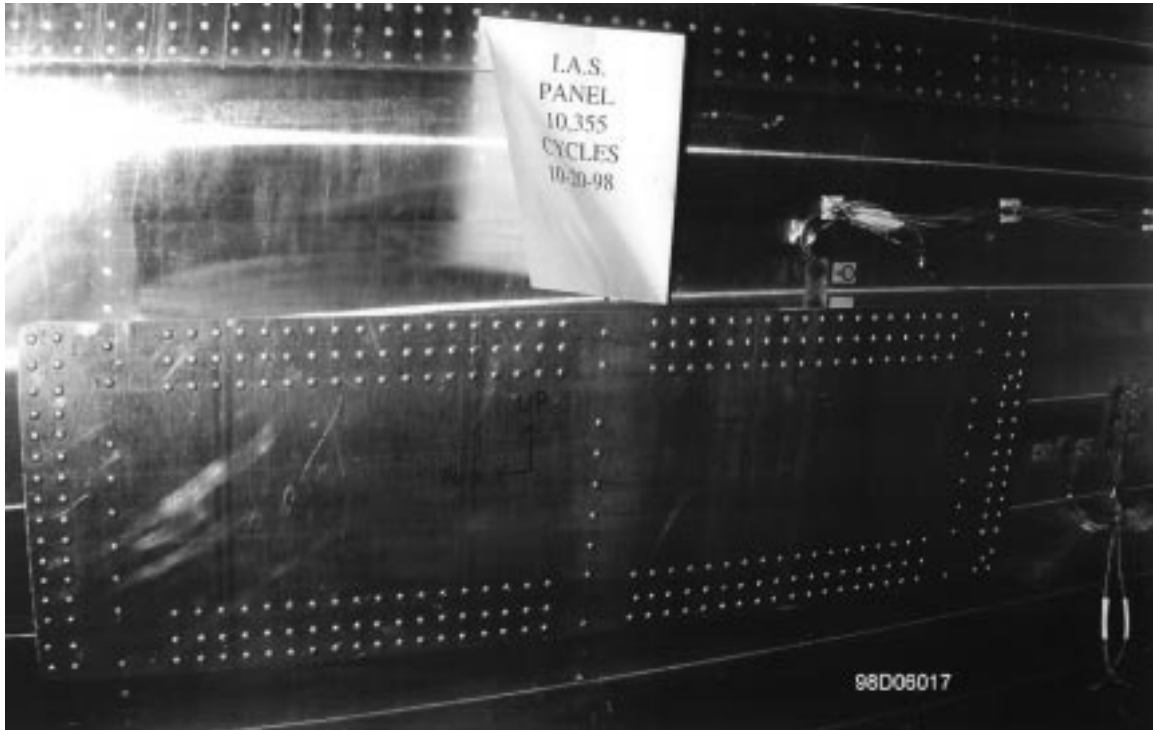
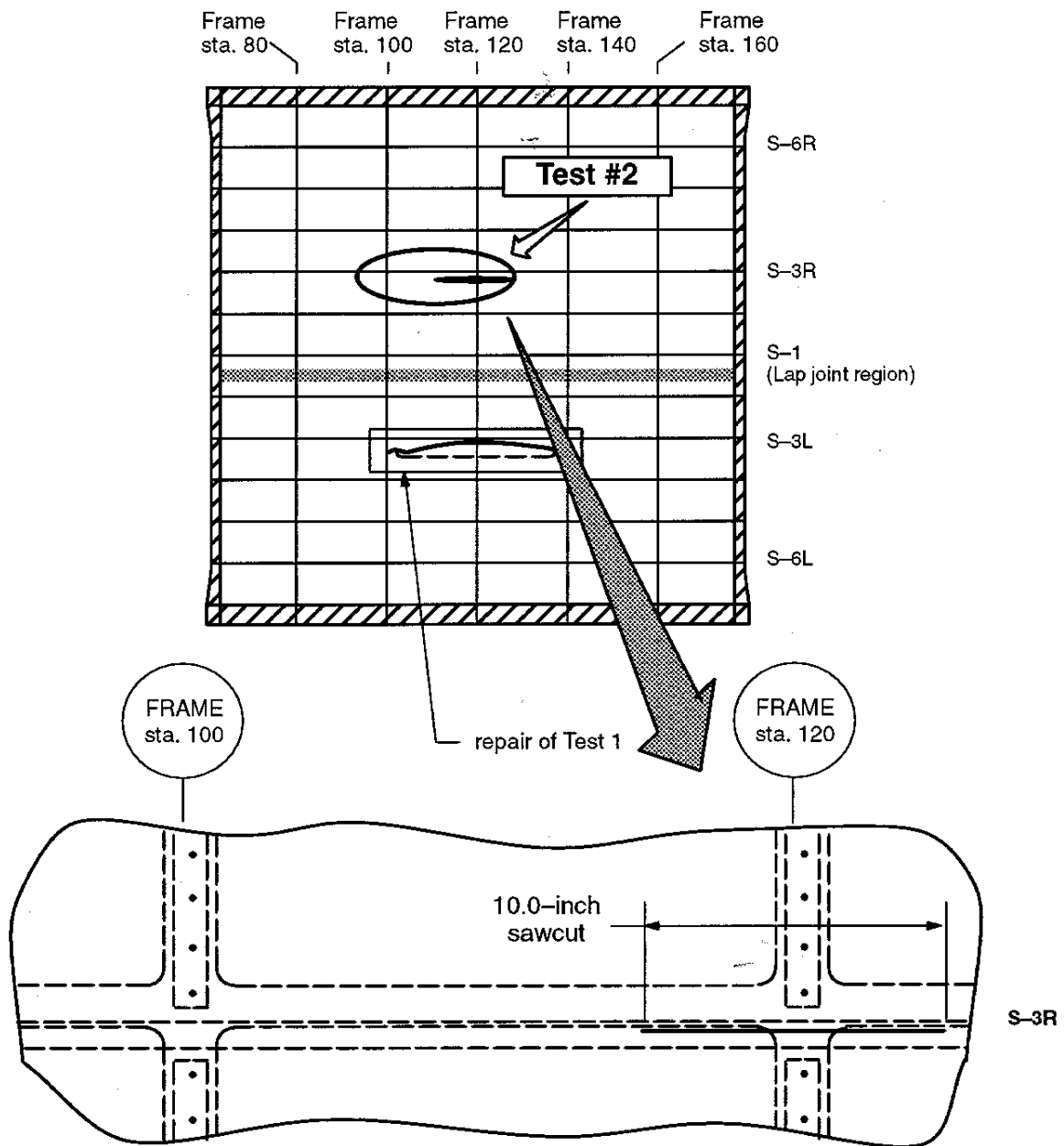


FIGURE 5-14. IAS PANEL, REPAIR OF TEST 1 LOCATION AT 10,355 CYCLES

5.4.5 Test 2—Summary

Unlike Test 1, Test 2 was conducted with the central frame severed. This testing consisted mainly of a residual strength test. However, a few pressure cycles were applied in order to generate some limited crack growth data from 10 inches with the central frame severed. The test was conducted at stringer S-3R, and centered in the panel (see Figure 5-15 and Figure 5-16).



Notes:

- 10-inch sawcut centered longitudinally on sta. 120 skin pad and circumferentially 0.15 inch below or to the left of the web of S-3R.

FIGURE 5-15. INITIAL SAWCUT DETAILS FOR TEST 2



FIGURE 5-16. IAS PANEL, 10-INCH SAWCUT AT TEST 2 LOCATION

The crack was later extended to 18 inches where, after a few cycles, it dynamically grew but arrested at the frame pads at a length of 38 inches.

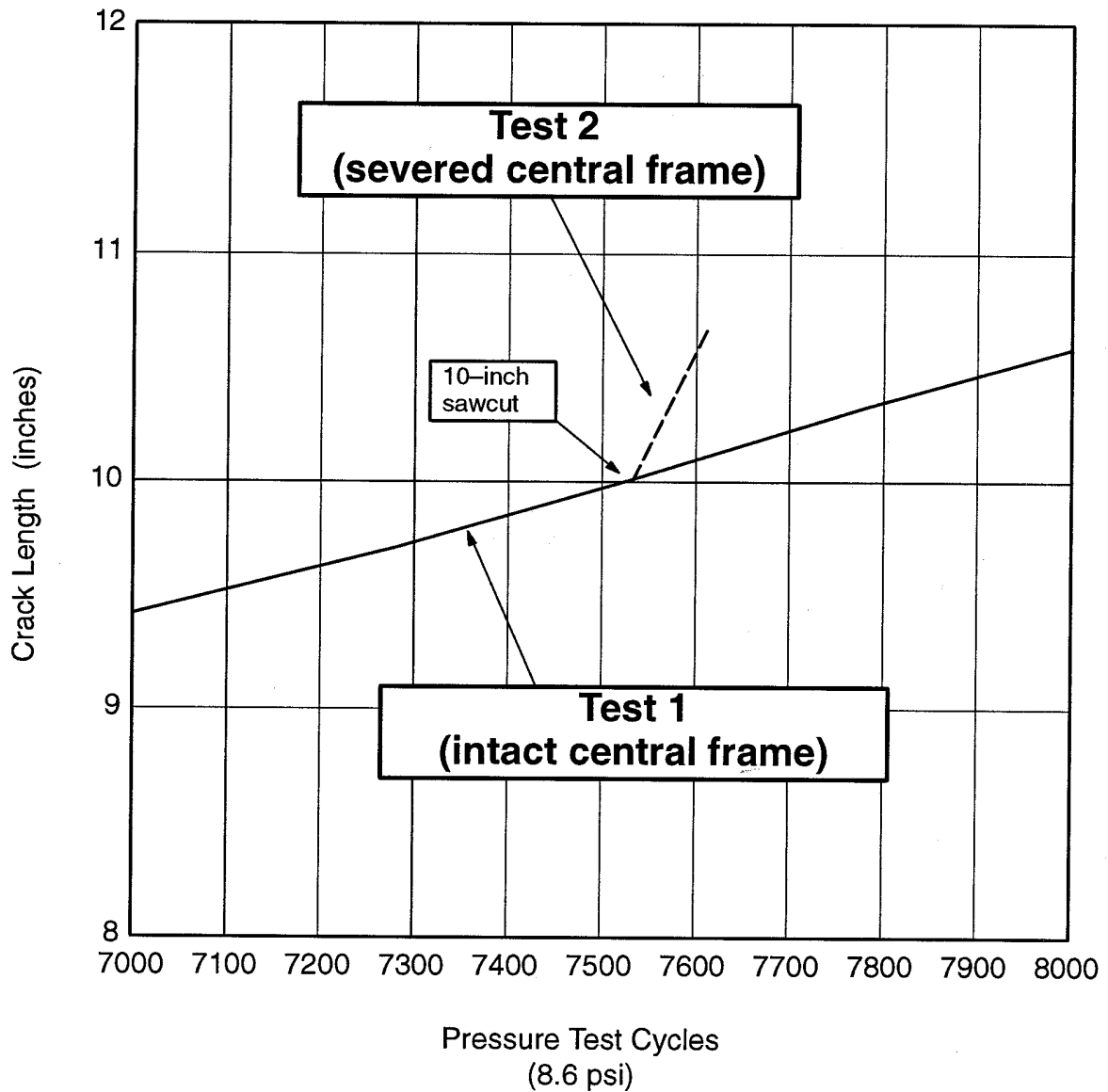
The residual strength test was conducted after small sawcuts were made emanating from the shear tie fastener holes. At 9.89 psi, the 38-inch crack dynamically ran to the edge of the panel, and the panel failed catastrophically.

Instrumentation details and strain gage readings for Test 2 are included in Appendix F.

5.4.6 Test 2—Crack Growth Results

Limited crack growth cycling was conducted at the location of Test 2. A 10-inch initial sawcut was made in the skin, and the central frame was severed.

The crack length versus pressure cycles plot is provided in Figure 5-17. It shows the growth from the initial 10-inch sawcut in contrast to the Test 1 crack growth data in the range of 10 inches. As expected, the change in rate is significant between the intact and severed central frame test. Table 5-2 contains the limited crack growth data from Test 2.



(after 10-inch sawcut installed for Test 2)

FIGURE 5-17. CRACK GROWTH HISTORY OF TEST 2

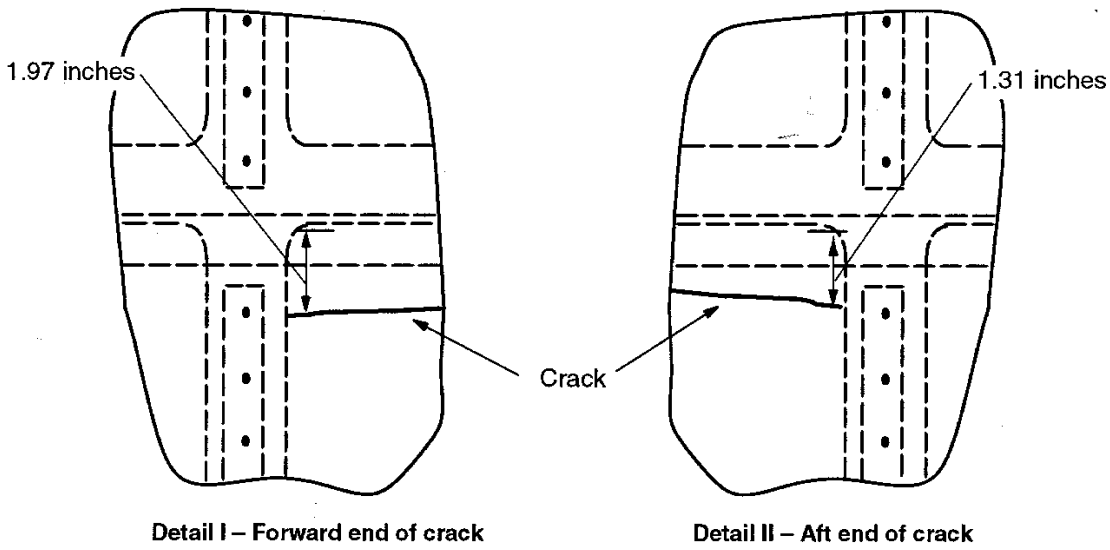
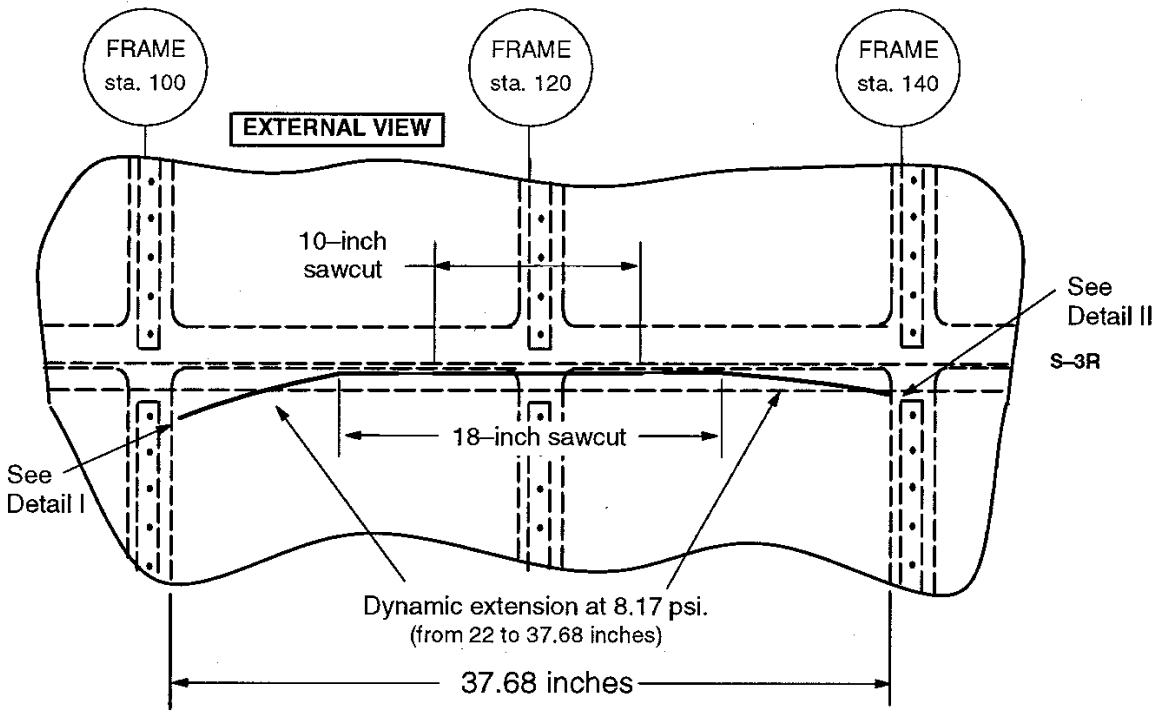


FIGURE 5-18. CRACK GROWTH TRAJECTORY OF TEST 2

TABLE 5-2. TEST RECORD OF CRACK LENGTH MEASUREMENTS FROM TEST 2

Test Cycle Number	Panel Cycle Number	Length of New Growth (inch)	Total (X) Dimension (inch)		Total (Y) Dimension (inch)		Total Crack Length (inch)
			Fwd Tip	Aft Tip	Fwd Tip	Aft Tip	
–	0	Intact	0	0	0	0	0
0	10355	Sawcut installed 10.00	–	–	–	–	10.00
80	10435	0.67	0.35	0.32	0.09	0.08	10.67
80	10438	Sawcut installed 18	–	–	–	–	18.00
9	10444	19.68	10.23	9.45	1.97	1.31	37.68

The crack was then extended to 18 inches with the intention of growing the crack cyclically to a length of 20 inches, at which the residual strength test would be conducted. However, upon cycling, at 8.17 psi and an estimated length of 22 inches, the crack dynamically ran out to a total length of 37.68 inches or approximately skin pad-to-skin pad (see Figure 5-18).

5.4.7 Test 2—Residual Strength Results

The residual strength test consisted of increasing the internal pressure until dynamic crack extension occurred. Events during the test were witnessed and recorded on videotape.

In an effort to avoid duplicating the performance of Test 1, in which the crack arrested in the shear tie fastener holes, small sawcuts, 0.05 inch long, were introduced emanating from the shear tie fastener holes (see Figure 5-19). The fasteners were removed to install these small sawcuts, then reinstalled after the sawcuts were made.

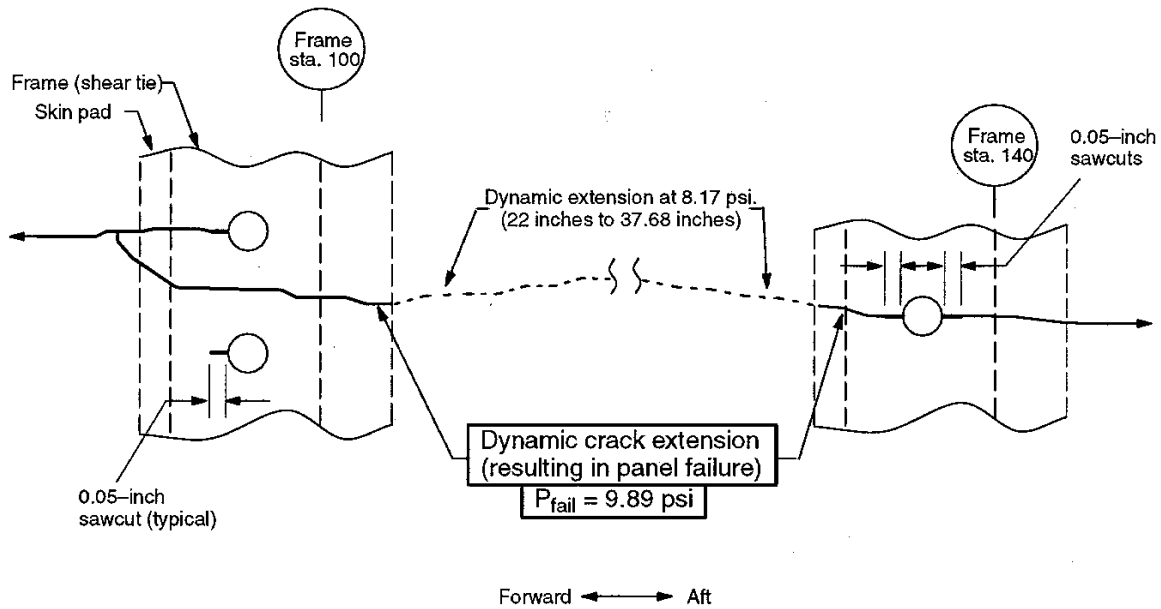


FIGURE 5-19. RESIDUAL STRENGTH CRACK CONFIGURATION OF TEST 2

The pressure was steadily increased at a rate of approximately 0.2 psi per minute. As the pressure was increased to 9.89 psi, the aft tip dynamically ran into, and out of, the shear tie fastener hole at frame station 140. The forward tip missed the shear tie fastener hole at frame station 100. The crack continued to extend dynamically to the panel edges, and catastrophically failed the panel. The test fixture suffered little damage due to the fused connection between the test panel and fixture. The dynamic crack trajectory is illustrated in Figure 5-20.

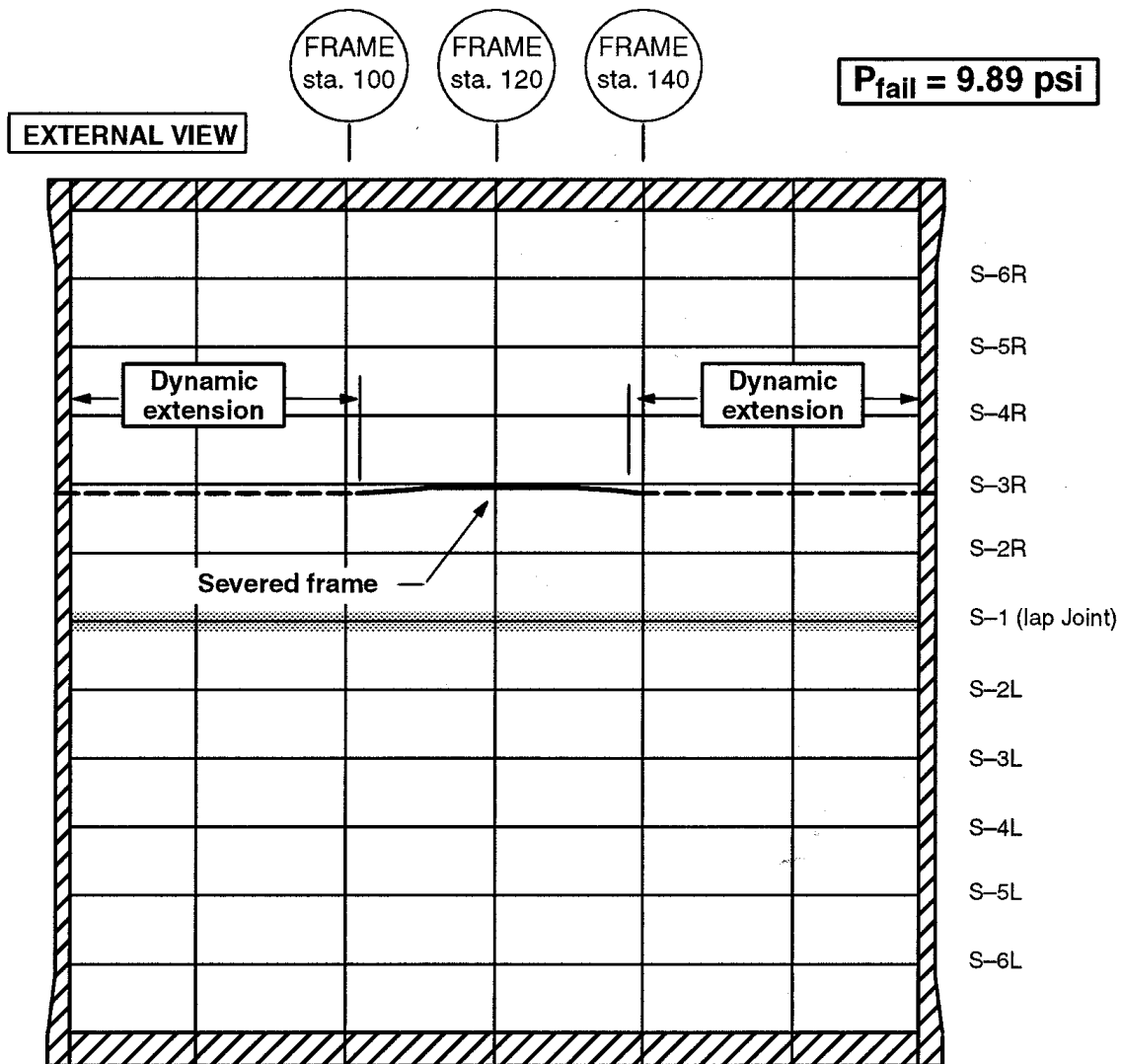


FIGURE 5-20. DYNAMIC PANEL FAILURE—TEST 2

5.5 Conclusions and Recommendations

The two-bay longitudinal crack panel test conducted on the IAS panel consisted of crack growth and residual strength testing. The crack growth and residual strength performance of the IAS panel was compared to built-up 2024 lap joint pressure panels tested by Boeing (Reference 6-1), which were tested under similar loading conditions. The comparisons that follow are unfortunately not head-to-head, because the built-up panel tests were conducted in the upper row of a lap joint, a location where load transfer and fastener hole net area reduction issues are involved.

Testing yielded the following general results:

- The total crack growth life of the IAS panel proved to be approximately three times longer than the built-up lap joint panels discussed in Reference 6-1. It should be noted that this trend between 7475 and 2024 material is experienced for large cracks growing at higher rates, in this case cracks growing from 5 to 38 inches. This trend, however, reverses for small cracks less than 5 inches, for which cracks in 2024 material grow at a lower rate than 7475. This is very relevant since the short crack region is typically targeted for crack detection opportunities on an airplane.
- No crack turning of significance was witnessed in either of the two tests conducted. The crack did deviate from the horizontal direction slightly under both cyclic propagation and dynamic extension. Surprisingly, the broken frame test showed no increased tendency of the crack to turn from the horizontal direction.
- The IAS panel demonstrated residual strength capability that was approximately 3% higher than the lap joint regions discussed in Reference 6-1.
- The IAS panel did not hold the typical limit pressure of a wide-body airplane having a two-bay crack with a severed central frame in the basic structure.

6 Longitudinal Two-Bay Analysis and Correlation

6.1 Summary

6.1.1 Deliverable

Analysis of test results and documentation for the tests of coupons and subcomponent panels called for in the test plan. (This work is associated with NASA SOW deliverable 3.7.)

6.1.2 Purpose

The panel analysis was performed to predict if the two-bay longitudinal crack panel configuration can hold a two-bay crack at the same pressure as built-up panels previously tested at Boeing Seattle. Also, panel analysis and actual test results were compared, to determine how accurately the selected analysis methods predicted actual structural behavior.

6.1.3 Summary of Results

A finite element model was generated to analyze the Integral Airframe Structure (IAS) program two-bay longitudinal crack panel. The model was sized at 15 stringer bays by 3 1/2 frame bays. Stress intensity factors determined from the analysis results for a crack centered on a broken frame were used to predict:

- The crack growth life for a crack growing from 5 to 38 inches total length
- The failure pressure for the panel containing a 38-inch crack

Because it represents the most critical case, the analysis assumed a straight crack, growing along a stringer and through the frame mouse-hole.

The residual strength prediction made from initial results provided the information required for the decision to build the IAS panel skin and stringers out of 7475-T7351 aluminum instead of 7050-T7351 aluminum.

The predicted skin stresses generally compared very well with corresponding test results in both magnitude and trend. However, stringer and frame stresses were typically not predicted as reliably.

The crack growth prediction using handbook crack growth rate data correlated surprisingly well with the test results. However, handbook crack growth data includes only lower stress intensity factors, while it is important to develop crack growth rate data at higher stress intensity factors. This importance was highlighted by the quality of the handbook data at the stress intensity factor levels reached in the panel test, and the sensitivity of the predicted results to the data.

A comparison of test and analysis results for the 7475-T7351 panel to predictions made for a panel made out of 2024-T3 aluminum shows that the 7475 panel would have a longer life than the 2024 panel by a factor of two for the crack lengths investigated in this program (5 to 38 inches). The 2024 panel would outperform the 7475 panel at shorter crack lengths.

The residual strength analysis results indicate that the skin was the most critical element for the two-bay crack scenario, because the rivets and frames did not pick up significant load from the skin until after the skin crack was predicted to extend dynamically. This was partly confirmed by the test results, by comparing predicted and test stresses in the frame and noting that none of the frames failed statically during testing. The failure pressure prediction for the two-bay crack case under-predicted the test results by less than 6%. The analysis, however, over-predicted the test results for a 22-inch crack centered on a broken frame by 17%. These predictions were performed with fracture data obtained from the 7475-T7651 material instead of 7475-T7351 material.

The analysis methods used to predict the IAS two-bay crack panel's behavior have been used at Boeing Seattle previously to model built-up structure. These methods are typically too time-consuming to be used in a design environment and would only be useful in analyzing the final configuration. Northrop Grumman investigated a simpler analytical approach to optimizing the IAS panel. The method and results of these analyses are provided in Appendix G.

Finally, crack growth and residual strength predictions need to be performed using material data obtained from the 7475-T7351 plates used in this program, once this data is developed from future planned NASA testing. These predictions would allow for the determination of the true accuracy of the analysis methods, without the influence of material variability.

6.2 Preliminary Analysis and Panel Design Modifications

The performance goal of the two-bay longitudinal crack test was for the integral panel to hold 9.4 psi with a two-bay crack and a broken central frame. This is the pressure held by the built-up pressure panels tested by Boeing Seattle (see Reference 6-1) under similar loading conditions. There were differences between the built-up and integral panel that make the comparison of results not quite head-to-head. One big difference was the fact that the built-up panel's crack was put in the lap joint, while the crack in the integral panel was in a typical bay. However, the Reference 6-1 data was public domain and provided a baseline to work with.

The initial design of the two-bay longitudinal crack panel called for the skin and stringers to be machined from 7050 aluminum plate. However, this material has low toughness properties in the orientation associated with a longitudinal crack in a fuselage (T-L). IAS team members were concerned about whether a panel made from 7050 material would be able to hold the required 9.4 psi.

To investigate these concerns, Boeing Seattle performed an analysis of an integral skin-stringer fuselage panel, to determine its residual strength capability with a two-bay longitudinal crack centered on a broken frame. Analysis results confirmed that the panel would not be capable of holding the required pressure.

Therefore, to improve the residual strength capability of the two-bay longitudinal test panel, the skin-stringer material was changed to 7475-T7351 plate. The panel was also redesigned to be more comparable to the referenced built-up panels, in terms of weight and static strength capability. Analysis of the revised panel for the two-bay crack scenario showed that 9.4 psi was achievable.

6.3 Modeling Assumptions

6.3.1 Test Fixture

Section 5 describes the test fixture, test panels, and test results. The test fixture was a general wide-body fuselage structure that had been thickened by approximately 75% to achieve a design life goal of one million pressure cycles. The test panel had dimensions more typical of fuselage crown structure. For this study, the test fixture was not included in the analysis; instead, a smaller, more detailed test panel model was developed. A disadvantage of this strategy was that the effect of the test fixture on the test panel was not modeled.

6.3.2 Model Elements and Dimensions

The scope of the analysis was limited to modeling the major structure of the test panel—the skins, stringers, and frames. Elements were included to model the load transfer at fasteners connecting the frames to the skin; however, local effects such as fastener holes and fillet radii were not modeled. Also, the actual test panel contained a lap joint adjacent to the central panel stringer, which was at least one and one-half bays away from the crack locations. This joint was assumed to not have an effect on the crack, so it was not included in the model. The structural configuration of the skin, stringer, and frame are shown in Figure 6-1. Figure 6-2 gives the dimensions of the structural elements.

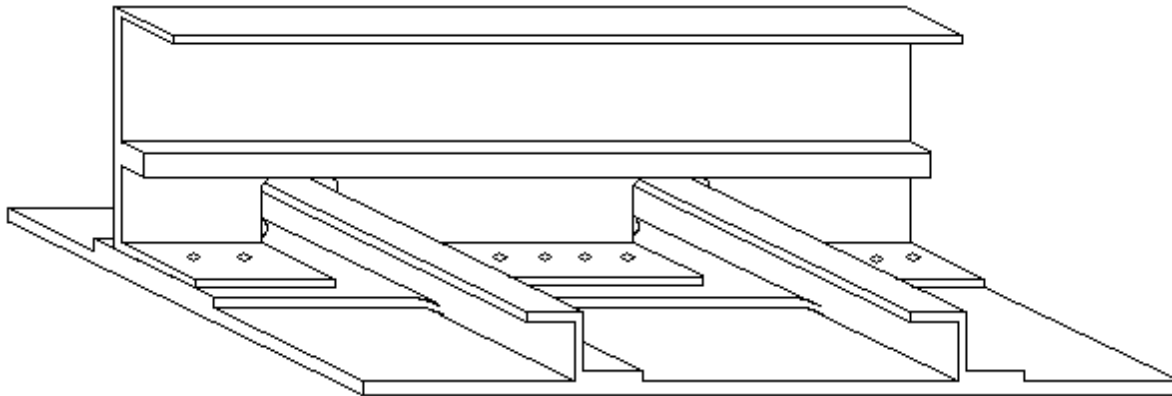


FIGURE 6-1. PANEL STRUCTURAL CONFIGURATION

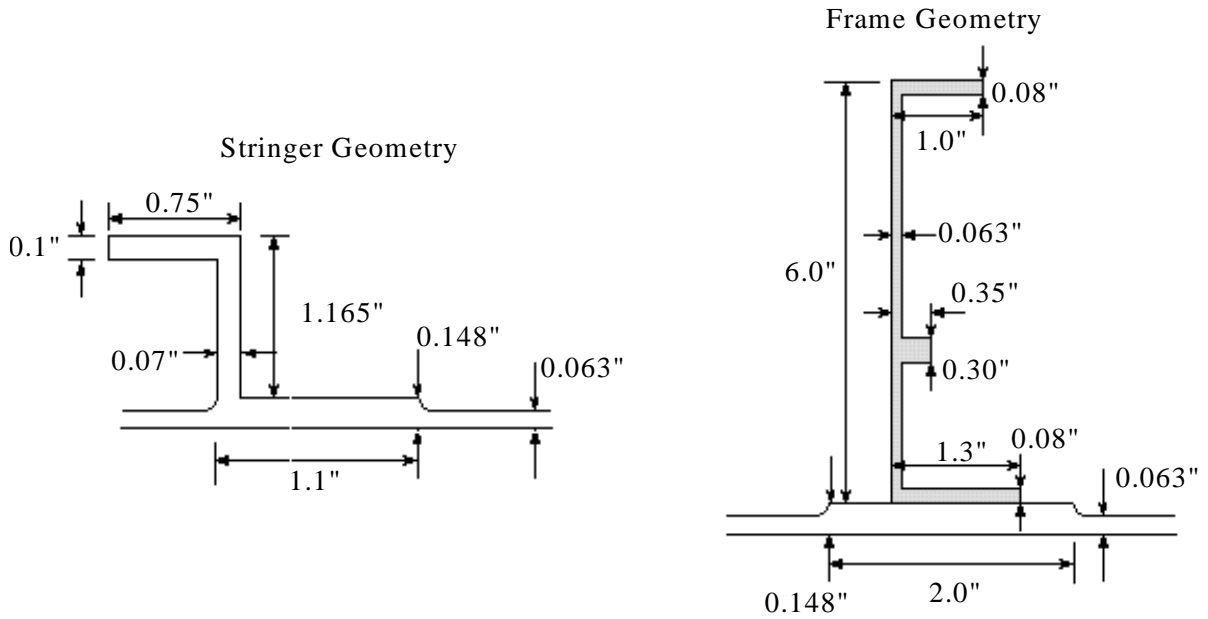


FIGURE 6-2. SKIN, STRINGER, AND FRAME DIMENSIONS

Figure 6-3 and Figure 6-4 show the skin and frame/stringer meshes. The model was 15 stringer bays wide ($\theta=62.6^\circ$) by $3\frac{1}{2}$ frame bays long ($z=70$ inch). Only the 6 stringer bays in the middle of the panel were modeled in detail. To reduce the model's size, the remaining stringer bays were coarsely meshed. Extending the model beyond 6 stringer bays was necessary to reduce boundary effects when analyzing the panel containing large damage. Significant interactions would have occurred if extensive damage was too close to a boundary, because symmetrical boundary conditions were used along all model boundaries; this implied that all damage was mirrored across the boundaries.

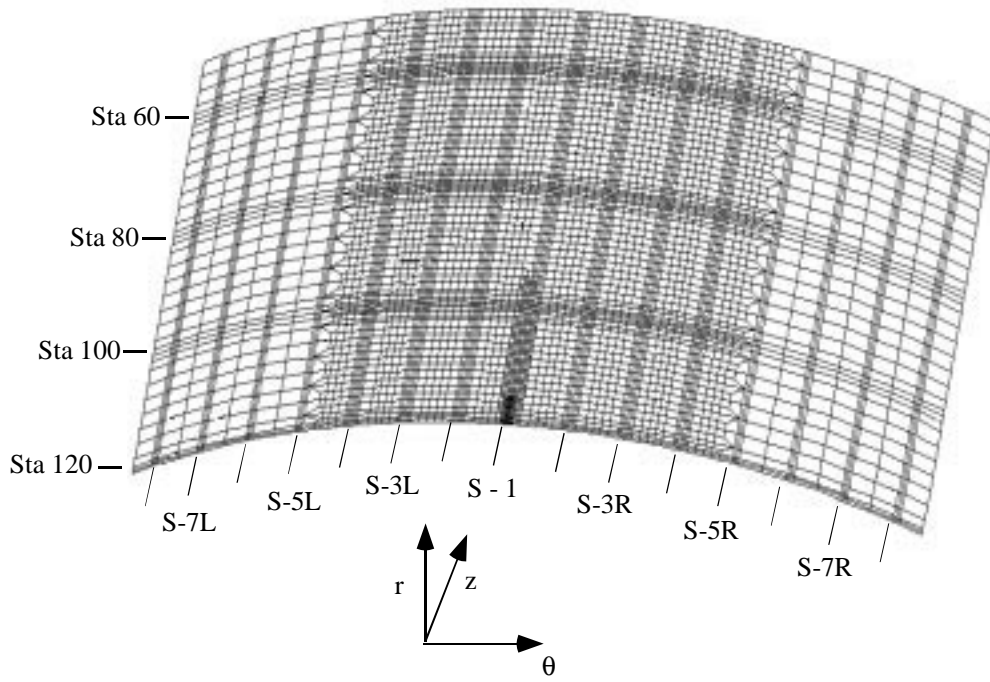


FIGURE 6-3. SKIN MESH

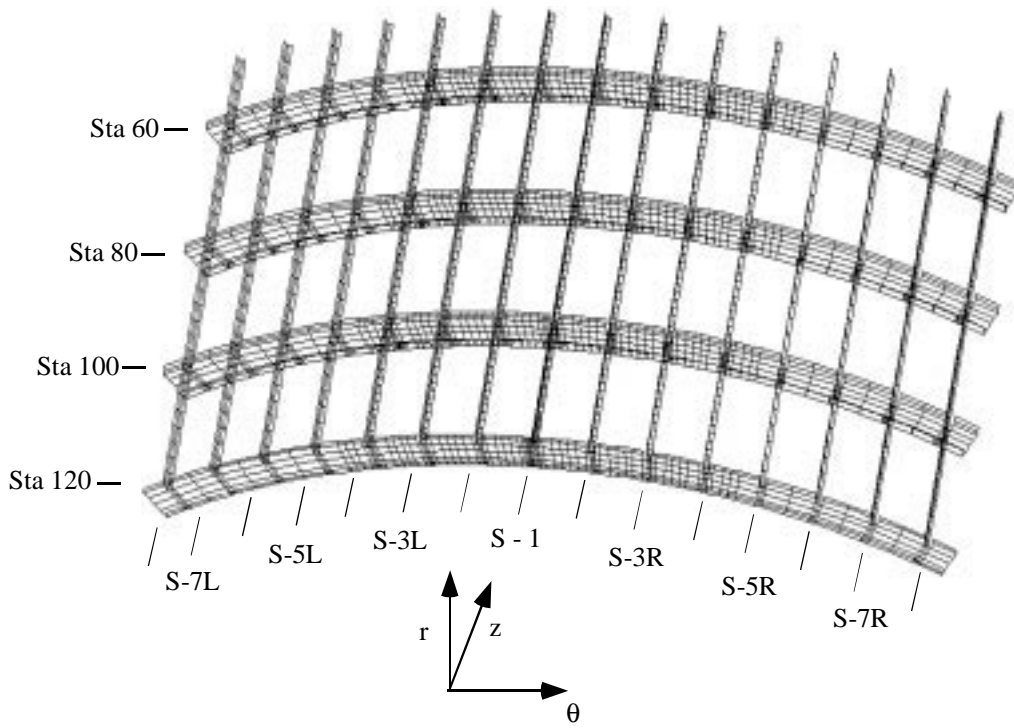


FIGURE 6-4. FRAME AND STRINGER MESH

6.3.3 Crack Location and Boundary Conditions

The longitudinal crack was introduced in the model along stringer S-1, centered on frame station 120. The crack was assumed to grow in a straight line and extend through the cut-out (or mouse-hole) in the frame used for passage of the continuous stringer. This scenario represented a more critical case than allowing the crack to pass between rivets in the frame-to-skin connection, since the frame, in this condition, would be better able to transfer load around the skin crack.

Symmetry boundary conditions were used to reduce the model's size. Displacement u_z and rotations ϕ_r and ϕ_θ for the skin and stringer nodes along the central frame location (station 120) were restrained, which made it possible to model only half of the panel and crack in the longitudinal (z) direction. This decision created a problem, because the frames were not symmetric, and early analyses demonstrated that restraining the central frame using symmetry boundary conditions made the frame too stiff. Therefore, the central frame was allowed to displace freely, but its area was reduced by a factor of two. This allowed the central frame to develop similar displacements and stresses as compared to the other frames for the intact case.

Symmetrical boundary conditions were also applied to all nodes at the other three edges of the model. Displacement u_θ and rotations ϕ_r and ϕ_z were fixed along boundaries running parallel to the stringers. Rotations ϕ_r and ϕ_θ were fixed, and displacement u_z was constrained to be constant for all nodes along station 50. A force per unit length of $\frac{p R}{2}$, where p is the applied pressure and R is the panel displacement, was applied to the station 50 edge to represent a pressure-loaded cylinder with capped ends. Hence, a load of

$(15 \text{ bays}) \cdot \left[(9.25 \text{ inches}) \frac{p R}{2} \right]$ was applied in the z direction to a node at station 50. An outward pressure load, p, was applied to all skin elements.

6.3.4 Elements and Material Properties

All models were solved using the ABAQUS finite element software. In the model, the skin, stringers, and frames were modeled with four-noded shell elements with six degrees of freedom per node (ABAQUS element S4R). The rivets attaching the frames to the skin were modeled using two-noded beam elements (ABAQUS element B31) with the radius set equal to the actual rivet diameter (3/16 inch).

Initial analyses were run assuming elastic properties for all elements. However, in subsequent analyses intended to predict the panel's residual strength, the frame and rivets near the crack were given elastic-plastic properties. The skins and stringers were always modeled as elastic, to facilitate calculation of stress intensity factors from the results. The material properties used for the skins, stringers, and frames in the analyses are shown in Table 6-1 and Table 6-2. Skins and stringers were given properties for 7475-T7351, while frames were given properties for 7050-T7451 plate. The elastic-plastic stress-strain relationship shown in Table 6-2 for 7050-T7451 plate was obtained from IAS static testing performed by NASA on specimen L15-2 (longitudinal grain orientation, 1.5-inch plate).

TABLE 6-1. MATERIAL ELASTIC PARAMETERS

Material	Modulus, E (Msi)	Poisson's Ratio, ν
7475-T7351 plate	10.3	.3
7050-T7451 plate	10.7	.3

TABLE 6-2. 7050-T7451 STRESS-STRAIN CURVE

Stress (ksi)	50.0	65.1	68.8	72.0	74.0	76.0	77.3	77.0
Strain (in/in)	.00467	.00683	.00909	.0215	.0320	.0455	.0607	.0808

Rivets near the crack path were modeled using a combination of six one-dimensional springs and rigid elements, to more easily introduce non-linear shear deformation (see Figure 6-5). The assumed load displacement diagram for the rivet's shear deformation is also shown in Figure 6-5. All rivet rotational and axial deformations were assumed to be linear and given a stiffness that was an order of magnitude greater than that for shear deflection.

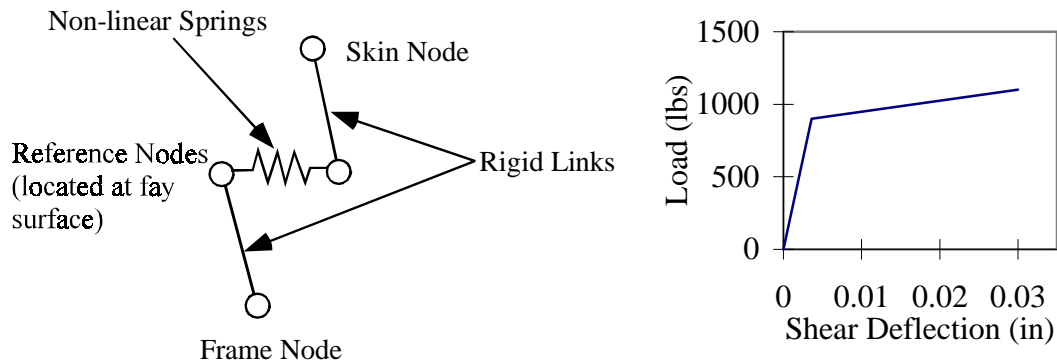


FIGURE 6-5. SCHEMATIC FOR NON-LINEAR RIVET ELEMENTS AND SHEAR DEFLECTION PROPERTIES

Both material non-linearity and geometric non-linearity were accounted for in the ABAQUS analyses. Also, the analyses were performed such that the intact model and subsequent crack analyses were solved in one run. Duplicate nodes along the crack path were held together with rigid springs during the intact analysis. Once the intact analysis was solved, the crack was introduced by removing these elements one by one and effectively growing the crack. Nodal displacements and the element force holding the crack-tip nodes together were printed out after each element was removed. Stress intensity factors were then calculated at each step using the force and displacement information from the model and the energy release rate methods described in Reference 6-2.

6.4 Analysis Results

6.4.1 Skin Deformation

Figure 6-6 shows the displaced shape of the skin mesh for the intact test panel with an applied pressure of 8.6 psi, which was the cyclic pressure used to grow the crack during testing. In this figure, the magnification factor on the displacements is high enough to see skin bulging between frame and stringer locations. Figure 6-7 shows the displaced shape of the mesh containing a 38-inch crack and an applied pressure of 8.6 psi. In this figure, the local bulging of the skin around the crack is much more significant than the bulging in the other parts of the panel.



**FIGURE 6-6. DISPLACED INTACT SKIN MESH, INTERNAL PRESSURE = 8.6 PSI,
MAGNIFICATION FACTOR = 100X**

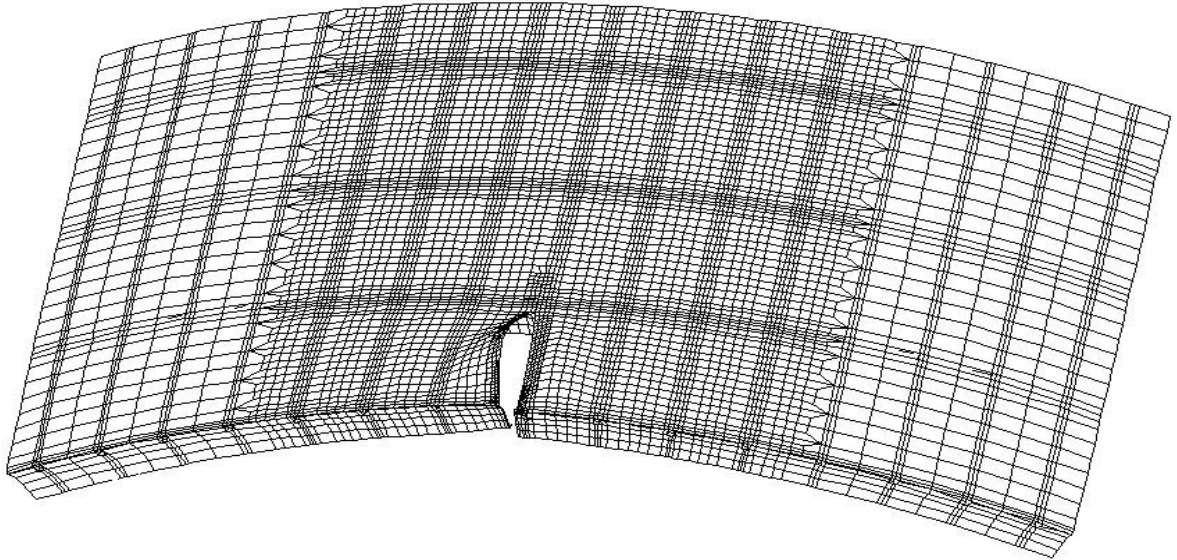


FIGURE 6-7. DISPLACED MESH WITH A 38-INCH CRACK, INTERNAL PRESSURE = 8.6 PSI, MAGNIFICATION FACTOR = 10X

6.4.2 Stress Intensity Factors

A total stress intensity factor representing the total strain energy release rate was used to make crack growth and residual strength predictions. Figure 6-8 contains a plot of the total stress intensity factors versus crack length for both an intact and broken central frame. Results are also provided at 8.6 and 9.4 psi for the broken frame case. The stress intensity curves for an applied pressure of 8.6 psi were developed assuming all elastic properties. The elastic results for the intact frame at a pressure of 8.6 psi were used to predict the life for the longitudinal crack under cyclically applied pressure. Correlation of these crack growth predictions with test results is provided in the next section.

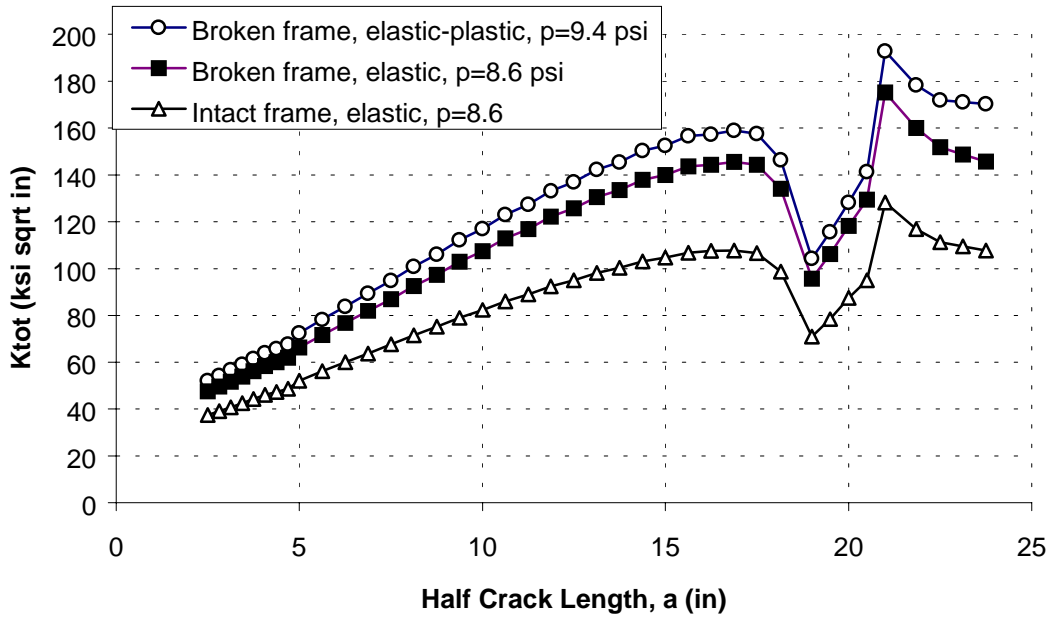


FIGURE 6-8. STRESS INTENSITY FACTORS FOR A LONGITUDINAL CRACK CENTERED ON A BROKEN FRAME

When the stress intensity curve for the 8.6 psi case is multiplied by a factor of 9.4 psi/8.6 psi, it is identical to the curve for 9.4 psi until the crack is well beyond the adjacent frame corresponding to a half crack length of 20 inches. This result indicates that the plasticity in the frames and rivets is not sufficient to affect the skin crack until it has grown past the adjacent frame. It also indicates that the frame does not work very hard (the stresses remain below yield) until the crack is larger than two bays. A review of frame stress results confirmed this conclusion.

6.4.3 Rivet Loads

The frame-to-skin attachment rivet loads for the frame adjacent to the central broken frame are shown in Figure 6-9. These forces represent shear loads transferred in the circumferential or hoop direction at an applied pressure of 9.4 psi. This pressure is equal to that determined to be critical for the skin containing a two-bay crack. All loads in the axial and longitudinal direction were small compared to the shear loads in the circumferential direction.

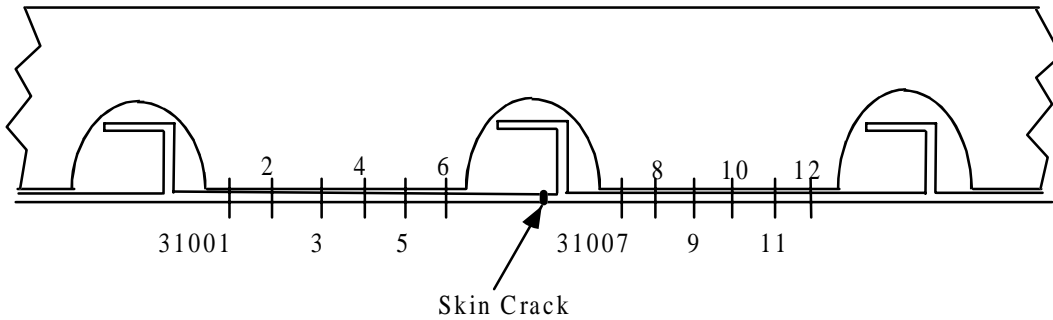
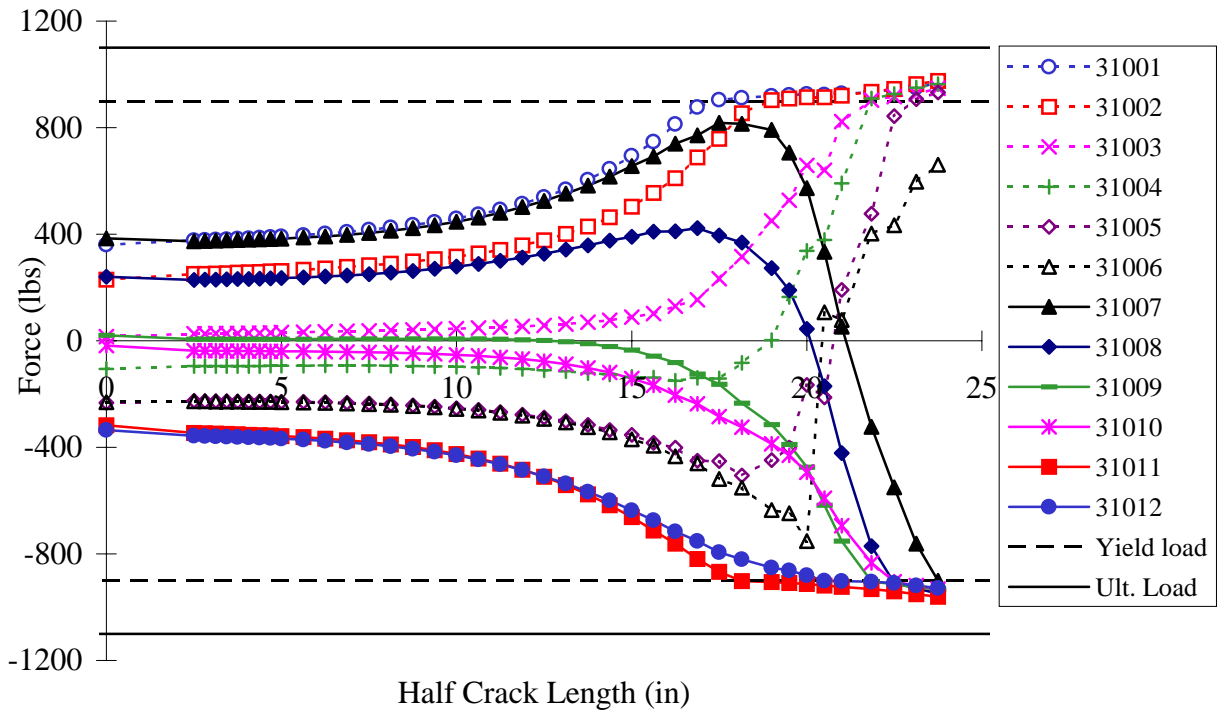


FIGURE 6-9. RIVET SHEAR LOADS AT ADJACENT FRAME LOCATION VERSUS CRACK LENGTH, APPLIED PRESSURE = 9.4PSI

The crack starts to influence the rivets when it reaches a half crack length of approximately 10 inches. Note that, as the crack approaches the frame, the direction (denoted by the sign) of the load changes for elements 31004, 31005, 31006, 31007, 31008 and 31009. For no-crack or small-crack cases, the rivets mainly transfer load in and out of the frame to get the load around the cut-outs (or mouse-holes) in the frame. As the crack grows larger, the rivets work in the same direction to shear load into the frame and around the skin crack. Also, once a fastener reaches the yield load, it does not continue to pick up more load. Therefore, the fasteners were not expected to be the critical element in the panel test.

6.4.4 Residual Strength

Examination of the analytical frame stresses and rivet loads at the predicted skin failure pressure showed that the frames and rivets were not critical. Therefore, predictions of panel residual strength containing a two-bay longitudinal crack with a broken central frame were made assuming the crack in the skin was the critical element. The calculation of when the skin crack became unstable and extended dynamically was performed by finding the tangency point between the stress intensity curves for the broken central frame case in Figure 6-8, and an R-curve for 7475-T7651 plate material found in Reference 6-3. Residual strength data for 7475-T7351 data was not available at the time the analysis was performed, so it was assumed that 7475-T7651 R-curve data would reasonably approximate -T7351 data.

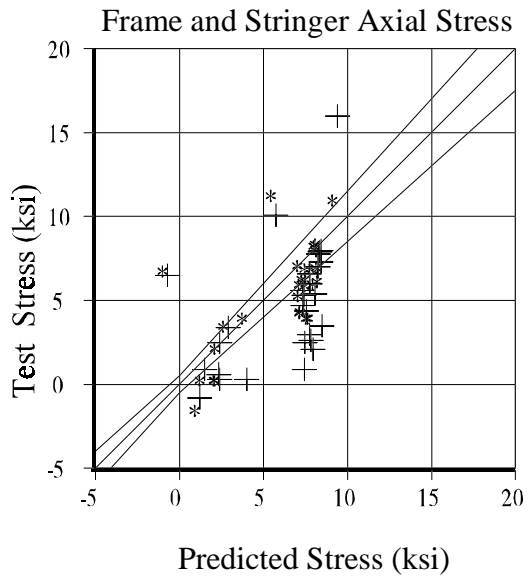
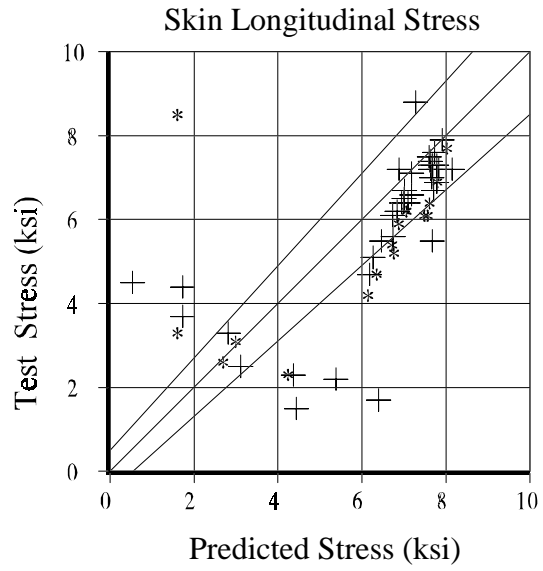
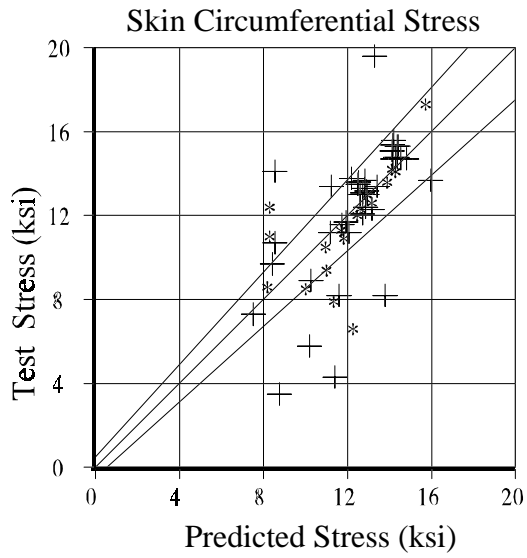
The elastic model results were used to initially assess the panel's residual strength containing a crack. After an approximate failure pressure was determined using the elastic results, elastic-plastic properties were added to the model, and the analysis was re-run at the estimated failure pressure. This iterative approach was determined to be unnecessary, as the frames and rivets had little plasticity at the point where the skin crack became critical. The predicted failure pressure for a 38-inch straight crack centered on a broken central frame was 9.4 psi.

6.5 Test and Analysis Correlation

6.5.1 Strain Gage Stress Comparisons

Stresses at each gage location were taken from the analysis results to make comparisons with the test gage results. The location of the gages on the test panel did not typically correspond to a nodal location in the model. For skin gages, the stresses were calculated by taking stresses in the model at the six closest nodes to the gage, and performing a least-squares estimation of the stress at the gage location. The mesh for the stringers and frames was not refined enough to perform the same type of estimation, so the stress from the closest node was used for comparison to the gage readings obtained from testing.

Figure 6-10 shows the predicted versus test stresses for an intact test panel (no sawcut). Results are given for gages located in test areas 1 and 2. Test areas 1 and 2 are defined in Section 5 and referenced here as Test 1 and Test 2, respectively. Included in each of the plots in Figure 6-10 are scatter bands that represent a 0.5 ksi stress offset plus another 10% error allowance. The circumferential stress comparisons for the skin gages show that the predictions generally fall within the scatter bands, with the outliers falling both above and below the 45-degree line that represents exact correlation. For the longitudinal skin stresses, the analysis tends to over-predict the test results; however, the majority of points still fall within the scatter bands. For the frame and stringer stresses, the comparison is not as good. The analysis typically over-predicts the test stresses for these gages. This result is not surprising, because of the refinement on the frames and stringers and the fact that many of the gage locations are near fastener holes and other stress concentrations not considered in the model.



+ Test area 1 gage results
 * Test area 2 gage results

FIGURE 6-10. TEST/ANALYSIS STRAIN GAGE CORRELATION FOR AN INTACT PANEL AT 8.6 PSI

For further comparison, membrane and bending stresses were calculated for locations on the test panel where gages were on both the inner and outer surfaces of a structural element. Line plots along a series of gages were then generated to show both stress values and trends at particular locations on the panel. These plots for the intact test panel are shown in Figure 6-11, Figure 6-12, and Figure 6-13. For both the circumferential and longitudinal membrane stresses, the analysis was able to predict both the trend and the magnitude of the test stresses quite well, although the longitudinal stresses tended to be over-predicted by the analysis. The difference in the results from the two different test areas was often more than the difference between the test and predicted values. Bending stresses were also predicted well, except at the station 120 and 140 pad-ups in Figure 6-11, where the test showed bending opposite than predicted. A positive bending stress in the plots corresponds to higher stress at the outer surface than the inner surface. Higher stress is typically expected on the inner surface at the pad-ups (negative bending stress), because the skin is pulled down by the frames at the pad-up and bulges outward in the middle of the bay. Therefore, the test results, which show higher stress on the outer surface of the pad-up, are not fully understood.

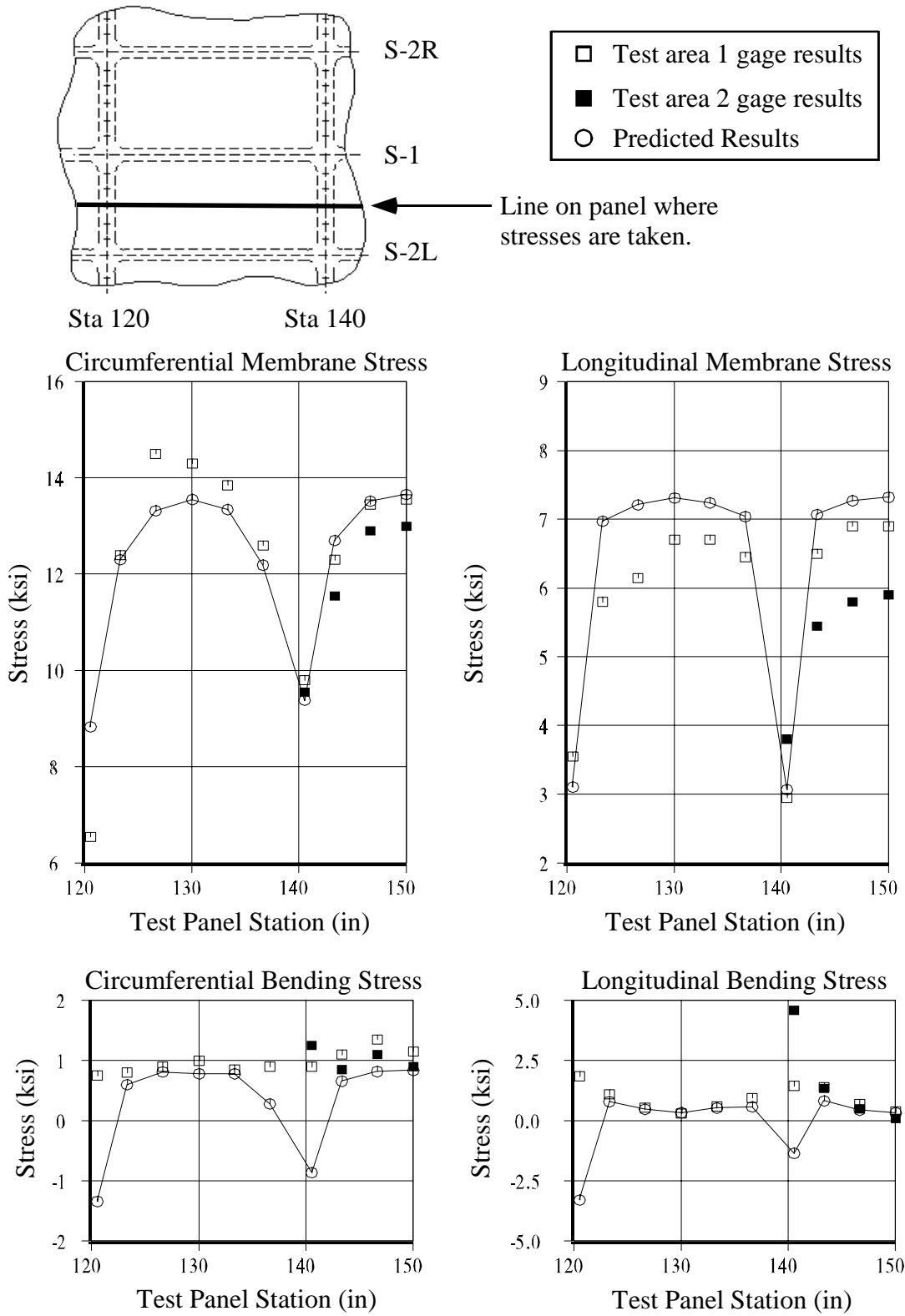


FIGURE 6-11. SKIN STRESS CORRELATION MIDWAY BETWEEN STRINGER S-1 AND S-2L FOR AN INTACT PANEL AT 8.6 PSI

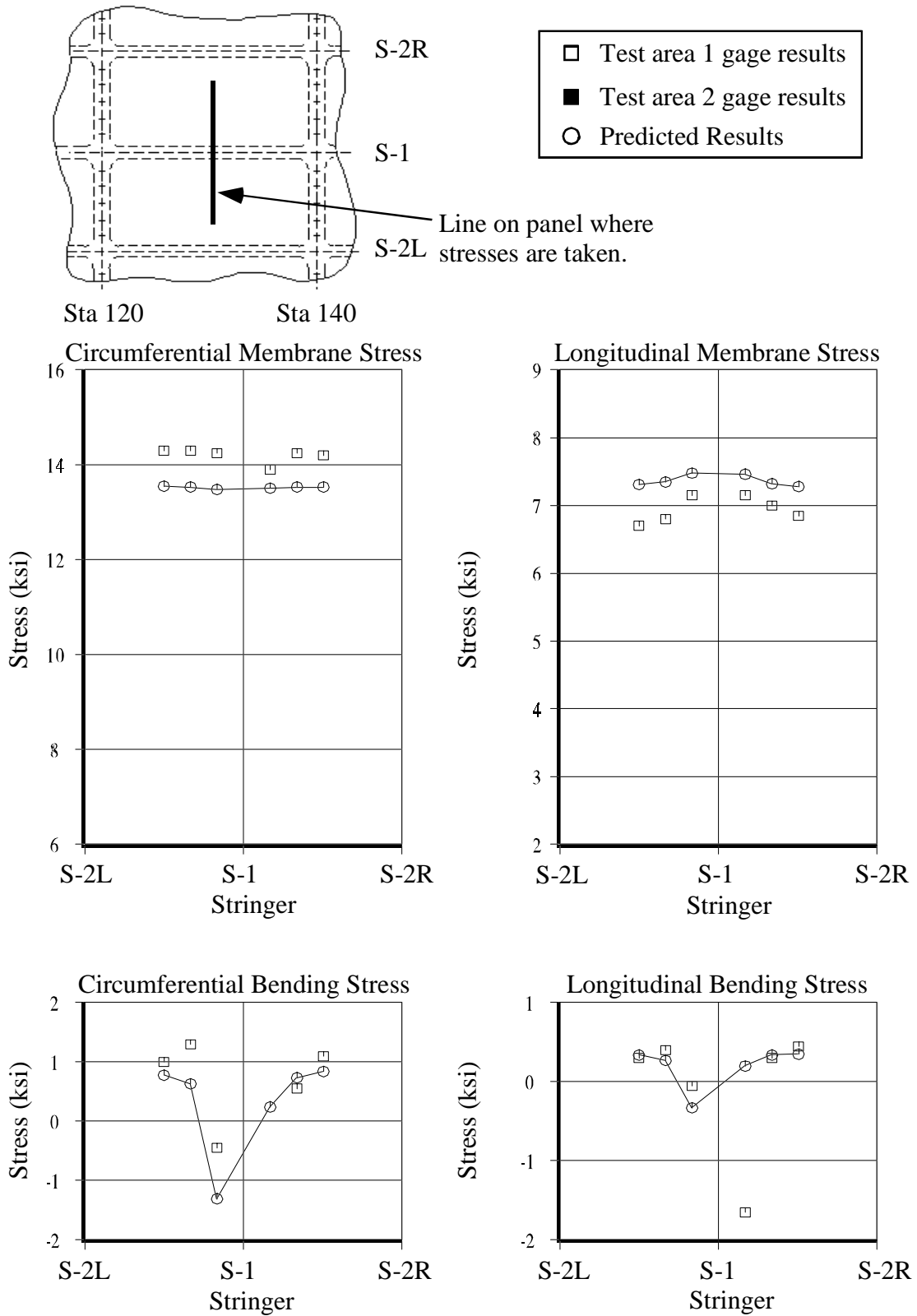


FIGURE 6-12. SKIN STRESS CORRELATION AT STATION 130 FOR AN INTACT PANEL AT 8.6 PSI

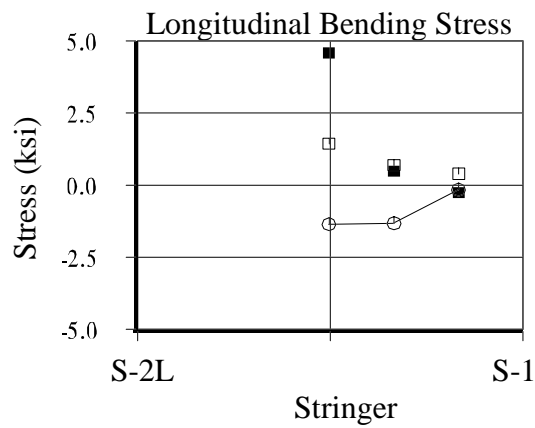
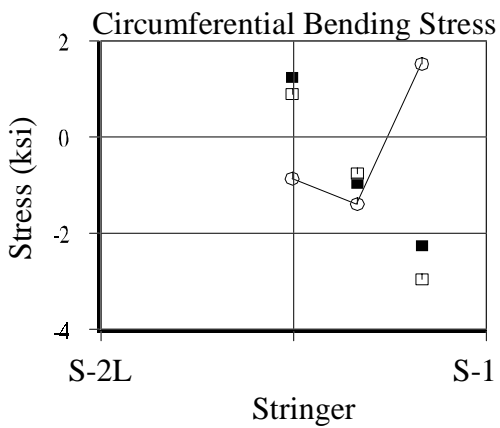
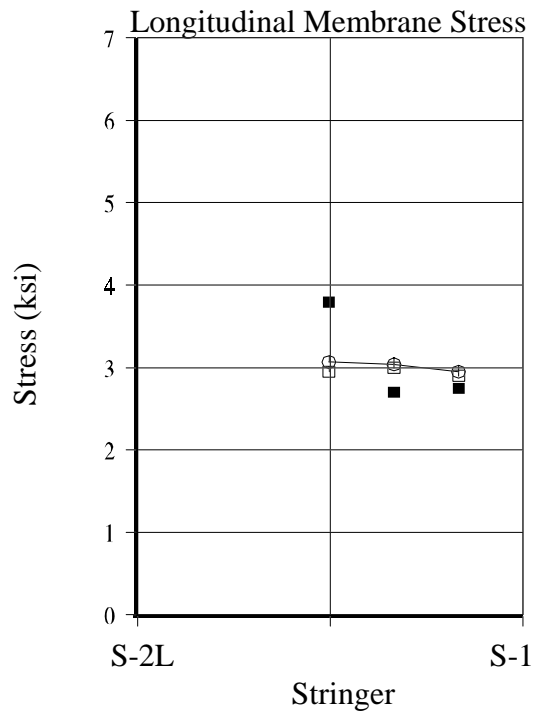
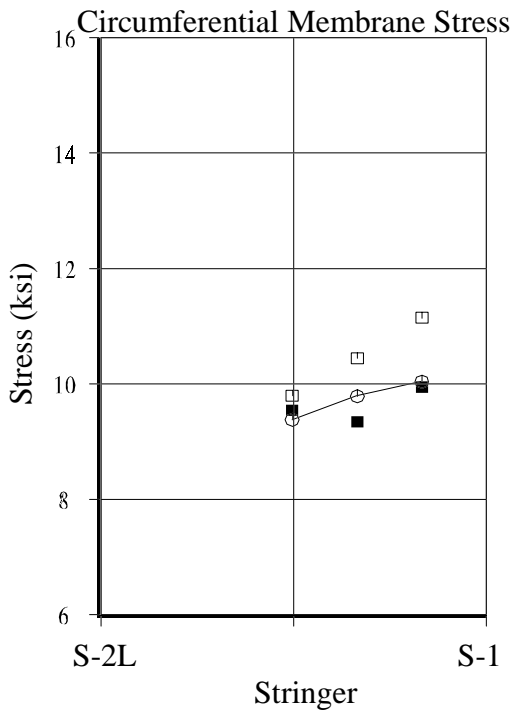
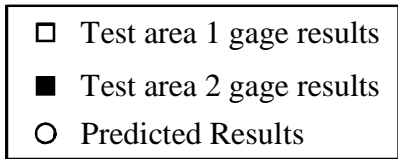
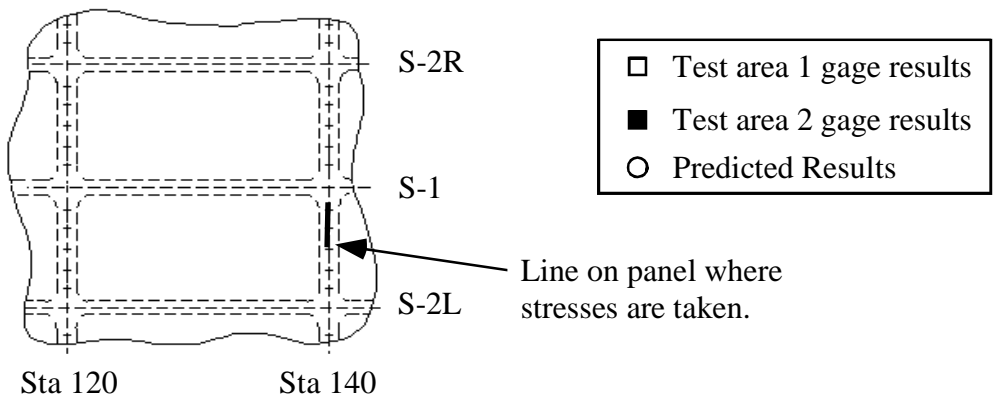


FIGURE 6-13. SKIN STRESS CORRELATION AT STATION 140 FOR AN INTACT PANEL AT 8.6 PSI

Figure 6-14, Figure 6-15, and Figure 6-16 show the corresponding line plots for the panel containing a 38-inch crack, centered on a broken frame. The stresses were taken at an applied pressure of 8.6 psi, which is about 1 psi less than the pressure needed in the tests to cause the 38-inch crack to extend dynamically. This pressure was used instead of the final failure pressure for ease in making comparisons with the intact case stresses. Also, stresses were available for comparison from both test areas, Test 1 and Test 2, since the same two-bay crack scenario was tested at both locations.

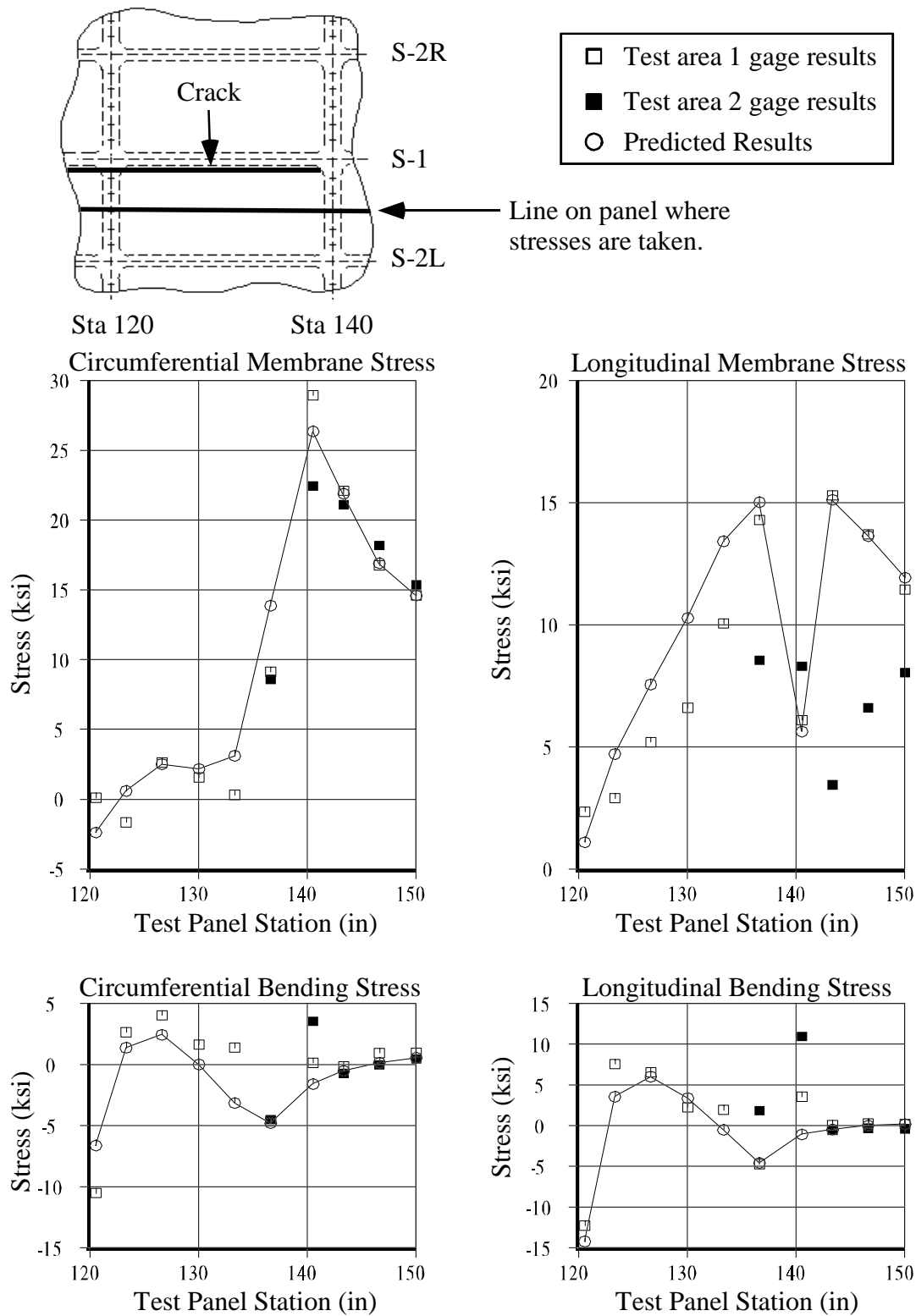


FIGURE 6-14. SKIN STRESS CORRELATION MIDWAY BETWEEN STRINGER S-1 AND S-2L FOR A PANEL CONTAINING A 38-INCH CRACK CENTERED ON A BROKEN FRAME

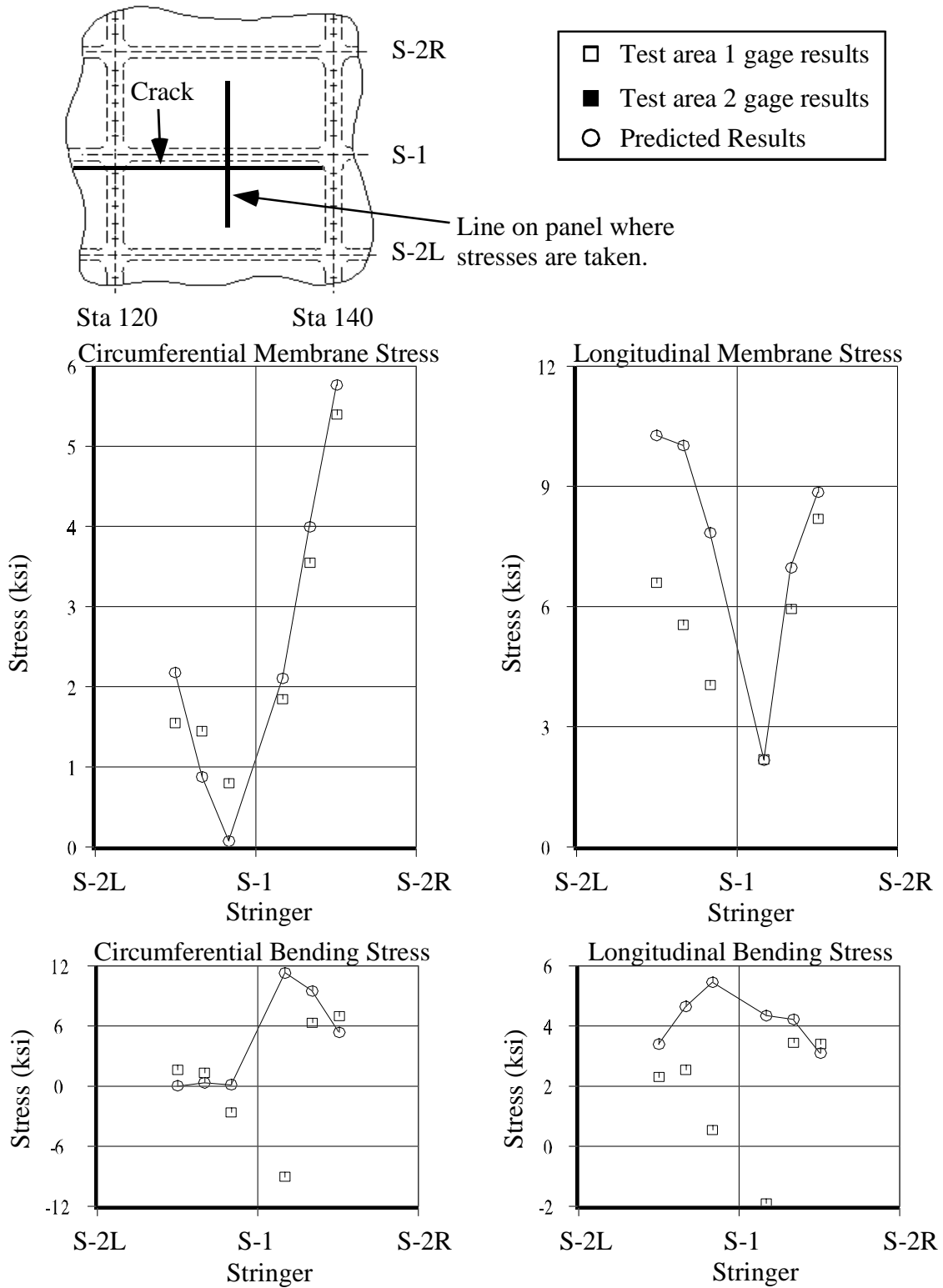


FIGURE 6-15. SKIN STRESS CORRELATION AT STATION 130 FOR A PANEL CONTAINING A 38-INCH CRACK CENTERED ON A BROKEN FRAME

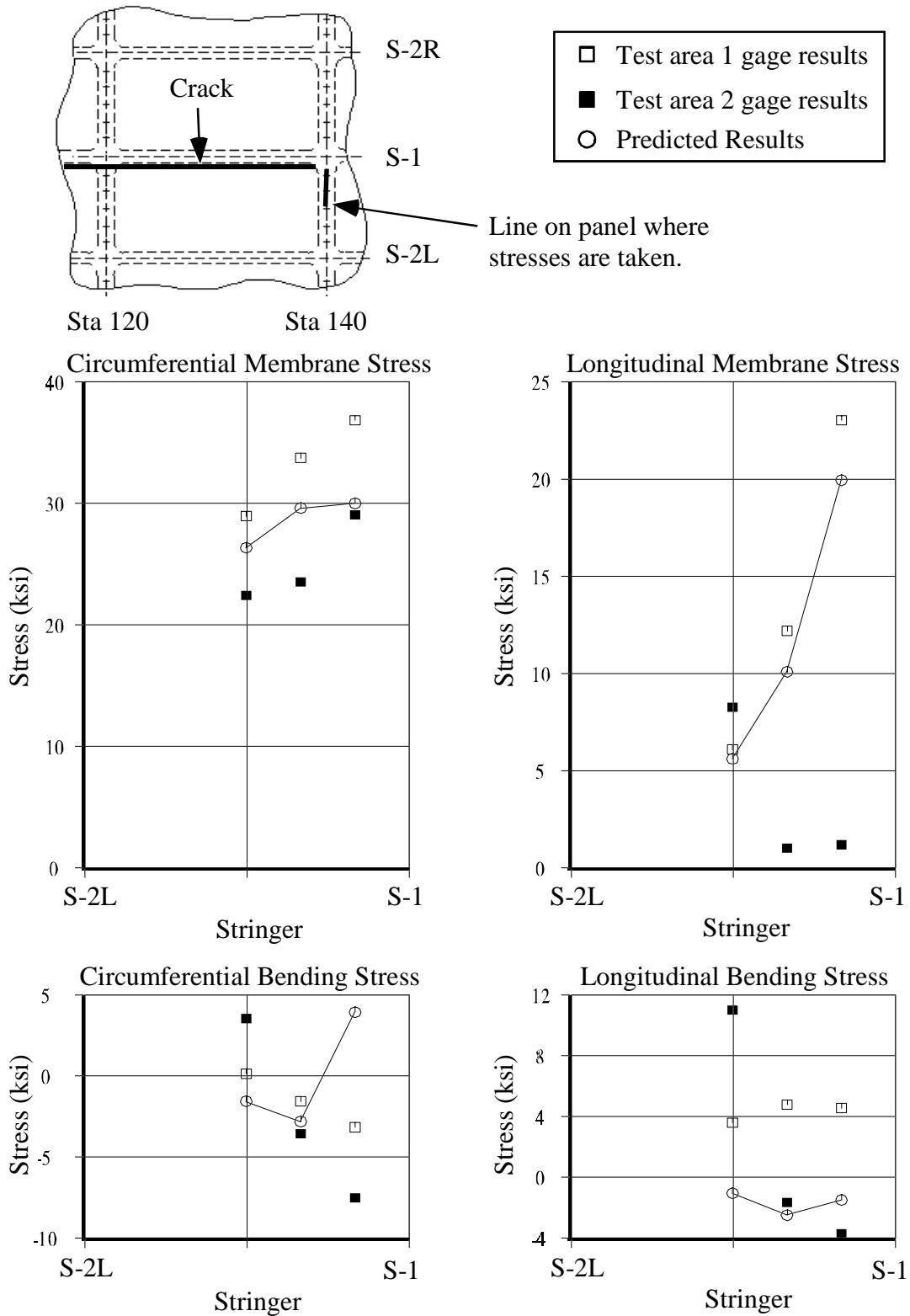


FIGURE 6-16. SKIN STRESS CORRELATION AT STATION 140 FOR A PANEL CONTAINING A 38-INCH CRACK CENTERED ON A BROKEN FRAME

The trends shown by the test data for the two-bay crack scenario are followed very well by the analysis. Figure 6-14 shows that the analysis is able to predict the dramatic rise and fall of the test membrane stresses in both the circumferential and longitudinal directions near the crack-tip location. The bending stress trends are also predicted well; however, there are a few cases where the analysis gives reverse bending compared to the test results. The analysis does not predict the magnitude of the test stresses as well as in the intact case, but, once again, the scatter between results obtained from the two different test areas is often more than the difference between analysis and test. Also, like the intact case, the longitudinal stresses tend to be over-predicted by the analysis.

For gages attached to the frame adjacent to the broken central frame, both the test and analysis results showed stresses that were low in comparison to the material's yield stress (65 ksi). For gages located above the crack location on the frame's fail-safe chord, which corresponds to the increased section area that is located along the top of the cutouts in the frame, the stresses were below 35 ksi for a two-bay crack and an applied pressure of 8.6 psi.

The results for the residual strength test conducted at test area 1 (Test 1) show that the fail-safe chord stress at the frame adjacent to the central broken frame remained below 50 ksi. This was true even after the crack-tips arrested in the fastener holes, and the panel was pressurized to 10.3 psi. In Test 2, the fail-safe chord gage did not reach the material's yield stress until after the failure pressure was reached and the crack extended dynamically past the frame. The frames did not break when total panel failure occurred in Test 2, as the fasteners tended to be the weak link and failed first.

6.5.2 Crack Growth Comparisons

Predictions of crack growth life were made to compare with results of crack growth testing performed in Test 1. In Test 1, the panel was cycled between 0.0 and 8.6 psi, with a skin crack and an intact central frame. The predictions were determined using the corresponding stress intensity factor curve shown in Figure 6-8. Note that the material crack growth rate properties used to make the prediction were obtained from the material database contained within the NASGRO crack growth program (see Reference 6-4) for 7475-T7351 T-L plate, since crack growth rate data, which was to be generated at NASA, had not yet been completed by the end of the Boeing contract.

Unfortunately, the range of ΔK used to develop the NASGRO crack growth rate equation parameters ended at 30 ksi inch^{1/2}, whereas the stress intensity factor at the beginning of testing (5-inch crack) was predicted to be almost 40 ksi inch^{1/2}.

Predictions were made using three different sets of crack growth rate data, including: the 7475-T7351 crack growth curve as defined in NASGRO; a straight line fit to the data used to generate the 7475-T7351 NASGRO curve; and 2024-T3 data from Reference 6-1. All three of these crack growth curves are presented in Figure 6-17 for $R = 0.0$, where $R = f_{\min}/f_{\max}$.

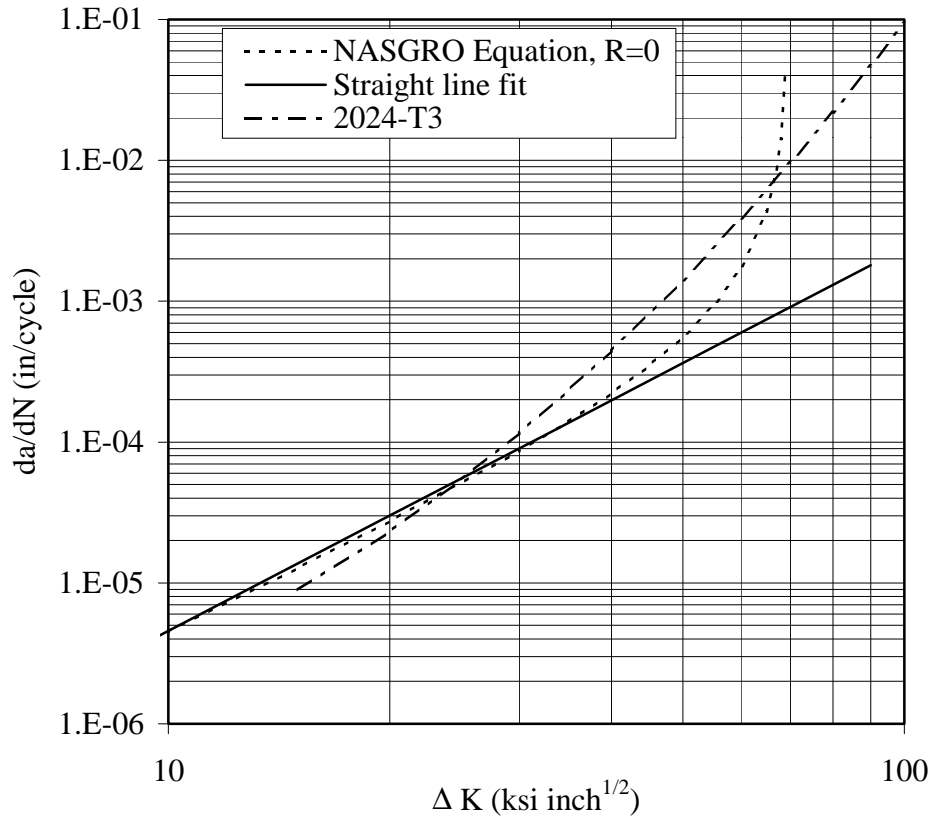


FIGURE 6-17. CRACK GROWTH RATE DATA FOR R = 0.0

The crack growth predictions made using these three crack growth rate curves are shown in Figure 6-18, along with the corresponding test data. A comparison of the predictions for the 7475-T7351 material to the test data shows that the prediction performed with the full NASGRO curve matches the test data very well. However, the NASGRO curve predicts the crack to extend dynamically after reaching 15 inches total length. At this crack length, the crack's stress intensity factor reaches the critical value specified by the NASGRO curve (70 ksi inch^{1/2}). This means that the crack would be expected to extend dynamically at this point. This critical stress intensity factor value is low, compared to that calculated from R-curve data used to perform residual strength predictions. Also, during the actual test, the crack grew fast, but in a stable manner, well beyond 15 inches.

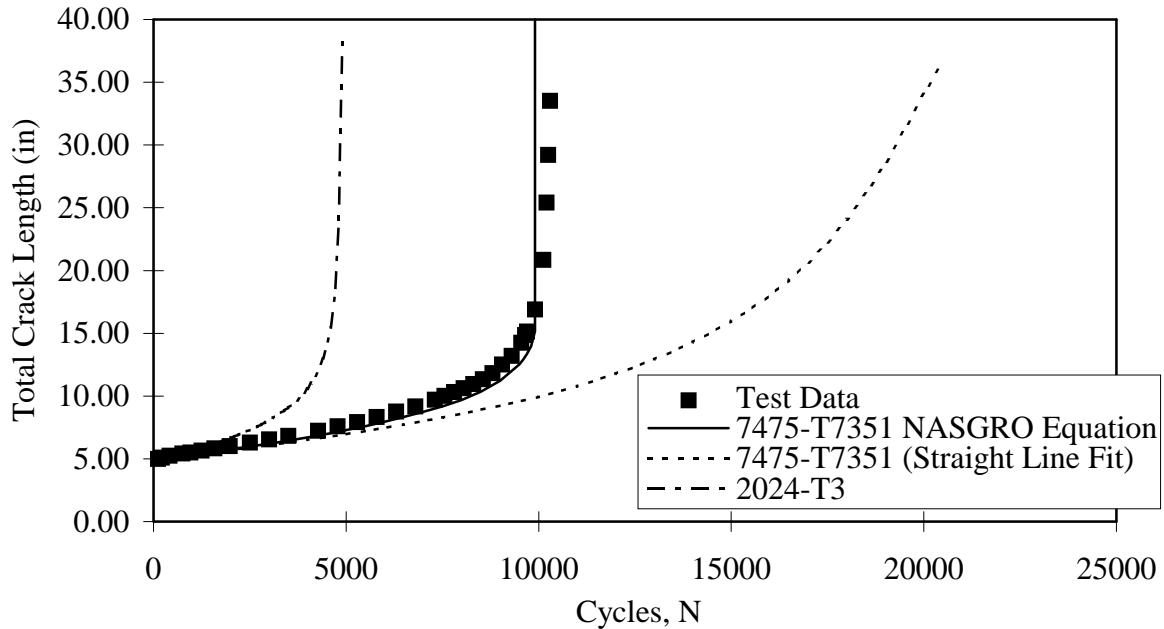


FIGURE 6-18. CRACK GROWTH PREDICTIONS AND TEST RESULTS FOR TEST 1

The prediction made using the straight-line fit of the NASGRO crack growth rate curve over-predicts the test data by a large margin. The results for this crack growth rate curve are included to show the sensitivity of the predictions to the crack growth rate data, and to highlight the need to develop crack growth rate data at higher ΔK levels for accurate prediction.

Finally, the prediction made using the crack growth rate data for 2024-T3 shows that a similar panel made from 2024-T3 would have about half the crack growth life for a crack growing from 5 inches to 40 inches total length. The reason for this result is that 2024-T3 has higher crack growth rates than 7475-T7351 at ΔK levels, where the crack is growing (above $35 \text{ ksi inch}^{1/2}$), as shown in Figure 6-17. However, 2024-T3 would outperform 7475-T7351 for crack growing at ΔK levels lower than about $25 \text{ ksi inch}^{1/2}$.

6.5.3 Residual Strength Comparisons

As presented earlier, the failure pressure for the panel containing a 38-inch crack centered on a broken frame was predicted to be 9.4 psi. This prediction compared very well with the Test 1 results for the corresponding cracking scenario, as the crack initially extended dynamically at approximately 9.7 psi. However, in the test, the crack-tips extended into the first frame-to-skin attachment fastener hole and were stopped from extending further. The analysis is not capable of predicting crack arrest in a hole, but it is assumed that if the cracks had missed the holes, or if a small crack had initiated at each hole prior to loading, the test panel would have failed at 9.7 psi.

A prediction was also made for Test 2, with the same methodology used in predicting Test 1. In Test 2, the plan was to cycle the panel at 8.6 psi with a 10-inch (total length) longitudinal crack and severed central frame. The crack was to be grown out to 20 inches to see if dynamic crack extension occurred. If the crack did not extend dynamically by the time it reached 20 inches, then the panel would be pressurized until failure. The analysis predicted that the crack would not extend dynamically at 8.6 psi for crack lengths up to 20 inches, and that it would take a pressure of 10.3 psi to get the crack to extend after reaching 20 inches.

During Test 2, the cyclic crack growth rate was too slow for a 10-inch crack cycled at a maximum pressure of 8.6 psi, so the crack was extended by sawcut to 18 inches. The panel was again cycled at 8.6 psi maximum pressure; from this length, the crack grew very rapidly. After eight cycles it had grown to approximately 22 inches, with a majority of the growth occurring on the last of the eight cycles. On the ninth cycle, the crack extended dynamically at 8.2 psi and arrested just before the pad-up on both sides, resulting in a 38-inch crack. Since the crack was slightly longer than the 20 inches specified for the previous prediction of Test 2, a prediction was made for a 22-inch crack. The failure pressure prediction for a 22-inch crack is 9.6 psi, which is 17% higher than the corresponding test result.

An estimate of the critical stress intensity factor, K_c , for the material used to fabricate the skins and stringers, 7475-T7351, was made from the Test 1 results. This was done to see if a more accurate prediction of the Test 2 instability pressure would result if more representative material properties were used (7475-T7651 material properties were used for the R-curve predictions). During Test 1, the crack extended about ½ inch on each side, to 39 inches total length, before going dynamic at approximately 9.7 psi. Using this result and the stress intensity factor curve presented in Figure 6-19 for a pressure of 9.7 psi and half crack length of 19.5 inches, K_c is determined to be approximately 120 ksi inch^{1/2}. Also shown in Figure 6-19 is the stress intensity curve for applied pressures of 9.0 psi; it intersects the critical stress intensity factor (120 ksi inch^{1/2}) at a half crack length of about 11 inches. This crack length corresponds to the Test 2 crack length at the point of crack instability (22 inches total length). Therefore, the critical stress intensity approach predicts the pressure at the point of dynamic extension to be 9.0 psi, which is 10% higher than the test results.

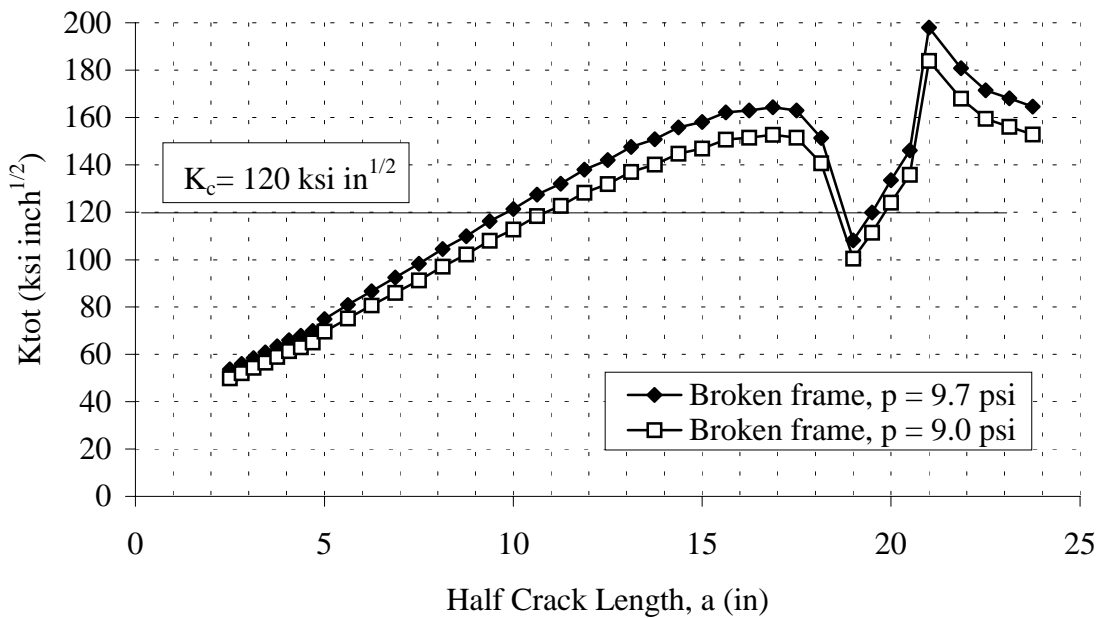


FIGURE 6-19. RESIDUAL STRENGTH PREDICTION USING K_c

Finally, after dynamic crack extension and subsequent arrest resulted in a 38-inch total length crack in Test 2, the panel was pressurized until failure. The panel failed by dynamic crack extension at 9.89 psi. The crack on one side hit a fastener hole; however, small notches were induced in the hole to prevent the hole from stopping the crack. This result shows that the crack would have kept going in Test 1 if the holes that stopped the main crack had small cracks in them. Also, the failure pressure for Test 2 was very close to that for Test 1 (9.7 psi) and the prediction (9.4 psi) made for this crack scenario using the R-curve analysis.

6.6 Outstanding Issues

The predictions made in the analyses of the two-bay crack panel were performed using crack growth and residual strength material properties that were not obtained from the actual 7475-T7351 plate or the same heat treatment lot as the plate used to build the two-bay longitudinal crack panel. Specimens were built to develop this data, but the tests were not completed prior to completion of this report. The predictions made using the material properties obtained from other resources were reasonable, compared to the test data. However, an effort should be made to perform these predictions with properties developed from the material used in this program. A comparison of the new predictions with the test data would provide a better measure of how well the analysis method works and the accuracy of stress intensity factor calculations—without the influence of material variation.

6.7 Conclusions

The crack growth and residual strength behavior of an integral skin/stringer pressure panel was investigated using a finite element approach. This study was initially performed to determine if the panel configuration would be able to hold a two-bay crack at the same pressure as built-up panels previously tested at Boeing Seattle—it provided the basis for the decision to build the integral panel out of 7475-T7351.

The predictions of skin stresses were generally very accurate as compared to test data. Frame and stringer stresses were not predicted as reliably as the skin stresses; this was attributed to the coarse mesh used for these structural elements.

Crack growth predictions using the NASGRO crack growth properties were surprisingly close to the results obtained in Test 1. However, since the accuracy of the NASGRO equation was questionable in the stress intensity range of interest, no real conclusions are possible at this time. Comparison of a prediction for a similar panel made out of 2024-T3 showed that the 7475-T7351 panel would have about twice the life for the crack lengths tested in this program. At smaller crack lengths, a 2024-T3 panel would outperform a 7475-T7351 panel.

The predicted residual strength pressure for the panel containing a 38-inch crack centered on a severed frame was very close to the crack instability point observed in Tests 1 and 2 for this crack scenario. The prediction of the crack instability point for Test 2 where the panel contained a 22-inch crack centered on a broken frame over-predicted the test result by 17%.

The difference between the test and analysis results was considered to be quite reasonable given the assumptions made in the finite element analysis and material properties. The assumptions in the finite element analysis were made to accomplish the desired results in a reasonable amount of time to provide test panel design support. Even so, the methods used for these predictions are too time-consuming to be used in a true design environment where the structure is continually being changed and optimized. A simpler analysis procedure that gives the relative effects of geometry changes was proposed by Northrop Grumman for use in optimizing the structure during the design phase. Northrop Grumman used this procedure to optimize the existing panel design (see Appendix G, specifically Task 2). However, because the method proposed by Northrop Grumman provides only relative effects of structural changes, the final design would ultimately have to be verified by a more complex analysis.

7 Inspection, Maintenance, and Repair Considerations

7.1 Overview

7.1.1 Deliverable

Inspection, maintenance, and repair concepts for integrally stiffened fuselage panel designs. (This work is associated with NASA SOW deliverable 3.8.)

7.1.2 Purpose

The monolithic nature of integral airframe structure (IAS) will present new inspection, maintenance, and repair challenges to the commercial aircraft industry. The purpose of this work was to begin to address the breadth of these issues by evaluating the inspection, maintenance, and repair of integral fuselage structure while considering various possible design configurations and materials properties.

7.1.3 Summary of Results

The conventional inspection methods currently used on built-up structure can also be applied to IAS—in specific, the equipment and techniques that will be used by the airlines to inspect integrally stiffened fuselage will be the same as those used on conventional fuselage structure.

Maintenance of the external surface of IAS should be better than built-up structure, because IAS is generally more corrosion-resistant, and because the design eliminates fastener holes. As the design is developed to accommodate structural repairs, the durability performance of the material used for the IAS fuselage skin will probably influence the IAS configuration design.

Analysis of durability properties of the selected panel material (7475) indicates that IAS skin repairs should terminate in stringer and frame lands for mechanically fastened attachments. This will ensure that the repairs terminate in the thicker areas of the panel.

7.2 A Review of Typical Airline Inspection and Maintenance Practices

7.2.1 Types of Inspections

Airlines inspect aircraft at specified intervals that are dependent on time, flight hours, or flight cycles. The three types of inspections are described in Table 7-1.

TABLE 7-1. TYPES OF AICRAFT INSPECTIONS

Inspection Type	Purpose	Inspection Interval
Scheduled initial inspections	For accidental damage or other incidents that are outside normal routines	Primarily time dependent
Corrosion prevention inspections (or environmental damage inspections)	Dictated by airline operations and the operations environment, they typically deal with inspecting for and preventing corrosion	Primarily time dependent
Fatigue related inspections	For aging aircraft where a portion (typically 75%) of the design service objective has been reached	Set according to the number of flight cycles an airplane accumulates

For fatigue related inspections of primary fuselage structure, the anticipated crack growth rate dictates the number of cycles allowed between maintenance and service checks of each component. The crack growth rate is in turn influenced by load, load profile, environment, component properties, applied tools, material alloy, temper, and surface treatments. Service experience and maintenance knowledge also highly influence the inspection interval.

7.2.2 Example: Inspection at Specific Intervals

Consider the example of an airline that performs inspections at specific intervals (see Table 7-2). In this example, the main types of inspections are called the “A” check, “C” check, and “D” check. Each of these inspections is performed at specified hourly or calendar time intervals, as described in the table.

TABLE 7-2. EXAMPLE: AIRLINE INSPECTION SCHEDULE

Check	Description	Interval
“A”	The primary or first-level air readiness inspection, intended to disclose the general condition of the aircraft. Conducted in conjunction with the lesser maintenance checks (preflight and transit).	Perform at intervals not to exceed 500 flight hours.
“C”	Requires a greater depth of inspection throughout the airplane to ensure continued airworthiness. Involves selected operational and functional checks and, to facilitate the inspection, requires such activities as removal of access doors and panels. Also requires completion of all items in the lesser checks.	Perform at intervals not to exceed 5000 flight hours or 15 calendar months, whichever comes first.
“D”	Requires a greater depth of inspection throughout the airplane, including disassembly of portions of the aircraft to facilitate inspection, to ensure continued airworthiness beyond the “C” check.	Perform at intervals not to exceed 25,000 flight hours or 5 calendar years, whichever comes first.

7.2.3 Maintenance

Fuselage maintenance during the design life of the aircraft consists primarily of inspection for accidental or environmental damage along with the repair of any other damage detected. Later in the life of the aircraft, additional inspections for fatigue damage are added to the maintenance requirements. Airlines perform maintenance at specified intervals, which are set by considering the number of flight cycles, airline operations, and operating environment.

The number of cycles allowed between maintenance and service checks for each component of primary structure is dictated by the anticipated damage growth rate. The damage tolerance criteria assumes that a detectable size crack is missed at the maintenance check. The recurring or repeat inspection interval is then defined as the time necessary for a *detectable* crack to grow to the critical size divided by a safety factor (typically a value of 2 for safety-critical structure). The detectable crack length is influenced by structured configuration factors, such as accessibility and the use of non-destructive examination (NDE) methods. The crack growth rate is influenced by component geometry, applied loads, material properties, and operating environment.

7.3 Inspection, Maintenance, and Repair Expectations for IAS

A series of inspections were conducted to evaluate and compare the IAS structure to a conventional built-up fuselage structure.

7.3.1 IAS Panel Initial Inspection

7.3.1.1 *Longitudinal Two-Bay Test Panel*

The IAS longitudinal two-bay crack panel was inspected during fabrication, following machining of the integrally stiffened skins. Both pieces of the panel were transported to a quality assurance lab to verify that machined-in features and design configuration had been maintained. To accomplish this, a lab technician used a coordinated measuring machine (CMM) and followed an inspection method to verify accurate fabrication.

After assembly of the skin, ultrasonic measuring equipment was used to measure thickness in the pockets. This verified that the panel met minimum skin gage requirements prior to testing. Also, rivet heads were manually measured to verify that button and head diameters at the top joint were correct.

7.3.1.2 *Extrusion Panels*

The IAS extrusion panels were inspected using fluorescent penetrant, coordinate measurement, and ultrasonics. These measurement methods allowed the team to investigate pits and surface characteristics, verify surface thickness, measure panel waviness, etc. For more information about the IAS extrusion panels, see Section 3.

7.3.2 Damage Tolerance Analysis for In-Service Inspection

In accordance with current FAA requirements, an in-service damage evaluation was considered during the initial design of the IAS panel. The primary damage considered for the fuselage structure consisted of a two-bay longitudinal crack in the skin with a broken center frame. With this damage present, IAS structure is required to meet specific residual strength requirements and also to demonstrate damage arrest capability by load redistribution into the adjacent structure (frames). 7050 aluminum plate material was initially considered for the IAS panel; however, after an evaluation of the fracture properties of 7050 material—particularly in the T-L orientation—it was determined that 7475 material would be better suited for this application.

The IAS longitudinal two-bay crack panel was required to successfully hold a two-bay crack, and to have a crack growth rate slow enough to support economical inspection. Initial analysis indicates that:

- The IAS panel can be designed to achieve the damage tolerance design requirements
- The monolithic outer skin of the IAS panel does exhibit damage arrest capability

Fortunately, existing equipment and techniques can be applied for in-service NDE inspection and measurement work for the IAS project. Conventional in-service inspection methods of assuring quality detection of problems include eddy current, ultrasonic, magneto-optical imaging, thermography, and florescent penetrant.

Although conventional inspection techniques apply, IAS also offers the opportunity to utilize and develop alternative inspection techniques, such as plate wave ultrasonics or acoustic emission, that can be used on built-up structure as well. These techniques would then be available to the customer as choices in addition to those available for conventional structure. Consequently, each customer could evaluate the possible time savings versus the additional capital expenditure for the various inspection options.

7.3.3 IAS Panel Maintenance

It is projected that slow crack growth will allow for economical inspection and maintenance cycles for airlines. This was addressed in the test and analysis portions of the IAS program (see Section 5 and Section 6). The IAS panel has some attractive maintenance-related design features:

- Corrosion resistance—The 7475 material used for the IAS panel has better general corrosion resistance than the 2024 material used for built-up structure.
- Maintainability—The elimination of thousands of fasteners and fastener holes will likely give the IAS panel a better maintainability rating than built-up structure.

7.3.4 IAS Repair Approach

During the *Affordable Design and Manufacturing (ADAM) for Commercial Transport Aircraft and Engines* proposal, a review of repair methods for integral versus built-up structure revealed that the same basic repair approach can be used for both types of structure. Low-cost repair methods, such as external patches with doublers, are preferred over replacing large skin panels or parts, provided that the repairs satisfy the service objectives. In the case of large integrally stiffened panels that are similar to large built-up fuselage panels, repair patches can be cost-effective. A conventional mechanical, external repair approach was used for the IAS program. The repair panel that was designed, fabricated, and tested during the IAS program (see Figure 7-1 and Figure 7-2) is a mechanically fastened repair typical of an in-service type fix. This panel demonstrated that new materials and methods are not required to ensure repairability of large integrated structures.



FIGURE 7-1. IAS REPAIR PANEL—INSIDE VIEW

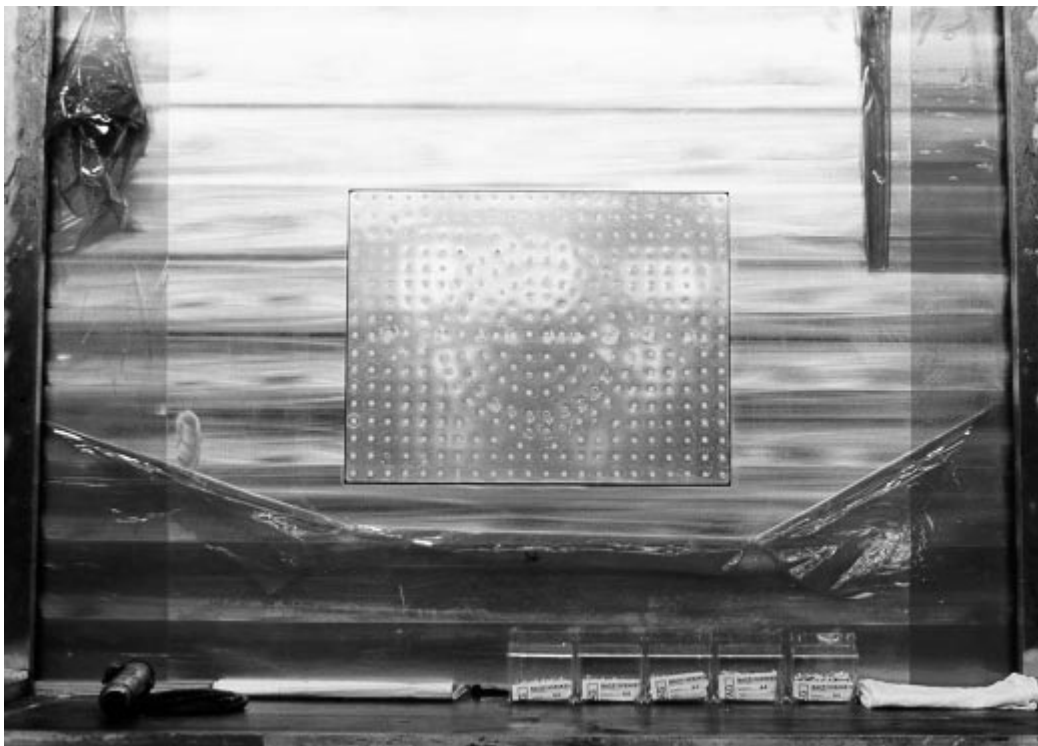


FIGURE 7-2. IAS REPAIR PANEL—OUTSIDE VIEW

The IAS panel repair procedure is anticipated to include the following steps:

1. Remove the damaged area.
2. Mechanically fasten doublers on both sides of the repair.
3. If needed, remove stiffener sections and splice in new pieces.
4. Apply sealant and finishes to provide corrosion protection.
5. Reinstall systems.

At this point, the airline can rapidly move the aircraft back into service.

7.3.5 Durability Analysis of Repairs

A durability (crack initiation) analysis was conducted on the IAS structure, to evaluate the 7475 material as compared to the 2024 material commonly used for skins on built-up fuselage structure. A comparison of the MIL Handbook 5 properties for open hole, $K_t = 3.0$, geometries shows that the 7475 material fatigue allowable is approximately 40% lower than the 2024 allowance for a typical aircraft life of 60,000 cycles (times a scatter factor of 4).

Typically, as part of the basic design requirements, the basic fuselage skin will be designed to accommodate an allowable open hole fatigue. This criteria was applied to the IAS structure to calculate the minimum skin thicknesses. Note that the basic hoop stress in the fuselage skin is defined by the following equation:

$$\text{Hoop stress} = \sigma = pr/t$$

where:

- p = fuselage pressure during a typical flight cycle (8.6 psi)
- r = fuselage radius (127 inches for the wide-body fuselage)
- t = skin thickness

A minimum skin thickness can be determined by setting the hoop stress equal to the open hole fatigue allowable for the two materials. For both materials, assume the following conditions:

$$K_t = 3.0$$

$$R = 0.0$$

$$N = 60,000 \times 4 = 240,000 \text{ cycles}$$

The allowable fatigue and minimum skin thickness calculated for each material are shown in Table 7-3.

TABLE 7-3. FATIGUE AND SKIN THICKNESS FOR PANEL MATERIALS

Material	Allowable Fatigue	Calculated Minimum Skin Thickness
2024-T3	Approximately 22,000	0.052 inches
7475-T74	Approximately 13,000	0.087 inches

This analysis indicates that durability will be a significant design consideration for the IAS panel if 7475 material is used. During the IAS program, an alternate material, 6013 aluminum, was evaluated. Its durability performance rivals the 2024 material. However, this material has producibility issues that must to be resolved to make it feasible for the IAS program.

The durability properties of 7475 material will likely influence IAS repair issues. The above durability analysis indicates that a conventional doubler repair will have to terminate in the thicker areas of the IAS panel skin (i.e., the lands). One possible consideration is to design the stringer geometries of the IAS structure so that the vertical leg of the stiffener is in the center of the land. This will allow the end fasteners of an internal doubler repair to pick up the thicker land.

In general, durability analysis represents an initial evaluation of a structure to address widespread fatigue damage (WFD). The analysis considers those design details and stress levels that, in combination, would eventually precipitate fatigue cracks in the structure. The IAS panel has several design features, such as the elimination of fastener holes, that would improve its resistance to WFD, provided that acceptable stress levels are maintained. However, it is crucial that sufficient time be allowed during the IAS production design phase for thorough assessment of factors affecting WFD, so it can be complete prior to drawing release.

7.4 Outstanding Issues

Built-up structure has been extensively investigated for WFD and micro-cracking around fastener holes. Monolithic and integrally stiffened structure have fewer fastener holes than built-up structure, and thus fewer sites for cracks to initiate WFD. However, it may be argued that integrally stiffened structure may have “hot spots” at fillet radius locations that could cause in-service problems. Design must account for possible fillet hot spots; however, there is flexibility in the structure to accommodate this. The IAS type of concept is expected to extend the life cycles of airplanes, which would help with aircraft structural safety.

Note that welded joints and weld repairs were not addressed fully by the IAS program. They should be considered in future follow-on efforts.

7.5 Conclusions and Recommendations

Conventional mechanical repair and inspection techniques can be applied to IAS panels. Inspection cycles are anticipated to be equivalent to those for built-up structure.

Durability performance of 7475 material is lower than conventional 2024 fuselage skin material; therefore, definition and evaluation of IAS durability and damage tolerance test and repair criteria is needed.

As a general rule, IAS skin repairs should terminate in stringer and frame lands to ensure adequate durability of mechanically fastened attachments.

8 Long-Range Plan

8.1 Overview

8.1.1 Deliverable

A documented assessment of higher-risk, longer-range manufacturing processes/design concepts for integral metallic fuselage construction. (This work is associated with NASA SOW deliverable 3.9.)

8.1.2 Purpose

The purpose of the long-range plan was to describe a possible path for the development work to follow the Integral Airframe Structure (IAS) program. This plan was specifically intended to target higher-risk, longer-range work associated with the development of metallic fuselage structure of integrally stiffened design. It was to encompass separate “chunks” of development work that can be conducted as independent small projects, but will work in combination with other efforts, to support an overall development path for fuselage structure design and manufacturing technology development. This path could shape efforts for the next two to four years; for especially high-risk ideas, the time frame could be even longer.

8.1.3 Summary of Results

This long-range plan recommends activity in ten areas:

1. Additional testing of 7475 plate and various extrusion materials in flat-panel configurations
2. Development of processes for producing flatter and wider extrusions
3. Development of tailored alloys for welding, casting, forming, and machining
4. Development of material alloys like second- or third-generation aluminum-lithium for decreased weight and increased performance for sheet, plate, and extrusions
5. Development of friction stir welding and other welding processes
6. Development of new innovative concepts for forming to contour, particularly compound contour
7. Development of processes to produce large-scale castings
8. Development and modeling of analysis tools
9. Development of analysis and certification methodologies

10. Development of processes for metal spray forming to contour and structural maintenance sensors

This list is not presented in any priority ordering.

Immediate efforts are warranted for flat panel testing in 7475 plate. On a longer term, three areas deserve special attention: extrusion process development; welding process development; and analysis tool development and modeling.

8.2 Basis For This Long-Range Plan

8.2.1 The IAS Vision

An overall goal of the aircraft industry is to develop multidiscipline, integrated concepts for the design and production of commercial aircraft that significantly reduce cost and cycle time while minimizing weight. One course for meeting this goal is to eliminate the majority of detail fabrication and mid-assembly steps by developing fuselage designs based on large integrally stiffened panels and super panels. The evolution of this research will take strategic thought and objectives that are focused on the application of collaborative projects. Product vision will be used to give guidance and to help select the correct or necessary enabling technology.

The long-term industry vision for fuselage assembly is to use self-tooling of large, consolidated parts, combined with precision assembly. Self-tooling implies the elimination of costly dedicated tooling. Flexible low-cost tool stands, coupled with large self-tooling primary structural members, provide locating and fixturing references. Precision assembly becomes the enabling technology, and it relies on electronic databases and computing design integration.

8.2.2 Commercial Transports Today

To make safe and reliable parts, the commercial aircraft industry has taken a traditional design approach that relies on:

- Embedded design practices
- An evolutionary design approach
- Reliance on discrete parts for damage tolerance
- Multiple load paths for fail safety

As a result, today's airframes typically are primarily conventional built-up structure of riveted aluminum skin and stringer construction. However, airframes are beginning to incorporate some innovative manufacturing technologies and monolithic designs, as castings and forgings, machined parts, and parts made by super plastic forming are beginning to replace built-up structure. These integral construction approaches for metal primary structure are being implemented slowly, on a limited basis, because they represent a particular challenge to each aspect of the traditional approach described above.

8.2.3 The IAS Program

The major components of airplane fuselage are panels composed of skins and stringers, body frames, floor beams, window frames, and door frames. Fuselage panel structure can be further differentiated, based on the functional requirements, as crown panels, side panels, and belly panels. Each of these parts is currently produced by built-up construction. For each of these major fuselage structural applications, multiple fabrication technologies can be employed to produce panels with large, integral structure designs. Each application/technology combination can be considered as an alternative to existing built-up structure.

The prospect of using integrally stiffened fuselage structure raises many unresolved questions about the damage tolerance and fail safety of such parts, and points the way toward a long-range and potentially high-risk, high-benefit development plan. The IAS program began the work needed to address manufacturing processes, part design, and part performance requirements.

As of this writing, the IAS team has completed the IAS test matrix, along with the IAS task activities (shown above in Figure 1-6). IAS program activity focused on integrally stiffened fuselage test panels produced from plate and by extrusion. An optimized design has been used for large panels, and analysis predictions were conducted to ensure successful two-bay longitudinal test validation for fuselage panels.

A screening type of test matrix was used for the test panels, with the intent of establishing trends to indicate whether the integral fuselage structure looks promising in terms of cost, weight, and performance. This test matrix was developed collaboratively by the IAS team members. If the trends indicated a positive result, then further development would be pursued, and a more thorough testing program would be needed. The results of this test program indicate that integral fuselage structure does in fact look very promising in each of the three evaluation areas.

However, the IAS program is only the beginning—in addition to the challenges of efficiently manufacturing integral fuselage structure, engineering issues, safety, and performance needs for structural reliability must be further and continually addressed. This long-range plan is an attempt to describe a possible path for the development work to follow.

8.2.4 Development of This Long-Range Plan

This assessment of longer-term manufacturing processes/design concepts for integral metallic fuselage construction is based on:

- Historical activity associated with the *Affordable Design for Manufacturing (ADAM) for Commercial Transport Aircraft and Engines* proposal
- Lessons learned from the IAS program, including the technology assessment, IAS design ideas, and a projection of possibilities for integral metallic fuselage construction
- Creative lists of processing, fabrication, and design concepts

Note that, while the scope of this long-range plan is focused on metallic fuselage primary structure for panels, it will also mention other structure (floor beams, doors, and bulkheads) and ideas for joining and welding.

8.3 Recommended Long-Range Activities

To further the status of integrally stiffened fuselage technology, this long-range plan recommends activity in ten areas, as described below. Each of these areas represents a stand-alone effort.

8.3.1 Additional Testing of 7475 Plate and Various Extrusion Materials in Flat-Panel Configurations

Past experience and lessons learned from the IAS program indicate that follow-on activities should include the production of additional machined-plate fuselage panels in flat and curved configurations. These panels should be tested and compared to built-up panels made out of the same material. This would provide data that would allow for the direct comparison of the differences between the two structures, in terms of strength, toughness, and residual strength, that are due to design features rather than material characteristics.

This work should include continued analysis and modeling for prediction comparison of analysis to actual machined flat panel tests. Continued analysis tool development will provide a stronger understanding of crack growth in integrally stiffened structure.

8.3.2 Development of Processes for Producing Wider and Flatter Extrusions

Producibility issues associated with extruded panels need to be resolved so that manufacturing can occur effectively. There are two areas of interest for long-term extrusion process development work:

- Producing wider near-net-shaped extruded panels to reduce the number of joints required
- Producing flat extrusion panels in a near-net-shaped form that are to machining tolerances

Cost and performance trends indicate that wider extrusion panels would be of “increased” value. The cost reduction trend associated with reducing the number of fuselage panels is illustrated in Figure 1-3. The extrusions produced for IAS by Alcoa were approximately 30 inches wide; in Russia, the panels are 40 to 45 inches wide. With some development, it could be possible to extrude a 60-inch wide panel.

Additional development work is needed on the post production flattening of the extrusion panels. Extruded panels for the IAS program were produced in a vee-shaped die with the intention of reducing the flattening and rolling operations. This was probably a reasonable assumption given that the IAS extrusions had a high degree of variation in the flattened area. This variation in panel flatness made it impossible to produce shear panels to a machining tolerance during the IAS program. A wider extrusion panel with machineable flatness is desired, so continued development effort on the flattening of extruded panels is recommended.

A possible longer-term, higher-risk opportunity would be the development of equipment to process the integrally stiffened panel extrusions after they leave the extrusion die. Imagine a process in which the raw extrusion exits the die in a vee shape and is stretched and flattened. Equipment would be needed to grab the extrusion and somehow flatten, stretch, and roll it, all while keeping the stringers in the correct alignment. This is a unique challenge and requires process development at the extrusion source.

Figure 8-1 depicts the concept of a vee-shaped extrusion being processed to a flat, machine-grade configuration. This geometry processing can conceivably be achieved to yield flat, wide extrusions and, therefore, to produce cost-effective structure.

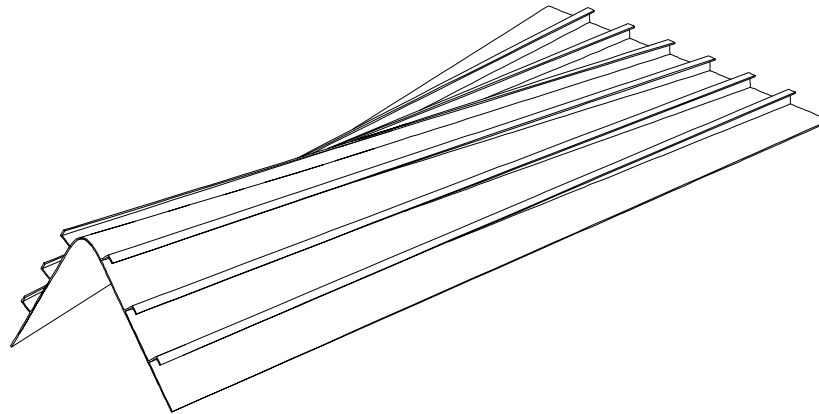


FIGURE 8-1. VEE-SHAPED EXTRUSION

Extrusion development work is on the rise, but the development risk for fuselage structure applications is still very high. Wide, near-net-shaped extrusion panel development would make a good follow on project to IAS. Near-net-shaped extrusions are a likely development path because they show a very high benefit and allow some long-range, high-risk, stretch technology when coupled with welding or friction stir joining. If successful, the application of near-net-shaped extrusions in combination with welded joints in fuselage structure could be a significant performance and cost breakthrough. This type of development will clearly define the path that the next generation of airframes will most likely follow—one featuring larger panels of welded extrusions or customized-build-ups.

8.3.3 Development of Tailored Alloys for Welding, Casting, Forming, and Machining

Tailored alloy development has long been a topic of interest as an enabling technology. Many processes, including welding, casting, forming, and machining, could potentially benefit from custom alloys. IAS forming issues and structural performance in particular could benefit from the development of new alloys.

In a comparison of strength and toughness for candidate airframe materials (see Figure 8-2), 2024 alloy is still the best performer among standard airframe skin materials. However there are promising alloys that may have new manufacturing benefits that can meet or exceed the performance of traditional materials.

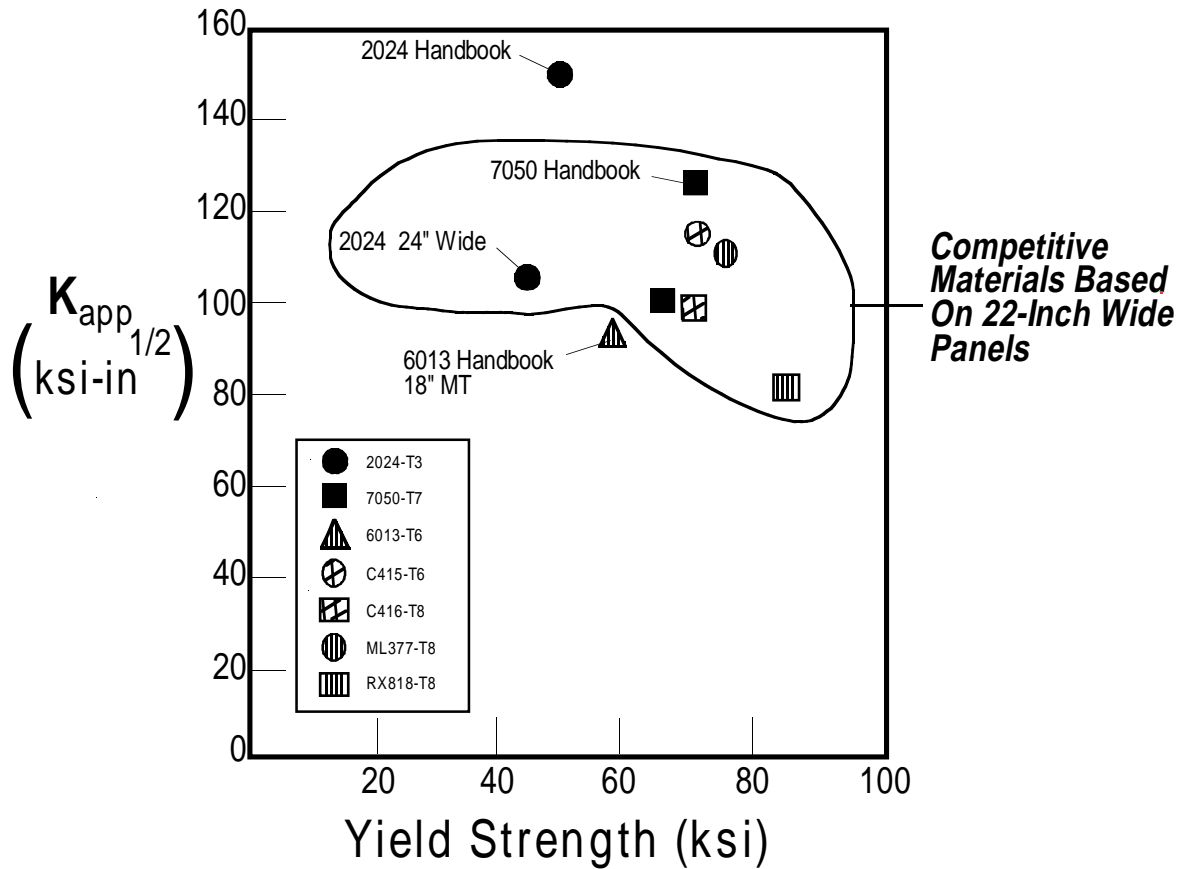


FIGURE 8-2. STRENGTH VERSUS TOUGHNESS OF CANDIDATE AIRFRAME MATERIALS

Source: Adapted from an illustration presented in “Emerging Alloy Processing and Characterization,” M. S. Domack, Integral Airframe Structures Program, Joint NASA/Industry Workshop, April 1998.

8.3.4 Development of Material Alloys Like Second- or Third-Generation Aluminum-Lithium

Another attractive material development type project is the development of material alloys like second- or third-generation aluminum-lithium. Such alloys could provide decreased weight and increased performance for sheet, plate, and extrusions. Tailored alloys that support welding, casting, forming, and machining, with performance competitive with 2024- and 7000-series alloys, would open up design and manufacturing innovations for reducing cost and customizing structure.

8.3.5 Development of Welding Processes

Welded fuselage structure is a potential technology breakthrough that would be a major shift from the traditional assembly and design methods used today. The use of welding joint techniques that are as fast as riveting to reduce the number of fasteners could be revolutionary. Welded fuselage joints would be the beginning; a long-range vision would include working up to large structural fuselage parts or sections. Theoretically, if a welded joint is 90% of the strength of the parent material and does not burden the structural weight of the part, it can be used to join any size extrusion.

This development work is high-risk and long-term, because it is radically different from traditional aircraft assembly and has some technical challenges in performance and life cycle. However, the European competition seems to be developing welded fuselage structure, and there seems to be more and more discussion of welded structure.

Friction stir welding is a development frontier that American industry is just starting to address. The only IAS contract activity in this area was simply to supply property data samples to be tested by NASA. It would be wise to expand this area of technology for producing lap joints and butt joints for fuselage structure.

Two potential advantages of welded joints stand out:

- Cost and weight savings through the elimination of fasteners and fastened joints
- The ability to join dissimilar materials

Consider the IAS vision shown in Figure 8-3. Welding rather than riveting the frames in place would reduce the fastener count. Welding the panels together would eliminate additional fasteners. The elimination of fasteners and fastened joints has the potential for cost and weight savings. For example, for the Boeing 747 fuselage, the cost savings averages over \$3 per fastener (see Table 8-1). If all the fasteners in the 747 fuselage could be eliminated, the cost savings would total nearly \$3 million.

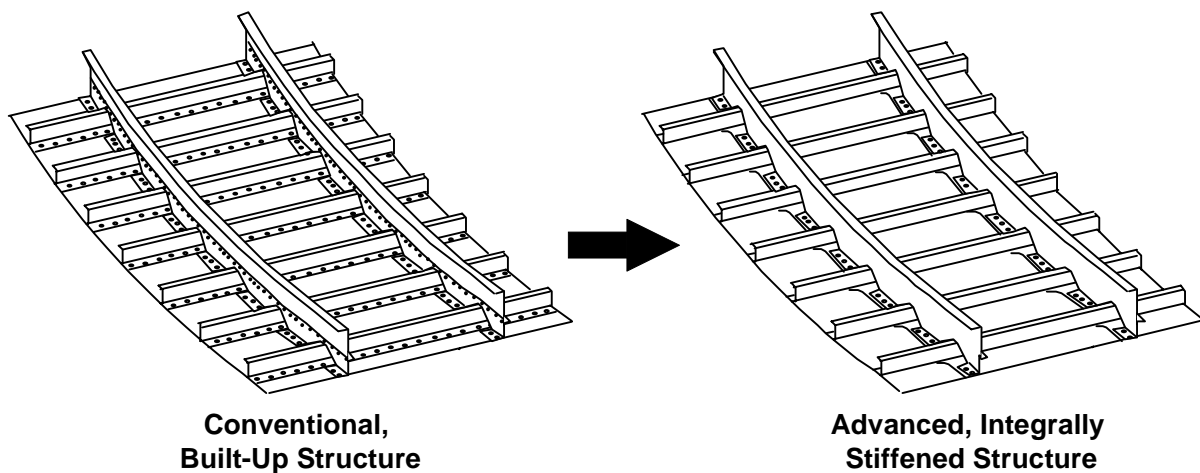


FIGURE 8-3. THE IAS VISION

TABLE 8-1. INSTALLED FASTENER COST—BOEING 747 FUSELAGE, SECTIONS 42–46

Fastener Type	Cost per Fastener	% of Fasteners
Rivet—Auto Installed	\$1.75	75%
Rivet—Hand Installed	\$5.00	15%
Hi-Lok Fastener	\$13.75	10%
Weighted Average For All Fasteners	\$3.44	—

Cost per Airplane Total of 850,000 Fasteners	\$2,924,000
---	-------------

Source: Northrop Grumman
(IAS Technical Review presentation, April 14–15, 1997)

Welding might allow some customization of materials at each quadrant—materials could be selected specific to the operational loads and intended functions. The joining of dissimilar materials would allow flexibility and tailoring of the design. Granted, this is a stretch of the imagination from traditional design philosophy. Built-up structure maybe visualized as net-shaped forgings welded to plate, sheet, or extrusions. This new approach offers the ability to have the thickness and properties where they are needed, and the thinness and weight savings where they can be easily taken.

The potential incorporation of extensive welding will also require different alloys to be considered, welding equipment to be developed, and design philosophies to be investigated. Figure 8-4 identifies some thoughts on incorporating a butt joint weld into the traditional fuselage. For damage tolerance, shear tied frames would be required locally at the joint.

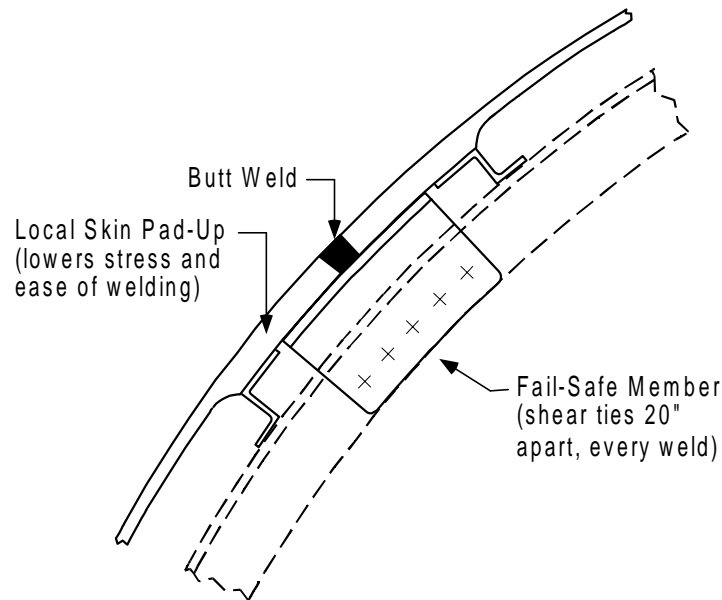


FIGURE 8-4. INCORPORATING A BUTT JOINT WELD INTO TRADITIONAL FUSELAGE STRUCTURE

This design would hold the fuselage together if there was a separation at the weld; the fail-safe member is the combination of shear tie and frame combination. The design would incorporate skin pad-ups locally at the weld sites for manufacturing ease and strengthening in the weld zone. Currently, there is no data on fatigue for welded joints in fuselage structure; this would be required to answer questions associated with such issues as porosity, micro-cracks, and corrosion resistance.

It has to be tested and proven that the welded joint is as good as the basic panel. However, if materials and welding techniques were successfully developed, then customized super panels could be made for the fuselage. Cost savings, weld quality, joint development, testing, etc., all need to be evaluated, but, nonetheless, welding has potential.

8.3.6 Development of Innovative Concepts for Forming to Contour, Particularly Compound Contour

IAS program activities indicate that it is very necessary to pursue options for forming parts to contour. A wide range of forming options is available, from the common and proven to the uncommon and unproven, such as:

- Bump forming
- Restained age creep forming
- Electro forming at high speed
- Forming by magnetic force
- Laser forming
- Stretch forming
- Peen forming
- Water peening
- Set shape forming
- Curved extensions
- Age creep forming
- Magna forming of large shapes
- Mechanical forming
- Local induction heating for forming complex contour
- Explosive forming
- Stretch SPF/DB
- Shot peening
- Soft media peening
- Spray forming of sheet or integral stiffened parts
- Casting to contour

These forming methods do not represent the total breadth of innovative forming ideas, nor do they indicate any specific priority. Forming technologies are required for single contour and compound contour of fuselage panels for each of the IAS applications; if the structure cannot be formed, fabrication is impossible. Some type of innovative forming would ultimately be a breakthrough for integral structure.

The IAS team discussed forming during the IAS program technology assessment workshop. These discussions indicated that age creep forming is a viable technology for compound contour fuselage structure. A follow-on project could be directed toward age creep forming development for compound contour fuselage panels, with the goal of assessing its viability and capability. A longer-range, higher-risk project might be to investigate some of the more embryonic innovative integral structure forming ideas, such as stretch forming. Stretch forming may not appear to be breakthrough technology, but stretch forming a panel with integral stiffeners is quite difficult; development of a process and equipment to accomplish this would be innovative, but not impossible.

Both the age creep and stretch forming projects would benefit from tailored material development—age creep-capable alloy tempers are still needed. This could offer motivation for pursuing the material development portion of the long-range plan.

8.3.7 Development of Processes to Produce Large-Scale Castings

In many applications, large-scale castings have been found to be cost-competitive with and weight-equivalent to more conventional structures. The United States Air Force CAST program and other similar activities have demonstrated a minimum 20% cost savings for cast structure as compared to baseline assemblies. More recent cost savings estimates have greatly exceeded 20%; for example, Airbus Industrie claims a 90% cost reduction on A330/A340 flap actuator torque boxes, an application in which cast parts replaced a large, crucial machined fitting.

Castings can potentially consolidate parts, reduce fastener counts, and effectively place structure where it is most needed in a design. Doors, door frames, and bulkheads are potential part candidates or concept prototypes. Casting lends itself to the forming of complex three-dimensional parts, and, in some applications, may produce near-net-shaped skin contours, which eliminates forming complications.

The advancement of custom casting alloys has the following technical needs:

- An increase in the strength ranges, which would directly translate to weight and operating cost savings.
- A decrease in crack growth rates, which would improve ownership costs for the airline operator

8.3.8 Development and Modeling of Analysis Tools

It is important to understand that engineering design and analysis are paramount to the development of the understanding and methodology necessary to use and apply monolithic or integrally stiffened, part consolidation projects in commercial aircraft. IAS activity is very important in helping to develop analysis methodology, modeling, and electronic analysis tools that can be validated by test. These tools have the potential to help establish new ways to develop, design, manufacture, and certify integrally stiffened or innovative structure.

The importance of design for manufacturing, or an electronic fingertip database for design, is increasing (see Figure 8-5). An integrated approach for design and manufacturing has become extremely important in the computer age. Therefore, there needs to be exploration of the perspective of how designers of the future will operate in the ideal environment of the future.

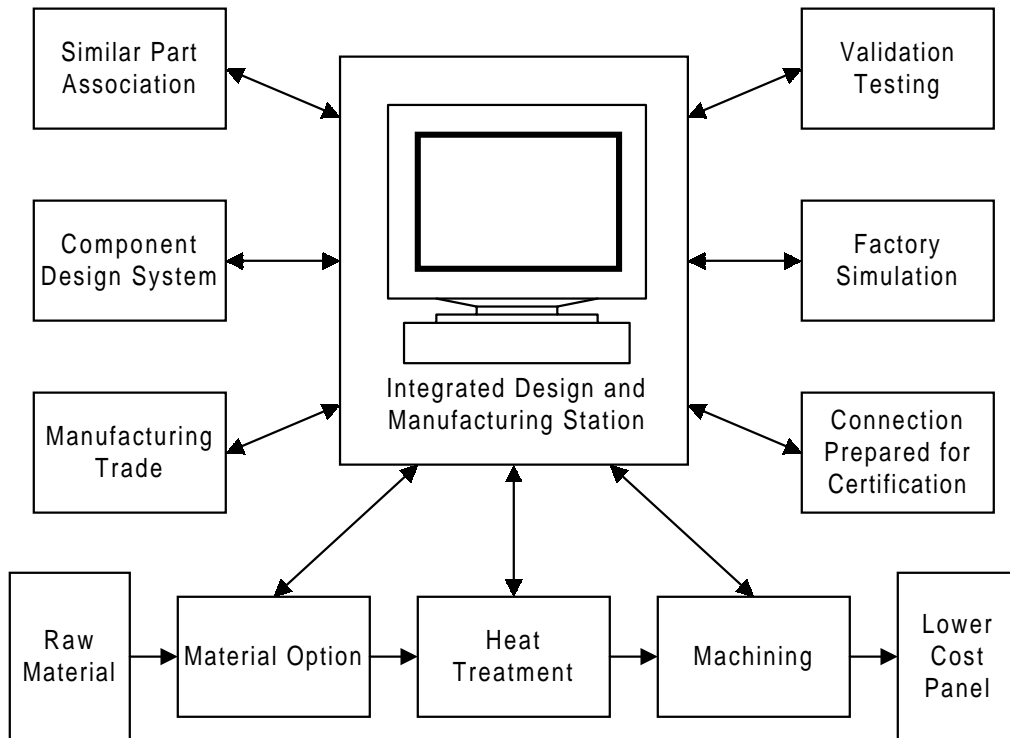


FIGURE 8-5. FUTURE INTEGRATED DESIGN

Effort needs to be continued to develop durability, damage tolerance, and fail-safe approaches for integrally stiffened structure. Material and structural behavior and crack growth data modeling are important for design and certification methodology. A design that incorporates the best characteristics for structural performance would be a strategic advantage. Such a design could be provided by the combination of:

- Computing design integration
- Advanced measurement technologies
- Electronic databases that give the designer tools that help design the structure, conduct trade studies, and make manufacturing and design choices that are based on prior knowledge and references

The capability to optimize structure weight, reduce manufacturing costs, and increase production flexibility is needed.

8.3.9 Development of Analysis and Certification Methodologies

Ultimately, airplane manufacturers are trying to avoid a heavy dependence on testing, which is costly. To achieve this, new certification methods will need to evolve and be developed along with the new technology. The Federal Aviation Administration, NASA, and industry must work together on certification methodologies and philosophies for the future commercial air transports.

8.3.10 Development of Processes for Metal Spray Forming to Contour and Structural Maintenance Sensors

Metal spray forming and structural maintenance sensors are two potentially breakthrough airframe industry fundamental research technologies that could be employed in commercial transports. Like the other technologies that have been discussed in this section, the potential needs to be explored and many questions answered. Research in these two fields could help revolutionize airframe design, construction, and maintenance.

8.4 Outstanding issues

Regardless of the status of integral structure development, the question remains: *Is integral structure the right way to go?* To answer this question, the risk associated with repair, forming, joining, etc., must be assessed for each enabling technology. In addition, damage tolerance and durability issues must be identified and resolved for any avenue of technology development or follow-on activity.

Also, despite the designation of a most likely candidate for each structural component application, not all of these large, integral structure concepts are guaranteed to provide improvements over built-up concepts. Each application/technology combination has a different value that depends on its application and focus. If differing levels of cost reduction potential, technical risk, and implementation costs are factored in, some combinations will apply to only one structural application type, whereas other combinations could produce spin-off benefits for many areas of aircraft structure.

8.5 Conclusions and Recommendations

This long-range plan suggests further development in several areas. However, five of these areas deserve immediate or near-term attention:

- **Flat-plate testing.** Given enough time and money, Boeing Seattle would expand on crack growth testing for integral and monolithic types of IAS fuselage structures, with additional flat panel testing in 7475 plate. This is an area where knowledge and understanding are starting to build, but there is no confidence in large-scale integral structure. Testing integrally stiffened and built-up panels made of the same material would allow for a comparison of pure knock-down differences between the two structural designs.
- **Plate and extrusion machining and joining.** Damage tolerance and fail safety issues are of particular concern with large-scale monolithic parts where there is no current certification approach or methodology. Based on what is currently known from the IAS program, Boeing Seattle would pursue continued efforts in plate and extrusion integrally stiffened panel development, utilizing high-speed machining and possibly innovative joining.
- **Analysis tools.** Engineering analysis tool development and, ultimately, a certification methodology are needed and are paramount for long-range development success. Therefore, **new analysis tool development should be continued.**
- **Welding.** Welding joints and structure to create body sections is another long-term industry vision for fuselage assembly that is radical and high-risk. Innovative joining techniques would replace and thus eliminate much of the need for manual fastening and automated riveting. **The ability to weld safe and reliable aircraft structure in an economical manufacturing scenario would be an industry breakthrough that could be used for the breakthrough vision of the future.**
- **Extrusions.** In a follow-on program, extrusions are very high on the development list, because the initial development and material properties work done during the IAS program shows promise. Near-net-shaped extrusions are a likely development path, because they show a very high buy-to-fly ratio and, in combination with welding or friction stir joining, allow some high-risk/long-range stretch technology. **The successful application of near-net-shaped extrusions in fuselage structure could be a huge breakthrough in both performance and cost.**

9 Full-Scale Validation Plan

9.1 Overview

9.1.1 Deliverable

A technology development, demonstration, and full-scale validation plan for integral metallic fuselage construction that includes panels (crown, keel, side, and window belt), doors, floor grids, and bulkheads. (This work is associated with NASA SOW deliverable 3.10.)

9.1.2 Purpose

The goal of this full-scale validation plan is to outline the steps necessary to give industry and the government the confidence to implement integrally stiffened metallic structure with its associated cost and performance benefits. This plan:

- Identifies the steps and activities required to initiate and conduct technology development activities that demonstrate that a concept part is viable
- Outlines what it would take for a full-scale validation plan for integral metallic fuselage construction

9.1.3 Summary of Results

Integrally stiffened structure falls outside the current design philosophy, and minimal experience has been logged with these types of parts. Structural integrity criteria for aircraft structure have evolved as new technologies have been proven by extensive verification tests and accumulation of operating experience. The safety criteria applied to Boeing aircraft structures (see 9.4.1) must be interpreted for any new technology structural concept developed, including integral structure.

This portion of the Integral Airframe Structure (IAS) program outlines an approach leading toward full-scale testing for the given candidate parts. Because crown panel structure is one of the most sensitive, highly-loaded, and high-performing pieces of structure, it is used as an example of how panels (crown, keel, side, window belt) go through testing to reach full-scale validation. Doors, floor grids, and bulkheads are similarly tested.

Because this crown panel is integrally stiffened, it does not have redundant load-carrying members. Alternate (fail-safe) load path characteristics need to be determined. Extensive testing is typically required for commercial aircraft structure validation. Testing will be especially extensive in this case, which involves a structure that is highly loaded, without multiple load paths, and without an experiential database.

9.2 Implementing New Airplane Technologies

At Boeing, there are typically three routes that lead eventually to the implementation of new technologies on airplanes:

- Technology champion
- Funded research
- Program application

These approaches are discussed below.

9.2.1 Technology Implementation Via the Technology Champion

The strongest and most effective approach in the past has been to have an operations or chief engineer champion ideas during a new product development activity. The Design Requirements and Objectives (DR&O) document specifically addresses the early airplane configuration and scenario. Its purpose is to assist in early program direction so that configuration development and key decisions can be made in a timely manner. The intent is to meet requirements and compliance objectives, by the design of a marketable product that meets regulatory requirements and satisfies government, Boeing, and customer standards for safety, design, performance.

Factors such as the DR&O, configuration, and market niche drive the initial trade study activities, much of which is done by pulling information from the existing design and manufacturing database. This is the point at which a technology champion can be of real help in defining new technology ideas of merit.

The issue of technology readiness and development plays a critical part at this point. Technology that is not ready and cannot support the business and development cycles of the product will not be used. However, if a case can be made that a technology can be made ready for development of the airplane, then the program will provide funding to make it happen. This is a very strong position for technology development; historically, it has been the best for successful implementation of new technology.

9.2.2 Technology Implementation Via Funded Research

Another way of developing technology is more traditional funded research in manufacturing or enabling technology. In these conditions, the technology is developed based on business needs and possible application projections. These technologies are not necessarily fast-tracked, so they may follow the traditional cycles of development that reflect the ebb and flow of research money. It is often possible to successfully implement these technologies and even retrofit them on existing airplanes. Usually, a compelling business case, backed by technical performance, drives these successes.

9.2.3 Technology Implementation Via Program Application

The third way of implementing new technologies occurs when a change is needed to solve a problem. In this case, the new technology is fully tested and proven before the solution is implemented.

9.3 Implementing IAS Technology

9.3.1 Implementing Technologies Like IAS

The implementation of applications like metallic fuselage concepts for integrally stiffened construction has typically been driven by cost-reduction initiatives or design for manufacturing trade studies. During such initiatives, candidate parts are identified, and new or existing application concepts are designed with one or several manufacturing technology options. An evolution of development produces a result that, from a business and technical aspect, may lead to hardware development.

The trade study can be long and costly; if it reaches testing it can be cost prohibitive to proceed. Testing is extensive and covers all possible verification scenarios, which can mean that thousands of coupons and hundreds of elements are processed before large panels and subcomponents are even designed.

This approach is similar to the IAS program development.

9.3.2 What This IAS Program Has Accomplished

The IAS program was developed by committee based on a need for lower cost manufacturing in the airframe industry. Its champions were key players from industry and government. One difference between the IAS program and other trade-study type programs is that the scale of the testing has been cut back to a few test pieces. The IAS team has completed a screening test matrix on a candidate part to determine if performance is acceptable and business trends are favorable.

9.3.3 Moving Forward With IAS Technology

At this point in IAS technology development, it is important to closely examine the requirements for this candidate part and select the “big hitters”—the test areas with the greatest potential impact and return. One possible activity is development of forming techniques to address producibility of a compound contour panel. Another is a fatigue test of a two-bay longitudinal crack that has been arrested at two bays.

From an airplane development view, the next activity is to establish a hardware development and test task required to validate and build confidence in the technology application and concept. IAS is close to this stage, enough to show promise, yet far enough away that replicate testing of coupons and panels is needed for an airplane. Engineering preliminary sizing of a body section using integrally stiffened panels might also be advantageous. This would help identify the advantages of the design and areas requiring detail development. IAS accomplished this to some degree by optimizing the design of the two-bay test panel. The panel was sized to be performance and weight competitive to built-up crown structure.

Other details still need to be screened before proceeding. For example, drainage of condensation on side panels and belly panels requires detail development of drain holes. After the identified detail issues have been addressed and enough confidence has been gained in the structure, the full-size barrel can be designed and analyzed, and drawings can be produced. Full barrel sections are typically used for structural stability, fatigue, and then static testing of the barrel as a combined structural system.

9.3.4 Example of This Approach—777 Testing

As an example of this approach for moving forward, consider Boeing's experience with 777 testing. Initially, even though the 777 design incorporated the best known improvements for built up structure, Boeing was not confident enough in the analysis process, analysis methodology, or structural understanding to immediately drive on to large scale testing. Therefore, Boeing tested multiple large panels in the 127-inch fixture before confidence was strong enough to build a full-scale barrel test for fuselage structure. Essentially, testing was needed to evolve the design, because the analysis and structural understanding did not drive the design.

9.4 Overview of Testing and Validation Criteria

9.4.1 Structural Criteria

To a large degree, structural design and structural integrity drive testing. Proof of structural integrity and safety is typically established by analysis, and supported by structural test. Structural integrity criteria for aircraft structure have evolved as new technologies have been proven through extensive verification tests and accumulation of operating experience. Little regulatory guidance is available for how much testing is required; however, a plan that covers theoretical situations can be discussed.

All structure designed by the Boeing Commercial Airplane Group for production and certification must satisfy criteria in nine structural areas, as well as follow good safety practices in general. The general criteria for the nine structural areas are described in Table 9-1.

TABLE 9-1. SUMMARY OF SAFETY CRITERIA IN NINE STRUCTURAL AREAS

Structural Area	Criteria
Static Strength and Stiffness	Primary structure must be designed to meet Federal Aviation Regulation (FAR) requirements for limit and ultimate load.
Durability	Primary structure must be designed to resist fatigue damage for the service objective.
Residual Strength	Primary flight-loaded structure must be designed to carry limit load with at least one major structural element assumed failed.
Fail Safety	Conventional structure must have multiple elements and/or redundant load paths and have adequate crack or damage arrest capability. (This criteria is not really applicable to integral structure, for which load distribution and redistribution need to be evaluated and understood.)
Damage Tolerance	Primary flight-loaded structure must have sufficient damage growth properties and inspection characteristics so that damage is detected before the residual strength of the structure is exceeded.
Corrosion Prevention	Structure must be designed to prevent corrosion and wear damage. Adequate drain paths and a program for corrosion inspection and control must be provided. (This needs to be incorporated into IAS panel design).
Inspectability	Ease of inspection must be achieved by appropriate access to primary and secondary structure.
Producibility	Structure must be designed to ensure a high level of producibility.
Repairability	All designs must meet the need for repairability.

9.4.2 Process Criteria

Full scale validation requires that the following five things be achieved:

- Stabilized material and processes
- Producibility
- Characterized mechanical properties
- Predictability of structural performance
- Supportability

9.5 Theoretical Scenario for Crown Panel

The IAS test matrix is a starting place for establishing a screening test for a candidate integrally stiffened structure. Assuming that the screening test trend looks good, and an alloy/material form is available (for example, wide extrusion)—from the view of a commercial airframe manufacturer, what types of testing would be necessary to progress toward full-scale validation? The following discussion offers one answer, by outlining the extensive testing that a commercial aircraft would typically undergo during development. For this discussion, assume that a crown fuselage panel is the candidate part for integrally stiffened structure.

Figure 9-1 illustrates the extensive amount of testing that occurs before a commercial transport reaches full-scale validation. However, reducing the need for extensive testing is one goal of the airframe community. To assist in the interpretation of fail safety and damage tolerance for integrally stiffened structure, there will be an evolution of testing of this type of structure and a database will be developed.

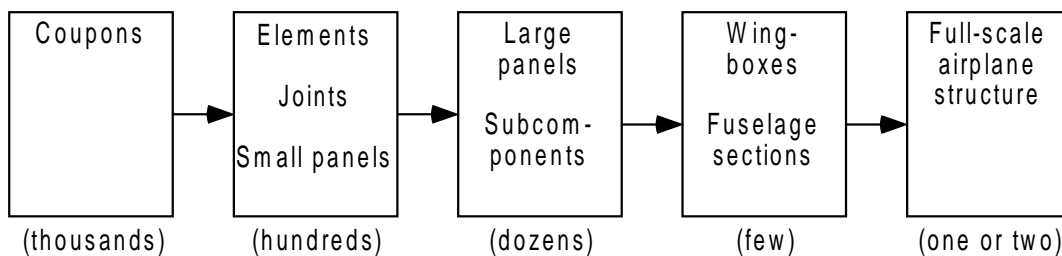


FIGURE 9-1. EXTENSIVE TESTING REQUIRED FOR FULL-SCALE VALIDATION

The ideal situation includes a material and a design with superior fatigue life and significantly slow crack growth. With integrally stiffened structure, the intent would be to design the structure so it never cracks; the only concern would be about critical crack length because of a secondary incident (such as impact with a foreign object). This situation would most likely never happen, so it would be necessary to develop the structure's durability fatigue rating. Doing so will require an extensive series of test hardware, evolutionary testing, and the latest analysis techniques. In broad terms, three types of testing would be required:

- Coupon
- Panel
- Barrel

9.5.1 Coupon Testing

The series of coupon tests is intended to yield the data that supplies the basis for sizing and capability of the local details. The term “coupon” in this context means anything that you can carry (for example, three-foot by three-foot or six-inch wide by four-foot long parts).

The first series of coupons would be **no-load transfer** coupons, to establish the no-load durability fatigue rating. The second series would be **joint transfer** or **load transfer** coupons. These might be three-row fastened joints, welded joints, or some other joint design style, and would require a series or evolution of little coupons to get a fatigue life data plan. These no-load transfer and load transfer sets of tests would indicate performance in the range of fuselage crown panel structure, with respect to some known baseline. 2024 sheet is typically used as the performance comparison baseline; testing would indicate performance better than, less than, or equal to the performance target.

Next, a series of **hardpoint** testing coupons would need to be developed, to address questions associated with hardpoint scenarios. These are all the situations that require riveted-on sheets for details, external doublers, and add-ons. These coupons establish that the structure has the capability to accept repairs and modifications in the field. For extrusion fuselage crown panels, this may require multiple coupons for shot peening, cold working, riveting on patches, and any other processing operation that may be required for a hardpoint.

If the structure continues to look good from a performance standpoint and the structural data is acceptable, it is necessary to establish fatigue ratings for the system. The fastening or joining system (mechanical, welding, etc.) must also be addressed, and a fatigue rating established for it as well.

During the coupon testing phase, multiple testing would also occur to investigate trends or scenarios for options that might improve the life of the structure (such as wider joints, four-row lap joints, cold worked holes, shot peening, etc.). The intent is to improve both the design and the established design goals. This is also an opportunity to reduce weight and optimize structure by test—that is, one of the activities is improvement of local details.

9.5.2 Panel Testing

If all coupon testing is acceptable, and the trend is favorable, the next activity would be panel testing. In general, panel testing would begin with flat panels and progress to curved panels.

9.5.2.1 Flat Panel Testing

Flat panel testing for the crown panel would include:

- Compression panel testing, which provides the opportunity to evaluate improvements that could be machined into the panels (such as discontinuous blade stiffeners between stringers).
- Crippling tests, short column for maximum load type panels
- Testing to demonstrate that the section joint design meets requirements. These tests would require a series of panels at various joint locations; this is necessary to represent the different types of joints and different loads.
- An investigation of crack growth in the circumferential direction.

For the circumferential crack growth tests, the panels might be six-feet wide by ten-feet long with no joints, and contain the basic stiffener design details with frames. These tests cycle sawcuts to investigate cross-grain crack growth. These tests also can be used to gather data about crack dwell time on stiffeners or as cracks approach stiffeners. There will also need to be a series of residual strength tests in which limit load is applied and crack arrest occurs in the outer members of the area; the test would be cycled again to investigate how the crack continues to grow into the next bays (and, ultimately, there would be three broken stiffeners). Depending on design performance, there might be a series of panels for different ultimate stress levels.

9.5.2.2 Curved Panel Testing

Curved panel testing for the crown panel might include strength tests involving shear panels and compression panels with multiple bays with frames. It might also include an investigation of the interplay between body bending and hoop loads. This would be done in the “ham can,” which is similar to the two bay longitudinal panel being done for IAS. In these tests, crack growth rate would be investigated in several areas of the panel, and sawcuts would be cycled to gather crack growth rate data. This might require several panels depending on the situation.

Much longer testing would be required for:

- Fatigue tests in panels
- Investigation of hard spots in hoop direction longitudinal lap joints
- Fatigue tests of joints

In these tests, the panels would be tested until they cracked, and, as the cracks develop, cycling would continue for crack growth data. Repairs may be made on these cracks to demonstrate the repair, further investigate additional crack growth, and test the effectiveness of the repair. This provides the opportunity to evolve a repair process. For example, if the first repair design is an underachiever, it provides an opportunity to develop ideas for repair design improvements. This may take several “improved” fatigue panels depending on the crack growth, the additive loads created by pressure, and the added stresses for the current structural design. The end product will be a worthy panel design that is lightweight and performs well.

Another series of panel tests that might occur before a full barrel section is the pressure with fore and aft loading of a curved panel to simulate body bending of a crown panel. This type of testing gives a hoop load effect at the same time there is pulling fore and aft. This is a very severe joint case, and it is conceivable that this could be done in parallel with the engineering of a barrel test.

9.5.3 Barrel Testing

On successful completion of coupon and panel testing, full-scale validation testing would finally be considered.

During panel testing, engineering and manufacturing databases grow large with information about design life, joints, and design improvements. During the testing trials, it is important to remember the perspective of the overall system view, to ensure that there is successful development across all design aspects. If this has occurred it might be possible to make a decision to begin full-scale barrel testing somewhere during the series of curved panel tests.

For barrel testing, an optimal section length must be determined. Typically, test lengths are based on the length of material that is available. This is typically approximately 35 feet. For fatigue and static testing, barrels are usually one or two body diameters in length. Longer barrel lengths can be advantageous for seeing more of the effects of bending and applied loads on the structure. For example, it may be necessary to evaluate the effect of compression loads on crown sections, in order to study the instability conditions that may occur in the panel. This phenomenon may occur only when the test barrel is long enough.

A simple barrel section could contain floor beams and beam-to-body joints. It could contain a series of windows with window cutouts, and windows could be installed to see design details in action during test. Passenger floors, cargo floors, and joint designs would be tested to ensure that the design will be viable in production.

The barrel could be attacked with sawcuts to show areas of potential weakness and to demonstrate how the barrel reacts to load redistribution and stresses. This might cause a cycle of test and redesign actions. During a full-scale barrel test, all the design details necessary to make the development producible may come into play, for example, static, shear and local bending, frame and skin connections, resolution of whether intercostals are needed in the design, and fore and aft destabilizing members.

At this point, the testing process will have led to one of two results:

- Success in answering the questions that validate analysis
- More questions are raised that require additional testing before validation is achieved

9.6 “Big Hitter” Testing Requirements for Various Structures

There is no question that airframes are vital to airplane safety and reliability. From the discussion above, it becomes apparent that, to guarantee safe and reliable performance, extensive testing is required for a commercial aircraft structure design development program. However, for each piece of structure, certain testing can be singled out as “big hitters” for the screening of performance (see Table 9-2).

TABLE 9-2. REQUIREMENTS FOR VARIOUS TYPES OF INTEGRALLY STIFFENED FUSELAGE STRUCTURES

Structure Type	Testing Requirements
Crown Panels	<ul style="list-style-type: none"> • Fatigue testing of a longitudinal two-bay arrested crack • Durability testing of larger panel
Side Panels	<ul style="list-style-type: none"> • Design development for drainage • Torsional stiffness testing • Design optimization
Window Belt	<ul style="list-style-type: none"> • Design optimization through, for example, design trades • Forming development for producibility
Belly Panels	<ul style="list-style-type: none"> • Extrusion and joining development for producibility • Design development for integration and for drainage/corrosion prevention
Floor Grid Floor Beams	<ul style="list-style-type: none"> • Accumulation of crack growth data to establish a database for damage tolerance and fail safety • Static and dynamic strength testing • Testing to determine survivability of 16-G crash loads
Doors	<ul style="list-style-type: none"> • Testing to address FAR concerns • Accumulation of crack growth data to establish a database for damage tolerance and fail safety
Bulkheads	<ul style="list-style-type: none"> • Accumulation of crack growth data to establish structure criteria • Addressing bird strike as discrete source damage, as necessary

9.7 Conclusions and Recommendations

The IAS program has been concerned with development of crack growth data, continued analysis development, interpretation of structure to meet damage tolerance and fail safety, and the methodology to achieve certification.

The plan leading to full-scale validation is one of testing to gain confidence in the structure and understand its behavior. Testing also validates analysis methods; as this evolves, it will help control the amount of testing required. Integrally stiffened metallic fuselage structure looks promising, but continued testing is needed to fully determine its merit. Large-scale use of integrally stiffened monolithic panels will require a significant testing program to establish an understanding of structural performance, validate structural integrity, and validate the analytical tools needed to effectively implement advanced designs.

10 References

- 6-1. Gruber, M. L., Mazur, C. J., Wilkins, K. E., Worden, R. E., “ Investigation of Fuselage Structure Subject to Widespread Fatigue Damage,” DOT/FAA/AR-95/47, October 1995.
- 6-2. Rankin, C. C., Brogan F. A., Riks, E., “Some computational tools for the analysis of through cracks in stiffened fuselage shells,” Computational Mechanics, 1993.
- 6-3. Larson, B. F., “C-17 Material Specimen Tests for Fracture Mechanics Data; Phase I, Lot 1 Aluminum Alloys; Final Technical Report,” MDC J9483-1, June 1987.
- 6-4. “Fatigue Crack Growth Computer Program ‘NASA/FLAGRO’ Version 2.0 Revision A,” JSC-22267A, May 1994

Appendix A

Forming Technology Assessment for Integral Airframe Structures

Following is the Boeing Seattle report “Forming Technology Assessment for Integral Airframe Structures (IAS),” also referred to as the “IAS White Paper,” dated December 12, 1996.

A. Ground rules:

1. Material: aluminum, 7XXX extrusion or plate (7050 is a candidate)
2. Thickness: begin with 2" - 2.5" thick then machine to final skin thickness with stiffeners
3. Panel size: 10' X 15'
4. Contour: simple contour

B. Design concept

1. **Machine integral iso-grid/bi-directional stiffener from a thick plate then form it (chip form, roll form, age/creep form)**

Advantage:

- Integrally stiffened structure

Disadvantage:

- Mark off (on smooth skin side) may be a problem.
- Need to know more about crack growth and Durability, Allowables, and Damage Tolerance (DADT)

Remark:

- This design had been tried in Space Station project at Huntsville in 1986. Mark-off and localized fracture had been experienced. To prevent mark off, machine pockets can be filled with rubber/urethane (liquid or machined block) so that the panel has an uniform thickness for forming. To prevent localized fracture, panel should be formed gradually in small increments. Age/creep formed panel may produce more consistently smooth contour than chip formed or roll formed panel. However, age/creep forming requires longer cycle time, support tooling, and more expensive autoclave to form. Roll forming is another alternative forming method. However, there is certain limit in panel size and thickness which can be investigated further when needed.

2. Machine integral channel/longitudinal stiffeners and skin from a thick plate then form it (chip form, roll form, age/creep form, stretch form, shrink form)

Advantage:

- Integrally stiffened structure
- Easier to form than Concept 1

Disadvantage:

- Mark off (on smooth skin side) may be a problem.
- Need to know more about crack growth and DADT

Remark:

- The main difference between this concept and concept 1 is that concept 2 uses channel stiffeners, while concept 1 panel is machined into iso-grid stiffener type. Forming is easier, machining is easier, but panel may be less stiff compared to concept 1. Stretch form is probably the best method for this concept.

3. Machine integral channel stiffened panel from a “comb” shape extrusion, then form it (chip form, roll form, age/creep form, stretch form, shrink form)

Advantage:

- Integrally stiffened structure
- Easier to form than Concept 1
- Easier to machine

Disadvantage:

- Mark off (on smooth skin side) may be a problem.
- Need to know more about crack growth and DADT
- Not strong as sheet or plate
- Residual stress may be a problem

Remark:

- This concept is similar to the concept 2, but panel is machined from an extrusion. Formability is about the same as, and machine will be less than concept 2. However, quality of extrusion can be a minus since porosity is a common problem with extrusion.

4. Form (stretch form, roll form, age/creep form) a thick plate to a contour then machine it.

Advantage:

- Integrally stiffened structure, one piece panel
- No mark off

Disadvantage:

- Difficult to machine, need 5-axis machine
- Blending (radius at stiffener leg and skin) can be a problem
- Need to know more about crack growth and DADT

Remark:

- This process is a reverse process to concepts 1 and 2. This process will eliminate mark off and the fracture problem as described in concept 1 and 2. The main problem for this concept is very difficult to machine (requires 5-axis machine), and also stress relief, spring back after machining is unknown.

5. Casting largest possible panels then join them together (riveting, welding)

Advantage:

- Integrally stiffened structure, one piece panel
- Quick cycle time, no machining or forming needed
- Consistent contour

Disadvantage:

- Not structurally strong as other concepts
- Defect in casting process
- Dimensional accuracy of large casting probably would require machining to correct configuration
- Need to know more about crack growth and DADT

Remark:

- This concept has low acceptability for integrally stiffened structure.

6. **Extrude skin and channel stiffener in one piece, then join them together (riveting, welding)**

Advantage:

- Integral stiffened structure
- Quick cycle time, no machining or forming needed
- Consistent contour
- Friction stir welding may work very well for this option

Disadvantage:

- Not structurally strong as other concepts
- Need to know more about crack growth and DADT

Remark:

- It can be done in small scale prototype, but we do not know if it can be done at a full size fuselage panel because distortion is one extrusion problem. Again, porosity in extrusion is another concern.

C. Forming technology assessment

High risk:

1. Drape forming
2. Shrink forming
3. Casting
4. Grid/frame and skin separate (Bonding together)

Moderate risk

1. Stretch forming (Longitudinal only)
2. Extruded then uncoil, plus friction stirring welding (Longitudinal only)
3. Creep forming
4. Chip forming
5. Roll forming
6. Shotpeen (Prestress) forming
7. 5 axis machining

Details:

1. Elastic drape forming

Advantage:

- Low tooling cost
- Short cycle time

Disadvantage:

- High stress/preload
- No experience

Remark:

- Low success possibility.
- It is formed by gravity pulling part into shape by its own weight.

2. Shrink forming:

Advantage:

- Somebody is doing it (Deutsche Aerospace)
- Low tooling cost
- No mark-off

Disadvantage:

- Limited compound contour capacity
- Labor intensive (A new tool that allows forming at multiple locations will help)
- Low repeatability, operator dependence factor may be high
- No experience
- No spec coverage

Remark:

- Low probability of success
- New technology to Boeing. A special tool grabs two adjacent stiffeners and pulls them closer as skin is bent to contour at the same time. It is labor intensive and requires a highly skilled operator. This technology can be improved if we have a tool that can form at multiple locations at once and fully automate process.

3. Casting:

Advantage:

- High repeatability contour

Disadvantage:

- Limit in minimum thickness
- Low in DADT
- Rough surface finish
- Defects (porosity)

Remark:

- Low probability of success
- Squeeze casting is believed better than conventional casting because it can produce thinner wall than conventional casting. Russia is doing some squeeze casting.

4. Grid/frame and separate skin, then bond them together:

Advantage:

- Easier to form, compared to integrally stiffened skin

Disadvantage:

- Difficult bonding them together (easy having void/unbond since contour of both pieces have to be matched near perfect.

Remark:

- Low probability of success
- Skin and stiffener are manufactured and formed separate, then bond them together. Not much advantage comparing to the current method of fuselage manufacturing.

5. Stretch forming:

Advantage:

- Moderate tool cost
- Quick cycle time
- Repeatable

Disadvantage

- Press tonnage availability
- Constant cross section
- Stiffener parallel to pull direction only, no Iso-grid type stiffener
- Limit thickness (depend on press tonnage)
- Temper limitation
- Require a lot of excess on both ends.

Remark:

- Medium risk
- Skin and stiffeners are machined from plate or extrusion then stretch form it.

6. Extruded, uncoil and Friction Stir Welding (FSW)

Advantage:

- No machining
- Easy to form without mark off
- Quick cycle time

Disadvantage:

- Low acceptance from engineering stand point comparing to sheet form
- Limit width to 80" diameter (251" or 20' if flatten out)
- Length limitation: unknown

Remark:

- Technology is available for at least ten years. However, because engineering prefers sheet form, therefore not much DADT available.
- Medium risk
- FSW is a fairly new technology that can weld aluminum alloy (similar or dissimilar), that conventional welding cannot. See section 12 for more information about FSW.

7. Creep/Age forming:

Advantage:

- Repeatable contour
- Some capability on compound contour
- Aging and forming at the same time

Disadvantage:

- Long autoclave time
- Facility/equipment availability
- Not good on some compound contour
- 2XXX alloy is generally not amenable to process as is used in T3 (However, 2XXX presently is alloy of choice for fuselage)
- Property change as forming

Remark:

- Textron is a major subcontractor of Airbus, doing a lot of age forming
- Boeing of Georgia had formed iso-grid panels for space station
- Medium risk

8. Chip forming

Advantage:

- Low tooling cost
- Short cycle time
- Adaptable to different contour
- Width is up to 28' (Boeing)

Disadvantage:

- Low contour repeatability
- Mark-off
- Simple contour only
- Buckling on stiffener that is perpendicular to contour direction
- Difficult to handle while forming.

Remark:

- Mark-off, repeatability are the main problems of this process. Fully automated chip forming will have more consistent contour.
- May need using urethane as support material in pockets/channels for forming.

9. Roll forming

Advantage:

- Low tooling cost
- Low cycle time
- Adaptable to different contour

Disadvantage:

- Mark-off
- Simple contour only
- Buckling on stiffener that is perpendicular to contour direction
- Difficult to handle while forming
- Limited thickness

Remark:

- Mark-off, repeatability are the main problems of this process
- May need to use urethane as support material in pockets/channels for forming.
- Wichita may have capability to roll form a panel 10' X 15' size

10. Shotpeen forming:

Advantage:

- No tooling cost
- Short cycle time
- No size limitation
- Good fatigue property

Disadvantage:

- No severe contour
- No clad skin
- Bi-directional contour occurs unless special efforts used (such as prestress)
- Channel stiffener forms better than Iso-grid type because Iso-grid type may result in oil canning/pillowing appearance.
- Little experience
- Moderate repeatability

11. 5-axis machining

Advantage:

- No forming required in some cases
- High repeatability
- Moderate cycle time

Disadvantage:

- No 5-axis machine available

Remark:

- A plate can be formed then prestressed flat again then machined in flat condition. This has been attempted in the past but not very successful. However, other option is form a plate then put it into a contour tool, vacuum the plate onto the tool and then machine.

Friction Stir Welding

It is a new technology which has been developed 6 years ago. No application yet for Boeing production, even though there are potential applications identified for the future. Application for industry wide is unknown. Airbus has shown interests in this technology in "welded airplane". There was demonstration of this technology in welding a space shuttle fuel tank, but not actual application yet. There is a team of Operations Technology, BMT, SDT, SMA evaluating this technology, that is including obtaining durability and damage tolerance (DADT). No spec yet available.

Process itself can be described as a sub-liquid welding (some people prefer it as solid welding state), because material is close to but not quite to liquid state during the process. Two pieces of material can be held together an adequate pressure, a high speed rotating pin (length is about as same as to the thickness of working piece) runs along the seam from one end to another. Friction between the rotating pin and working material creates heat, bringing material on both pieces to near liquid state, and they are joined.

This technology will be used in Boeing only after material issues addressed and acceptable design concepts can be offered. Ops Tech is running test to obtain data on Durability and Damage Tolerance (DADT), and crack growth. Ops Tech is putting in an experimental unit of Friction Stir Welding in 17-04 building in Auburn (Cost about \$300,000.00) and it will be ready for test by 1997. Working envelop for this machine is 4' X 10'.

Advantage:

- Can weld aluminum (even alloys not conventionally weldable), including dissimilar aluminum alloys. About 1/3" wide strip along the join, it will have a mixture of both alloys (if they are different alloy), therefore that strip will have mixed property of both.
- Smaller heat affected zone than conventional welding or diffusion bonding.
- Lighter weight comparing to a conventional panel with rivets.

Disadvantage:

- Large, heavy machine
- Butted join is the best way to weld, cannot do lap join
- No spec coverage at this time
- No DADT data
- Little experience
- Strength loss is about 15 - 20% at the join area
- Lower corrosion resistant than original material
- Limit welding length, unless there is a tool is specially set up for it
- May require local aging to provide acceptable property

Remark:

- Ability to weld aluminum alloys, even dissimilar, which cannot be done well by conventional welding.
- Lower strength alloy is easier to weld
- Clad skin is not recommended
- Speed: 1/2" thick plate can be welded at a speed of 5-6 feet per minute. Speeds are expected to improve with development

Appendix B

IAS Program Test Matrix

Following is the final IAS program test matrix.

Integral Aircraft Structures Test Matrix

Test Group	Type	Configurations	No Specimens Per Lot					Assignee (d=design, f=fab, t=test)					
			Plate			Extr.		Other	MDC	BAC	LM	NG	NAS A
			7050-T7451, 1.5"	7050-T7451, 2.5"	7475-T7351, 1.5"	7050-T74511	6013-T651X						
Material Properties	1	Static Tensile	L	3	3	3	3	3			d,f		t
			LT	3	3	3	3	3			d,f		t
			ST	2	2	2	2	2			d,f		t
	2	Fatigue (Unnotched, R=.05)	L (flush side)	5	5		5				d,f		t
			LT (flush side)	5	5		5				d,f		t
			L (t/2)	5	5						d,f		t
		Fatigue (Open Hole, R=.05)	L (flush side)	5	5		5				d,f		t
			LT (flush side)	5	5		5				d,f		t
			L (t/2)	5	5						d,f		t
	3	Crack Growth/R-Curve flush side	CCT, 24 in, t=.06 L-T	1	1	1	1	1			d,f		t
			CCT, 24 in, t=.06, T-L	1	1	1	1	1			d,f		t
			CCT, 24 in, t=.148, T-L			1					d,f		t
			CCT, 12", T-L, t=.12	1	1		1				d,f		t
			CCT, 12", L-T, t=.06	2	2		1				d,f		t
			CCT, 12", T-L, t=.12	1	1		1				d,f		t
			CT, L-S, t=.06	1	1		1				d,f		t
	CT, L-S, t=.06	1	1		1				d,f		t		
	4	Determination of r _c flush side	DCB (L-T)	9						d,t	f		
			DCB (T-L)	9						d,t	f		
			DCB (T-L)					5		d,f,t			
			DCB/SDCB (L-T)				7		d	f,t			
DCB/SDCB (T-L)						7		d	f,t				
Structural Details	5	Thickness Interface	-3 (24", Rfillet=.063)	2						d,f	t		
			-5 (24", Rfillet=.188)	2						d,f	t		
			-9 (18", Rfillet=.188)	4						d,f	t		
			-11 (12", Rfillet=.063)	2						d,f,t			
			-13 (12", Rfillet=.188)	2						d,f,t			(1)t
	6	Basic Stiffener Fatigue	Rfillet=.063	10						d,f			t
			Rfillet=.120	10						d,f			t
			Rfillet=.188	10						d,f			t
	7	Mechanical Joints	Static	Longitudinal	1					d,f			t
			Fatigue		4					d,f		t	
Static			Transverse	1					d,f			t	
Fatigue				4					d,f		t		
8	Friction Stir Weld	Static	LT	6					d,f			t	
		Fatigue	LT	10					d,f			t	
		Corrosion		2					d,f			t	

Test Group	Type	Configurations	No Specimens Per Lot					Assignee (c=design, f=fab, t=test)					
			Plate			Extr.		Other*	MDC	BAC	LM	NG	NAS A
			7050-T7451, 1.5"	7050-T7451, 2.5"	7475-T7351, 1.5"	7050-T74511	6013-T651X						
Panels	9	Flat Repair Panel (Fatigue)			1			d	f			t	
	11	Unpressurized Circ. Crack (FCGR/Res. Strength)	Panel #1	1				d			f	t	
			Panel #2				1	d			f	t	
	12	Pressurized Circ. Crack (FCGR/Res. Strength)	Panel #1	1				d			f	t	
			Panel #2				1	1	d			f	t
	13	Tens., Press.: FCGR/Res. Strength	Long. Crack #1			1			d,f,t				
	14	Compr.: Static unnotched	Curved long.#1	1					d			f	t
			Curved long.#2					1	d			f	t
	15	Shear: Static unnotched	Curved shear#1	1					d,f,t				
			Curved shear#2					1	d,f,t				
16	Demo Panels	Singly curved				1			d,f				
		Doubly curved		1				d		f			

*Other materials include: 7050-T6511 extrusion, 7475-T7351 plate (a different lot than the one IAS purchased), and 2324-T39 plate.

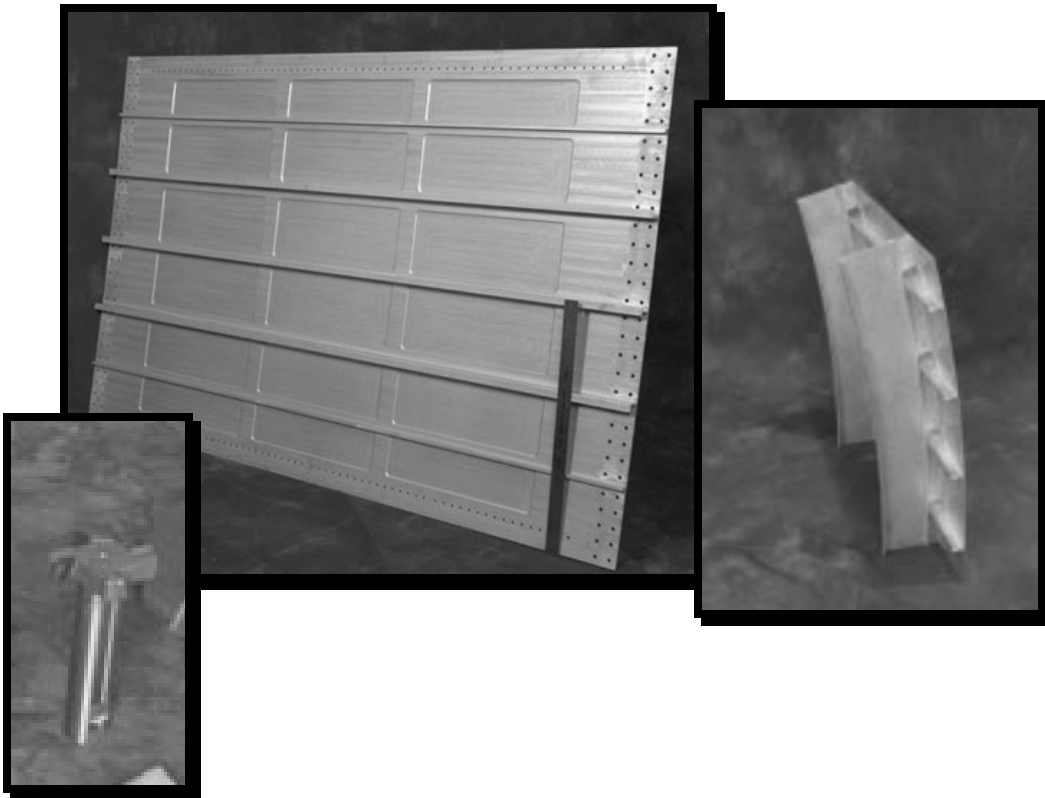
Note: Shaded boxes indicate tests not completed under this phase of the program.

Appendix C

Integral Airframe Structures Test Panel Fabrication

Following is the Northrop Grumman report “Integral Airframe Structures Test Panel Fabrication,” dated February 23, 1998.

**Northrop Grumman
Commercial Aircraft Division
Manufacturing Technology**



Integral Airframe Structures

Test Panel Fabrication

February 23, 1998

Project Manager

Jerry Griffith

Project Engineer

Patrick Porowski

Table of Contents

1.0 Abstract	C-5
2.0 Introduction	C-5
3.0 Material	C-7
4.0 Project Description	C-8
5.0 Cutter Tools and Machining Equipment	C-8
6.0 Process Flow	C-10
7.0 Vericut Model Machining Times	C-11
8.0 Actual Machining Times	C-14
9.0 Test Panel Weight Study	C-16
10.0 Dimensional Accuracy of the Panels	C-17
11.0 Conclusion	C-18
12.0 Appendix	C-19

List of Figures

Figure 2.1: IAS Compression Panel	C-6
Figure 2.2: IAS Tension Panel	C-6
Figure 2.3: End Grip	C-7
Figure 2.4: Strut Plate	C-7
Figure 5.1: Cutters Used on IAS Panels	C-9
Figure 5.2: CNC Mill Used to Machine IAS Panels	C-10
Figure 9.1: Material Utilization Using Monolithic Machining	C-16

List of Tables

Table 7.1: Vericut Data on Tension Panels	C-13
Table 7.2: Vericut Data on Compression Panel	C-13
Table 7.3: Vericut Data on Compression Panel Frames	C-14
Table 8.1: Actual Machining Times for the Tension Panel	C-15
Table 9.1: Aircraft Structure Weight	C-17

Integral Airframe Structures

Test Panel Fabrication

1.0 Abstract:

The Integral Airframe Structures project is a NASA program and was established to develop methods for manufacturing aerostructures more economically. This is to be accomplished through the development and validation of integral stiffened structure. The areas of study include; application of advanced materials processes, durability and damage tolerance testing and analysis, cost modeling, and the fabrication and testing of integrally stiffened subcomponents. Through this approach, the objective of significantly reducing the manufacturing costs of fuselage structure is hoped to be achieved. This phase of the program is focusing on machined from plate structure.

2.0 Introduction:

The manufacturing of aircraft is a very time consuming and expensive process. Many technologies are currently being implemented to reduce the manufacturing cost and time in order to improve quality and satisfy demand. Perhaps the greatest success in technology has evolved in the use of monolithic manufacturing. Monolithic manufacturing consists of machining a solid billet of material into a part that would otherwise be built up from many different parts and fasteners. With this technology however, many variables must be accounted for to assure strength, weight, and performance characteristics.

There are three main characteristics in monolithic manufacturing that must be validated to be successful. First, the structural performance must be maintained. The part must be able to arrest cracks within itself, avoiding crack propagation. In a built up fuselage, the structure is made up of separate components which include skins, longerons, and z-frames. These built up structures allow cracks to arrest within a specified area in an individual component preventing large fractures from occurring. The purpose of this task

is to determine how a monolithic fuselage panel, such as the one shown in figure 2.2, will react by initiating a crack in the structure under a specified stress.



Figure 2.1: IAS Compression Panel



Figure 2.2: IAS Tension Panel

Northrop Grumman has the task to fabricate 3 static test panels and Boeing, South has the design responsibility. Two tensile and one compression panel were fabricated for the task, shown in figure 2.1 & 2.2. In addition, several other pieces of hardware were needed which include the following. First, a pair of end grips that are to be attached to the ends of the two tension panels built. These end grips, as seen in figure 2.3, will be used to connect the panels to the tensile machine that will be used in pulling the part at NASA Langley. Second, a set of six strut plates were manufactured to support the panels in the test, shown in figure 2.4. Third, a set of eight angle iron brackets were fabricated to support the strut plates. Fourth, a wooden box was built which will be mounted to the skin side of the tension panels and a vacuum will be pulled on it during the test. This vacuum box is designed to simulate a pressurized fuselage during the experiment.



Figure 2.3: End Grip



Figure 2.4: Strut Plate

3.0 Material:

The material used to manufacture the three panels is a 7050 series aluminum alloy composed of zinc and magnesium that results in a heat-treatable alloy of high strength. The material is a precipitation heat treated by a process that provides good corrosion resistance while maintaining high strength characteristics. The two tension panels are made of 1.5 inch thick 7050 - T7451 plate stock that was provided to us by Boeing, South. The material used to fabricate the compression panel and test hardware was provided by Northrop Grumman. The compression panel was made from 1.5 inch thick 7050 - T7451 plate stock. The end grips were fabricated out of 3 inch thick 7075-T651 plate which has a slightly higher yield and ultimate tensile strength than 7050 plate.

The truss plates are made of $\frac{3}{4}$ inch thick 2024-T3 aluminum alloy plate which is largely composed of copper as the principal alloying element. This material does not have the corrosion resistance that the 7050 series has but provides moderate strength that is needed in the support of the panel for this given test. Finally, the vacuum box was built out of 1.5 inch thick plywood, which will be used to secure the tension panels during the test.

4.0 Project Description:

Three test panels were fabricated along with the support fixturing according to engineering tolerances. In addition, several other requirements were established.

- NC programming on the panels and support fixturing is to be done by Northrop Grumman.
- A Vericut simulation of the NC program will be run and a report detailing process parameters and total run time will be generated.
- Setup time and cutter change times will be measured during production to validate the Vericut data.
- The Vericut simulation will be run to provide data that would be representative of fabricating these panels as production items.
- Data will be provided on the total wetted area of the finished part and the machined excess area based on the Unigraphics model.
- The three panels are to be bump formed to a 118.5” radius by Micro Craft located in Hampton, VA.
- Upon the completion of all parts, the report will be sent to the NASA Langley Research Center.

5.0 Cutter Tools and Machining Equipment:

The cutting tools used in this program consist of six different cutters which include standard end mills and two custom made cutters as seen in figure 5.1. The tools are described below and specifications on the tools can be seen in table 7.1.

- Tool 1 is a six inch diameter face mill which is used in facing the material during the material preparation stage of the process.
- Tools 2 and 3 are custom made cutters used to cut the radius specifications called out by the engineering design drawings. The tools were designed not only to cut the given radius dimensions, but also had to be of a diameter that could reach under the

integral stringer flanges to cut the designed profile. Both cutters are four flute with two effective cutting surfaces. Each cutter is three inches in diameter with a seven inch overall length and a 1.25 inch shank diameter. The main difference between the two cutters is in the cutting radius. Cutter 2 is responsible for cutting the radius along the integral stringers of .09 inch and cutter 3 is responsible for cutting the floor pocket at a radius of .190 inch.

- Tool 4 is a 2 inch diameter end mill that was used to remove large amounts of material in rough cutting the panels during the initial stages of the process.
- Tool 5 is a 1.5 inch diameter end mill that was used to remove large amounts of material in rough cutting the panels during the initial stages of the process.
- Tool 6 is a ¾ inch diameter end mill that was used to part the panels from the excess stock.

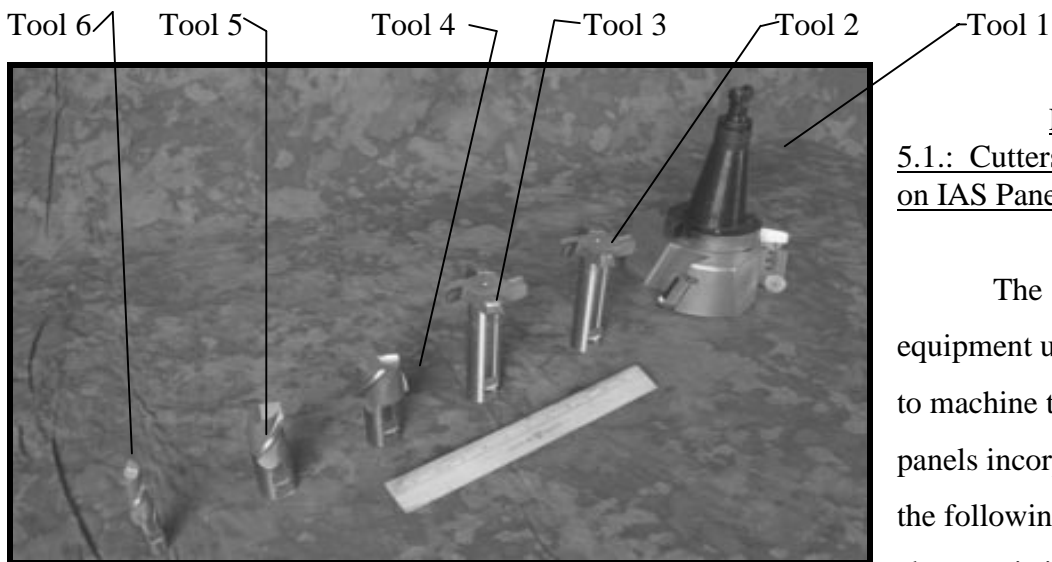


Figure 5.1.: Cutters Used on IAS Panels

The equipment utilized to machine the IAS panels incorporated the following characteristics.

The machine used was a Cincinnati Milacron horizontal spindle CNC mill, model TC-15 as seen in figure 5.2.

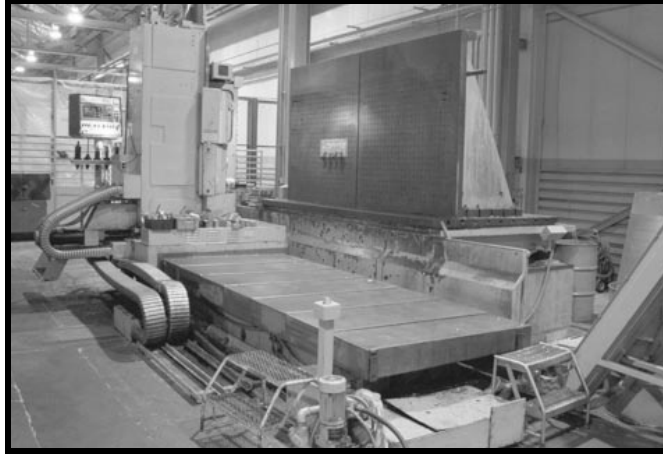


Figure 5.2: CNC Mill Used to Machine IAS Panels:

The three axis mill is powered by a 25 HP motor that is capable of producing spindle speeds between 20 and 2500 rpm. The machine has the following travel parameters; X Axis = 120”, Y Axis = 60”, and Z Axis = 32”.

6.0 Process Flow:

The tension panels, compression panel, and compression panel frames were made with the following sequence.

- Material was sent from Boeing, South to Northrop Grumman for the tension panels at precut lengths. Material for the compression panel and the compression frames was provided by Northrop Grumman.
- Engineering files on the parts were supplied to us in Unigraphics by Boeing, South.
- N/C programming on the parts was completed by Northrop Grumman.
- A vacuum fixture was used to secure both the tension and compression panels throughout the machining process.
- Material for the parts were surfaced on one side using tool 1, the 6 inch diameter face mill. Pin-up holes were placed in the excess material to aid in securing the parts during machining.

- The parts were then fabricated using the Vericut generated machining programs on the Cincinnati three axis machine.
- The parts were removed from the machine and separated from the excess material.
- Deburring using scotch bright and sandpaper was completed.
- Inspection of the physical features of the parts was done using various measuring aids and dye penetrant inspection was performed to assure no cracks existed within the machined parts.
- The tension and compression panels were sent to Micro Craft, Hampton VA. for bump forming. Both the compression panel and tension panels are to be formed to a 118.5 inch radius to simulate a consistent section of fuselage.
- Following bump forming, the two tension panels were delivered to NASA LaRC by Micro Craft.
- The compression panel will be sent back to Northrop Grumman after bump forming for assembly of the frames. The frames are attached to the compression panel with NAS counter sunk fasteners. The compression panel assembly was then shipped to NASA LaRC.

The test fixture components, which include the end grips, angle iron braces, strut plates, and vacuum box were made with a similar process flow. The panels and test fixture components were then shipped to NASA LaRC.

7.0 Vericut Model Machining Times:

Vericut was used to determine the optimum machining sequences to manufacture both the tension panels, compression panel, and frames. Data was collected and placed in table form as seen in tables 7.1 for the tension panels, 7.2 for the compression panel, and 7.3 for the compression frames. The data includes many machining characteristics on the three different parts. The tools are listed in the order that they were used and the cutting times are listed for each tool. These times do not include set-up time or tool changes throughout the process. The tables include the following information in column form.

- The T/S and Profile column is a code number assigned to the tool being used.
- The tool diameter section gives the cutting diameter of the tool.
- The cutting time column gives the time that the cutter is machining. This figure is taken from the time the cycle start button is pushed to the time the tool finishes its operation including traverse movements throughout the cycle.
- The chip load column gives the load on the tool in inches.
- The number of flutes column tells the amount of cutting surfaces the tool incorporates.
- The spindle speed column gives the rotational speed of the spindle in revolutions per minute.
- The feed rate is given in inches per minute which is the distance the cutter moves in inches during a minutes time.
- The cutting speed is given in square feet per minute.
- The depth of cut section in the tables consist of the maximum material removal using the particular cutter.
- The material removal rate is given in cubic inches per minute.

According to the Vericut simulation the parts had the following machining times. Table 7.1 shows a tension panel required 1069 minutes, or 17.8 hours, of continuous machining time. Table 7.2 shows that a compression panel required 412 minutes, or 6.87 hours, of continuous machining time. Table 7.3 shows that a frame for the compression panel required 152.9 minutes, or 2.55 hours, of continuous machining time.

Table 7.1: Vericut Data on Tension Panels

Tool #	T/S and Profile #	Tool Diameter	Cutting Time	Chip Load	# of Flutes	Spindle Speed	Feed	Cutting Speed	Depth of Cut	MRR
1	Ingersoll I-MAX	6.00 inch	37.43 min.	.002 in	6	2500 rpm	30 in/min	4000 SFM	.06 in	11 in cub. / min
2	115.055-2004 52330	2.00 inch	685.54 min	.01 in	2	1530 rpm	30 in/min	800 SFM	.25 in	15 in cub. / min
3	115.055-1501 50510	1.5 inch	220.39 min.	.006 in	2	1950 rpm	25 in/min	950 SFM	.25 in	9 in cub. / min
4	115.055-1006 51830	1.0 inch	41.28 min.	.004 in	2	2500 rpm	20 in/min	650 SFM	.125 in	2.5 in cub. / min
5	Custom T Cutter	3.0 inch	47.34 min.	.009 in	4	2500 rpm	90 in/min	2000 SFM	.25 in	65 in cub. / min
6	Custom T Cutter	3.0 inch	7.75 min.	.009 in	4	2500 rpm	90 in/min	2000 SFM	.25 in	65 in cub. / min
7	112.019-0059	.109 inch	7.26 min.	.001 in	3	2500 rpm	10 in/min	100 SFM	.0625 in	.5 in cub. / min
8	112.023-4204	.312 inch	2.79 min.	.04 in	1	2400 rpm	18 in/min	200 SFM	.25 in	1.5 in cub. / min
9	112.034-1066 NUCON 77	.250 inch	2.64 min.	.07 in	1	2400 rpm	20 in/min	170 SFM	.25 in	1 in cub. / min
10	115.055-0701 53950	.75 inch	16.8 min	.025 in	2	1950 rpm	90 in/min	380 SFM	.5 in	35 in cub. / min
			Total Cutting Time =	1069.22 min						

Table 7.2: Vericut Data on Compression Panel

Tool #	T/S and Profile #	Tool Diameter	Cutting Time	Chip Load	# of Flutes	Spindle Speed	Feed	Cutting Speed	Depth of Cut	MRR
1	Ingersoll I-MAX	6.00 inch	10.51 min	.002 in	6	2500 rpm	30 in/min	4000 SFM	.06 in	11 in cub. / min
2	115.055-2004 52330	2.00 inch	206.41 min	.01 in	2	1530 rpm	30 in/min	800 SFM	.25 in	15 in cub. / min
3	115.055-1501 50510	1.5 inch	112.62 min	.006 in	2	1950 rpm	25 in/min	950 SFM	.25 in	9 in cub. / min
4	115.055-1006 51830	1.0 inch	36.63 min	.003 in	2	2500 rpm	15 in/min	650 SFM	.125 in	1.3 in cub. / min
5	Custom T Cutter	3.0 inch	18.55 min	.009 in	4	2500 rpm	90 in/min	2000 SFM	.25 in	65 in cub. / min
6	Custom T Cutter	3.0 inch	8.84 min	.009 in	4	2500 rpm	90 in/min	2000 SFM	.25 in	65 in cub. / min
7	115.055-0701 53950	.75 inch	18.64 min	.025 in	2	1950 rpm	90 in/min	380 SFM	.5 in	35 in cub. / min
			Total Cutting Time =	412.20 min						

Table 7.3: Vericut Data on Compression Panel Frames

Tool #	T/S and Profile #	Tool Diameter	Cutting Time	Chip Load	# of Flutes	Spindle Speed	Feed	Cutting Speed	Depth of Cut	MRR
1	115.055-1006 50920	1 in	123.77 min	0.025	2	1900 rpm	100 in/min	500 SFM	.25 in	25 in cub. / min
2	115.055-0701 52570	.75 in	29.15 min	0.003	2	2400 rpm	15 in/min	480 SFM	.5 in	6 in cub. / min
			Total Cutting Time = 152.92 min							

Vericut gives a good indication of what the machining times would be in a production setting. However, in building a first article prototype there are always things that must be reevaluated to optimize the process.

8.0 Actual Machining Times:

The actual machining times were observed to validate the accuracy of the vericut data, shown in table 8.1. However, the data that was collected does not correctly represent the time it would take to machine the panels in a production setting. The data collected correctly represents a first article prototype. The tool number column represents the percentage of the predicted vericut times that the process was run at. The large panel took 1603 minutes or 27 hours of cutting time which is 9.2 hours more than the vericut simulation. The reason for the actual cutting time being only 66 percent of the vericut data is a result of many factors. First, the N\C machining code was over ridden several times. This is due to being a first article prototype job which required additional set-up time for the material and tool changes. Second, in a production setting larger equipment would be used to machine the parts which would work faster than the milling machine used.

Table 8.1: Actual Machining Times for the First Article Tension Panel

Tool #	T/S and Profile #	Tool Diameter	Cutting Time	Chip Load	# of Flutes	Spindle Speed	Feed	Cutting Speed	Depth of Cut	MRR
1 @ 62%	Ingersoll I-MAX	6.00 inch	60 min.	0.002 in	6	2500 rpm	19 in/min	4000 SFM	.06 in	6.5 in cub. / min
2 @ 76%	115.055-2004 52330	2.00 inch	900 min.	0.007 in	2	1530 rpm	23 in/min	800 SFM	.25 in	11 in cub. / min
3 @ 56%	115.055-1501 50510	1.5 inch	390 min.	0.004 in	2	1950 rpm	14 in/min	950 SFM	.25 in	5 in cub. / min
4 @ 69%	115.055-1006 51830	1.0 inch	60 min.	0.003 in	2	2500 rpm	14 in/min	650 SFM	.125 in	1.5 in cub. / min
5 @ 53%	Custom T Cutter	3.0 inch	90 min.	0.004 in	4	2500 rpm	47 in/min	2000 SFM	.25 in	35 in cub. / min
6 @ 43%	Custom T Cutter	3.0 inch	18 min.	0.004 in	4	2500 rpm	38 in/min	2000 SFM	.25 in	28 in cub. / min
7 @ 29%	112.019-0059	.109 inch	25 min.	0.001 in	3	2500 rpm	3 in/min	100 SFM	.0625 in	.5 in cub. / min
8 @ 40%	112.023-4204	.312 inch	7 min.	0.003 in	1	2400 rpm	7 in/min	200 SFM	.25 in	.5 in cub. / min
9 @ 33%	112.034-1066 NUCON 77	.250 inch	8 min.	0.003 in	1	2400 rpm	7 in/min	170 SFM	.25 in	1 in cub. / min
10 @ 37%	115.055-0701 53950	.75 inch	45 min.	.008 in	2	1950 rpm	33 in/min	380 SFM	.5 in	17 in cub. / min
			Total Cutting Time =	1603 min.						

In conclusion, the two panels provided the data necessary to free the process of anomalies and would follow the Vericut data closely in a production setting. The data in table 8.1 should only be used for an estimate on a prototype panel.

The set up time for this job which includes tool changes, material preparation, and set-up was approximately 8 hours. The total time for the job is 35 hours which does not represent the time it would take to manufacture this part in a production environment. In a production environment the panels can be made closer to the Vericut data found in table 7.1 due to many characteristics. First, in a production setting the programs are proved and the operators are more familiar with the machine movements which allows for faster machining. Second, the production equipment is more rigid than the machine used to make the test panels. A gantry machine used in production is able to absorb the shock

produced in taking the larger cuts in the metal. Third, having proved set-up instructions for a job also makes a big difference in cutting time in an operation such as this. During the process of machining the test panels, many bugs were found in the program as well as the set up that had to be worked out before a successful outcome prevailed. Finally, automated tool changers are found on some of our machining centers that could be implemented into this process for quicker tool changes.

9.0 Test Panel Weight Study:

After the three panels were machined weight measurements were taken to evaluate material utilization efficiency for the process, shown in figure 9.1 below. First, the two tension panels had a final weight of 48 lbs. each but were of different initial raw stock sizes. In tension panel #1 the raw weight of the material was 612 lbs. with a finished panel weight of 48 lbs. This amounts to 92 percent of material removal from the initial stock for tension panel #1. Second, the compression panel had an initial raw weight of 273.6 lbs. with a finished panel weight of 11.6 lbs. This amounts to 96 percent material removal from the raw stock. Finally, the compression panel frames had an initial raw weight of 57 lbs. with a finished weight of 1.96 lbs. This amounts to 96 percent material removal from the raw stock.

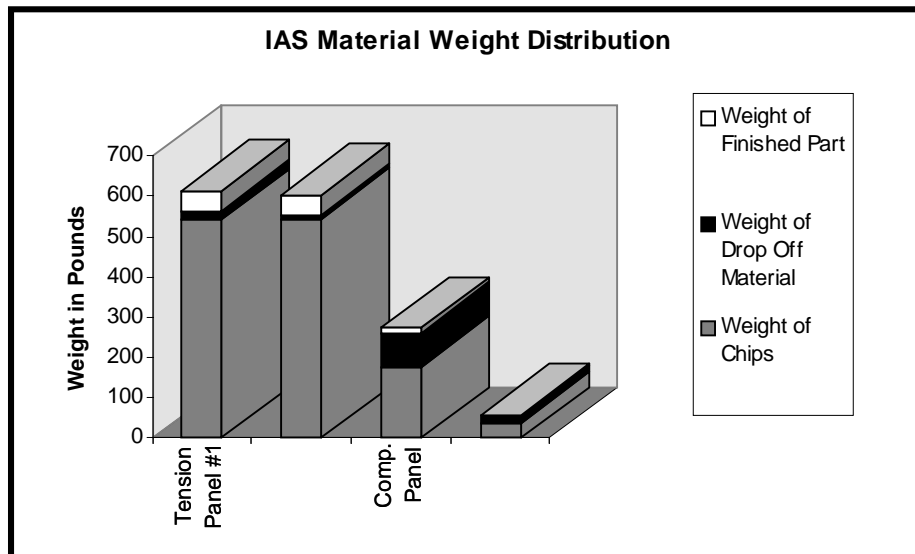


Figure 9.1: Material Utilization Using Monolithic Machining

After the initial weight measurements were found for the panels, a general study on a larger scale was performed to evaluate the use of integrally stiffened panels on a 100 foot long, 20 foot diameter fuselage, seen in table 9.1. This study gives us an idea of what type of material requirements are needed in applying this type of technology. First, it was determined that 242 panels would be needed to produce the 100' structure. If we assume that the raw material needed in producing a panel is 600 lbs. than the raw material needed in building the structure would be 145,200 lbs. The finished weight of the structure material would be 11,616 lbs. which is 8 percent of the raw material weight.

Table 9.1: Aircraft Structure Weight

Surface Area of 100' fuselage	904780.8 sq in.
Surface Area of fuselage test panel	3744 sq in.
# of Panels to Build Aircraft	242 panels
Raw Material Weight for panels	600 lbs
Total Weight of Raw Material	145,200 lbs
Finished Weight of Structure	11,616 lbs
# of Stiffeners	94
Total length of material for stiffeners	1.78 Miles

The main idea to note in this study is if this technology is to ever be widely used in an aircraft, the cost of the material must be evaluated to the labor savings gained in producing this type of structure over conventional methods of manufacturing used currently. In addition, thoughts on being able to obtain the necessary amount of aluminum to produce this type of structure must be studied to assure availability on the larger scale.

10.0 Dimensional Accuracy of the Panels:

Thickness and stiffener spacing data was taken for all panels to insure that they were manufactured to engineering specifications. The panels showed very good dimensional accuracy overall with the following characteristics. First, on the two tension

panels, the maximum deviation from the engineering tolerances for the floor thickness of .17” and pocket thickness .06” was .008” and was below .005” in most places. The flange thickness deviation on these two panels was a maximum .008” with most of the flange measurements deviating less than .005”. The compression panel found very similar results in dimensional accuracy. After the panels were measured they were inspected for cracks through a die penetrant inspection process. All three panels passed the inspection showing no cracks anywhere on the structure.

11.0 Conclusion:

The following conclusions were drawn from this test panel fabrication task:

- Coordination in the design phase between manufacturing engineering and product design is critical to developing a cost effective process.
- Fabrication of complex integrally stiffened panels is compatible with today’s design systems and machine tools.
- N/C process provided accurate parts that will lead to reduced variability in down stream assembly operations.
- Material ‘buy to fly’ ratios are very high, typically over 90% of the raw material is removed and will be scrap.

12.0 Appendix

List of Appendix

Vericut Data on IAS Panels, Tension Panels 1 & 2	C-20
Vericut Data on IAS Panels, Compression Panel	C-21
Vericut Data on IAS Panels, Compression Frames	C-22
Actual Cutting Data on IAS Tension Panel #1	C-23
Weight Calculations for IAS Panels	C-24
Study on Aircraft Structure Weight	C-25
Graph on IAS Material Weight Distribution	C-26
Compression Panel Floor Thickness Measurements	C-27
Compression Panel Stiffener Thickness Measurements	C-28
Compression Panel Stiffener Location Measurements	C-29
Compression Panel Pocket Location Measurements	C-30
Tension Panel 1 & 2, Floor Thickness Measurements	C-31
Tension Panel 1, Stiffener Thickness Measurements	C-32
Tension Panel 2, Stiffener Thickness Measurements	C-33
Tension Panel 1 & 2, Stiffener Location Measurements	C-34
Tension Panel 1 & 2, Pocket Location Measurements	C-35
Tension Panel 1 & 2, Pocket Location Measurements	C-36
Compression Frame 1 & 2, Inspection Sheet	C-37

Vericut Data on IAS Panels

Tension Panels #1 and #2

Tool #	Assembly Number	T/S and Profile #	Tool Diameter	Cutting Time	Chip Load	# of Flutes	Spindle Speed	Feed	Cutting Speed	Depth of Cut	MRR
1	55000095	Ingersoll I-MAX	6.00 inch	37.43 min.	.002 in	6	2500 rpm	30 in/min	4000 SFM	.06 in	11 in cub. / min
2	50000227	115.055-2004 52330	2.00 inch	685.54 min	.01 in	2	1530 rpm	30 in/min	800 SFM	.25 in	15 in cub. / min
3	50000437	115.055-1501 50510	1.5 inch	220.39 min.	.006 in	2	1950 rpm	25 in/min	950 SFM	.25 in	9 in cub. / min
4	50000351	115.055-1006 51830	1.0 inch	41.28 min.	.004 in	2	2500 rpm	20 in/min	650 SFM	.125 in	2.5 in cub. / min
5	99999991	Custom T Cutter	3.0 inch	47.34 min.	.009 in	4	2500 rpm	90 in/min	2000 SFM	.25 in	65 in cub. / min
6	99999992	Custom T Cutter	3.0 inch	7.75 min.	.009 in	4	2500 rpm	90 in/min	2000 SFM	.25 in	65 in cub. / min
7	10000015	112.019-0059	.109 inch	7.26 min.	.001 in	3	2500 rpm	10 in/min	100 SFM	.0625 in	.5 in cub. / min
8	20000280	112.023-4204	.312 inch	2.79 min.	.04 in	1	2400 rpm	18 in/min	200 SFM	.25 in	1.5 in cub. / min
9	20000429	112.034-1066 NUCON 77	.250 inch	2.64 min.	.07 in	1	2400 rpm	20 in/min	170 SFM	.25 in	1 in cub. / min
10	50000546	115.055-0701 53950	.75 inch	16.8 min	.025 in	2	1950 rpm	90 in/min	380 SFM	.5 in	35 in cub. / min
				Total Cutting Time =	1069.22 min						

Compression Panel

Tool Graph #	Tool Assembly Number	T/S and Profile #	Tool Diameter	Cutting Time	Chip Load	# of Flutes	Spindle Speed	Feed	Cutting Speed	Depth of Cut	MRR
1	55000095	Ingersoll I-MAX	6.00 inch	10.51 min	.002 in	6	2500 rpm	30 in/min	4000 SFM	.06 in	11 in cubed / min
2	50000227	115.055-2004 52330	2.00 inch	206.41 min	.01 in	2	1530 rpm	30 in/min	800 SFM	.25 in	15 in cubed / min
3	50000437	115.055-1501 50510	1.5 inch	112.62 min	.006 in	2	1950 rpm	25 in/min	950 SFM	.25 in	9 in cubed / min
4	50000351	115.055-1006 51830	1.0 inch	36.63 min	.003 in	2	2500 rpm	15 in/min	650 SFM	.125 in	1.3 in cubed / min
5	99999991	Custom T Cutter	3.0 inch	18.55 min	.009 in	4	2500 rpm	90 in/min	2000 SFM	.25 in	65 in cubed / min
6	99999992	Custom T Cutter	3.0 inch	8.84 min	.009 in	4	2500 rpm	90 in/min	2000 SFM	.25 in	65 in cubed / min
7	50000546	115.055-0701 53950	.75 inch	18.64 min	.025 in	2	1950 rpm	90 in/min	380 SFM	.5 in	35 in cubed / min
				Total Cutting Time =	412.20 min						

Compression Frames

Tool Graph #	Tool Assembly Number	T/S and Profile #	Tool Diameter	Cutting Time	Chip Load	# of Flutes	Spindle Speed	Feed	Cutting Speed	Depth of Cut	MRR
1	50000096	115.055-1006 50920	1 in	123.77 min	0.025	2	1900 rpm	100 in/min	500 SFM	.25 in	25 in cubed / min
2	50001179	115.055-0701 52570	.75 in	29.15 min	0.003	2	2400 rpm	15 in/min	480 SFM	.5 in	6 in cubed / min
				Total Cutting Time =	152.92 min						

Actual Cutting Data on IAS Tension Panel

Tension Panels #1

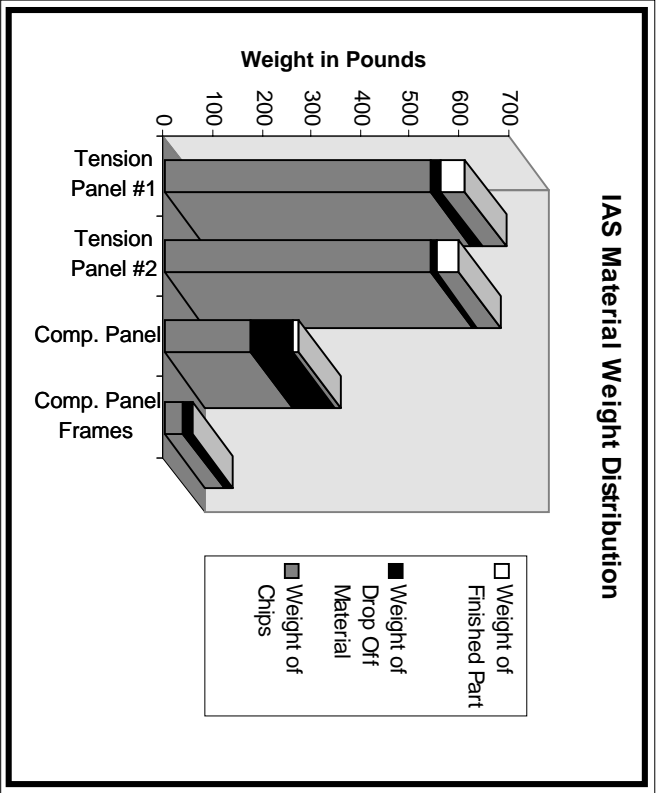
Tool #	T/S and Profile #	Tool Diameter	Cutting Time	Chip Load	# of Flutes	Spindle Speed	Feed	Cutting Speed	Depth of Cut	MRR
1 @ 62%	Ingersoll I-MAX	6.00 inch	60 min.	0.002 in	6	2500 rpm	19 in/min	4000 SFM	.06 in	6.5 in cub. / min
2 @ 76%	115.055-2004 52330	2.00 inch	900 min.	0.007 in	2	1530 rpm	23 in/min	800 SFM	.25 in	11 in cub. / min
3 @ 56%	115.055-1501 50510	1.5 inch	390 min.	0.004 in	2	1950 rpm	14 in/min	950 SFM	.25 in	5 in cub. / min
4 @ 69%	115.055-1006 51830	1.0 inch	60 min.	0.003 in	2	2500 rpm	14 in/min	650 SFM	.125 in	1.5 in cub. / min
5 @ 53%	Custom T Cutter	3.0 inch	90 min.	0.004 in	4	2500 rpm	47 in/min	2000 SFM	.25 in	35 in cub. / min
6 @ 43%	Custom T Cutter	3.0 inch	18 min.	0.004 in	4	2500 rpm	38 in/min	2000 SFM	.25 in	28 in cub. / min
7 @ 29%	112.019-0059	.109 inch	25 min.	0.001 in	3	2500 rpm	3 in/min	100 SFM	.0625 in	.5 in cub. / min
8 @ 40%	112.023-4204	.312 inch	7 min.	0.003 in	1	2400 rpm	7 in/min	200 SFM	.25 in	.5 in cub. / min
9 @ 33%	112.034-1066 NUCON 77	.250 inch	8 min.	0.003 in	1	2400 rpm	7 in/min	170 SFM	.25 in	1 in cub. / min
10 @ 37%	115.055-0701 53950	.75 inch	45 min.	.008 in	2	1950 rpm	33 in/min	380 SFM	.5 in	17 in cub. / min
Total Cutting Time =			1603 min.							

Weight Calculations for IAS Panels

Description	Weight in Pounds
Tension Panel #1	
Weight of Raw Material	612 lbs
Weight of Cut Off Material	22.64 lbs
Weight of Finished Tension Panel #1	48 lbs
Weight of Chips	541.36 lbs
Tension Panel #2	
Weight of Raw Material	601.45 lbs
Weight of Cut Off Material	10.48 lbs
Weight of Finished Tension Panel #2	48 lbs
Weight of Chips	542.97 lbs
Compression Panel	
Weight of Raw Material	273.6 lbs
Weight of Cut Off Material	84.31 lbs
Weight of Finished Compression Panel	11.63 lbs
Weight of Chips	177.66 lbs
Compression Panel Frames	
Weight of Raw Material	57.08 lbs
Weight of Cut Off Material	16.52 lbs
Weight of Finished Compression Panel	1.96 lbs
Weight of Chips	38.6 lbs

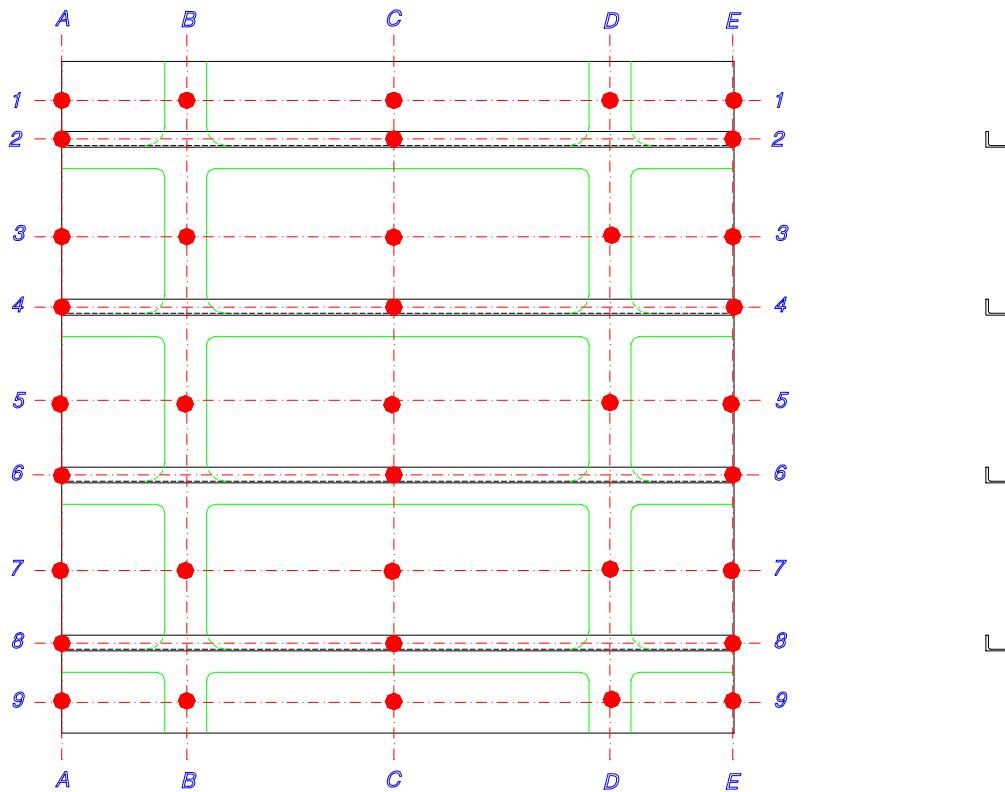
Study on Aircraft Structure Weight

Surface Area of 100' fuselage	904780.8 sq in.
Surface Area of fuselage test panel	3744 sq in.
# of Panels to Build Aircraft	242 panels
Raw Material Weight for panels	600 lbs
Total Weight of Raw Material	145,200 lbs
Finished Weight of Structure	11,616 lbs
# of Stiffeners	94
Total length of material for stiffeners	1.78 Miles



Floor Thickness Measurements

Vertical Position	A	Dev. +-	B	Dev. +-	C	Dev. +-	D	Dev. +-	E	Dev. +-	F	Dev. +-	G	Dev. +-	Horizontal Position
1	0.065	-0.005	0.166	-0.004	0.061	0.001	0.06	0	0.064	0.004	0.167	-0.003	0.06	0	
3	0.063	-0.007	0.17	0	0.063	0.003	0.061	0.001	0.062	-0.002	0.165	-0.005	0.061	0.001	
5	0.065	-0.005	0.168	-0.002	0.062	0.002	0.061	0.001	0.061	0.001	0.165	-0.005	0.061	0.001	
7	0.062	-0.008	0.166	-0.004	0.06	0	0.06	0	0.06	0	0.165	-0.005	0.059	-0.001	
9	0.067	-0.003	0.168	-0.002	0.067	0.007	0.065	0.005	0.066	0.006	0.168	-0.002	0.06	0	
Nominal Dimension	0.06		0.17		0.06		0.06		0.06		0.17		0.06		



Stiffener Thickness Measurements

Measurements Along Horizontal Position A

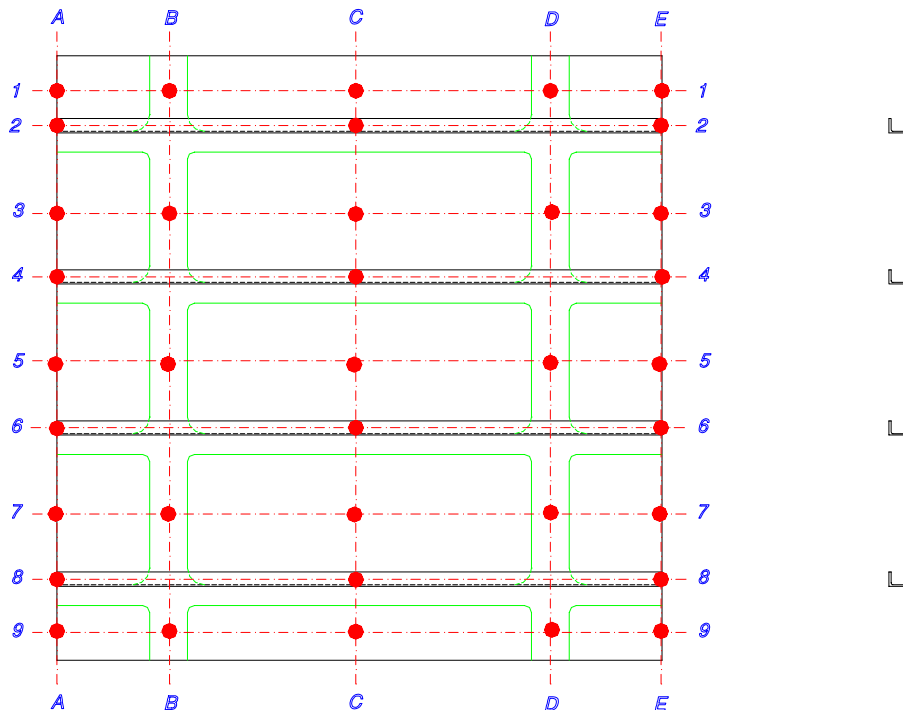
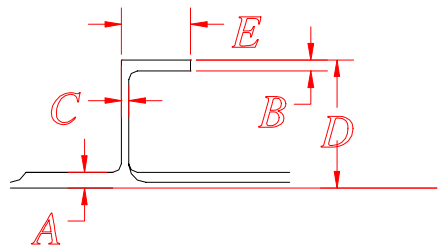
Vertical Position	A	Dev. +/-	B	Dev. +/-	C	Dev. +/-	D	Dev. +/-	E	Dev. +/-
2A	0.169	-0.001	0.113	0.001	0.086	0.006	1.39	0	0.75	0
4A	0.168	-0.002	0.113	0.001	0.086	0.006	1.388	-0.002	0.75	0
6A	0.168	-0.002	0.113	0.001	0.085	0.005	1.388	-0.002	0.75	0
8A	0.169	-0.001	0.113	0.001	0.084	0.004	1.39	0	0.75	0
Nominal Dimension	0.17		0.12		0.08		1.39		0.75	

Measurements Along Horizontal Position D

Vertical Position	A	Dev. +/-	B	Dev. +/-	C	Dev. +/-	D	Dev. +/-	E	Dev. +/-
2D	0.166	-0.004	0.113	-0.007	0.086	0.006	1.386	-0.004	0.75	0
4D	0.168	-0.002	0.113	-0.007	0.086	0.006	1.385	-0.005	0.75	0
6D	0.169	-0.001	0.114	-0.006	0.087	0.007	1.385	-0.005	0.75	0
8D	0.17	0	0.114	-0.006	0.085	0.005	1.386	-0.004	0.75	0
Nominal Dimension	0.17		0.12		0.08		1.39		0.75	

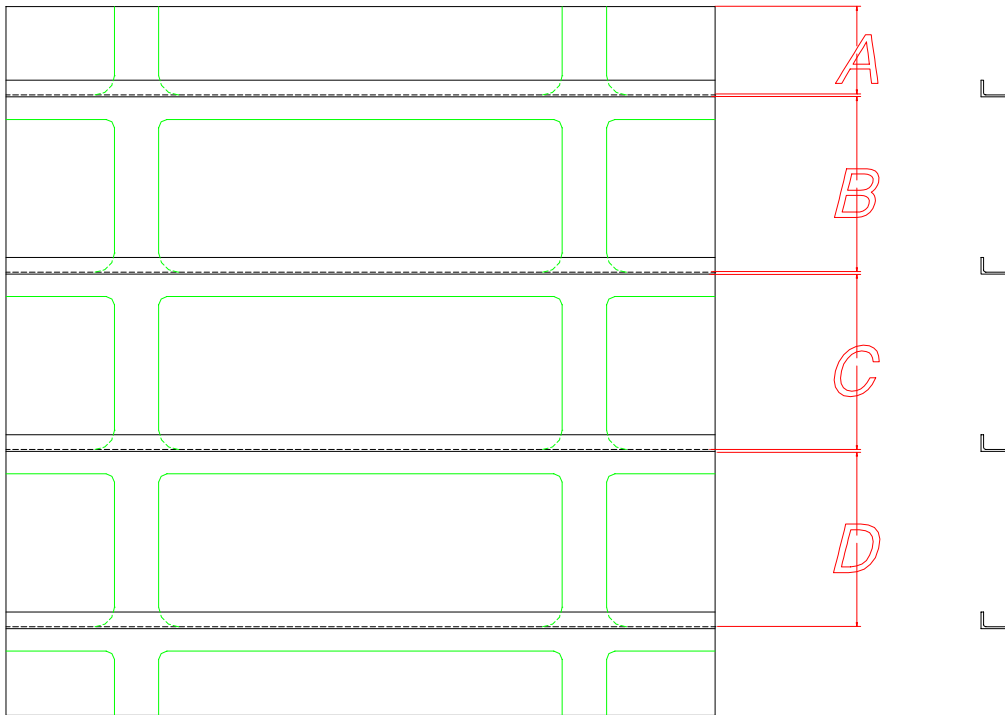
Measurements Along Horizontal Position G

Vertical Position	A	Dev. +/-	B	Dev. +/-	C	Dev. +/-	D	Dev. +/-	E	Dev. +/-
2G	0.169	-0.001	0.112	-0.008	0.087	0.007	1.384	-0.006	0.75	0
4G	0.169	-0.001	0.112	-0.008	0.087	0.007	1.382	-0.008	0.75	0
6G	0.162	-0.008	0.112	-0.008	0.087	0.007	1.382	-0.008	0.75	0
8G	0.168	-0.002	0.112	-0.008	0.086	0.006	1.382	-0.008	0.75	0
Nominal Dimension	0.17		0.12		0.08		1.39		0.75	



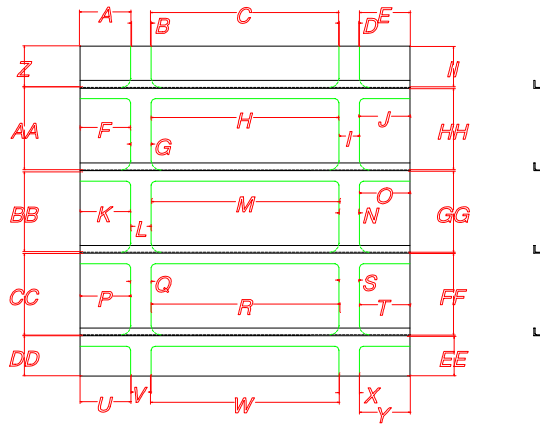
Stiffener Location Measurements

Dimension Ref.	Inches
A	4.006
B	7.915
C	7.915
D	7.916



Pocket Location Measurements

Dimension Ref.	Inches	Nom Dim	Dev. +/-
A	4.898	4.9	-0.002
B	2.008	2	0.008
C	18.2	18.2	0
D	2.005	2	0.005
E	4.896	4.9	-0.004
F	4.902	4.9	0.002
G	2.008	2	0.008
H	18.2	18.2	0
I	2.005	2	0.005
J	4.899	4.9	-0.001
K	4.9	4.9	0
L	2.008	2	0.008
M	18.198	18.2	-0.002
N	2.005	2	0.005
O	4.902	4.9	0.002
P	4.902	4.9	0.002
Q	2.008	2	0.008
R	18.199	18.2	-0.001
S	2.005	2	0.005
T	4.9	4.9	0
U	4.901	4.901	0
V	2.008	2	0.008
W	18.198	18.2	-0.002
X	2.005	2	0.005
Y	4.902	4.9	0.002
Z	4.009	4	0.009
AA	6.896	6.9	-0.004
BB	6.892	6.9	-0.008
CC	6.892	6.9	-0.008
DD	2.899	2.9	-0.001
EE	2.899	2.9	-0.001
FF	6.892	6.9	-0.008
GG	6.892	6.9	-0.008
HH	6.896	6.9	-0.004
II	4.006	4	0.006
JJ	4.001	4	0.001
KK	6.894	6.9	-0.006
LL	6.897	6.9	-0.003
MM	6.9	6.9	0
NN	2.899	2.9	-0.001



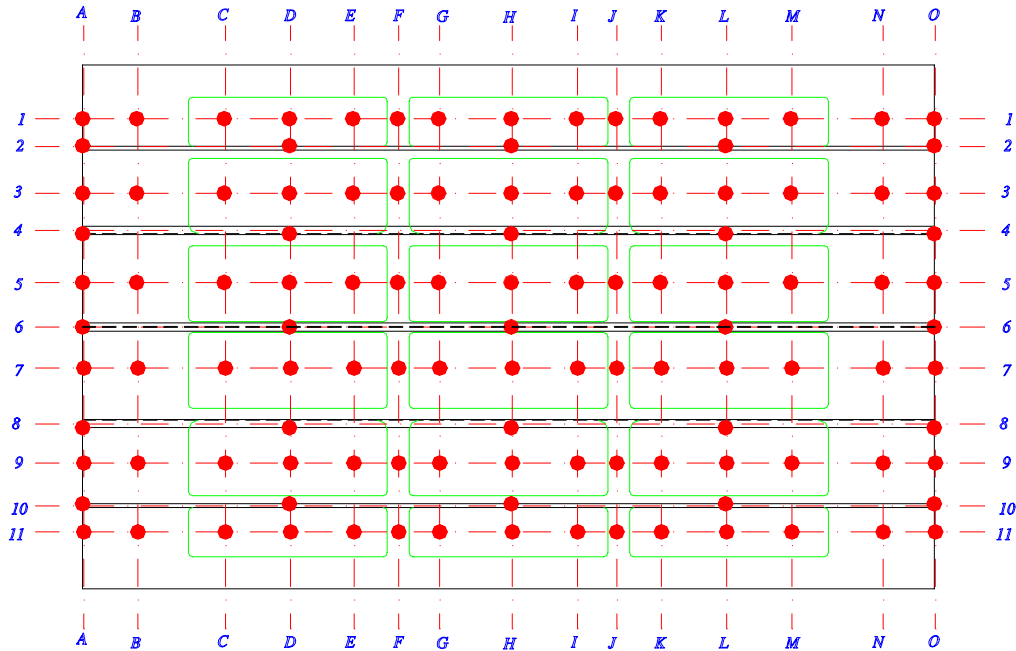
Inspection Sheet for Tension Panel #1

Floor Thickness Measurements

Vertical Position	A	Dev. +/-	B	Dev. +/-	C	Dev. +/-	D	Dev. +/-	E	Dev. +/-	F	Dev. +/-	G	Dev. +/-	Horizontal
1	0.162	-0.008	0.163	-0.007	0.054	-0.006	0.054	-0.006	0.053	-0.007	0.161	-0.009	0.053	-0.007	
3	0.165	-0.005	0.164	-0.006	0.055	-0.005	0.052	-0.008	0.054	-0.006	0.161	-0.009	0.052	-0.008	
5	0.165	-0.005	0.166	-0.004	0.056	-0.004	0.053	-0.007	0.054	-0.006	0.163	-0.007	0.055	-0.005	
7	0.166	-0.004	0.167	-0.003	0.057	-0.003	0.056	-0.004	0.056	-0.004	0.163	-0.007	0.056	-0.004	
9	0.166	-0.004	0.167	-0.003	0.058	-0.002	0.057	-0.003	0.058	-0.002	0.164	-0.006	0.058	-0.002	
11	0.166	-0.004	0.169	-0.001	0.06	0	0.06	0	0.06	0	0.166	-0.004	0.059	-0.001	
Nominal Dimension	0.17		0.17		0.06		0.06		0.06		0.17		0.06		

Floor Thickness Measurements Continued

Vertical Position	H	Dev. +/-	I	Dev. +/-	J	Dev. +/-	K	Dev. +/-	L	Dev. +/-	M	Dev. +/-	N	Dev. +/-	O	Dev. +/-	Horizontal Position
1	0.053	-0.007	0.051	-0.009	0.16	-0.01	0.053	-0.007	0.055	-0.005	0.055	-0.005	0.165	-0.005	0.165	-0.005	
3	0.053	-0.007	0.051	-0.009	0.16	-0.01	0.055	-0.005	0.054	-0.006	0.055	-0.005	0.165	-0.005	0.163	-0.007	
5	0.054	-0.006	0.053	-0.007	0.16	-0.01	0.055	-0.005	0.056	-0.004	0.056	-0.004	0.166	-0.004	0.165	-0.005	
7	0.055	-0.005	0.055	-0.005	0.164	-0.006	0.056	-0.004	0.057	-0.003	0.057	-0.003	0.166	-0.004	0.165	-0.005	
9	0.057	-0.003	0.058	-0.002	0.164	-0.006	0.058	-0.002	0.058	-0.002	0.056	-0.004	0.166	-0.004	0.165	-0.005	
11	0.059	-0.001	0.059	-0.001	0.166	-0.004	0.059	-0.001	0.06	0	0.059	-0.001	0.167	-0.003	0.169	-0.001	
Nominal Dimension	0.06		0.06		0.17		0.06		0.06		0.06		0.17		0.17		



Inspection Sheet for Tension Panel #2

Floor Thickness Measurements

Vertical Position	A	Dev. +/-	B	Dev. +/-	C	Dev. +/-	D	Dev. +/-	E	Dev. +/-	F	Dev. +/-	G	Dev. +/-	Horizontal
1	0.16	-0.01	0.163	-0.007	0.056	-0.004	0.055	-0.005	0.053	-0.007	0.157	-0.013	0.052	-0.008	
3	0.163	-0.007	0.164	-0.006	0.056	-0.004	0.056	-0.004	0.055	-0.005	0.159	-0.011	0.054	-0.006	
5	0.162	-0.008	0.165	-0.005	0.056	-0.004	0.055	-0.005	0.055	-0.005	0.16	-0.01	0.056	-0.004	
7	0.166	-0.004	0.163	-0.007	0.056	-0.004	0.056	-0.004	0.055	-0.005	0.161	-0.009	0.057	-0.003	
9	0.164	-0.006	0.167	-0.003	0.058	-0.002	0.058	-0.002	0.056	-0.004	0.168	-0.002	0.06	0	
11	0.166	-0.004	0.165	-0.005	0.061	-0.001	0.059	-0.001	0.059	-0.001	0.164	-0.006	0.059	-0.001	
Nominal Dimension	0.17		0.17		0.06		0.06		0.06		0.17		0.06		

Floor Thickness Measurements Continued

Vertical Position	H	Dev. +/-	I	Dev. +/-	J	Dev. +/-	K	Dev. +/-	L	Dev. +/-	M	Dev. +/-	N	Dev. +/-	O	Dev. +/-	Horizontal Position
1	0.05	-0.01	0.052	-0.008	0.161	-0.009	0.054	-0.006	0.056	-0.004	0.057	-0.003	0.165	-0.005	0.164	-0.006	
3	0.055	-0.005	0.053	-0.007	0.16	-0.01	0.055	-0.005	0.056	-0.004	0.056	-0.004	0.163	-0.007	0.163	-0.007	
5	0.056	-0.004	0.056	-0.004	0.16	-0.01	0.055	-0.005	0.055	-0.005	0.058	-0.002	0.164	-0.006	0.162	-0.008	
7	0.057	-0.003	0.057	-0.003	0.163	-0.007	0.057	-0.003	0.056	-0.004	0.057	-0.003	0.165	-0.005	0.163	-0.007	
9	0.059	-0.001	0.059	-0.001	0.162	-0.008	0.056	-0.004	0.06	0	0.059	-0.001	0.165	-0.005	0.168	-0.002	
11	0.061	0.001	0.061	0.001	0.167	-0.003	0.061	0.001	0.06	0	0.06	0	0.169	-0.001	0.168	-0.002	
Nominal Dimension	0.06		0.06		0.17		0.06		0.06		0.06		0.17		0.17		

Stiffener Thickness Measurements Panel #1

Measurements Along Horizontal Position 2 & 10

Position	A	Dev. +-	B	Dev. +-	C	Dev. +-
2A	0.358	0.002	0.664	-0.006	0.165	-0.005
2D	0.357	0.001	0.666	-0.004	0.166	-0.004
2H	0.358	0.002	0.665	-0.005	0.165	-0.005
2L	0.358	0.002	0.664	-0.006	0.165	-0.005
2O	0.359	0.003	0.665	-0.005	0.164	-0.006
10A	0.36	0.004	0.669	-0.001	0.17	0
10D	0.359	0.003	0.668	-0.002	0.171	0.001
10H	0.359	0.003	0.668	-0.002	0.17	0
10L	0.359	0.003	0.669	-0.001	0.169	-0.001
10O	0.359	0.003	0.669	-0.001	0.17	0
Nominal Dimension	0.356		0.67		0.17	

Measurements Along Horizontal Position 4

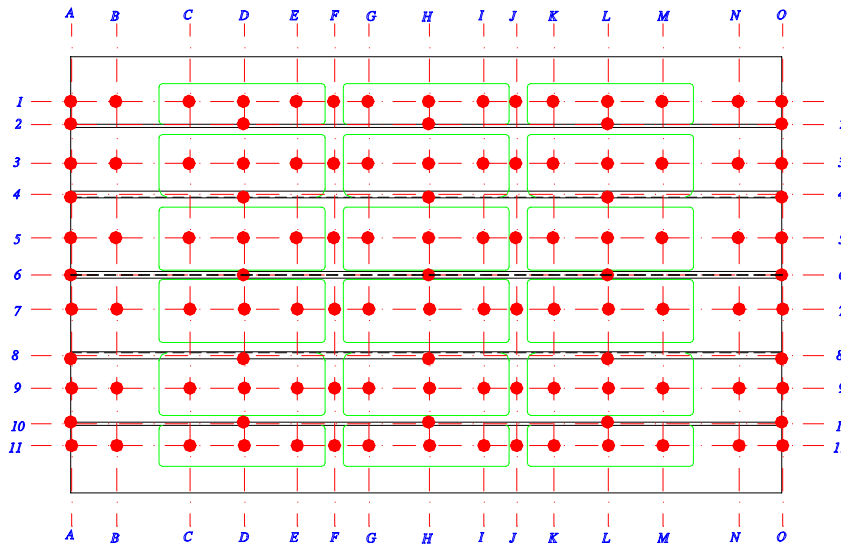
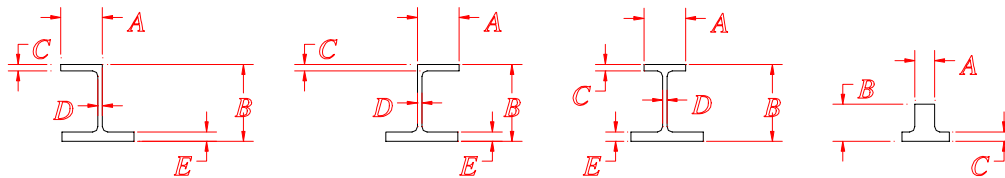
Position	A	Dev. +-	B	Dev. +-	C	Dev. +-	D	Dev. +-	E	Dev. +-
4A	0.755	0.005	1.387	-0.003	0.116	-0.004	0.082	0.002	0.166	-0.004
4D	0.754	0.004	1.385	-0.005	0.116	-0.004	0.082	0.002	0.166	-0.004
4H	0.754	0.004	1.386	-0.004	0.117	-0.003	0.081	0.001	0.165	-0.005
4L	0.754	0.004	1.387	-0.003	0.117	-0.003	0.081	0.001	0.167	-0.003
4O	0.755	0.005	1.388	-0.002	0.117	-0.003	0.083	0.003	0.167	-0.003
Nominal Dimension	0.75		1.39		0.12		0.08		0.17	

Measurements Along Horizontal Position 6

Position	A	Dev. +-	B	Dev. +-	C	Dev. +-	D	Dev. +-	E	Dev. +-
6A	0.755	0.005	1.387	-0.003	0.116	-0.004	0.079	-0.001	0.167	-0.003
6D	0.755	0.005	1.387	-0.003	0.116	-0.004	0.079	-0.001	0.167	-0.003
6H	0.758	0.002	1.387	-0.003	0.117	-0.003	0.08	0	0.167	-0.003
6L	0.755	0.005	1.387	-0.003	0.117	-0.003	0.08	0	0.167	-0.003
6O	0.755	0.005	1.387	-0.003	0.117	-0.003	0.08	0	0.167	-0.003
Nominal Dimension	0.75		1.39		0.12		0.08		0.17	

Measurements Along Horizontal Position 8

Position	A	Dev. +-	B	Dev. +-	C	Dev. +-	D	Dev. +-	E	Dev. +-
8A	0.754	0.004	1.389	-0.001	0.116	-0.004	0.083	0.003	0.168	-0.002
8D	0.754	0.004	1.389	-0.001	0.116	-0.004	0.083	0.003	0.168	-0.002
8H	0.754	0.004	1.389	-0.001	0.116	-0.004	0.083	0.003	0.168	-0.002
8L	0.755	0.005	1.388	-0.001	0.116	-0.004	0.082	0.002	0.169	-0.001
8O	0.755	0.005	1.388	-0.001	0.116	-0.004	0.083	0.003	0.169	-0.001
Nominal Dimension	0.75		1.39		0.12		0.08		0.17	



Stiffener Thickness Measurements Panel #2

Measurements Along Horizontal Position 2 & 10

Position	A	Dev. +/-	B	Dev. +/-	C	Dev. +/-
2A	0.357	0.001	0.663	-0.007	0.162	-0.008
2D	0.356	0	0.662	-0.008	0.161	-0.009
2H	0.357	0.001	0.663	-0.007	0.162	-0.008
2L	0.357	0.001	0.664	-0.006	0.163	-0.007
2O	0.357	0.001	0.664	-0.006	0.163	-0.007
10A	0.358	0.002	0.668	-0.002	0.167	-0.003
10D	0.357	0.001	0.668	-0.002	0.166	-0.004
10H	0.357	0.001	0.667	-0.003	0.166	-0.004
10L	0.357	0.001	0.666	-0.004	0.167	-0.003
10O	0.358	0.002	0.666	-0.004	0.166	-0.004
Nominal Dimension	0.356		0.67		0.17	

Measurements Along Horizontal Position 4

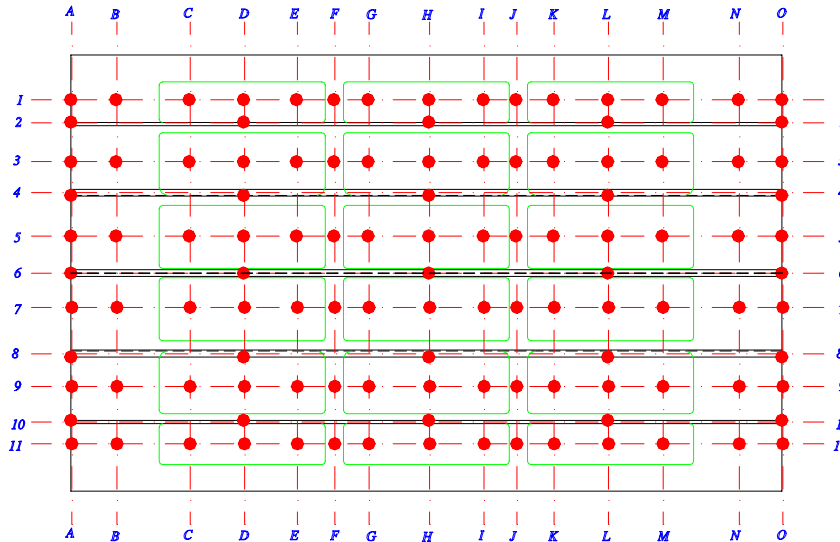
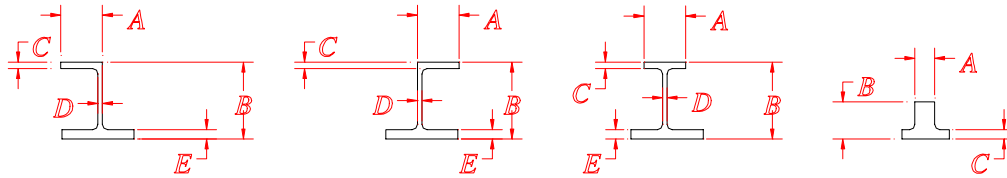
Position	A	Dev. +/-	B	Dev. +/-	C	Dev. +/-	D	Dev. +/-	E	Dev. +/-
4A	0.754	0.004	1.384	-0.006	0.114	-0.006	0.076	-0.004	0.164	-0.006
4D	0.755	0.005	1.385	-0.005	0.113	-0.007	0.074	-0.006	0.164	-0.006
4H	0.756	0.006	1.384	-0.006	0.113	-0.007	0.074	-0.006	0.164	-0.006
4L	0.755	0.005	1.385	-0.005	0.113	-0.007	0.073	-0.007	0.165	-0.005
4O	0.755	0.005	1.386	-0.004	0.113	-0.007	0.075	-0.005	0.165	-0.005
Nominal Dimension	0.75		1.39		0.12		0.08		0.17	

Measurements Along Horizontal Position 6

Position	A	Dev. +/-	B	Dev. +/-	C	Dev. +/-	D	Dev. +/-	E	Dev. +/-
6A	0.755	0.005	1.388	-0.002	0.115	-0.005	0.067	-0.013	0.164	-0.006
6D	0.755	0.005	1.388	-0.002	0.116	-0.004	0.066	-0.014	0.164	-0.006
6H	0.755	0.005	1.387	-0.003	0.114	-0.006	0.065	-0.015	0.164	-0.006
6L	0.755	0.005	1.386	-0.004	0.114	-0.006	0.066	-0.014	0.165	-0.005
6O	0.755	0.005	1.386	-0.004	0.114	-0.006	0.066	-0.014	0.165	-0.005
Nominal Dimension	0.75		1.39		0.12		0.08		0.17	

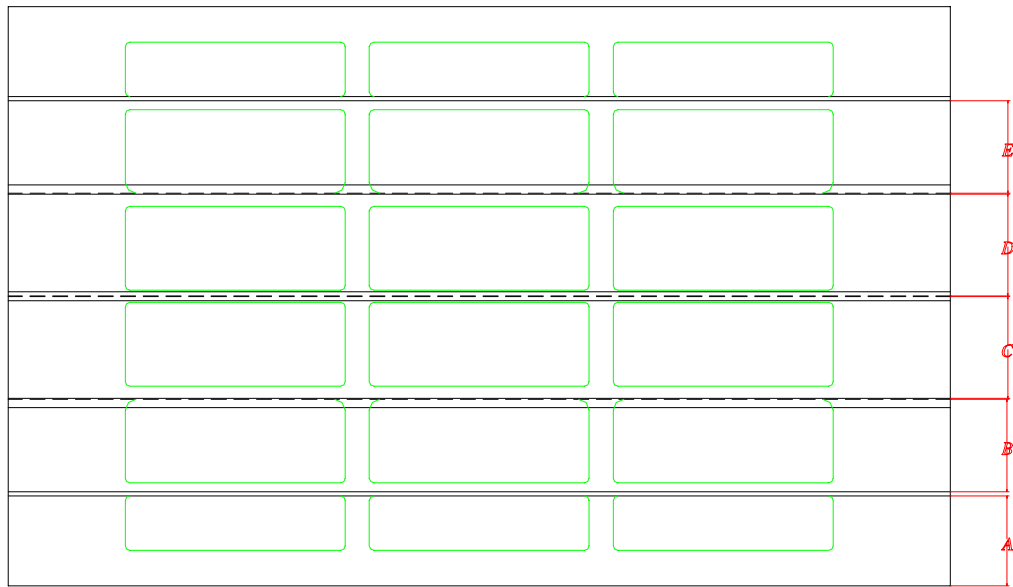
Measurements Along Horizontal Position 8

Position	A	Dev. +/-	B	Dev. +/-	C	Dev. +/-	D	Dev. +/-	E	Dev. +/-
8A	0.754	0.004	1.387	-0.003	0.114	-0.006	0.074	-0.006	0.164	-0.006
8D	0.754	0.004	1.386	-0.004	0.113	-0.007	0.074	-0.006	0.164	-0.006
8H	0.754	0.004	1.387	-0.003	0.113	-0.007	0.074	-0.006	0.164	-0.006
8L	0.754	0.004	1.386	-0.004	0.113	-0.007	0.074	-0.006	0.165	-0.005
8O	0.754	0.004	1.386	-0.004	0.114	-0.006	0.074	-0.006	0.165	-0.005
Nominal Dimension	0.75		1.39		0.12		0.08		0.17	



Stiffener Location Measurements Panel #1

Dimension Ref.	Inches
A	7.446
B	7.636
C	8.424
D	8.42
E	7.637

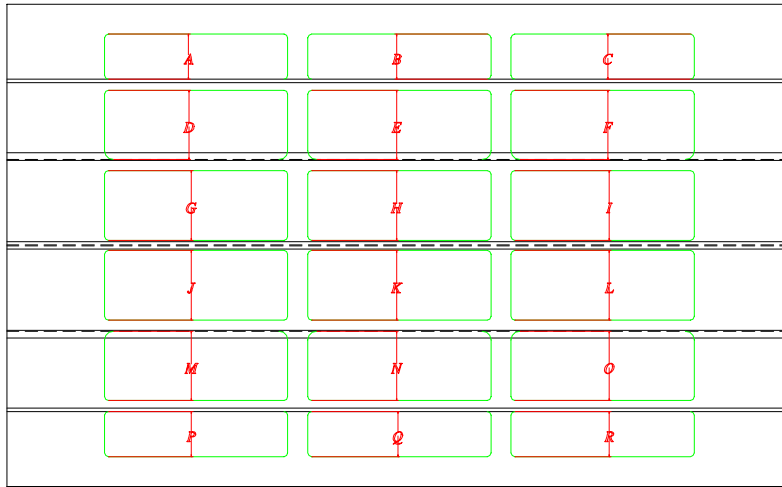


Stiffener Location Measurements Panel #2

Dimension Ref.	Inches
A	7.424
B	7.652
C	8.436
D	8.435
E	7.652

Pocket Location Measurements Panel #1

Dimension Ref.	Inches	Nom Dim	Dev. +/-
A	4.505	4.5	0.005
B	4.505	4.5	0.005
C	4.505	4.5	0.005
D	6.878	6.9	-0.022
E	6.879	6.9	-0.021
F	6.878	6.9	-0.022
G	6.868	6.9	-0.032
H	6.868	6.9	-0.032
I	6.867	6.9	-0.033
J	6.888	6.9	-0.012
K	6.887	6.9	-0.013
L	6.888	6.9	-0.012
M	6.869	6.9	-0.031
N	6.869	6.9	-0.031
O	6.87	6.9	-0.03
P	4.5	4.5	0
Q	4.5	4.5	0
R	4.5	4.5	0



Pocket Location Measurements Panel #2

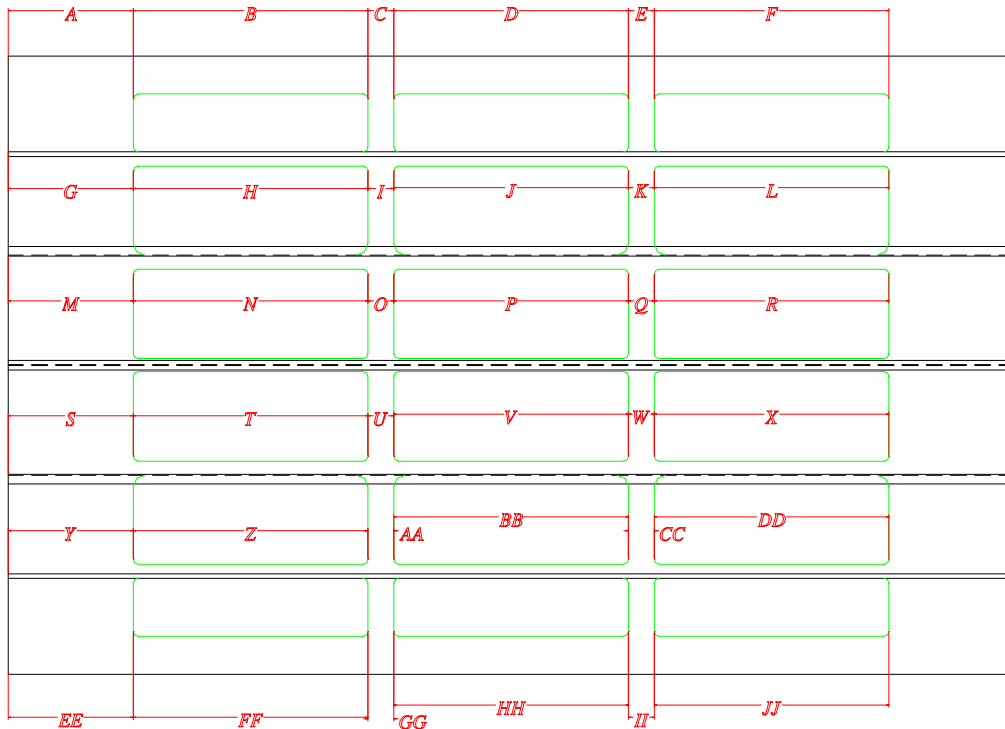
Dimension Ref.	Inches	Nom Dim	Dev. +/-
A	4.5	4.5	0
B	4.5	4.5	0
C	4.5	4.5	0
D	6.9	6.9	0
E	6.9	6.9	0
F	6.9	6.9	0
G	6.89	6.9	-0.01
H	6.89	6.9	-0.01
I	6.89	6.9	-0.01
J	6.9	6.9	0
K	6.9	6.9	0
L	6.9	6.9	0
M	6.9	6.9	0
N	6.9	6.9	0
O	6.9	6.9	0
P	4.5	4.5	0
Q	4.5	4.5	0
R	4.5	4.5	0

Pocket Location Measurements Panel #1

Dimension Ref.	Inches	Nom Dim	Dev. +/-
A	9.7	9.7	0
B	18.2	18.2	0
C	2	2	0
D	18.2	18.2	0
E	2	2	0
F	18.2	18.2	0
G	9.7	9.7	0
H	18.2	18.2	0
I	2	2	0
J	18.2	18.2	0
K	2	2	0
L	18.2	18.2	0
M	9.7	9.7	0
N	18.2	18.2	0
O	2	2	0
P	18.2	18.2	0
Q	2	2	0
R	18.2	18.2	0
S	9.7	9.7	0
T	18.2	18.2	0
U	2	2	0
V	18.2	18.2	0
W	2	2	0
X	18.2	18.2	0
Y	9.7	9.7	0
Z	18.2	18.2	0
AA	2	2	0
BB	18.2	18.2	0
CC	2	2	0
DD	18.2	18.2	0
EE	9.7	9.7	0
FF	18.2	18.2	0
GG	2	2	0
HH	18.2	18.2	0
II	2	2	0
JJ	18.2	18.2	0

Pocket Location Measurements Panel #2

Dimension Ref.	Inches	Nom Dim	Dev. +/-
A	9.7	9.7	0
B	18.2	18.2	0
C	2	2	0
D	18.2	18.2	0
E	2	2	0
F	18.2	18.2	0
G	9.7	9.7	0
H	18.2	18.2	0
I	2	2	0
J	18.2	18.2	0
K	2	2	0
L	18.2	18.2	0
M	9.7	9.7	0
N	18.2	18.2	0
O	2	2	0
P	18.2	18.2	0
Q	2	2	0
R	18.2	18.2	0
S	9.7	9.7	0
T	18.2	18.2	0
U	2	2	0
V	18.2	18.2	0
W	2	2	0
X	18.2	18.2	0
Y	9.7	9.7	0
Z	18.2	18.2	0
AA	2	2	0
BB	18.2	18.2	0
CC	2	2	0
DD	18.2	18.2	0
EE	9.7	9.7	0
FF	18.2	18.2	0
GG	2	2	0
HH	18.2	18.2	0
II	2	2	0
JJ	18.2	18.2	0



IAS Compression Frame Inspection Sheet

Frame 1: Thickness Measurements

Location #	Measurement
1	0.0830
2	0.0850
3	0.0815
4	0.0630
5	0.0620
6	0.0610
7	0.3490
8	0.3500
9	0.3500
10	0.0630
11	0.0610
12	0.0600
13	0.0610
14	0.0620
15	0.0800
16	0.1210
17	0.1230
18	0.0810
19	0.1220
20	0.1230
21	0.0810
22	0.1230
23	0.1230
24	0.0820
25	0.1220
26	0.1210
27	0.0810
28	0.2990
29	0.3000
30	0.3010

Frame 1: Dimensional Verification

Location	Measurement
A	3.6750
B	1.6000
C	6.3930
D	1.5980
E	6.3930
F	1.6000
G	6.3950
H	1.6030
I	2.7130
J	1.1875
K	1.1860
L	5.9750
M	6.0000

IAS Compression Frame Inspection Sheet

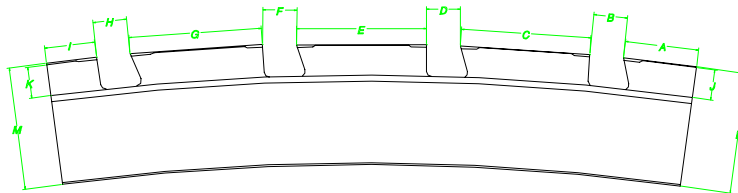
Frame 2: Thickness Measurements

Location #	Measurement
1	0.0860
2	0.0840
3	0.0840
4	0.0625
5	0.0625
6	0.0625
7	0.3500
8	0.3490
9	0.3500
10	0.0625
11	0.0615
12	0.0615
13	0.0620
14	0.0635
15	0.0820
16	0.1220
17	0.1250
18	0.0810
19	0.1220
20	0.1230
21	0.0820
22	0.1220
23	0.1230
24	0.0825
25	0.1250
26	0.1210
27	0.0810
28	0.3000
29	0.2960
30	0.3000

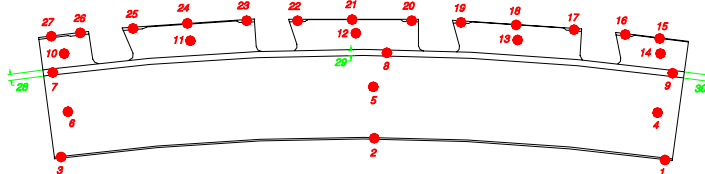
Frame 2: Dimensional Verification

Location	Measurement
A	3.6760
B	1.6020
C	6.3960
D	1.6000
E	6.3900
F	1.6000
G	6.3950
H	1.6000
I	2.1750
J	1.1850
K	1.1875
L	6.0000
M	6.0000

DIMENSIONAL VERIFICATION DRAWING



THICKNESS MEASUREMENT DRAWING



Appendix D

IAS Material Characterization Test Plan

Following is the Boeing Seattle “Material Characterization Test Plan.”

IAS Material Characterization Test Plan

Purpose

The purpose of this testing is to characterize the mechanical, fatigue, and fracture behavior of 7050-T7451 plate, 7050-T74511 and 6013-T651X extrusion, and 7475-T7351 plate. This same lot of 7475 plate was used to build the two-bay longitudinal crack panel. The data generated as part of this test program was used (if available) in an analysis effort aimed at predicting the behavior of these integrally stiffened structure tests.

Test Descriptions:

Static Tensile Tests:

Forty-one tensile coupons listed in the test matrix are to be tested per ASTM E-8 to develop yield, ultimate, and stress-strain relationship.

Instructions:

- Measure and record actual specimen dimensions prior to testing.

Fatigue (Unnotched):

Forty unnotched fatigue test specimens listed in the enclosure 3 test matrix are to be cycled to failure, using constant amplitude loading at a frequency of 10Hz.

Instructions:

- Run each specimen at the net section stress level shown in the enclosed test matrix.
- Measure and record actual specimen dimensions prior to testing.
- Record total cycles at failure and the origin of the failure.
- Terminate testing at 10^6 cycles.
- Save failed specimens.

Fatigue (Open-Hole):

Forty open-hole fatigue test specimens listed in the enclosure 3 test matrix are to be cycled to failure, using constant amplitude loading at a frequency of 10Hz.

Instructions:

- Run each specimen at the net section stress level shown in the enclosed test matrix.
- Measure and record actual specimen dimensions prior to testing.
- Record total cycles at failure and the origin of the failure.
- Terminate testing at 10^7 cycles.
- Save failed specimens.

Crack Growth and R-Curve:

40-inch, 24-inch and 12-inch Wide Center Crack Panels

Six 40-inch wide, eight 24-inch wide and eleven 12-inch wide center crack tension panels listed in the enclosure 3 test matrix are to be tested per the following:

Crack growth test instructions:

- Conduct test per ASTM E647.
- Run each specimen at the stress level shown in the enclosed test matrix.
- 40-inch wide panels: grow cracks from initial notch to 13.0 inch tip-to-tip.
- 24-inch wide panels: grow cracks from initial notch to 8.0 inch tip-to-tip.
- 12-inch wide panels: grow cracks from initial notch to 4.0 inch tip-to-tip.
- Cycle at 10 Hz.
- Record crack length as a function of cycles (minimum of 20 measurements).

Residual strength test (R-Curve) instructions:

- Conduct test per ASTM E561.
- Physically measure crack lengths from specimen centerline.
- Install buckling restraints and crack opening displacement gage.
- Manually load specimen in stroke control.
- Above 50% of the expected failure load, hold every 10 kips and measure crack extension.
- Above 75% of the expected failure load, hold every 2 kips and measure crack extension.
- Conduct a minimum of five buckling checks during the test (back down 10% of load).
- Make a minimum of eight visual crack extension measurements.
- Photograph each failed specimen.
- Save one-half of each failed specimen.

Crack Growth and R-Curve:

Compact Tension Tests

Ten compact crack tension specimens listed in the attached test matrix are to be tested per the following:

Crack growth test instructions:

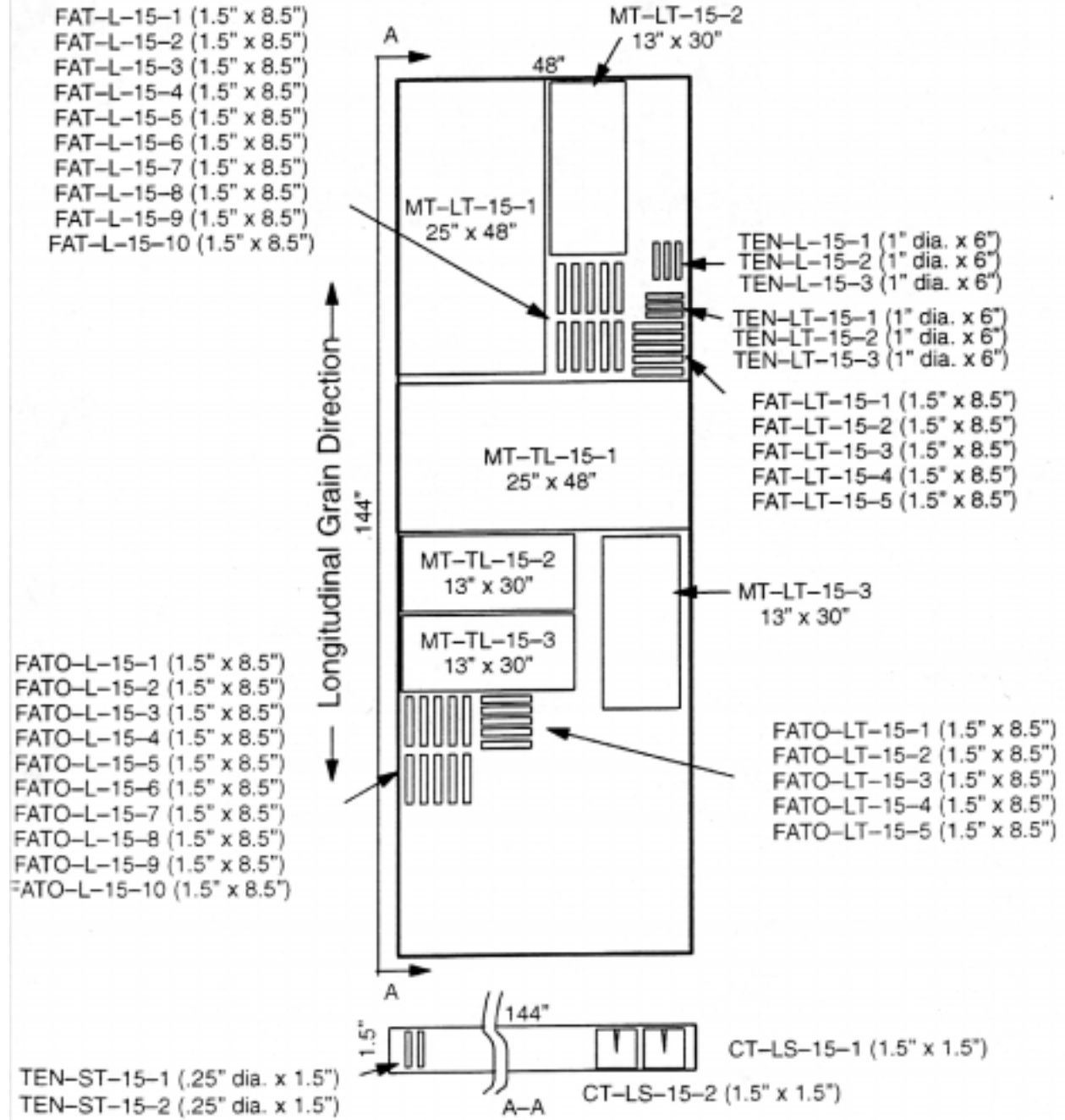
- Conduct test per ASTM E647.
- Run each specimen at the stress level shown in the enclosed test matrix.
- Grow cracks from the initial notch to approximately $0.5W$.
- Cycle at 10 Hz.
- Record crack length as a function of cycles.

Residual strength test (R-Curve) instructions:

- Conduct test per ASTM E561.
- Physically measure crack lengths on both sides of the specimen.
- Install buckling restraints as required and a crack opening displacement gage.
- Load specimen in COD control at a maximum stress intensity factor rate of 10 ksi sqrt in/min.
- Make a minimum of five visual crack extension measurements.
- Conduct a minimum of five buckling checks during the test (back down 10% of load).
- Photograph each failed specimen.
- Save one-half of each specimen.

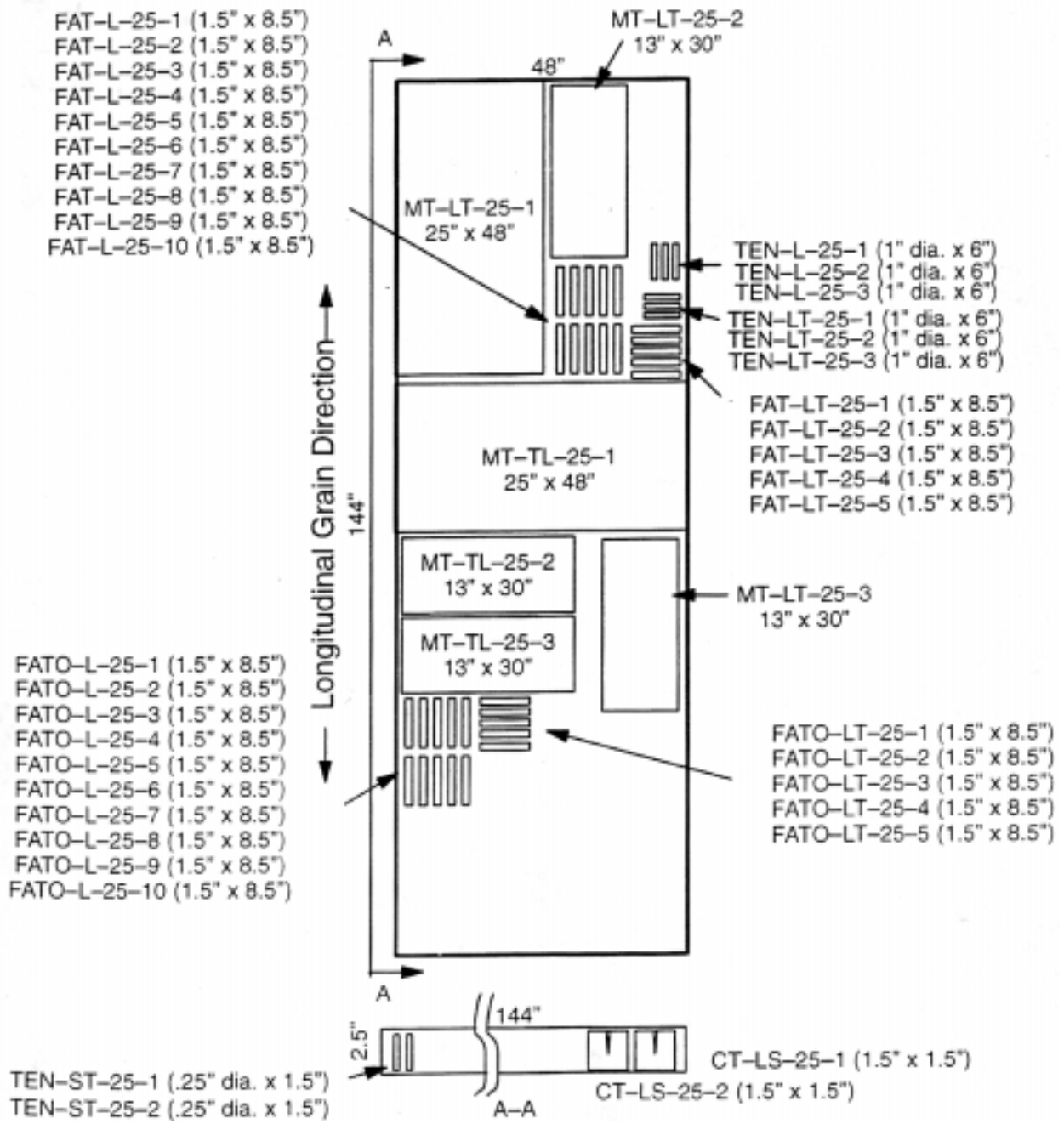
IAS Material Properties Cutting Diagram

7050 Plate (t = 1.5")
48" x 144"



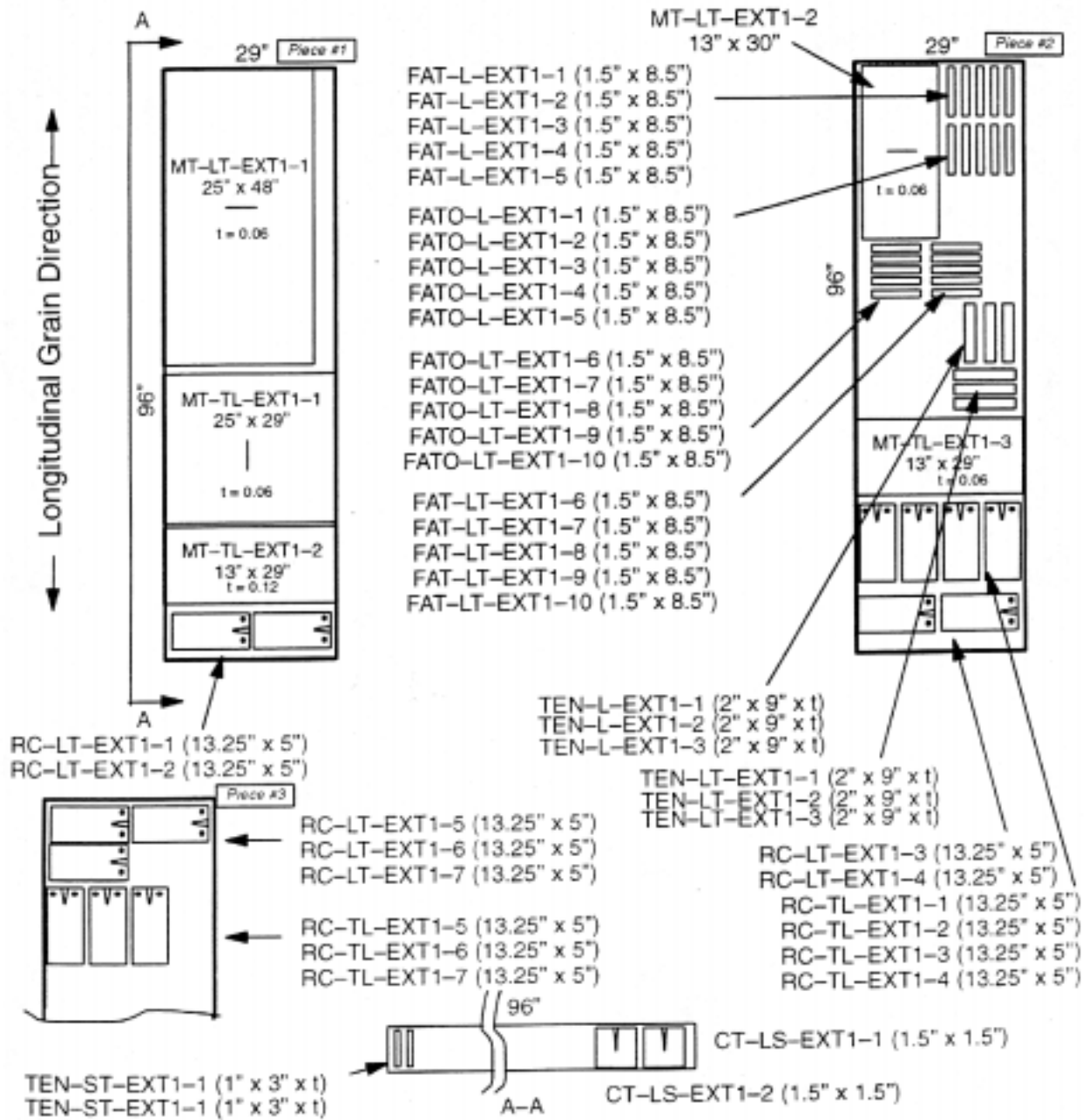
IAS Material Properties Cutting Diagram

7050 Plate (t = 2.5")
48" x 144"



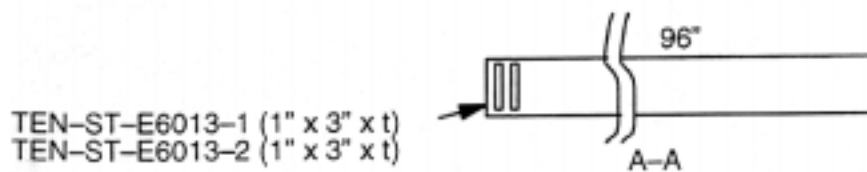
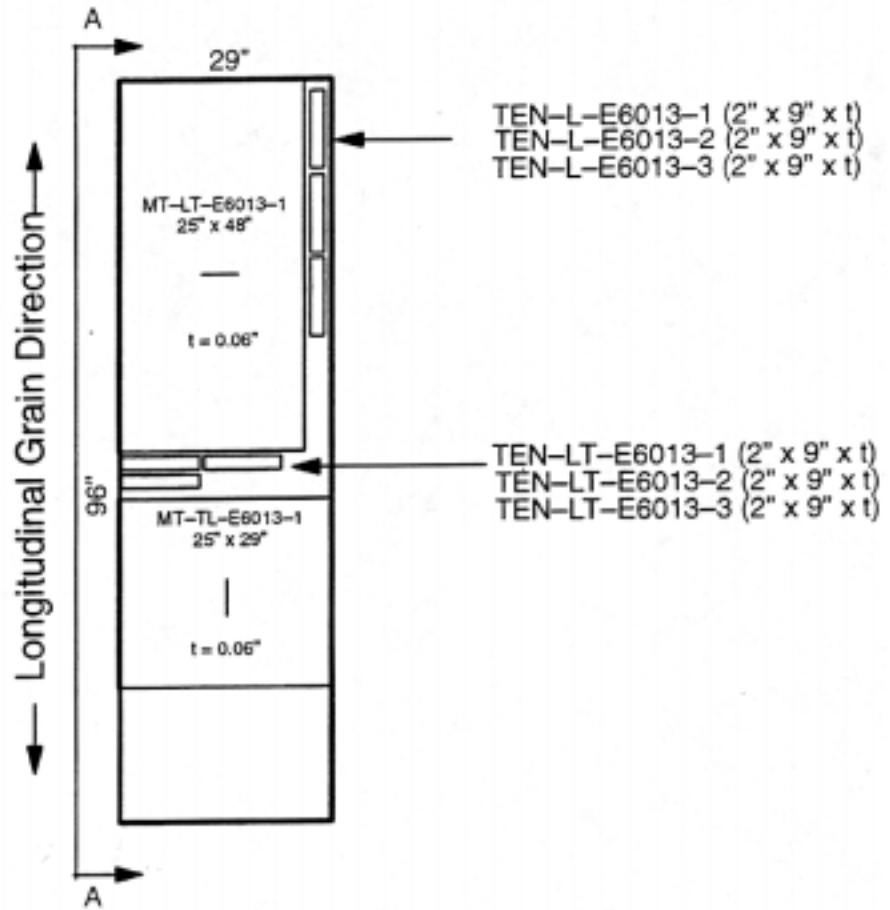
IAS Material Properties Cutting Diagram

7050 Extrusion (t = 0.2")
29" x 96"



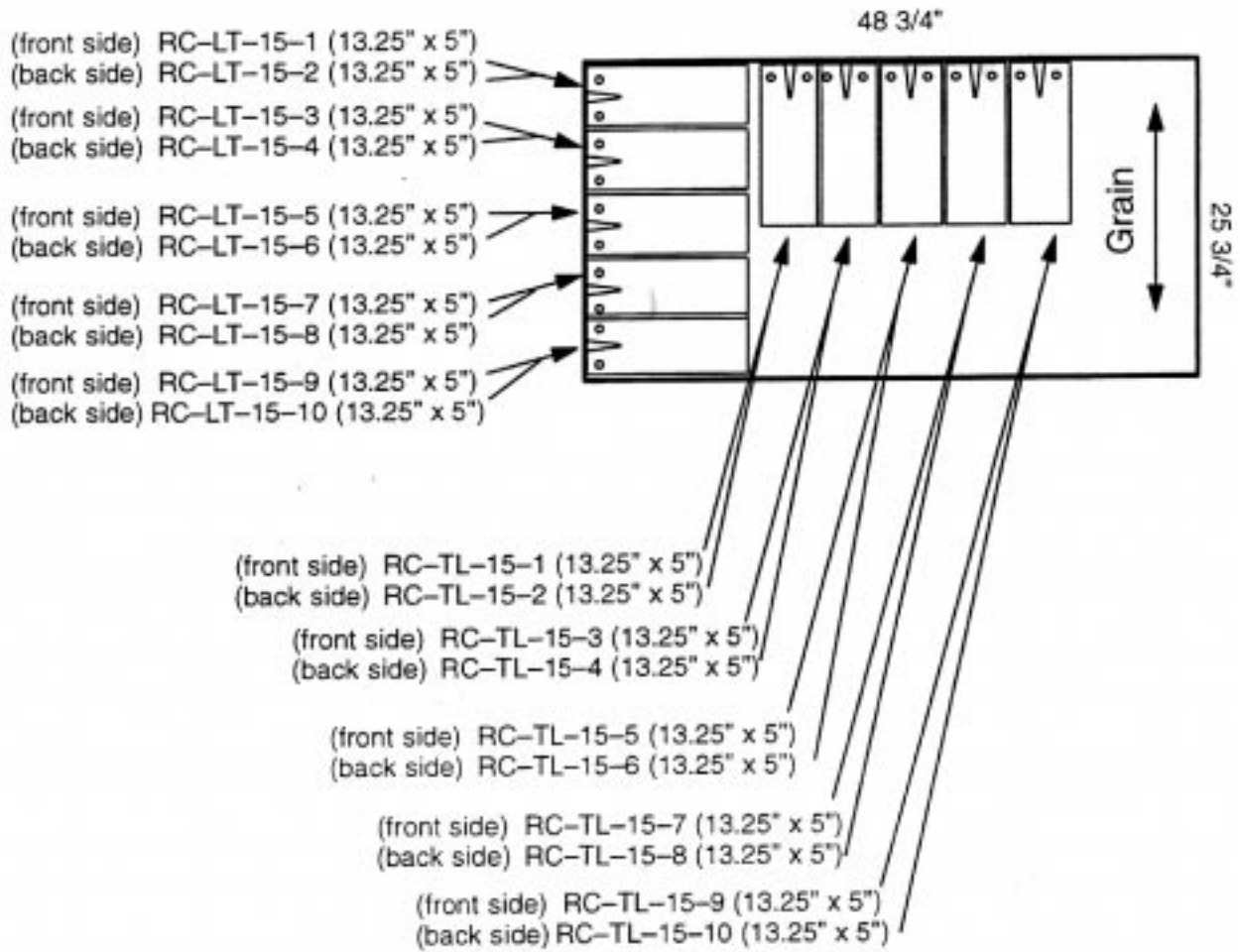
IAS Material Properties Cutting Diagram

6013 Extrusion (t = 0.2)
29" x 96"



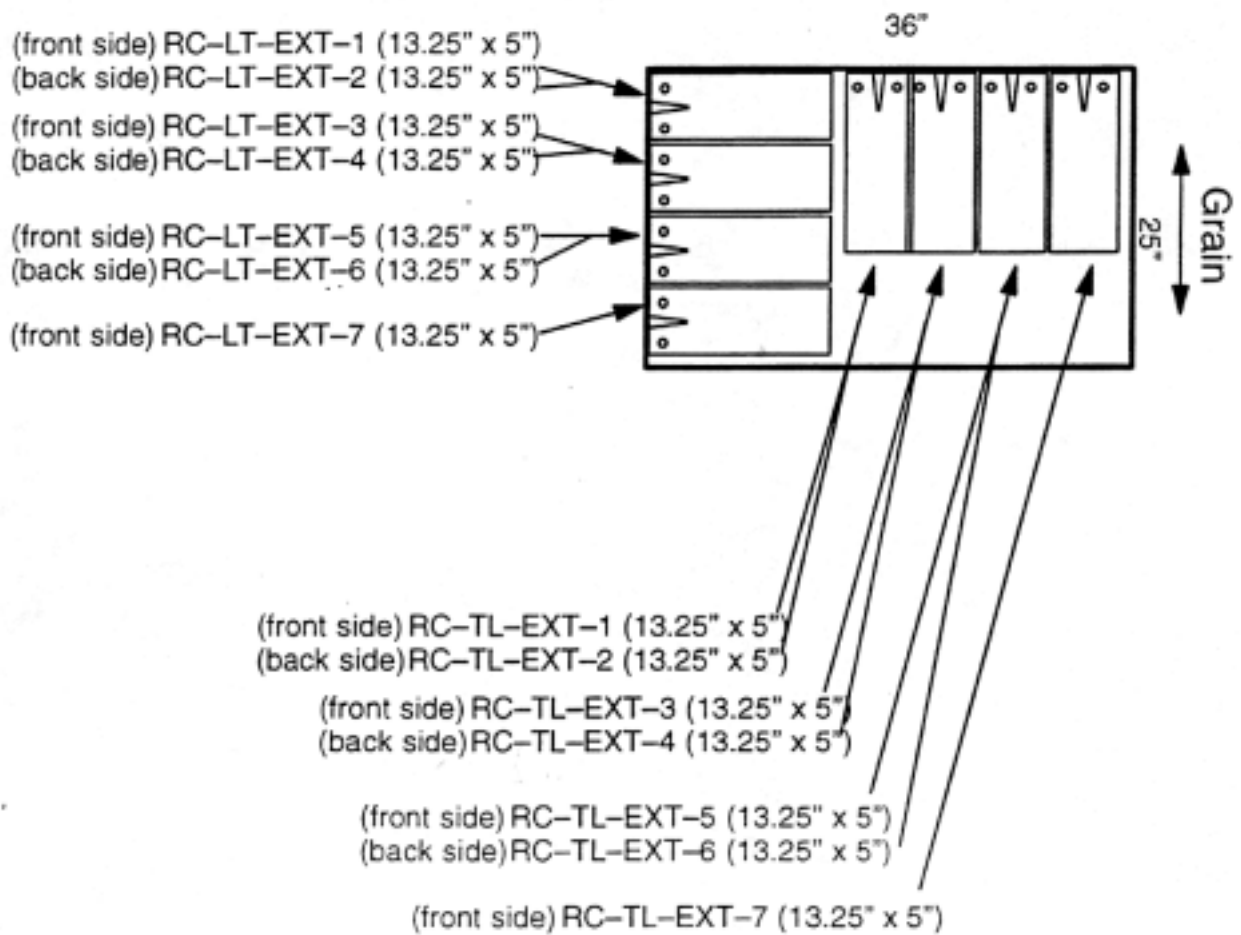
IAS Material Properties Cutting Diagram

7050 Plate (t = 1.5")
25 3/4" x 48 3/4"



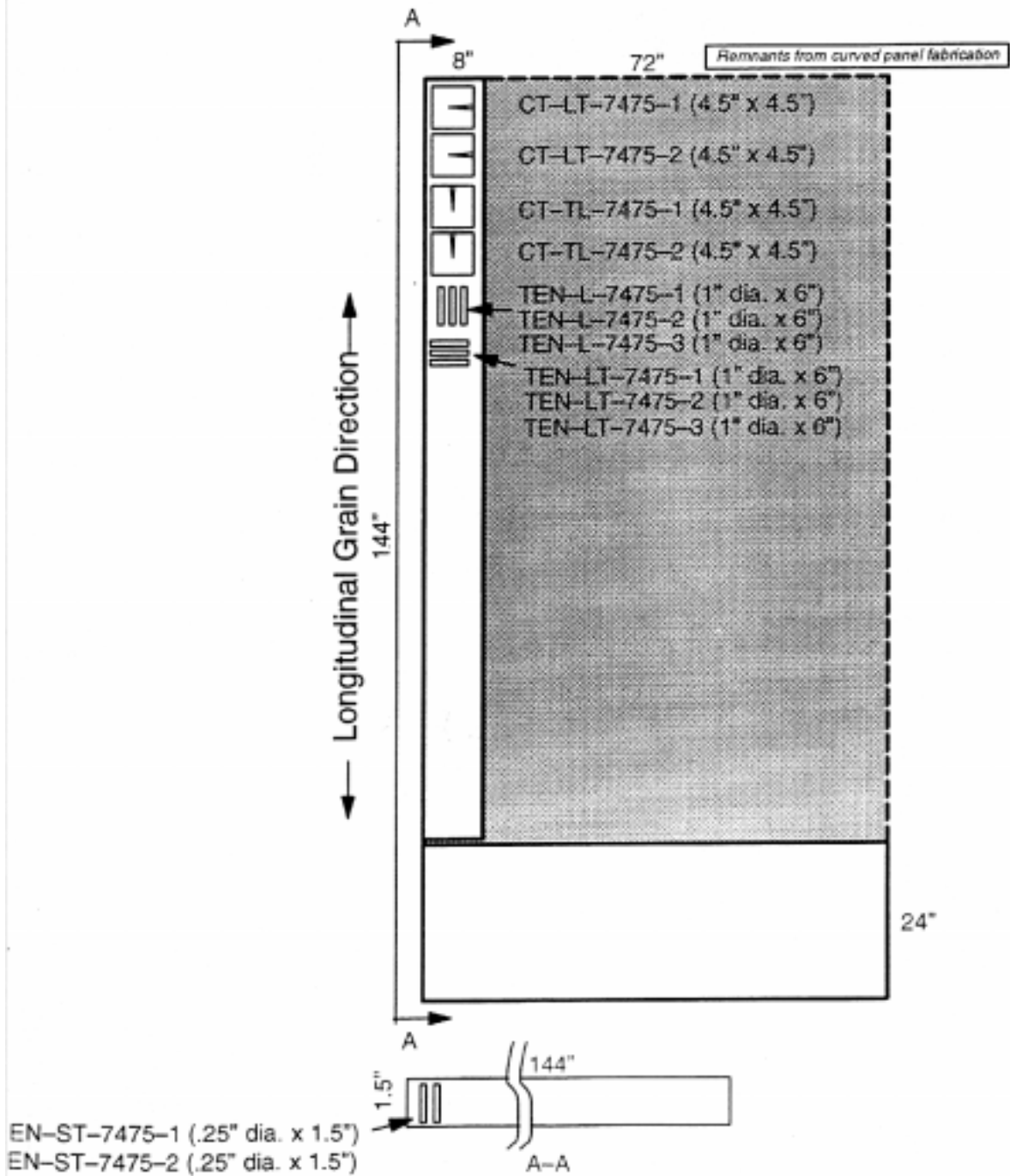
IAS Material Properties Cutting Diagram

7050 Extrusion (t = 1.5")
25" x 36"



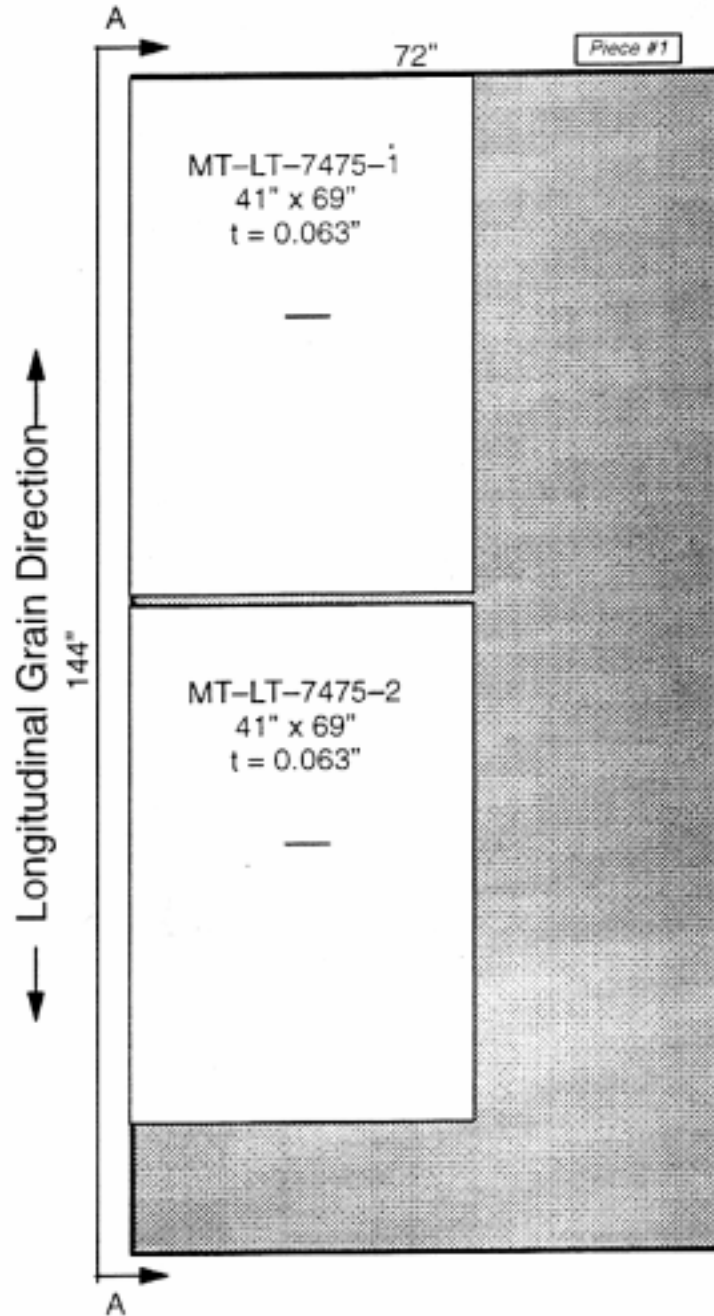
IAS Material Properties Cutting Diagram

7475-T7351 Plate (t = 1.5")
72" x 144"
(panel fabrication remnants)



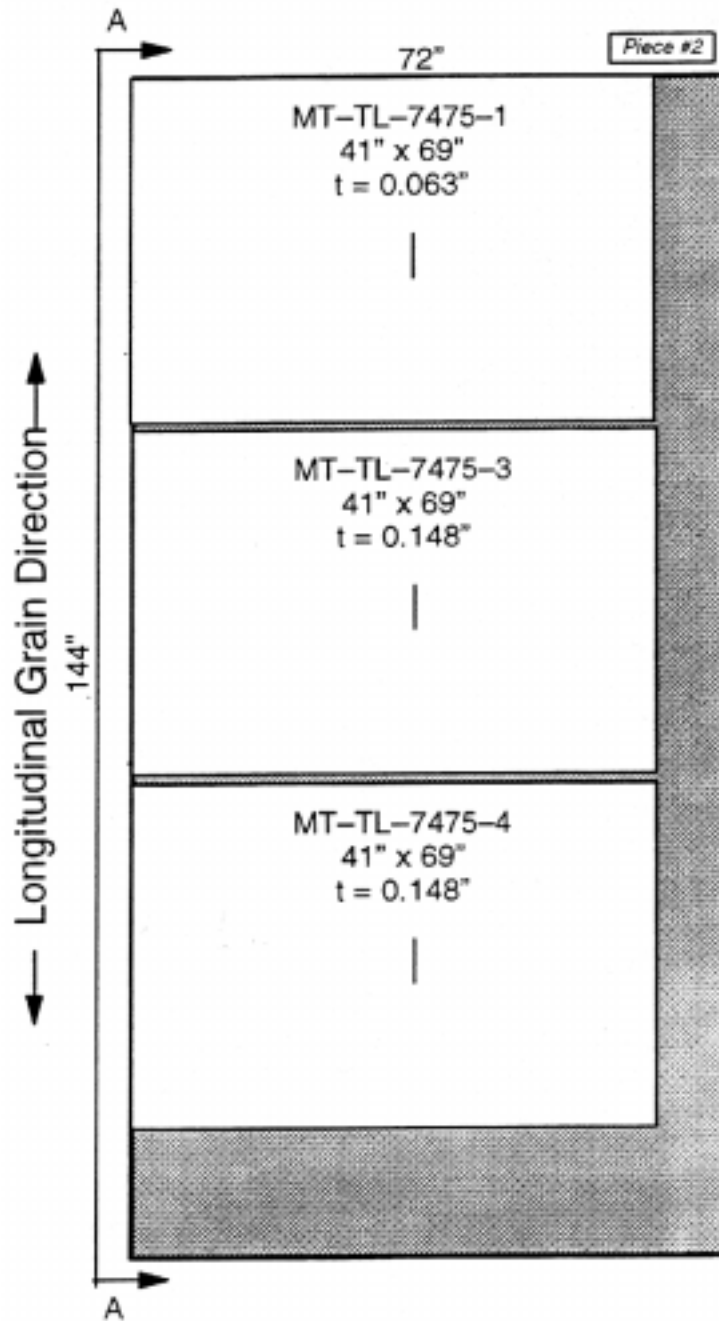
IAS Material Properties Cutting Diagram

7475-T7351 Plate (t = 1.5")
72" x 144"



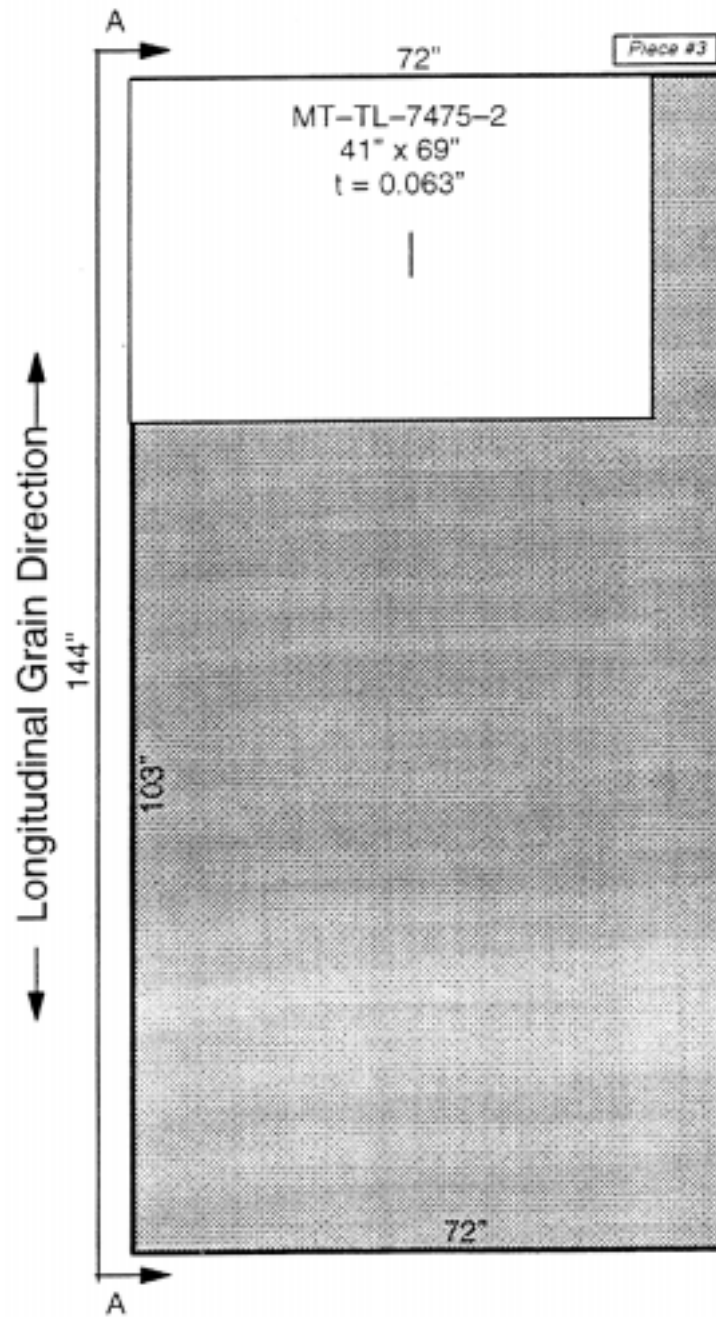
IAS Material Properties Cutting Diagram

7475-T7351 Plate (t = 1.5")
72" x 144"



IAS Material Properties Cutting Diagram

7475-T7351 Plate (t = 1.5")
72" x 144"



IAS Material Properties Test Matrix

Test Group	Test Type	Grain	Thickness (original / final)	Location	Specimen ID	Specimen Drawing No.
1	Static Tensile	L	1.5/7475	1/2	TEN-L-7475-1	D6-4671-856-2 (Rough size = 1"D x 6")
		L	1.5/7475	flush	TEN-L-7475-2	
		L	1.5/7475	flush	TEN-L-7475-3	
		L	1.5/7050	1/2	TEN-L-15-1	
		L	1.5/7050	flush	TEN-L-15-2	
		L	1.5/7050	flush	TEN-L-15-3	
		L	2.5/7050	1/4	TEN-L-25-1	
		L	2.5/7050	flush	TEN-L-25-2	
		L	2.5/7050	flush	TEN-L-25-3	
		L	ext. #1/7050	1/2	TEN-L-EXT1-1	D6-4671-877 (Rough size = 2" x 9" x t)
		L	ext. #1/7050	flush	TEN-L-EXT1-2	
		L	ext. #1/7050	flush	TEN-L-EXT1-3	
		L	ext. 6013	1/2	TEN-L-E6013-1	
		L	ext. 6013	flush	TEN-L-E6013-2	
		L	ext. 6013	flush	TEN-L-E6013-3	
		LT	1.5/7475	1/2	TEN-LT-7475-1	D6-4671-856-1 (Rough size = 1"D x 6")
		LT	1.5/7475	flush	TEN-LT-7475-2	
		LT	1.5/7475	flush	TEN-LT-7475-3	
		LT	1.5/7050	1/2	TEN-LT-15-1	
		LT	1.5/7050	flush	TEN-LT-15-2	
		LT	1.5/7050	flush	TEN-LT-12-3	
		LT	2.5/7050	1/4	TEN-LT-25-1	
		LT	2.5/7050	flush	TEN-LT-25-2	
		LT	2.5/7050	flush	TEN-LT-25-3	
		LT	ext. #1/7050	1/2	TEN-LT-EXT1-1	D6-4671-877 (Rough size = 2" x 9" x t)
		LT	ext. #1/7050	flush	TEN-LT-EXT1-2	
		LT	ext. #1/7050	flush	TEN-LT-EXT1-3	
		LT	ext. 6013	1/2	TEN-L-E6013-1	
		LT	ext. 6013	flush	TEN-L-E6013-2	
		LT	ext. 6013	flush	TEN-L-E6013-3	
		ST	1.5/7475	-	TEN-ST-7475-1	D6-4671-881 (Rough size = .25"D x 1.5")
		ST	1.5/7475	-	TEN-ST-7475-2	
		ST	1.5/7050	-	TEN-ST-15-1	
		ST	1.5/7050	-	TEN-ST-15-2	
		ST	2.5/7050	-	TEN-ST-25-1	
		ST	2.5/7050	-	TEN-ST-25-2	
ST	ext. #1/7050	-	TEN-SL-EXT1-1	D6-4671-142 (Rough size = 1" x 3" x t)		
ST	ext. #1/7050	-	TEN-SL-EXT1-2			
ST	ext. 6013	-	TEN-SL-E6013-1			
ST	ext. 6013	-	TEN-SL-E6013-2			

IAS Material Properties Test Matrix With Stress Level

Test Group	Test Type	Grain	Thickness (original / final)	Location	Specimen ID	Stress Level	Specimen Drawing No.	
2	Fatigue (unnotched, R=.05) as machined finish	L	1.5 / 0.1 7050	Flush side	FAT-L-15-1	40	net section (ksi.)	
					FAT-L-15-2			
					FAT-L-15-3			30
					FAT-L-15-4			
			2.5 / 0.1 7050		FAT-L-15-5	20		
					FAT-L-25-1			
					FAT-L-25-2			40
					FAT-L-25-3			
			ext. #1 / 0.1 7050		FAT-L-25-4	30		
					FAT-L-25-5			
					FAT-L-EXT1-1			40
					FAT-L-EXT1-2			
		1.5 / 0.1 7050	1/2	FAT-L-EXT1-3	30			
				FAT-L-EXT1-4				
				FAT-L-EXT1-5	20			
				FAT-L-15-6				
				2.5 / 0.1 7050	FAT-L-15-7	40		
					FAT-L-15-8			
		FAT-L-15-9	30					
		FAT-L-15-10						
		LT	1.5 / 0.1 7050	Flush side	FAT-L-25-6	40		
					FAT-L-25-7			
					FAT-L-25-8	30		
					FAT-L-25-9			
2.5 / 0.1 7050	FAT-L-25-10				20			
	FAT-LT-15-1							
	FAT-LT-15-2		40					
	FAT-LT-15-3							
	ext. #1 / 0.1 7050		FAT-LT-15-4			30		
			FAT-LT-15-5					
FAT-LT-15-6			20					
FAT-LT-15-7								
2.5 / 0.1 7050	1/2	FAT-LT-25-1	40					
		FAT-LT-25-2						
		FAT-LT-25-3	30					
		FAT-LT-25-4						
ext. #1 / 0.1 7050	1/2	FAT-LT-25-5	20					
		FAT-LT-EXT1-6						
		FAT-LT-EXT1-7						
		FAT-LT-EXT1-8		30				
		FAT-LT-EXT1-9						
		FAT-LT-EXT1-10		20				

IAS Material Properties Test Matrix With Stress Level (concluded)

Test Group	Test Type	Grain	Thickness (original / final)	Location	Specimen ID	Stress Level	Specimen Drawing No.
2 cont.	Fatigue (open hole R=.05)	L	1.5 / 0.1 7050	Flush side	FATO-L-15-1	20	net section (ksi.)
					FATO-L-15-2		
					FATO-L-15-3	15	
			FATO-L-15-4		15		
			FATO-L-15-5		10		
			FATO-L-25-1		20		
			FATO-L-25-2		20		
			FATO-L-25-3		15		
			FATO-L-25-4		15		
			FATO-L-25-5		10		
			FATO-L-EXT1-1		20		
			FATO-L-EXT1-2		20		
		FATO-L-EXT1-3	15				
		FATO-L-EXT1-4	15				
		FATO-L-EXT1-5	10				
		FATO-L-15-6	20				
		FATO-L-15-7	20				
		FATO-L-15-8	15				
		FATO-L-15-9	15				
		FATO-L-15-10	10				
		FATO-L-25-6	20				
		FATO-L-25-7	20				
		FATO-L-25-8	15				
		FATO-L-25-9	15				
FATO-L-25-10	10						
							SP00043-1 (Rough size = 1.5" x 8.5")
		LT	1.5 / 0.1 7050	Flush side	FATO-LT-15-1	20	
					FATO-LT-15-2		
					FATO-LT-15-3	15	
			FATO-LT-15-4		15		
			FATO-LT-15-5		10		
			FATO-LT-25-1		20		
			FATO-LT-25-2		20		
			FATO-LT-25-3		15		
			FATO-LT-25-4		15		
		FATO-LT-25-5	10				
			ext. #1 / 0.1 7050		FATO-LT-EXT1-1	20	
				FATO-LT-EXT1-2	20		
				FATO-LT-EXT1-3	15		
					FATO-LT-EXT1-4	15	
					FATO-LT-EXT1-5	10	

IAS Material Properties Test Matrix With Cyclic/Failure Loads

Test Group	Test Type	Grain	Thickness (original / final)	Location	Specimen ID	Loads cyclic/failure	Specimen Drawing No.	
3	Crack Growth R-Curve	L-T	1.5 / 0.063/7475 1.5 / 0.063/7475	Flush side	MT-LT-7475-1 MT-LT-7475-2		D6-4671-5 -664-3 (Rough size = 41" x 69")	
			1.5 / 0.06/7050 2.5 / 0.06/7050 ext.#1/0.06/7050 ext. 6013 / 0.06		MT-LT-15-1 MT-LT-25-1 MT-LT-EXT1-1 MT-LT-E6013-1	Cyclic load=10.7 kips $K_I = 6.7$ ksi sqrt in $K_{II} = 28.3$ ksi sqrt in Anticipated failure: 32.1 kips	D6-4671-5 -555-2 (Rough size = 25" x 48")	
		T-L	1.5 / 0.063/7475 1.5 / 0.063/7475 1.5 / 0.148/7475 1.5 / 0.148/7475		MT-TL-7475-1 MT-TL-7475-2 MT-TL-7475-3 MT-TL-7475-4		D6-4671-5 -664-3 (Rough size = 41" x 69")	
			1.5 / 0.06/7050 2.5 / 0.06/7050 ext.#1/0.06/7050 ext. 6013 / 0.06		MT-TL-15-1 MT-TL-25-1 MT-TL-EXT1-1 MT-TL-E6013-1	Cyclic load= 6.6 kips $K_I = 4.0$ ksi sqrt in $K_{II} = 17.3$ ksi sqrt in Anticipated failure: 19.7 kips	D6-4671-5 -555-2 (Rough size = 25" x 48")	
		T-L	1.5 / 0.12/7050 2.5 / 0.12/7050 ext.#1/0.12/7050 ext.#1/0.06/7050		MT-TL-15-2 MT-TL-25-2 MT-TL-EXT1-2 MT-TL-EXT1-3	Cyclic load= 9.3 kips $K_I = 5.7$ ksi sqrt in $K_{II} = 17.3$ ksi sqrt in Anticipated failure: 27.8 kips	D6-4671-5 -547-2 (Rough size = 13" x 30")	
		L-T	1.5 / 0.06/7050 2.5 / 0.06/7050 ext.#1/0.06/7050		MT-LT-15-2 MT-LT-15-3 MT-LT-25-2 MT-LT-25-3 MT-LT-EXT1-2	Cyclic load= 7.6 kips $K_I = 9.3$ ksi sqrt in $K_{II} = 28.3$ ksi sqrt in Anticipated failure: 22.7 kips		
		T-L	1.5 / 0.12/7050 2.5 / 0.12/7050		MT-TL-15-3 MT-TL-25-3	Cyclic load= 9.3 kips $K_I = 5.7$ ksi sqrt in $K_{II} = 17.3$ ksi sqrt in Anticipated failure: 27.8 kips		
		L-T	1.5 / 0.063/7475 1.5 / 0.063/7475		Flush side	CT-LT-7475-1 CT-LT-7475-2		SP00136-7 (Rough size = 4.5" x 4.5")
		T-L	1.5 / 0.063/7475 1.5 / 0.063/7475			CT-TL-7475-1 CT-TL-7475-2		
		L-S	1.5 / 0.06/7050 2.5 / 0.06/7050 ext.#1/0.06/7050		-	CT-LS-15-1 CT-LS-25-1 CT-LS-EXT1-1	Cyclic load= 0.1 kips $K_I = 7.1$ ksi sqrt in $K_{II} = 16.1$ ksi sqrt in Anticipated failure: 0.15 kips	SP00136-1 (Rough size = 1.5" x 1.5")
			1.5 / 0.12/7050 2.5 / 0.12/7050 ext.#1/0.12/7050			CT-LS-15-2 CT-LS-25-2 CT-LS-EXT1-2	Cyclic load= 0.2 kips $K_I = 7.1$ ksi sqrt in $K_{II} = 16.1$ ksi sqrt in Anticipated failure: 0.3 kips	

IAS Material Properties Test Matrix With Pre-crack/Failure Loads

Test Group	Test Type	Grain	Thickness (original / final)	Location	Specimen ID	Loads Pre-crack/failure	Specimen Drawing No.
4	r_c	L-T	1.5 / 0.09 7050	Flush side	RC-LT-15-1*	TBD by McDonnell Douglas	MDC-3
					RC-LT-15-2		
					RC-LT-15-3*		
					RC-LT-15-4		
					RC-LT-15-5		
					RC-LT-15-6		
					RC-LT-15-7		
					RC-LT-15-8		
					RC-LT-15-9		
					RC-LT-15-10		
		T-L	1.5 / 0.09 7050		RC-TL-15-1		MDC-3
					RC-TL-15-2		
					RC-TL-15-3		
					RC-TL-15-4		
					RC-TL-15-5		
					RC-TL-15-6		
					RC-TL-15-7		
					RC-TL-15-8		
					RC-TL-15-9		
					RC-TL-15-10		
		L-T	ext. #1 / 0.09 7050		RC-LT-EXT1-1		MDC-3
					RC-LT-EXT1-2		MDC-5
					RC-LT-EXT1-3		MDC-7
					RC-LT-EXT1-4		MDC-9
					RC-LT-EXT1-5		MDC-11
					RC-LT-EXT1-6		MDC-13
					RC-LT-EXT1-7		MDC-15
		T-L	ext. #1 / 0.09 7050		RC-TL-EXT1-1		MDC-3
RC-TL-EXT1-2	MDC-5						
RC-TL-EXT1-3	MDC-7						
RC-TL-EXT1-4	MDC-9						
RC-TL-EXT1-5	MDC-11						
RC-TL-EXT1-6	MDC-13						
RC-TL-EXT1-7	MDC-15						

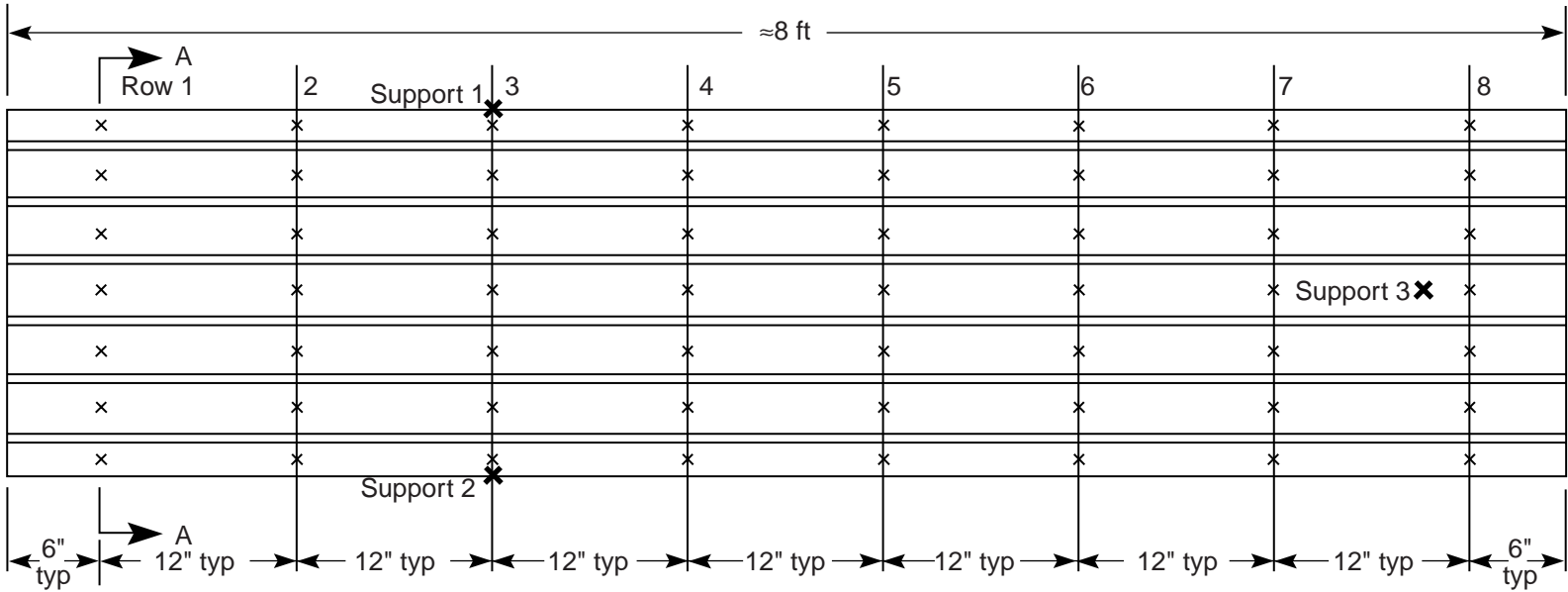
* Damaged specimen on fabrication (did not re-make)

Appendix E

Extruded Panel Measurements

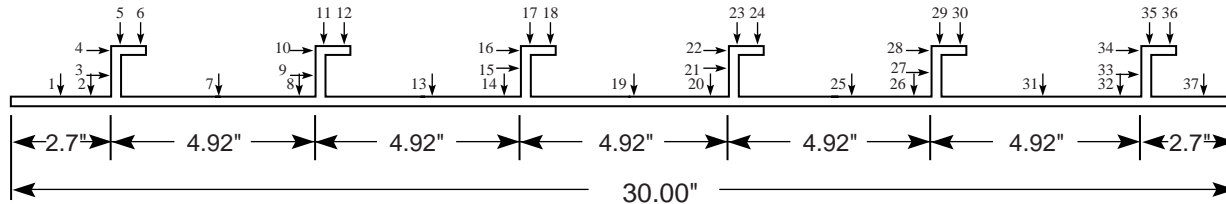
Following are measurements of the Alcoa extrusion panels taken at Boeing Seattle.

Draft Example of Panel Measurement



PLAN VIEW OF 30 in. x 96 in. EXTRUDED PANEL

Point Locations



Section A-A

✕ = Panel Supports

Supports 1 & 2 located
30 inches from end of panel,
0.4 inches from side.

Support 3 located on C₁,
9.25 inches from end of panel.

Figure 1.0-1. Extruded Panel.

		Change in top of flange					Panel 1
Points		6	12	18	24	30	36
Row							
1	z	1.146	1.128	1.070	1.162	1.159	1.336
	x	3.060	8.018	12.879	17.769	22.780	27.540
2	z	1.189	1.129	1.028	1.101	1.115	1.264
	x	3.061	8.018	12.879	17.766	22.779	27.540
3	z	1.300	1.149	1.075	1.100	1.090	1.231
	x	2.833	8.019	12.879	17.768	22.779	27.540
4	z	1.254	1.176	1.080	1.130	1.106	1.234
	x	3.086	8.020	12.940	17.770	22.779	27.540
5	z	1.219	1.202	1.150	1.167	1.155	1.262
	x	3.164	8.021	12.940	17.768	22.779	27.592
6	z	1.228	1.238	1.140	1.202	1.218	1.344
	x	3.164	8.020	12.940	17.773	22.780	27.593
7	z	1.257	1.272	1.197	1.283	1.313	1.457
	x	3.163	8.018	12.940	17.769	22.780	27.594
8	z	1.270	1.307	1.275	1.371	1.408	1.580
	x	3.163	8.019	12.922	17.769	22.779	27.594
Δz		0.154	0.179	0.247	0.271	0.318	0.349

		Change in top of flange					Panel 2
Points		6	12	18	24	30	36
Row							
1	z	1.251	1.157	1.103	1.066	1.183	1.198
	x	3.163	8.079	12.992	17.870	22.780	27.693
2	z	1.224	1.136	1.074	1.063	1.124	1.210
	x	3.164	8.079	12.992	17.869	22.780	27.693
3	z	1.259	1.143	1.058	1.091	1.170	1.261
	x	3.124	8.079	12.992	17.869	22.739	27.643
4	z	1.257	1.153	1.046	1.107	1.218	1.317
	x	3.122	8.079	12.992	17.869	22.738	27.643
5	z	1.262	1.196	1.139	1.132	1.247	1.270
	x	3.125	8.079	12.992	17.869	22.740	27.643
6	z	1.292	1.226	1.174	1.178	1.300	1.336
	x	3.123	8.079	12.992	17.870	22.740	27.644
7	z	1.294	1.257	1.202	1.180	1.326	1.425
	x	3.125	8.080	12.992	17.871	22.739	27.644
8	z	1.321	1.288	1.229	1.222	1.406	1.540
	x	3.123	8.086	12.992	17.869	22.740	27.643
Δz		0.097	0.152	0.183	0.159	0.282	0.342

Rows	Change in z							Panel 1
	1	2	3	4	5	6	7	8
Location								
1	1.259							
	.052	.097	0.150	0.155	0.159	0.173	0.193	0.206
								Δ 0.154
7	5.040							
	0.033	.052	0.073	0.096	0.109	0.130	0.159	0.178
								Δ 0.145
13	9.960							
	0.002	-0.016	0.003	0.031	0.067	0.100	0.142	0.179
								Δ 0.195
19	15.060							
	0.009	-0.048	-0.049	-0.016	0.022	0.070	0.140	0.199
								Δ 0.242
25	19.80							
	0.065	0.016	0.006	0.025	0.061	0.118	0.203	0.288
								Δ 0.242
31	24.720							
	0.137	0.083	0.060	0.069	0.109	0.178	0.276	0.374
								Δ 0.314
37	28.440							
	0.248	0.182	0.157	0.150	0.178	0.252	0.380	0.505
								Δ 0.355
	Δ	Δ	Δ	Δ	Δ	Δ	Δ	Δ
	0.246	0.230	0.206	0.166	0.156	0.182	0.240	0.327

Delta change in skin amplitude down the panel

Rows	Change in z							Panel 2
	1	2	3	4	5	6	7	8
1A	1.259							
	0.195	0.166	0.181	.185	.188	0.221	0.229	0.256
								Δ .090
7A	5.040							
	0.119	0.096	0.115	0.136	0.119	0.149	0.183	0.216
								Δ 0.120
13A	9.960							
	0.048	0.028	0.020	0.048	.086	0.115	0.139	0.183
								Δ 0.163
19A	15.059							
	0.048	0.029	0.006	.002	.081	0.123	0.157	0.190
								Δ 0.188
25A	19.80							
	0.014	-0.028	-0.030	.028	0.088	0.119	0.126	0.170
								Δ 0.200
31A	24.719							
	0.080	.050	0.109	0.175	0.132	0.164	0.214	0.322
								Δ 0.178
37A	28.439							
	<u>0.151</u>	<u>0.108</u>	<u>0.162</u>	<u>0.224</u>	<u>0.197</u>	<u>0.248</u>	<u>0.332</u>	0.468
								Δ 0.360
	Δ 0.137	Δ 0.194	Δ 0.211	Δ 0.222	Δ 0.116	Δ 0.133	Δ 0.206	Δ 0.378

		Stringer Wave x-Direction					Panel 1
Points		4	10	16	22	28	34
Row							
1		2.505 1.019	7.468 1.020	12.333 .999	17.222 1.030	22.194 1.060	27.007 1.179
2		2.523 1.019	7.476 1.020	12.369 0.990	17.235 1.030	22.196 1.059	27.030 1.180
3		<u>2.337</u> 1.066	7.471 1.018	12.360 0.990	17.234 1.021	22.207 1.047	27.046 1.150
4		2.505 1.106	7.474 1.020	12.367 0.990	17.234 1.020	22.212 1.046	27.060 1.150
5		2.569 1.105	7.478 1.103	12.351 0.990	17.241 1.020	22.207 1.046	27.068 1.150
6		2.565 1.106	7.473 1.102	12.363 1.090	17.247 1.081	22.201 1.086	27.053 1.150
7		2.571 1.181	7.474 1.180	12.362 1.090	17.236 1.200	22.216 1.186	27.077 1.271
8		<u>2.577</u> 1.201	7.468 1.200	12.334 1.090	17.227 1.230	22.216 1.278	27.072 1.424
Δ		<u>0.240</u>	<u>0.010</u>	0.036	0.025	0.022	0.070

		Stringer Wave x-Direction					Panel 2
Points		4	10	16	22	28	34
Row							
1		2.574 1.150	7.514 1.070	12.437 1.020	17.326 1.000	22.196 1.060	27.140 1.105
2		2.584 1.150	7.530 1.070	12.434 0.989	17.322 0.970	22.210 1.021	27.123 1.106
3		2.558 1.150	7.524 1.070	12.426 0.990	17.292 0.970	22.182 1.021	27.109 1.105
4		2.546 1.150	7.514 1.070	12.430 0.990	17.286 0.970	22.176 1.120	27.104 1.171
5		2.561 1.150	7.508 1.118	12.418 1.040	17.298 .970	22.191 1.121	27.110 1.171
6		2.570 1.187	7.506 1.120	12.425 1.040	17.309 1.030	22.192 1.121	27.109 1.171
7		2.585 1.191	7.510 1.160	12.433 1.100	17.327 1.080	22.200 1.181	27.107 1.271
8		2.579 1.220	7.499 1.190	12.441 1.140	17.327 1.120	22.198 1.271	27.116 1.390
Δ		0.039	0.031	0.023	0.041	0.034	0.036

Flange Wave w/o Skin Influence

Panel 2

Points	6	12	18	24	30	36
Row	2	8	14	20	26	32
1	(1.081) 0.170 z 1.251 x 3.163	(1.073) 0.084 1.157 8.079	(1.066) 0.037 1.103 12.992	(1.079) -0.013 1.066 17.870	(1.119) 0.064 1.183 22.780	(1.075) 0.123 1.198 27.693
2	(1.071) 0.153 z 1.224 x 3.164	(1.060) 0.076 1.136 8.079	(1.069) 0.005 1.074 12.992	(1.085) -0.022 1.063 17.869	(1.129) 0.005 1.124 22.780	(1.103) 0.107 1.210 27.693
3	(1.087) 0.172 z 1.259 x 3.124	(1.063) 0.080 1.143 8.079	(1.051) -0.007 1.058 12.992	(1.102) -0.011 1.091 17.869	(1.136) 0.034 1.170 22.739	(1.100) 0.161 1.261 27.643
4	(1.083) .174 z 1.257 x 3.122	(1.046) .107 1.153 8.079	(1.026) .020 1.046 12.992	(1.101) .006 1.107 17.869	(1.109) .109 1.218 22.738	(1.096) .221 1.317 27.643
5	(1.075) .187 z 1.262 x 3.125	(1.064) .132 1.196 8.079	(1.068) .071 1.139 12.992	(1.092) .040 1.132 17.869	(1.096) .151 1.247 22.740	(1.072) .198 1.270 27.643
6	(1.076) .216 z 1.292 x 3.123	(1.075) .151 1.226 8.079	(1.067) .107 1.174 12.992	(1.091) .087 1.178 17.870	(1.125) .175 1.300 22.740	(1.094) .242 1.336 27.644
7	(1.069) .225 z 1.294 x 3.125	(1.080) .177 1.257 8.080	(1.073) .129 1.202 12.992	(1.081) .099 1.180 17.871	(1.120) .206 1.326 22.739	(1.106) .319 1.425 27.644
8	(1.075) .246 z 1.321 x 3.123	(1.079) .209 1.288 8.086	(1.062) .167 1.229 12.992	(1.082) .140 1.222 17.869	(1.129) .277 1.406 22.740	(1.090) 0.450 1.540 27.643
Δz	0.097	0.152	0.183	0.159	0.282	0.342
Δz	0.018	0.034	0.047	0.023	0.040	0.034
Not due to skin						

Appendix F

Strain Gage Readings and Gage Locations

Following is the Boeing Seattle report “Strain Gage Readings and Gage Locations,” which details this information for Test 1 and Test 2 of the two-bay longitudinal crack panel.

Strain Gage Readings and Gage Locations

The contents of this appendix are defined below:

- Strain gage survey for both test locations

Test 1 - Intact skin and frame at 8.6 psi Page F-3
- 38 inch skin crack with severed central frame at 8.6 psi Page F-4

Test 2 - Intact skin and frame at 8.6 psi Page F-5
- 38-inch skin crack with severed central frame at 8.6 psi Page F-6

Assumed mechanical properties and nomenclature:

Frames: $E = 10.7 \times 10^6$ psi Poisson's ratio = 0.33
 $E_c = 10.6 \times 10^6$ psi $G = 3.9 \times 10^6$ psi
 $F_{ty} = 68$ ksi $F_{cy} = 64$ ksi $F_{sy} = 39$ ksi

Skin stringer: $E = 10.3 \times 10^6$ psi Poisson's ratio = 0.33
 $E_c = 10.6 \times 10^6$ psi $G = 3.9 \times 10^6$ psi
 $F_{ty} = 62$ ksi $F_{cy} = 60$ ksi $F_{sy} = 35$ ksi

gage# = strain gage identification
fa1 = stress in the hoop or circumferential direction
fc1 = stress in the longitudinal direction
fmax1 = maximum principal stress
fmin1 = minimum principal stress
tac1 = shear stress between the hoop and longitudinal direction
tacm1 = maximum principal shear stress
angle1 = angle to the principal stress measured from the hoop direction

Note: Stress reported in ksi, and angle reported in degrees.

- Strain gage locations/drawing number 115X8003 (20 pages)

- Test 1 was conducted at the "R.H. Strain Gage Area"
- Test 2 was conducted at the "L.H. Strain Gage Area"

TEST NUMBER: TEST 1
 TEST DESCRIPTION: Intact - gage readings
 PANEL CONDITION: Intact
 NOTE: Stress in ksi

PANEL NUMBER: IAS
 PEAK PRESSURE: 8.6 psi
 CYCLE PRESSURE: 8.6 psi
 CYCLE NUMBER: 18

gage1	gage2	fa1	fc1	fmax1	fmin1	tac1	tacm1	angle1	fa2	fc2	fmax2	fmin2	tac2	tacm2	angle2
1	2	3.5	4.5	4.6	3.3	-0.4	0.7	-69.4	4.3	2.2	4.4	2.0	-0.7	1.2	-16.3
3	4	7.3	5.4	7.3	5.4	-0.2	1.0	-4.5	5.8	1.7	5.8	1.7	-0.1	2.0	-1.2
5	6	13.2	6.9	13.5	6.7	-1.2	3.4	-10.2	11.6	4.7	11.9	4.4	-1.4	3.8	-11.1
7	8	15.4	6.7	15.4	6.7	0.5	4.4	3.2	13.6	5.6	13.6	5.6	0.3	4.0	2.2
9	10	15.3	7.3	15.4	7.2	0.9	4.1	6.0	13.1	6.4	13.2	6.3	0.8	3.5	6.9
11	12	14.8	7.3	15.0	7.2	1.1	3.9	7.8	13.7	6.7	13.7	6.6	0.7	3.6	5.3
13	14	8.2	5.5	8.5	5.2	1.0	1.7	17.4	19.6	8.8	19.6	8.8	0.6	5.4	3.1
15	16	13.8	7.1	13.9	7.0	0.7	3.4	6.0	14.7	7.2	14.8	7.2	0.7	3.8	5.6
17	18	15.6	7.2	15.7	7.2	0.7	4.3	4.6	13.0	6.4	13.1	6.4	0.8	3.3	6.5
19	20	15.3	7.0	15.3	6.9	0.5	4.2	3.5	13.3	6.4	13.4	6.3	0.6	3.5	5.1
21	22	14.7	7.3	14.8	7.2	0.7	3.8	5.2	13.0	6.1	13.0	6.1	0.5	3.5	4.4
23	24	13.5	7.4	13.5	7.4	0.5	3.1	4.7	11.7	5.5	11.8	5.4	0.8	3.2	7.3
25	26	8.2	3.3	8.5	3.0	1.2	2.7	13.0	14.1	2.5	14.2	2.4	-1.1	5.9	-5.4
27	28	9.7	3.7	9.8	3.7	0.3	3.0	2.9	11.2	2.3	11.2	2.2	0.2	4.5	1.4
29	30	10.7	4.4	10.7	4.4	0.4	3.2	3.2	8.9	1.5	9.0	1.4	0.8	3.8	6.0
31	32	13.4	7.9	13.6	7.6	1.1	3.0	10.9	11.2	5.1	11.2	5.1	0.7	3.1	6.4
33	34	14.8	7.6	15.0	7.5	1.0	3.7	7.4	12.1	6.2	12.2	6.0	1.0	3.1	9.1
35	36	13.4	7.2	13.5	7.1	0.9	3.2	7.8	13.7	7.2	13.8	7.1	0.9	3.4	7.3
37	38	15.1	7.5	15.2	7.4	0.8	3.9	6.2	12.3	6.6	12.4	6.5	0.8	2.9	7.6
39	40	14.7	7.3	14.8	7.2	0.9	3.8	6.9	12.4	6.5	12.5	6.5	0.7	3.0	6.7
! 66		5.6													
! 68		5.4													
! 80		6.6													
! 82		6.5													
! 42		1.6													
! 44		0.3													
! 46		3.0													
! 48		2.5													
! 50		0.9													
! 52		-0.3													
! 54		0.3													
! 56		3.4													
! 58		5.8													
! 60		2.6													
! 62		0.6													
! 64		-0.8													
! 70		6.0													
! 72		2.5													
! 74		16.0													
! 76		4.4													
! 78		0.9													
! 84		5.3													
! 86		2.6													
! 88		10.1													
! 90		4.7													
! 92		2.1													
! 94		3.5													
! 96		7.3													
! 98		7.9													
! 100		7.8													
! 102		7.0													
* 104		8.0	5.4	10.4	3.1	-3.3	3.7	-34.7							

TEST NUMBER: TEST 1
 TEST DESCRIPTION: 38 inch - gage readings
 PANEL CONDITION: 38 inch skin crack / severed frame
 NOTE: Stress in ksi

PANEL NUMBER: IAS
 PEAK PRESSURE: 8.6 psi
 CYCLE PRESSURE: 8.6 psi
 CYCLE NUMBER: 10,355

gage1	gage2	fa1	fc1	fmax1	fmin1	tac1	tacm1	angle1	fa2	fc2	fmax2	fmin2	tac2	tacm2	angle2
1	2	-9.6	-10.3	-8.7	-11.3	-1.2	1.3	-37.8	12.0	13.8	13.8	12.0	0.2	0.9	84.1
3	4	-10.4	-9.9	-8.8	-11.5	1.3	1.4	49.4	10.6	14.6	16	9.3	-2.7	3.3	-63.1
5	6	1.0	10.5	11.2	0.3	2.6	5.4	75.7	-4.3	-4.7	-2.1	-7.0	-2.4	2.5	-42.8
7	8	6.7	11.8	11.9	6.5	-0.8	2.7	-81.4	-1.4	-1.4	1.1	-4.0	-2.5	2.6	-44.8
9	10	12.4	11.6	19.9	4.1	8.0	7.9	43.6	-1.6	4.8	11.2	-8.2	9.1	9.7	54.8
11	12	9.9	9.4	17.3	2.1	7.6	7.6	44.1	-2.8	2.5	8.6	-9.2	8.4	8.9	53.7
13	14	-7.2	0.3	4.6	-11.6	7.1	8.1	58.7	10.9	4.1	15.3	-0.3	7.0	7.8	31.9
15	16	-1.8	4.6	4.8	-2.1	-1.3	3.4	-78.8	3.4	3.5	6.9	0	-3.4	3.4	-45.4
17	18	2.8	8.1	9.6	1.3	-3.3	4.2	-64.5	0.1	3.0	4.5	-1.4	-2.6	2.9	-59.4
19	20	3.2	8.9	11.3	0.8	-4.4	5.2	-61.7	-0.1	4.3	5.9	-1.8	-3.1	3.8	-62.9
21	22	1.7	12.0	16.8	-3.2	-8.5	10	-60.7	-1.1	8.1	10.2	-3.3	-4.9	6.7	-66.6
23	24	4.5	9.6	24.4	-10.6	-17.3	17.5	-49.2	13.8	19.0	27.8	5.0	-11.2	11.4	-51.5
25	26	33.7	27.6	34.3	26.9	-2.1	3.7	-17.1	40.0	18.5	42.9	15.6	-8.5	13.7	-19.1
27	28	32.2	17.0	33.5	15.7	4.7	8.9	15.7	35.3	7.4	36.0	6.7	4.5	14.7	8.8
29	30	29.1	9.7	29.3	9.6	1.7	9.9	4.9	28.8	2.5	29.5	1.9	4.3	13.8	8.9
31	32	22.0	15.4	26.2	11.2	6.8	7.5	32.0	22.2	15.2	25.6	11.8	6.0	6.9	29.8
33	34	17.7	14.0	20.3	11.4	4.1	4.5	32.8	15.8	13.4	18.8	10.3	4.1	4.3	36.9
35	36	14.2	12.2	14.7	11.8	1.0	1.4	22.5	14.6	12.6	15.3	11.8	1.5	1.8	27.7
37	38	15.8	12.5	16.7	11.6	2.0	2.6	25.1	13.1	12.0	14.8	10.3	2.2	2.3	38.2
39	40	15.6	11.7	17.1	10.2	2.9	3.5	28.4	13.6	11.2	15.5	9.2	2.9	3.1	33.8
! 66		0.8													
! 68		0.1													
! 80		14.5													
! 82		13.8													
! 42		-5.7													
! 44		-17.9													
! 46		-28.3													
! 48		-4.1													
! 50		-13.0													
! 52		-21.4													
! 54		-4.5													
! 56		11.6													
! 58		24.4													
! 60		7.8													
! 62		10.0													
! 64		14.3													
! 70		1.2													
! 72		-1.7													
! 76		-0.5													
! 78		-2.6													
! 84		11.6													
! 86		5.4													
! 88		28.7													
! 90		9.8													
! 92		3.2													
! 94		5.6													
! 96		18.8													
! 98		18.3													
! 100		13.6													
! 102		10.9													
* 104		20.4	16.6	26.8	10.2	-7.8	8.3	-38.4							

TEST NUMBER: TEST 2
 TEST DESCRIPTION: Intact - gage readings
 PANEL CONDITION: Intact
 NOTE: Stress in ksi

PANEL NUMBER: IAS
 PEAK PRESSURE: 8.6 psi
 CYCLE PRESSURE: 8.6 psi
 CYCLE NUMBER: 18

gage1	gage2	fa1	fc1	fmax1	fmin1	tac1	tacm1	angle1	fa2	fc2	fmax2	fmin2	tac2	tacm2	angle2
23	24	6.4	12.7	12.8	6.4	0.4	3.2	86.3	11.1	4.6	11.1	4.5	0.7	3.3	5.7
25	26	7.7	2.5	7.7	2.5	0	2.6	0.3	12.2	3	12.8	2.4	2.4	5.2	13.6
27	28	8.4	3.2	8.4	3.2	0.6	2.6	6.8	10.3	2.2	10.3	2.2	-0.1	4.1	-1.0
29	30	10.8	8.4	14.4	4.8	-4.7	4.8	-37.9	8.3	-0.8	8.3	-0.8	0.7	4.6	4.4
31	32	12.4	6.8	12.5	6.7	0.8	2.9	8.3	10.7	4.1	10.8	4.1	0.5	3.3	4.1
33	34	14.0	6.3	14.0	6.3	0.5	3.9	3.9	11.8	5.3	11.9	5.2	0.5	3.3	4.3
35	36	9.2	5.1	9.3	5.1	0.5	2.1	6.2	17.1	7.6	17.1	7.6	0.2	4.7	1.3
37	38	13.4	6.0	13.4	5.9	0.3	3.7	2.6	12.8	6.1	12.8	6.1	0.2	3.3	1.7
39	40	13.9	6.0	14.0	6.0	0.5	4.0	3.9	12.1	5.8	12.1	5.8	0.3	3.2	2.7
! 42		-0.1													
! 44		3.7													
! 46		5.6													
! 48		1.9													
! 50		0.0													
! 52		-1.3													
! 54		-0.0													
! 56		3.2													
! 58		5.5													
! 60		1.9													
! 62		-0.0													
! 64		-1.8													
! 70		6.0													
! 72		4.1													
! 74		10.7													
! 76		6.0													
! 78		4.0													
! 84		5.7													
! 86		3.7													
! 88		11.0													
! 90		5.0													
! 92		3.7													
! 94		5.9													
! 96		7.7													
! 98		8.1													
! 100		8.0													
! 102		5.7													
* 104		6.7	2.0	6.7	2.0	0.1	2.4	1.7							
! 66		6.8													
! 68		6.6													
! 80		6.6													
! 82		6.5													

TEST NUMBER: TEST 2
 TEST DESCRIPTION: 38 inch - gage readings
 PANEL CONDITION: 38 inch skin crack/severed frame
 NOTE: Stress in ksi

PANEL NUMBER: IAS
 PEAK PRESS 8.6 psi
 CYCLE PRESSURE: 8.6 psi
 CYCLE NUMBER: 10,445

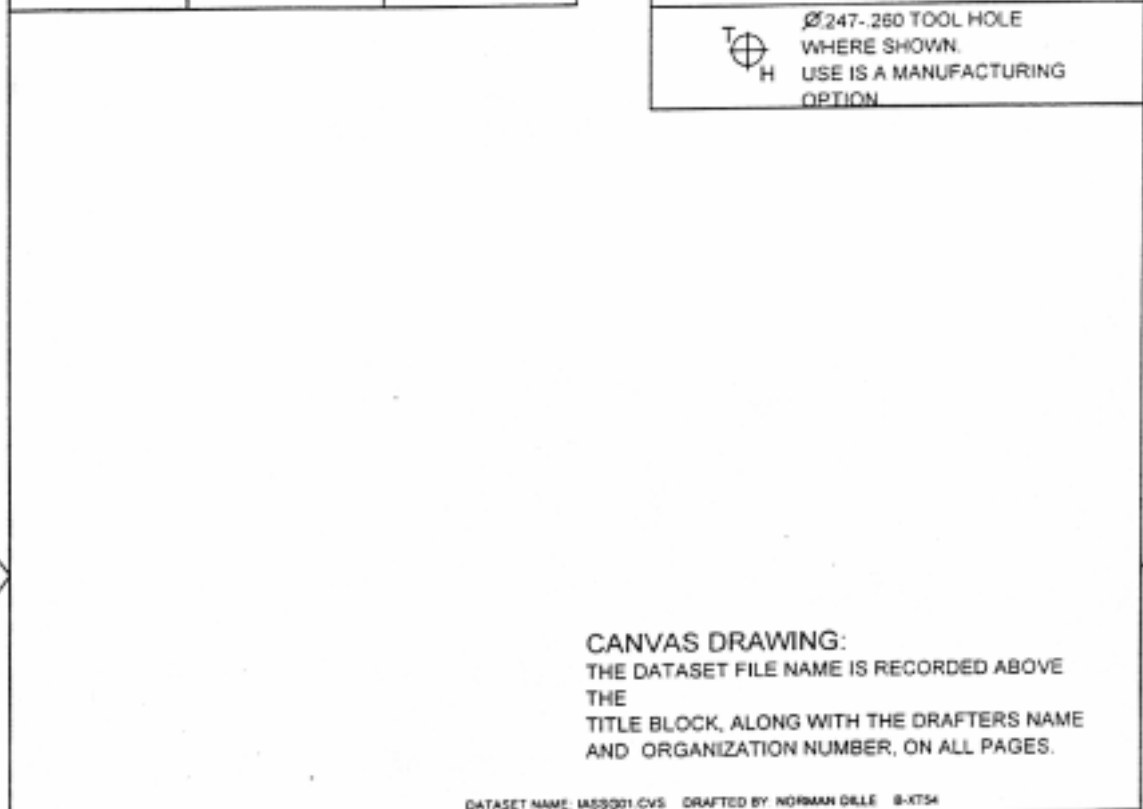
gage1	gage2	fa1	fc1	fmax1	fmin1	tac1	tacm1	angle1	fa2	fc2	fmax2	fmin2	tac2	tacm2	angle2
23	24	4.1	10.4	22.4	-8.1	14.9	15.3	51	13.1	6.7	23.3	-3.6	13.1	13.5	38.1
25	26	21.6	-2.5	21.6	-2.5	0.3	12.1	0.8	36.6	4.9	37.3	4.2	4.9	16.6	8.5
27	28	20	-0.6	20.4	-1	3	10.7	8	27.1	2.7	27.1	2.7	0	12.2	-0.1
29	30	26	19.3	38.7	6.6	-15.8	16.1	-39	18.9	-2.7	19	-2.7	-0.6	10.8	-1.5
31	32	20.4	2.9	20.5	2.8	-1	8.8	-3.1	21.8	4	21.9	3.9	-1.6	9	-4.9
33	34	18.2	6.3	19.1	5.3	-3.5	6.9	-15	18.2	6.9	19.3	5.7	-3.7	6.8	-16.6
35	36	11	9.5	13.9	6.6	-3.6	3.6	-38.9	18.4	12.6	20.6	10.4	-4.2	5.1	-27.6
37	38	15	9	16.8	7.2	-3.8	4.8	-25.7	14.9	10.1	17.3	7.6	-4.3	4.9	-30.2
39	40	15.8	7.7	17	6.5	-3.4	5.3	-19.9	14.9	8.4	16.6	6.6	-3.8	5	-24.7
!	80	14.6													
!	82	14.4													
!	42	-5.8													
!	44	-18.9													
!	46	-30.7													
!	48	-3.1													
!	50	-13.6													
!	52	-22.9													
!	54	-4.5													
!	56	13.7													
!	58	28.2													
!	60	7.9													
!	62	10.6													
!	64	15.7													
!	70	0.6													
!	72	0.5													
!	74	0													
!	84	11.8													
!	86	5.2													
!	88	31													
!	90	9.5													
!	92	4													
!	94	10.6													
!	96	14.4													
!	98	13.9													
!	100	11.3													
!	102	4.7													
*	104	14.4	3.2	14.7	2.9	-2	5.9	-10							

APPLICATION		
PART NO.	NEXT ASSY	USED ON

UNLESS OTHERWISE SPECIFIED
DIMENSIONS ARE IN INCHES

TOLERANCES:
 $\text{ANGLES} \pm 2^\circ$ $\text{DECIMALS} \pm .03$

 $\varnothing 247-260$ TOOL HOLE
WHERE SHOWN,
USE IS A MANUFACTURING
OPTION



CANVAS DRAWING:
THE DATASET FILE NAME IS RECORDED ABOVE
THE
TITLE BLOCK, ALONG WITH THE DRAFTER'S NAME
AND ORGANIZATION NUMBER, ON ALL PAGES.

DATASET NAME: 115X8003.CVS DRAFTED BY: NORMAN DILLE 8-XT54

DRAWN NORMAN B. DILLE	DATE 06/24/98	THE BOEING COMPANY			
CHECKED <i>Norman B. Dille</i>	8/25/98				
STRESS <i>K. Williams</i>	8/26/98				
ENGR <i>Norman B. Dille</i>	7/7/98	TITLE STRAIN GAGE LOCATIONS - INTEGRAL AIRFRAME STRUCTURE LONGITUDINAL CRACK TEST (TEST ONLY)			
LEAD <i>Norman B. Dille</i>	7/7/98				
GROUP <i>Norman Jackson</i>					
PROJ N/A					
STRUCTURES <i>Chris For</i>		SIZE A	CAGE CODE 81205	DWG NO. 115X8003	
USED ON N/A	SECT NO.	SCALE NONE	SHEET 1	PAGE 01	REV
CHG ON EWA 5-B6E52-TST1	GROUP ORG B-XT54				

84003 001 MAC/CAN REV 7/98

Norman B. Dille 9/16/98

LIST OF ACTIVE PAGES

PAGE NUMBER	REV	ADDED PAGES				PAGE NUMBER	REV	ADDED PAGES			
		PAGE NUMBER	REV	PAGE NUMBER	REV			PAGE NUMBER	REV	PAGE NUMBER	REV
1											
2											
3											
4											
5											
6											
7											
8											
9											
10											
11											
12											
13											
14											
15											
16											
17											
18											
19											
20											

DATA SET NAME: WSSG02.CVS DRAFTED BY: NORMAN DILLE 8-ETM

DRAWN BY: MADDAN REV: 000

THE BOEING COMPANY

SIZE

A

CAGE CODE

81205

DWG NO.

115X8003

SHEET 1

PAGE 02

REV

SEE PAGE 1 FOR DETAILS

REVISIONS

REV	DESCRIPTION	DATE	APPROVAL

DATASET NAME: 115X8003.CVS DRAFTED BY: NORMAN DILLS B-JT54

THE BOEING COMPANY

SIZE
A

CAGE CODE
81205

DWG NO.

115X8003

SHEET 1

PAGE

03

REV

SEE PAGE 1 FOR DETAILS

115X8003-004-115X8003-REV-0183

TABLE OF CONTENTS

PAGE

TITLE PAGE	1
LIST OF ACTIVE PAGES	2
REVISION PAGE	3
TABLE OF CONTENTS	4
INDEX (STRAIN GAGE)	5-6
LIST OF MATERIALS	7
NOTES	8-10
OVERVIEW	11
STRAIN GAGE INSTALLATION DRAWINGS	12-20

DATASET NAME: 14SS004.CVS DRAFTED BY: NORMAN DILLE E-KT54

THE BOEING COMPANY

SIZE

A

CAGE
CODE

81205

DWG NO.

115X8003

SHEET 1

PAGE 04

REV

SEE PAGE 1 FOR DETAILS

115X8003-004-115X8003-REV-001

INDEX

NAME	PAGE NO.	NAME	PAGE NO.	NAME	PAGE NO.
IAS-L001	12	IAS-L037	15		
IAS-L002	12	IAS-L038	15		
IAS-L003	12	IAS-L040	15		
IAS-L004	12	IAS-L042	16		
IAS-L005	13	IAS-L044	16		
IAS-L006	13	IAS-L046	16		
IAS-L007	13	IAS-L048	16		
IAS-L008	13	IAS-L050	16		
IAS-L009	13	IAS-L052	16		
IAS-L010	13	IAS-L054	16		
IAS-L011	13	IAS-L056	16		
IAS-L012	13	IAS-L058	16		
IAS-L013	13	IAS-L060	16		
IAS-L014	13	IAS-L062	16		
IAS-L015	13	IAS-L064	16		
IAS-L016	13	IAS-L066	17		
IAS-L017	13	IAS-L068	17		
IAS-L018	13	IAS-L070	17		
IAS-L019	13	IAS-L072	17		
IAS-L020	13	IAS-L074	17		
IAS-L021	13	IAS-L076	17		
IAS-L022	13	IAS-L078	17		
IAS-L023	13	IAS-L080	19		
IAS-L024	13	IAS-L082	19		
IAS-L025	14	IAS-L084	19		
IAS-L026	14	IAS-L086	19		
IAS-L027	14	IAS-L088	19		
IAS-L028	14	IAS-L090	19		
IAS-L029	14	IAS-L092	19		
IAS-L030	14	IAS-L094	19		
IAS-L031	15	IAS-L096	19		
IAS-L032	15	IAS-L098	19		
IAS-L033	15	IAS-L100	19		
IAS-L034	15	IAS-L102	19		
IAS-L035	15	IAS-L104	19		
IAS-L036	15				

DATASET NAME: IAS8003.CVS DRAFTED BY: NORMAN DILLE 8-XT54

81205 025 MACQUAN REV 7/92

THE BOEING COMPANY

SIZE	CAGE CODE
A	81205

DWG NO. **115X8003**

SHEET 1	PAGE 05	REV
---------	---------	-----

SEE PAGE 1 FOR DETAILS

INDEX

NAME	PAGE NO.	NAME	PAGE NO.	NAME	PAGE NO.
IAS-R023	13	IAS-R078	17		
IAS-R024	13	IAS-R080	19		
IAS-R025	14	IAS-R082	19		
IAS-R026	14	IAS-R084	19		
IAS-R027	14	IAS-R086	19		
IAS-R028	14	IAS-R088	19		
IAS-R029	14	IAS-R090	19		
IAS-R030	14	IAS-R092	19		
IAS-R031	15	IAS-R094	19		
IAS-R032	15	IAS-R096	19		
IAS-R033	15	IAS-R098	19		
IAS-R034	15	IAS-R100	19		
IAS-R035	15	IAS-R102	19		
IAS-R036	15	IAS-R104	19		
IAS-R037	15				
IAS-R038	15				
IAS-R039	15				
IAS-R040	15				
IAS-R042	16				
IAS-R044	16				
IAS-R046	16				
IAS-R048	16				
IAS-R050	16				
IAS-R052	16				
IAS-R054	16				
IAS-R056	16				
IAS-R058	16				
IAS-R060	16				
IAS-R062	16				
IAS-R064	16				
IAS-R066	17				
IAS-R068	17				
IAS-R070	17				
IAS-R072	17				
IAS-R074	17				
IAS-R076	17				

DATA SET NAME: V35G06.CVS DRAFTED BY: NORMAN DILLE 8/27/84

81205 025 MANG/CAW REV 198

THE BOEING COMPANY

SIZE
A

CAGE CODE
81205

DWG NO.

115X8003

SHEET 1

PAGE 06

REV

SEE PAGE 1 FOR DETAILS

NOTES

SPECIFICATIONS AND STANDARDS FOR THE CONTROL OF MANUFACTURING OPERATION (AS APPLICABLE) ARE AS FOLLOWS:

UNLESS OTHERWISE SPECIFIED DIMENSIONS ARE IN INCHES.

DIMENSIONING AND TOLERANCING PER ANSI Y14.5M (1982) AS SUPPLEMENTED BY D6-55369; EXCEPT DRAWINGS PREPARED PRIOR TO 8-27-84 COMPLY WITH ANSI Y14.5 (1973).

1. INSTALL STRAIN GAGES, TERMINAL STRIPS AND APPLY PROTECTIVE COATING PER "STRAIN GAGE INSTALLATION TECHNIQUES", BOEING CORPORATE STRAIN GAGE DOCUMENT (USE AE10/15 ADHESIVE SYSTEMS FOR BONDING STRAIN GAGES AND TERMINAL STRIPS, SUITABLE ALTERNATE MAY BE USED FOR TERMINAL STRIP BONDING.
 2. INSTALL AN IDENTIFICATION LABEL NEXT TO GAGE. INSTALL I.D. LABEL ON LEAD WIRES, PRINTED ON TMS-SCE-1/8-2.04 HEAT SHRINK, AT GAGE END AND ON PATCH PANEL END.
 3. LEAD WIRES TO BE MADE FROM AWG 26, 3 CONDUCTOR RIBBON WIRE AND CUT TO LENGTH ON INSTALLATION. LENGTH WILL BE DETERMINED BY DISTANCE FROM STRAIN GAGE INSTALLATION TO PATCH PANEL.
 4. AXIAL STRAIN GAGE DIMENSIONS ARE TO THE CENTERLINES OF THE GRID. ROSETTE STRAIN GAGE DIMENSIONS ARE TO THE INTERSECTION OF THE CENTERLINES OF THE THREE LEGS. DIMENSIONS ARE IN THE X,Y,Z PLANES UNLESS OTHERWISE SPECIFIED ON THE STRAIN GAGE DRAWING.
- 5
- LOCATE STRAIN GAGE AS CLOSE TO EDGE, ANOTHER STRAIN GAGE, STRUCTURE OR OTHER INDICATED OBJECT AS POSSIBLE. WHEN THE STRAIN GAGE IS INSTALLED ADJACENT TO A RADIUS, CARE MUST BE TAKEN TO PLACE THE GAGE NEXT TO BUT NOT INTO THE RADIUS.
 6. LETTERED FLAGNOTES PERTAIN ONLY TO THE PAGE ON WHICH THEY APPEAR.
 7. ALL GAGES ARE ON ALUMINUM UNLESS OTHERWISE NOTED ON DRAWING.
 8. ABBREVIATIONS PER BDS3010.

DATASET NAME: IAS5208.DVS DRAFTED BY: NORMAN DELLE 8-2784

81205-008-000-000-REV-1-190

THE BOEING COMPANY

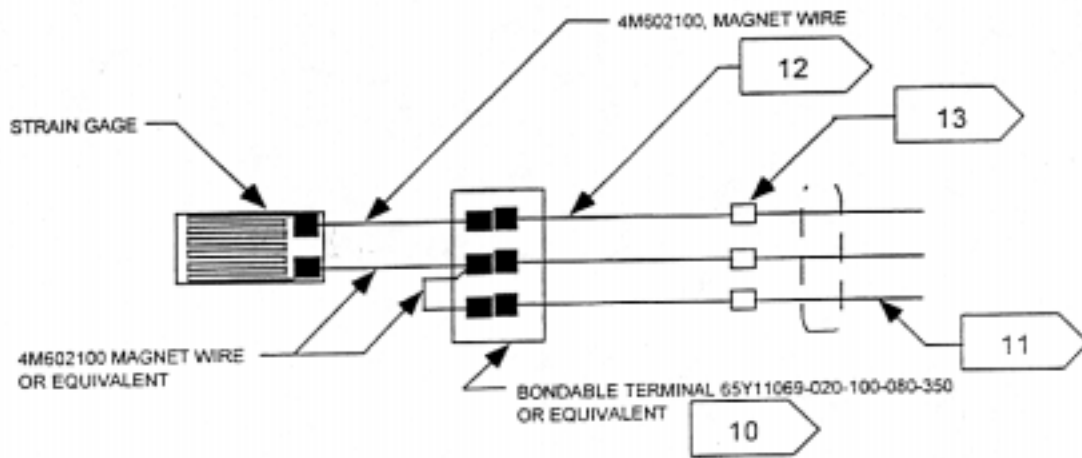
SIZE	CAGE CODE	DWG NO.
A	81205	115X8003
	SHEET 1	PAGE 8
		REV

SEE PAGE 1 FOR DETAILS

NOTES

9. THE SYMBOLS SHOWN BELOW ARE USED THROUGHOUT THE STRAIN GAGE INSTALLATION DRAWING PAGES TO REPRESENT STRAIN GAGES AS THEY APPEAR IN DIFFERENT VIEWS:

STRAIN GAGE SYMBOL	EXPLANATION
	AXIAL GAGE, PLAN VIEW, NEAR SIDE
	AXIAL GAGE, PLAN VIEW, FAR SIDE
	AXIAL GAGE, END VIEW, NEAR SIDE
	AXIAL GAGE, END VIEW, FAR SIDE
	AXIAL GAGE, SIDE VIEW, NEAR SIDE
	AXIAL GAGE, SIDE VIEW, FAR SIDE
	ROSETTE GAGE, PLAN VIEW, NEAR SIDE
	ROSETTE GAGE, PLAN VIEW, FAR SIDE
	ROSETTE GAGE, SIDE VIEW
	IDENTIFICATION SYMBOL & LETTER, NEAR SIDE
	IDENTIFICATION SYMBOL & LETTER, FAR SIDE



TYPICAL STRAIN GAGE INSTALLATION

DATASET NAME: 115X8003.CVS DRAFTED BY: NORMAN DILLE B-XTM

THE BOEING COMPANY

SIZE	CAGE CODE	DWG NO.
A	81205	115X8003
SHEET 1	PAGE 9	REV

SEE PAGE 1 FOR DETAILS

81028-108-AMERICAN-REV-3183

NOTES

10

BONDABLE TERMINALS 65Y11069-020-100-080-350 OR SUITABLE ALTERNATE.
INSTALL TERMINALS AS NEAR TO STRAIN GAGE AS PRACTICAL (SEE NOTE 1).
TERMINAL STRIPS ARE SUPPLIED IN TERMINAL GROUPS, DIVIDE AS REQUIRED.

11

SIZE 20 SHIELDED 3 CONDUCTOR CABLE (BELDON 8772 3 COND. SHIELDED) (2H1220000).

12

SIZE 26 AWG. 3 CONDUCTOR RIBBON WIRE.

13

SOLDER SPLICE OR PATCH PANEL CONNECTION.

DATASET NAME: ISS5G10.CVS DRAFTED BY: NORMAN DILLE B-JT54

THE BOEING COMPANY

SIZE

A

CAGE
CODE

81205

DWG NO.

115X8003

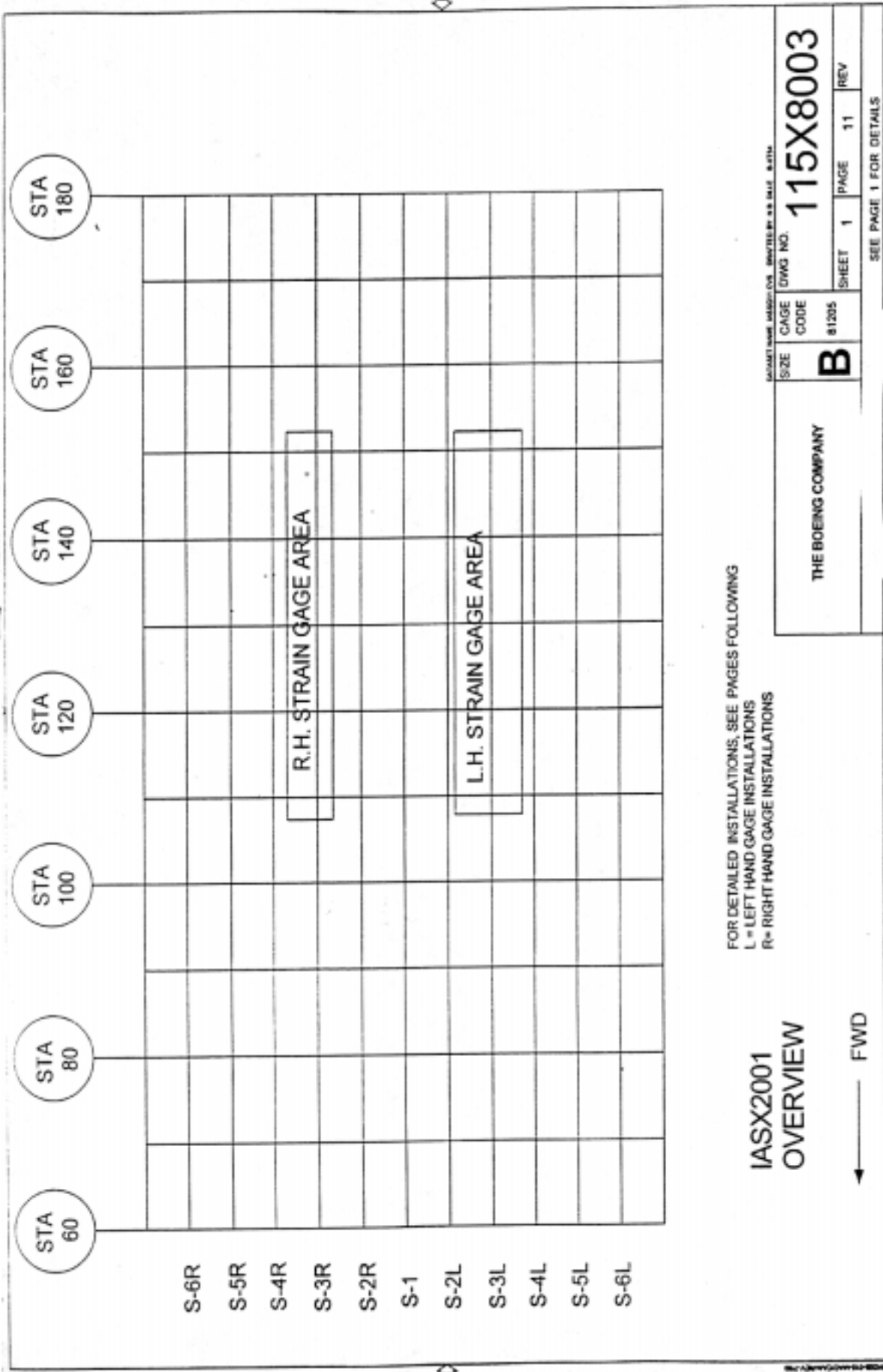
SHEET 1

PAGE 10

REV

SEE PAGE 1 FOR DETAILS

81228-008-1M/C/D/CALL REV. 1783



FOR DETAILED INSTALLATIONS, SEE PAGES FOLLOWING
 L = LEFT HAND GAGE INSTALLATIONS
 R = RIGHT HAND GAGE INSTALLATIONS

**IASX2001
 OVERVIEW**

← FWD

PROJECT NAME: IASX2001 SHEET NO. 115X8003

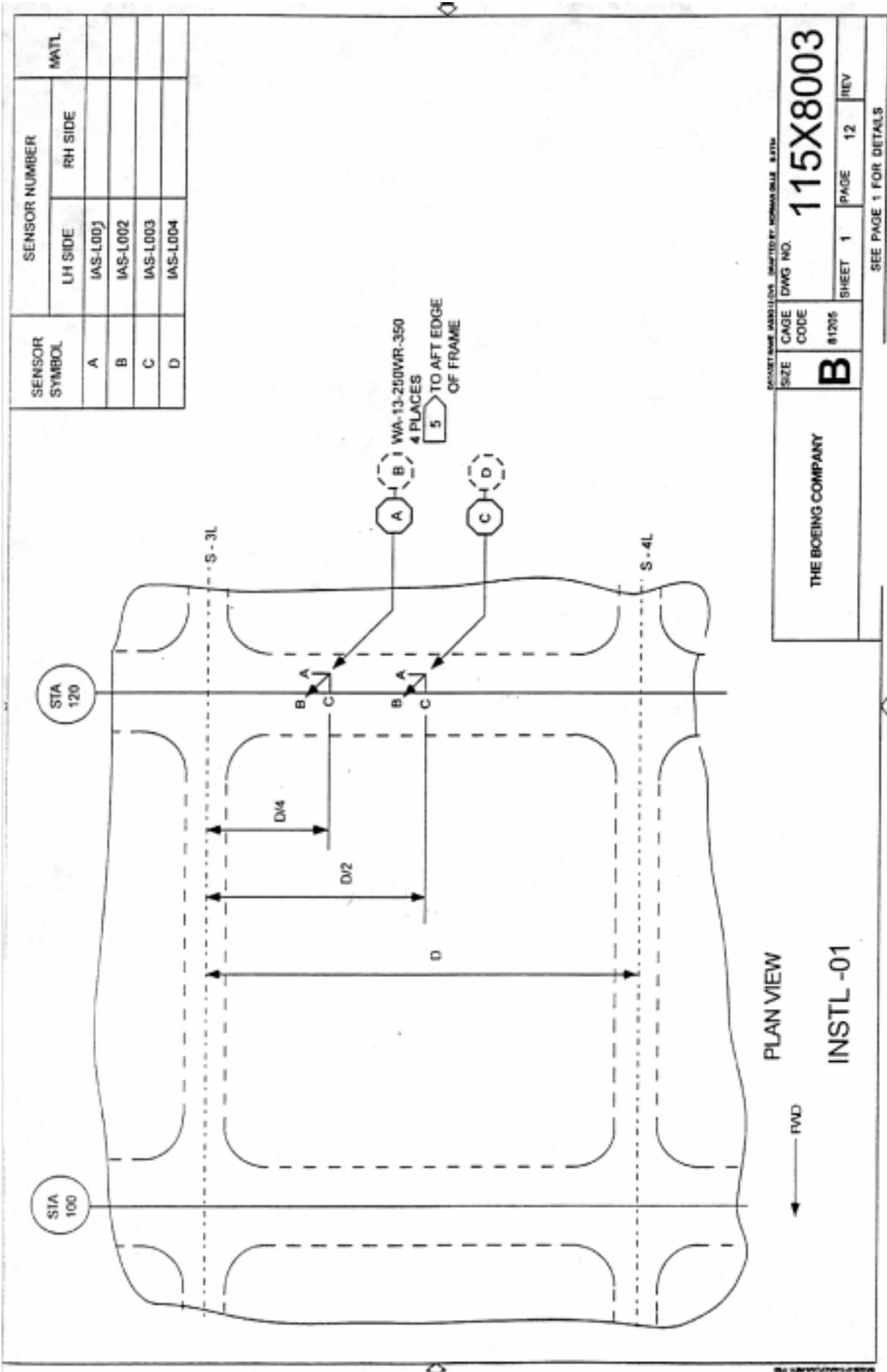
DWG NO. **115X8003**

SIZE GAGE CODE
B 81205

SHEET 1 PAGE 11 REV

THE BOEING COMPANY

SEE PAGE 1 FOR DETAILS



SENSOR SYMBOL	SENSOR NUMBER		MNTL
	LH SIDE	RH SIDE	
A	IAS-L001		
B	IAS-L002		
C	IAS-L003		
D	IAS-L004		

PLAN VIEW
INSTL-01

← FWD

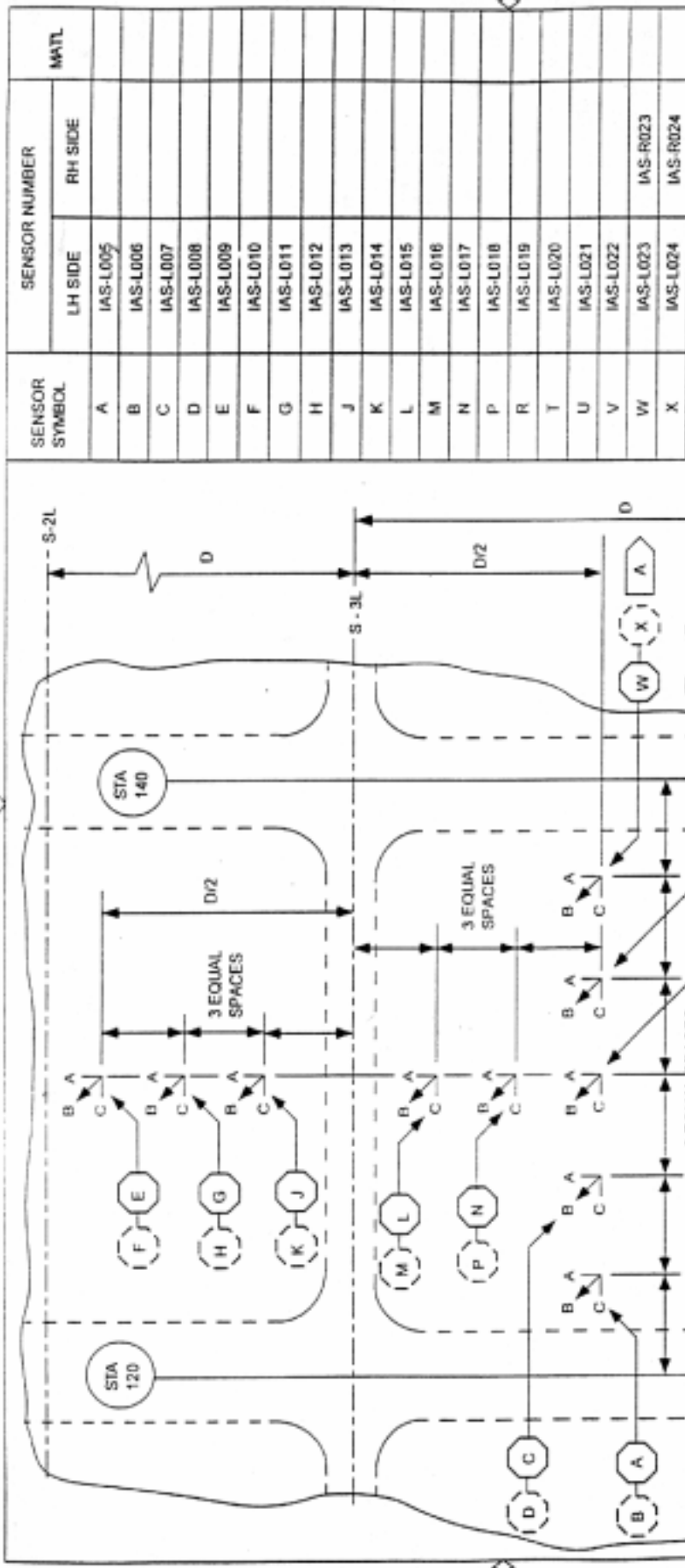
THE BOEING COMPANY

SIZE CAGE CODE 81205

DWG NO. 115X8003

SHEET 1 PAGE 12 REV

SEE PAGE 1 FOR DETAILS



INSTL -03
L.H. SHOWN ONLY

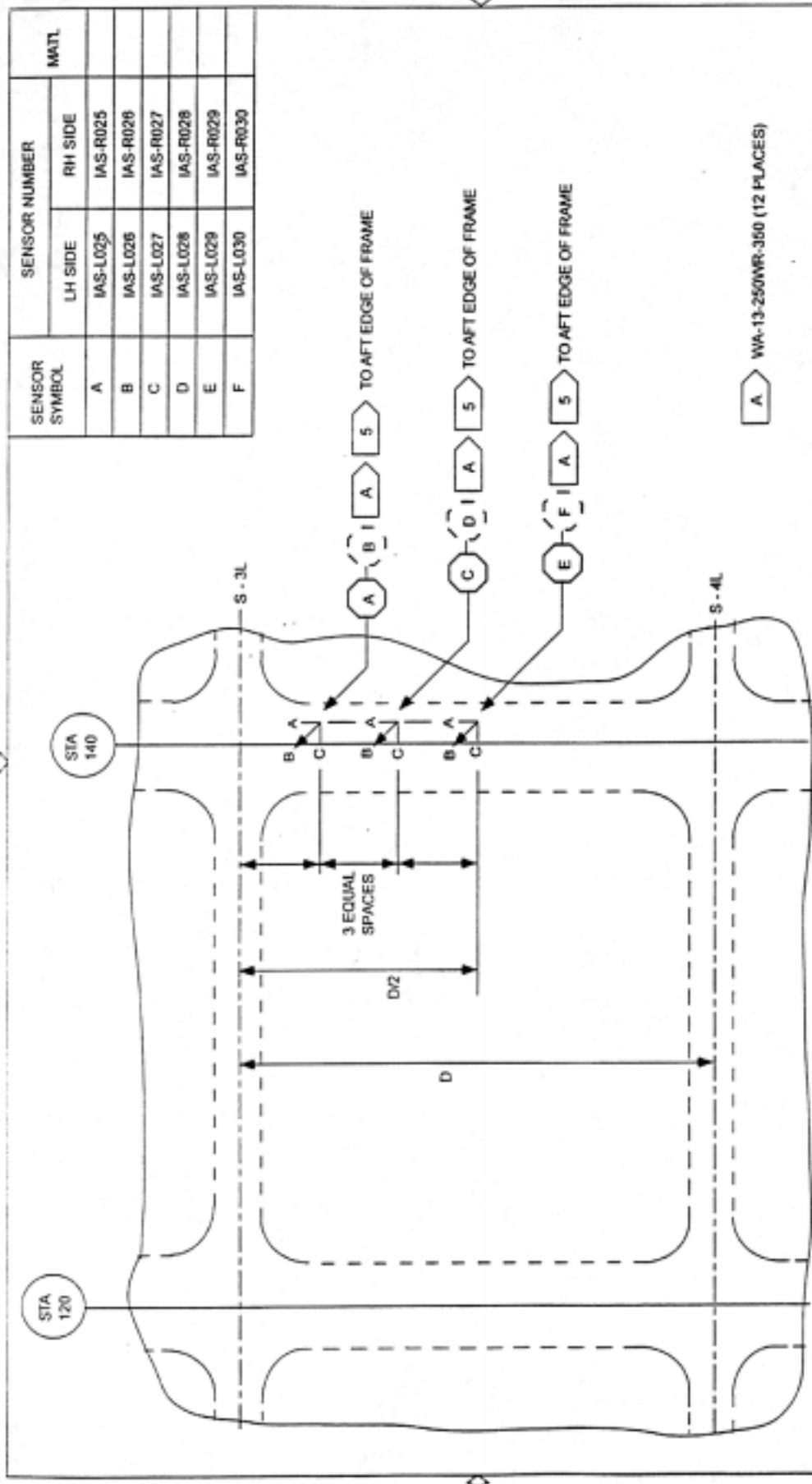
A WA-13-250MR-350 (22 PLACES)

SENSOR SYMBOL	SENSOR NUMBER		MATL
	LH SIDE	RH SIDE	
A	IAS-L005		
B	IAS-L006		
C	IAS-L007		
D	IAS-L008		
E	IAS-L009		
F	IAS-L010		
G	IAS-L011		
H	IAS-L012		
J	IAS-L013		
K	IAS-L014		
L	IAS-L015		
M	IAS-L016		
N	IAS-L017		
P	IAS-L018		
R	IAS-L019		
T	IAS-L020		
U	IAS-L021		
V	IAS-L022		
W	IAS-R023	IAS-R023	
X	IAS-L024	IAS-R024	

PROJECT: **115X8003**
 CAGE CODE: **B**
 DWG NO: **115X8003**
 THE BOEING COMPANY
 SHEET 1 PAGE 13 REV

PLAN VIEW

SEE PAGE 1 FOR DETAILS



SENSOR SYMBOL	SENSOR NUMBER		MATT.
	LH SIDE	RH SIDE	
A	IAS-L025	IAS-R025	
B	IAS-L026	IAS-R026	
C	IAS-L027	IAS-R027	
D	IAS-L028	IAS-R028	
E	IAS-L029	IAS-R029	
F	IAS-L030	IAS-R030	

PLAN VIEW
 INSTL -05
 L.H. SHOWN ONLY

THE BOEING COMPANY

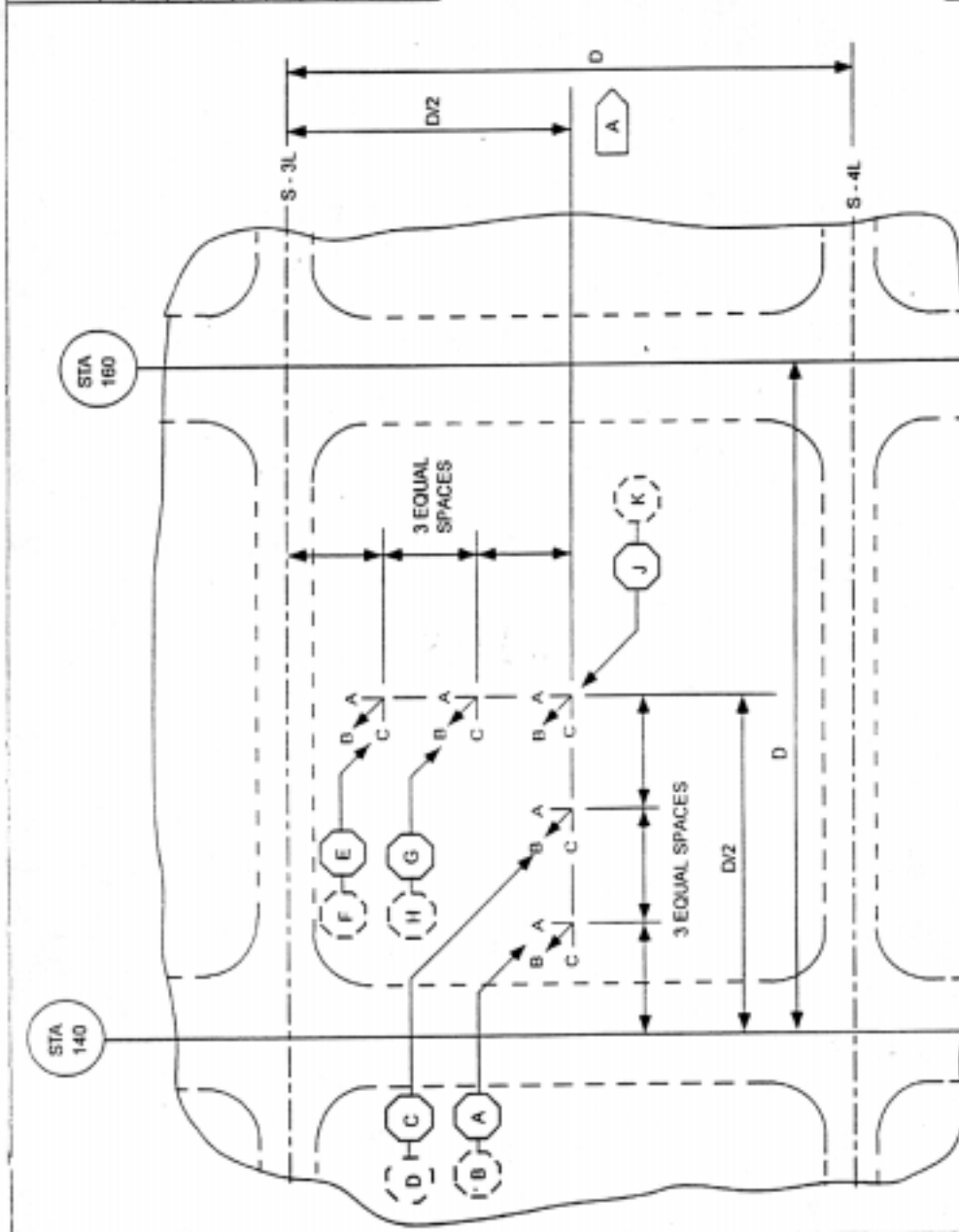
WA-13-250WR-360 (12 PLACES)

115X8003

SHEET 1 PAGE 14 REV

SEE PAGE 1 FOR DETAILS

SENSOR SYMBOL	SENSOR NUMBER		MATL
	LH SIDE	RH SIDE	
A	IAS-L031	IAS-R031	
B	IAS-L032	IAS-R032	
C	IAS-L033	IAS-R033	
D	IAS-L034	IAS-R034	
E	IAS-L035	IAS-R035	
F	IAS-L036	IAS-R036	
G	IAS-L037	IAS-R037	
H	IAS-L038	IAS-R038	
J	IAS-L039	IAS-R039	
K	IAS-L040	IAS-R040	



INSTL -07
L.H. SHOWN ONLY

A WA-13-250WR-350 (20 PLACES)

THE BOEING COMPANY

SIZE: B

CAGE CODE: 81205

DWG NO.: 115X8003

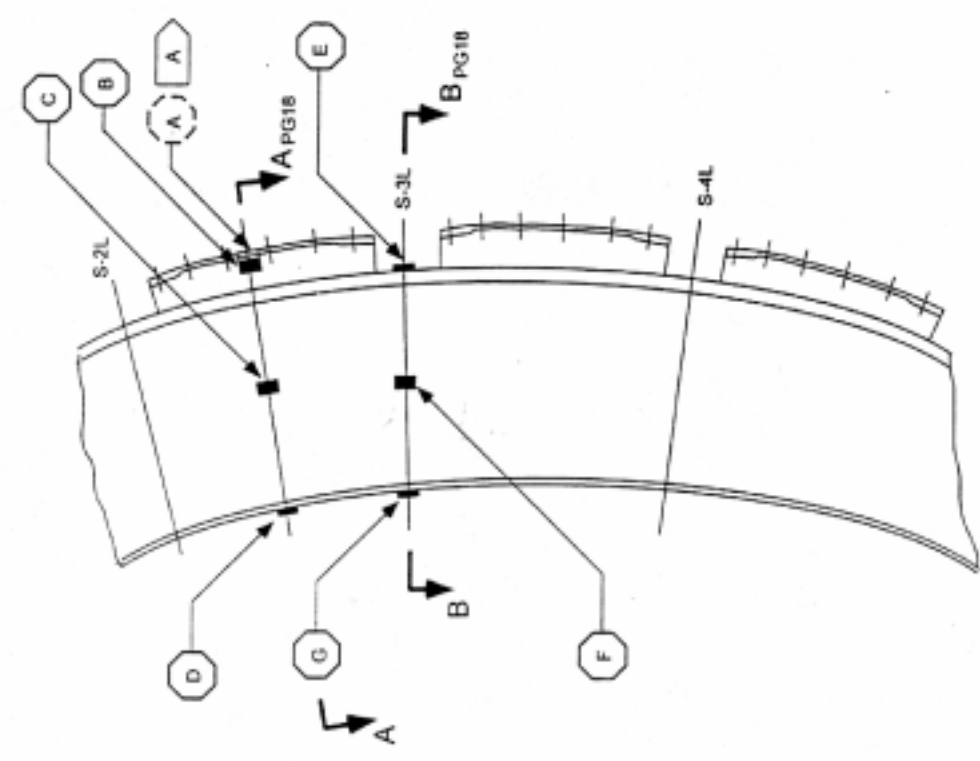
SHEET 1 PAGE 15 REV

SEE PAGE 1 FOR DETAILS

PLAN VIEW

FWD

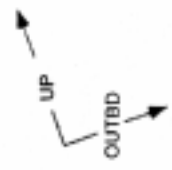
SENSOR SYMBOL	SENSOR NUMBER		MNTL
	LH SIDE	RH SIDE	
A	IAS-L066	IAS-R068	
B	IAS-L068	IAS-R068	
C	IAS-L070	IAS-R070	
D	IAS-L072	IAS-R072	
E	IAS-L074	IAS-R074	
F	IAS-L076	IAS-R076	
G	IAS-L078	IAS-R078	



INSTL -11
 FRAME STA. 120
 L.H. SHOWN ONLY

VIEW LOOKING AFT

A CEA-13-250UN-350 (14 PLACES)



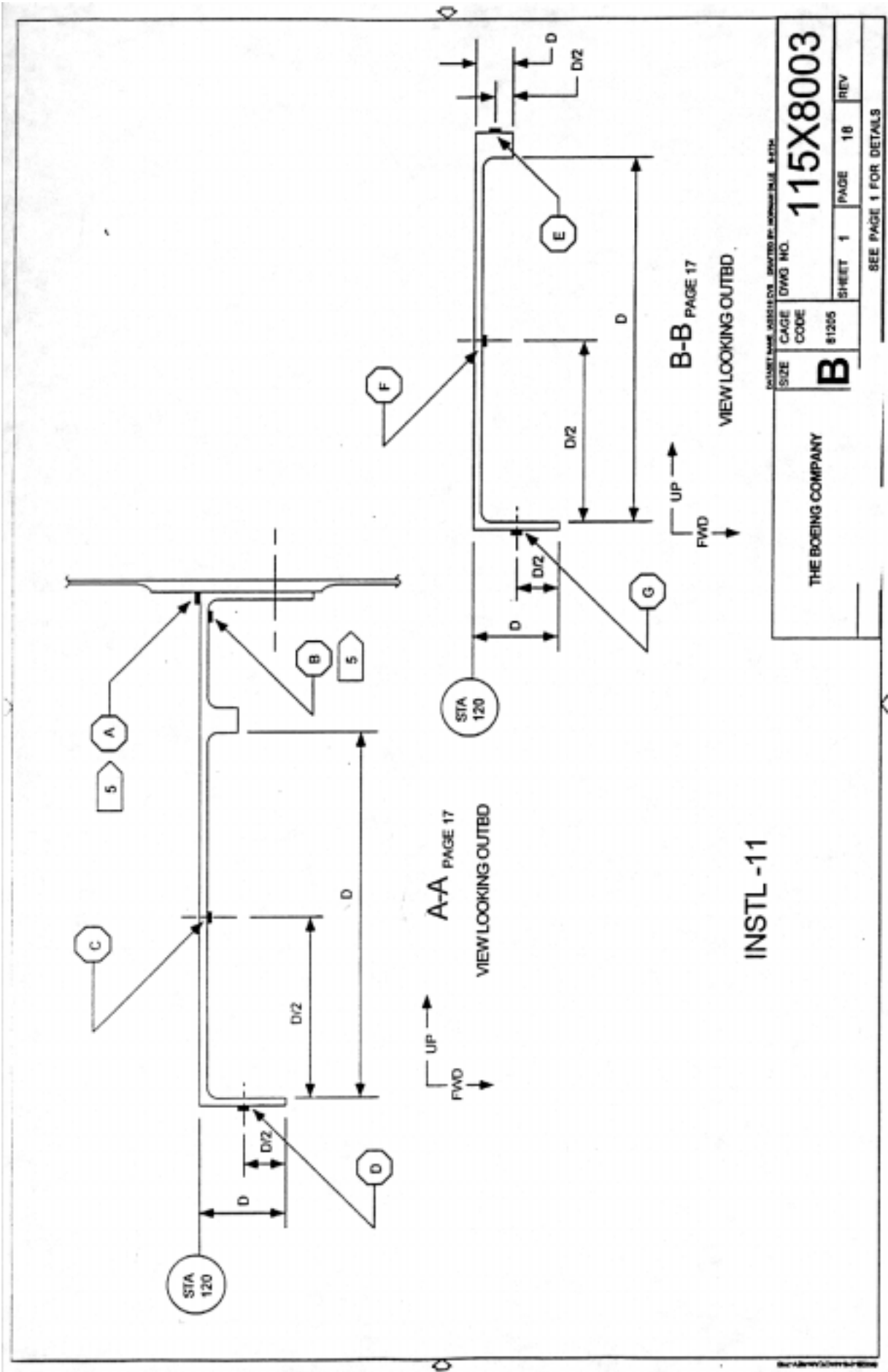
THE BOEING COMPANY

PROJECT NAME: AIRCRAFT ROUTER: WINGMOUNTABLE - 8170

SIZE	CAGE CODE	115X8003	
B	81285	SHEET 1	PAGE 17

REV

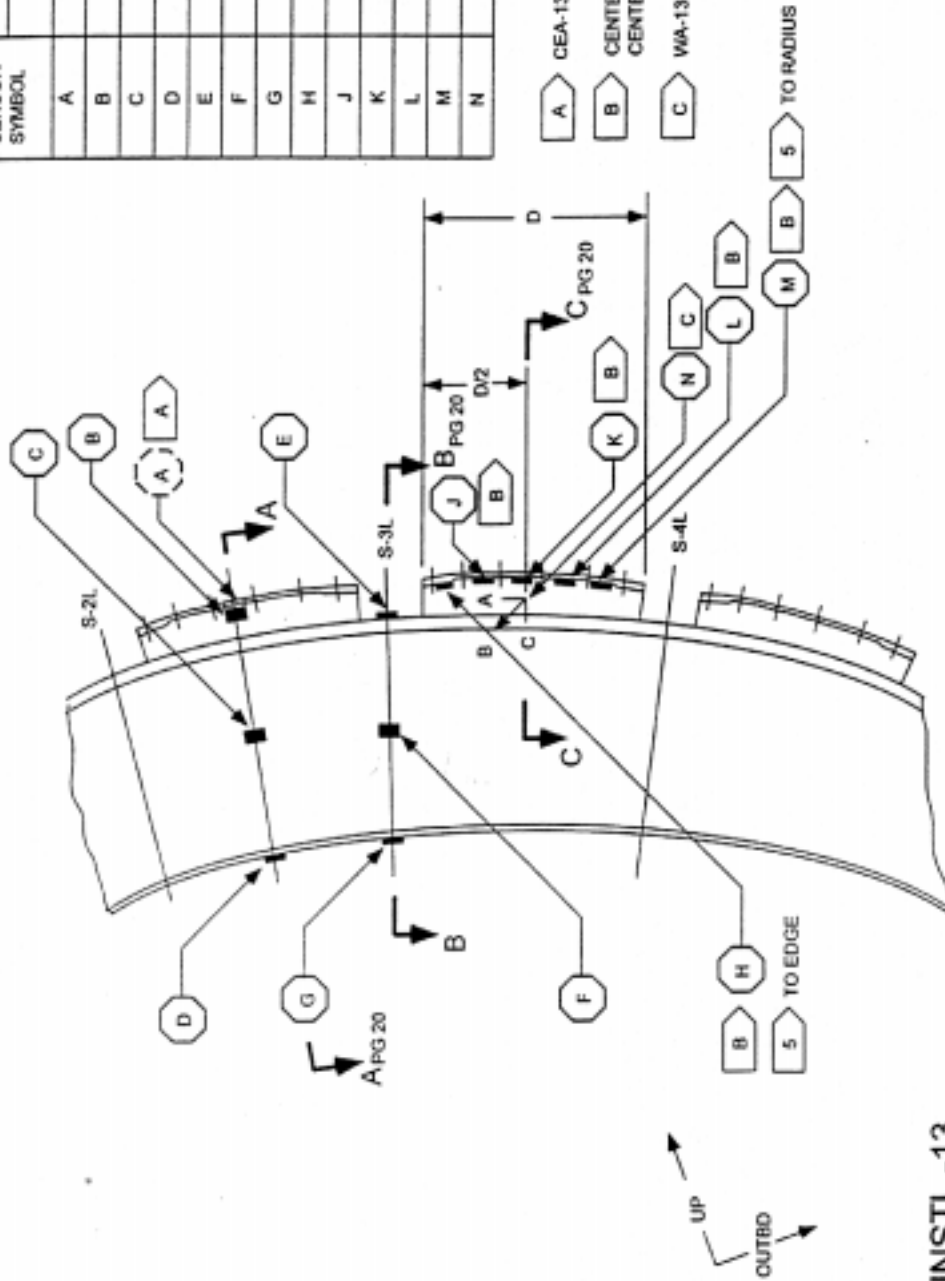
SEE PAGE 1 FOR DETAILS



INSTL -11

THE BOEING COMPANY
 DRAWING ASSOCIATION CONTROL BY WORKSTATION 4474
 CAGE CODE
 CODE
 81205
B
 115X8003
 SHEET 1 PAGE 18 REV
 SEE PAGE 1 FOR DETAILS

SENSOR SYMBOL	SENSOR NUMBER		MATERIAL
	LH SIDE	RH SIDE	
A	IAS-L080	IAS-R080	
B	IAS-L082	IAS-R082	
C	IAS-L084	IAS-R084	
D	IAS-L086	IAS-R086	
E	IAS-L088	IAS-R088	
F	IAS-L090	IAS-R090	
G	IAS-L092	IAS-R092	
H	IAS-L094	IAS-R094	
J	IAS-L098	IAS-R098	
K	IAS-L098	IAS-R098	
L	IAS-L100	IAS-R100	
M	IAS-L102	IAS-R102	
N	IAS-L104	IAS-R104	



INSTL -13
 FRAME STA. 140
 L.H. SHOWN ONLY

VIEW LOOKING AFT

ALL DIMENSIONS UNLESS OTHERWISE SPECIFIED ARE IN INCHES

SIZE CAGE DWG NO.

115X8003

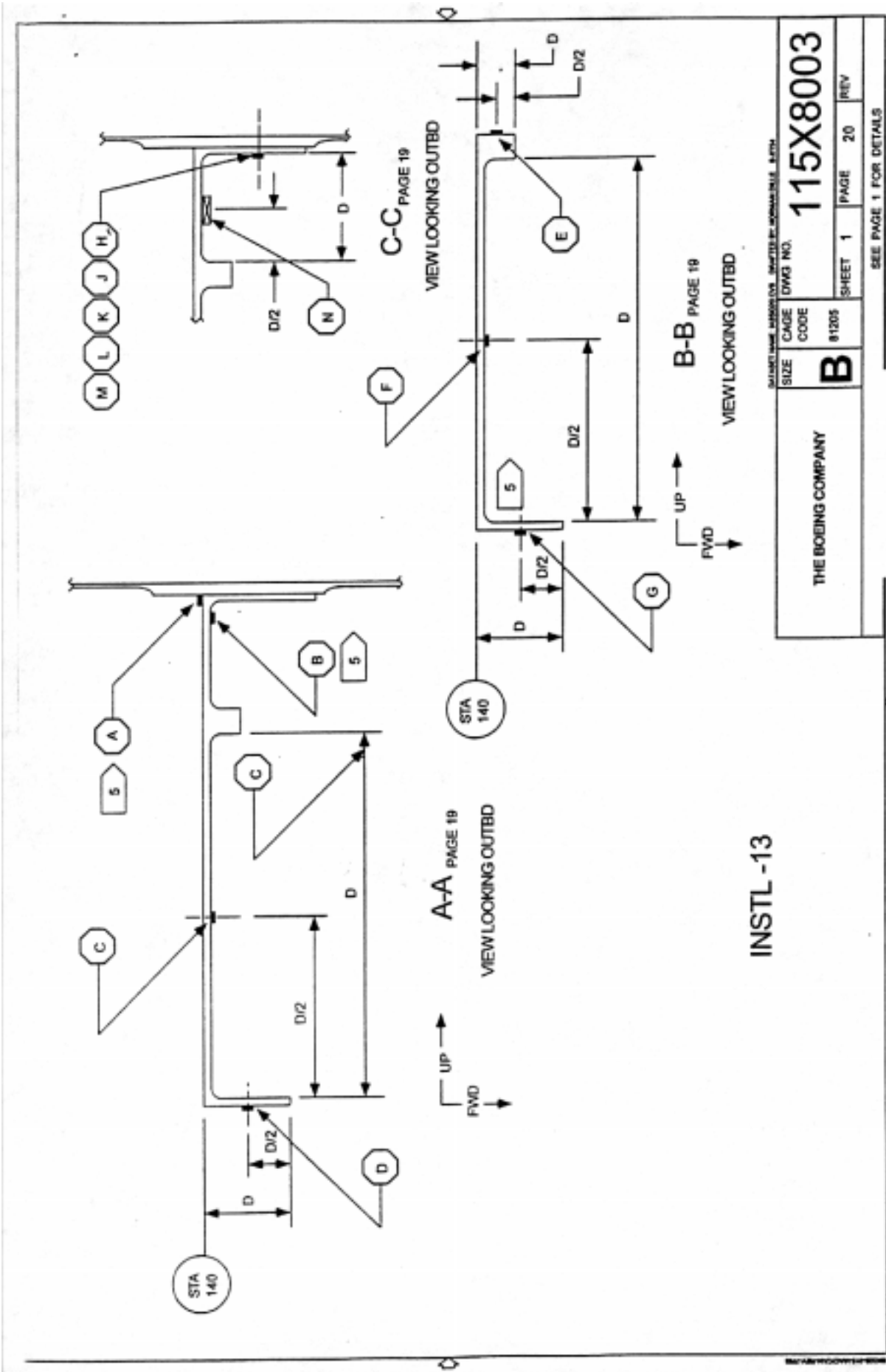
THE BOEING COMPANY

B

#1205

SHEET 1 PAGE 19 REV

SEE PAGE 1 FOR DETAILS



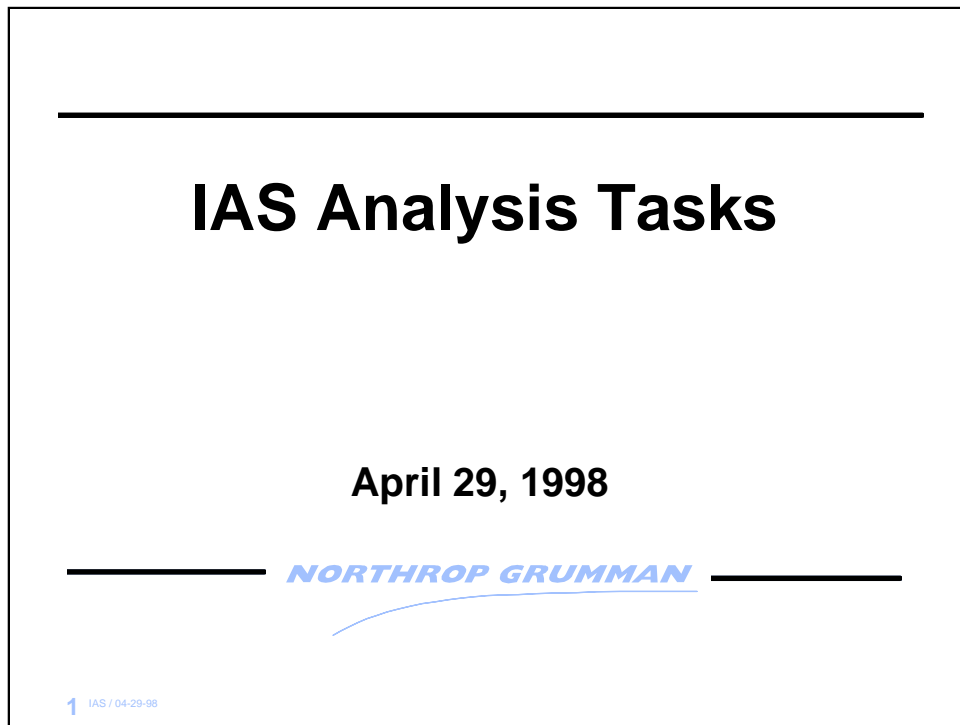
INSTL -13

Appendix G

Northrop Grumman Analytical Task 1 and Task 2

Following are the Northrop Grumman reports “Northrop Grumman Analytical Task 1,” dated April 29, 1998, and “Northrop Grumman Analytical Task 2” dated November 1998.

X.X Northrop Grumman Analytical Task 1



Northrop Grumman had two IAS analytical tasks for 1998 which used the finite element program called "Mechanica":

- 1) evaluate stress concentrations in IAS
- 2) evaluate stress intensity in IAS for longitudinal cracking.

This section documents the results of task 1, which was presented at the IAS meeting held in Norfolk on April 29, 1998.

Purpose

- **Mechanica can be a quick and effective way to help size structure in a production design environment (D&DT).**
Northrop-Grumman has two Mechanica modeling tasks:
 - **Task 1 addresses Durability**
 - **2 dimensional analysis (sensitivity of stress concentrations to changes in stringer spacing, land thickness and machined pocket radii).**
 - **3 dimensional analysis (combined Kt from bi-axial loading).**
 - **Determine how stress concentrations in Integral Aircraft Structure (IAS) compare with those in Built-up Aircraft Structure (BAS) in fuselage panels.**
 - **Task 2 will address Damage Tolerance**
 - **To be performed next**

2 IAS / 04-29-98

The aerospace industry is particularly interested in tools that can be used in a design effort. In that environment an engineer needs something that is quick and efficient so that he can help size the structure in a timeframe that will meet aggressive milestones.

Mechanica is good for that because of its use of the “p element”, a high order element that contains curved lines and surfaces. This allows the analyst to model complex geometry quickly and accurately with few elements. It’s still a linear approach, but it’s evolving to do both large deflection and non-linear material property analyses.

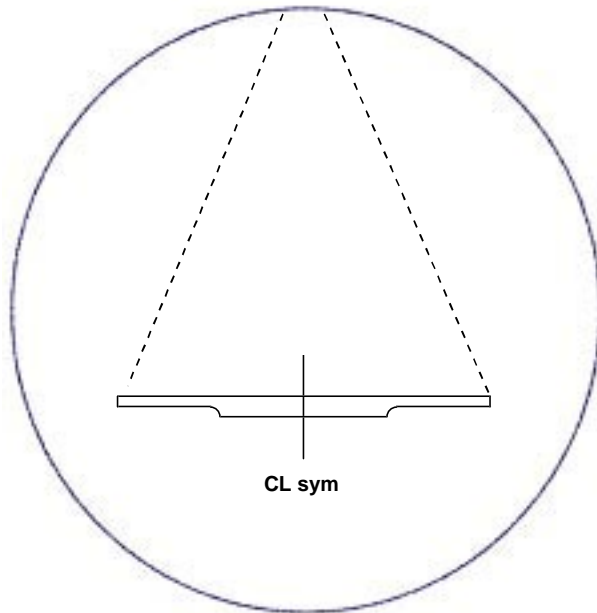
In this task durability is addressed, that is, what local stresses can we expect, how does this compare with built-up aircraft structure (BAS), and how should we make IAS evolve to produce durability equal to or better than BAS

First we’ll look at some two dimensional models and evaluate the sensitivity of local stress to changes in geometry.

Then we’ll look at some three dimensional modeling and evaluate combined Kt’s and bi-axial loading.

We’ll end by making some comparisons between IAS and BAS.

Two Dimensional Analysis



- Start with a 1" slice of the fuselage
- Concentrate on one repeatable section
- Due to symmetry, look at one half

radius of fuselage = 127"

3 IAS / 04-29-98

In the two dimensional analysis we'll start with a one inch slice of a round fuselage with a radius of 127 inches (as shown in the figure). We'll concentrate on one repeatable section containing a stringer land. Due to symmetry, we can model one half of this.

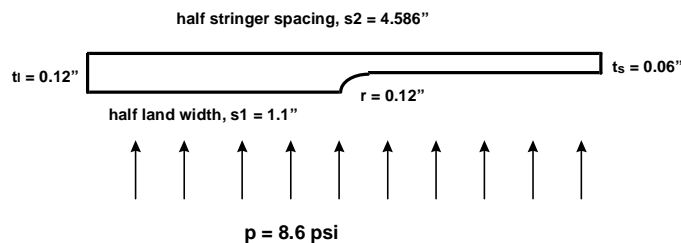
Baseline Geometry and Applied Load

$R = 127''$ (fuselage radius)

Ends constrained to act
as part of cylinder

$$S_{hoop} = pR/t_s = 18,200 \text{ psi}$$

$$S_{axial} = pR/2t_s = 9,100 \text{ psi}$$



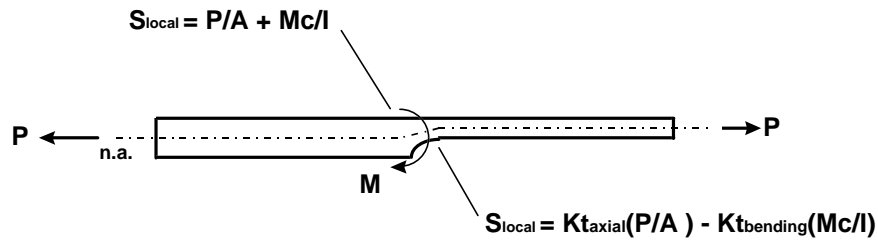
4 IAS / 04-29-98

For the baseline, a skin thickness of 0.06 inches and a land thickness of 0.12 inches is assumed, along with a machined land radius of 0.12 inches. The land width is 2.2 inches (half width is 1.1) and the stringer land spacing is 9 inches (half width is 4.5). The ends are constrained cylindrically to act like a fuselage and an 8.6 psi pressure is applied which yields a reference hoop stress (pR/t) of 18,200 psi. The axial stress in the fuselage would be one half of this ($pR/2t$), or 9,100 psi.

Internal Loads and Stresses

P - hoop load caused by pressure

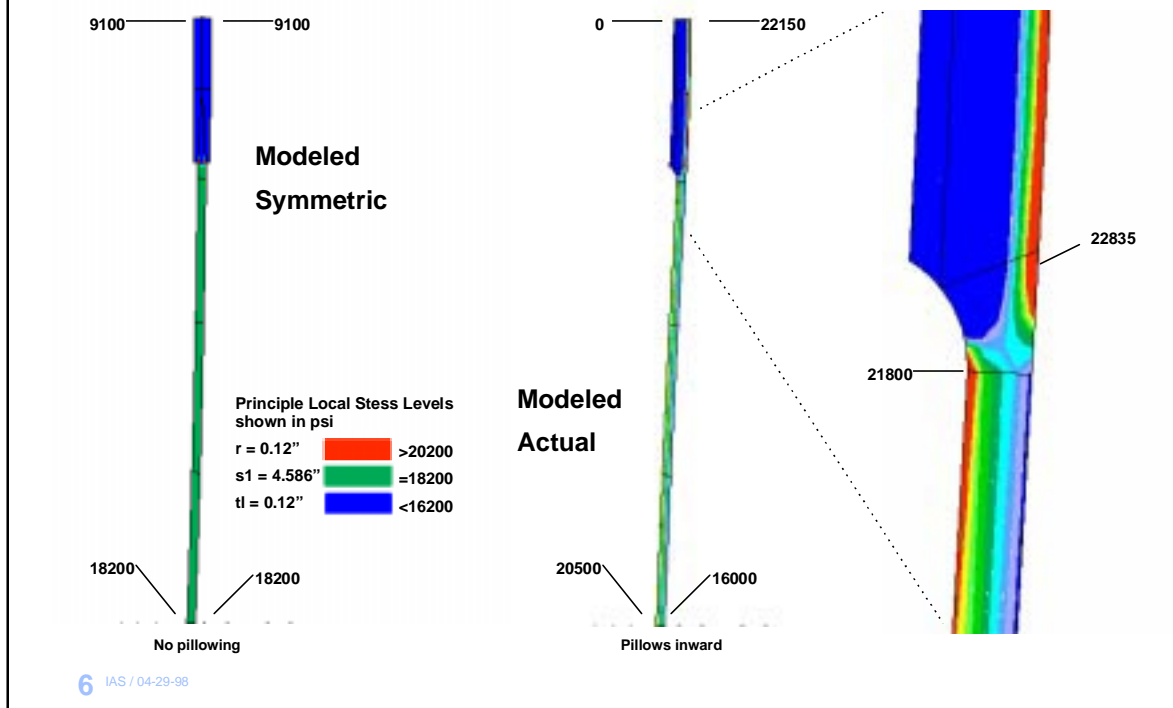
M - bending moment due to offset in load path



5 IAS / 04-29-98

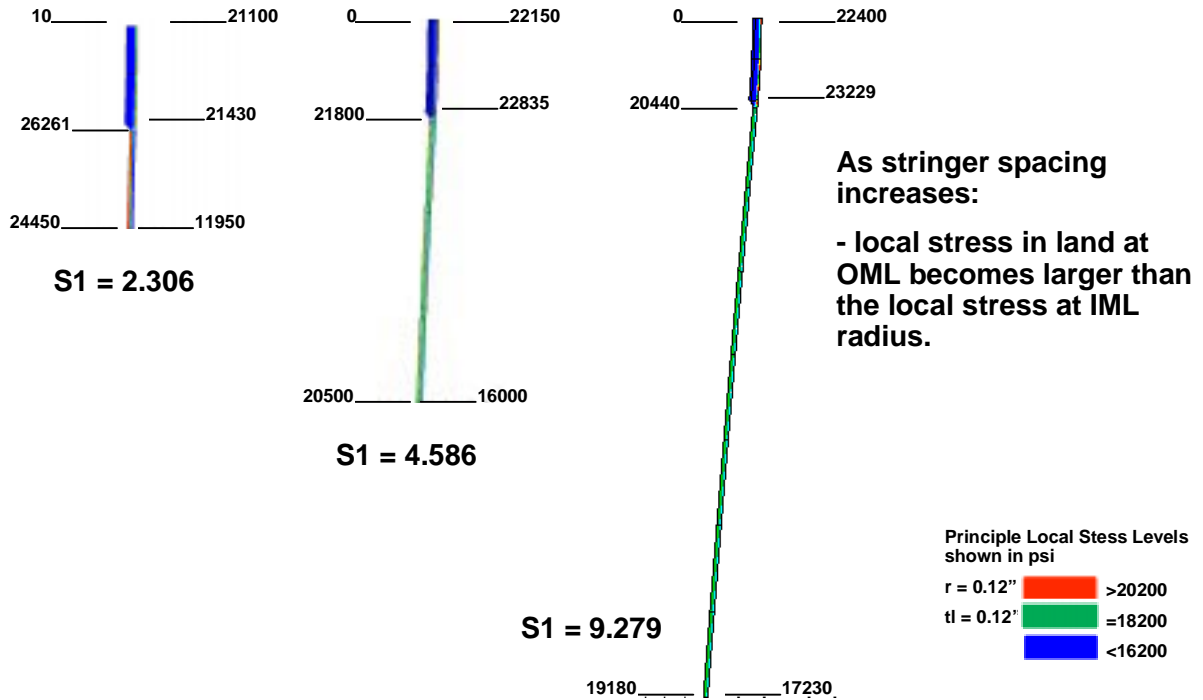
The hoop load produces an internal axial load, as shown. Due to the difference in thickness between the land and skin, the eccentricity in the load path causes an internal bending moment at the radius. Intuitively, we would expect a high local stress on the outer mold line (OML) because the tension due to axial and bending loads combine ($P/A + Mc/I$). We would also expect a high local stress on the inner mold line (IML) because of the stress concentration, even though the bending stress relieves the tension stress due to the axial loading ($P/A - Mc/I$). To define the magnitude of these local high stresses, a two dimensional mechanical model was built and loaded.

Symmetric vs Actual Geometry Results (Baseline)



The results are shown in the Figure above. As expected, there are hot spots at both locations, with 21,800 ksi at the IML and 22,835 ksi at the OML. This gives an effective K_t of about 1.20 to 1.25 based on a reference hoop stress of 18,200 ksi in the skin. Note that there is a pillowing effect in the skin, with the pillowing toward the center of the fuselage. This is reflected by the stress in the skin halfway between the stringer lands, which is 20.5 and 16.0 ksi at the IML and OML surface, respectively. With a symmetric geometry, and therefore no bending due to an eccentric load path, there is no bending, as shown on the left of the Figure.

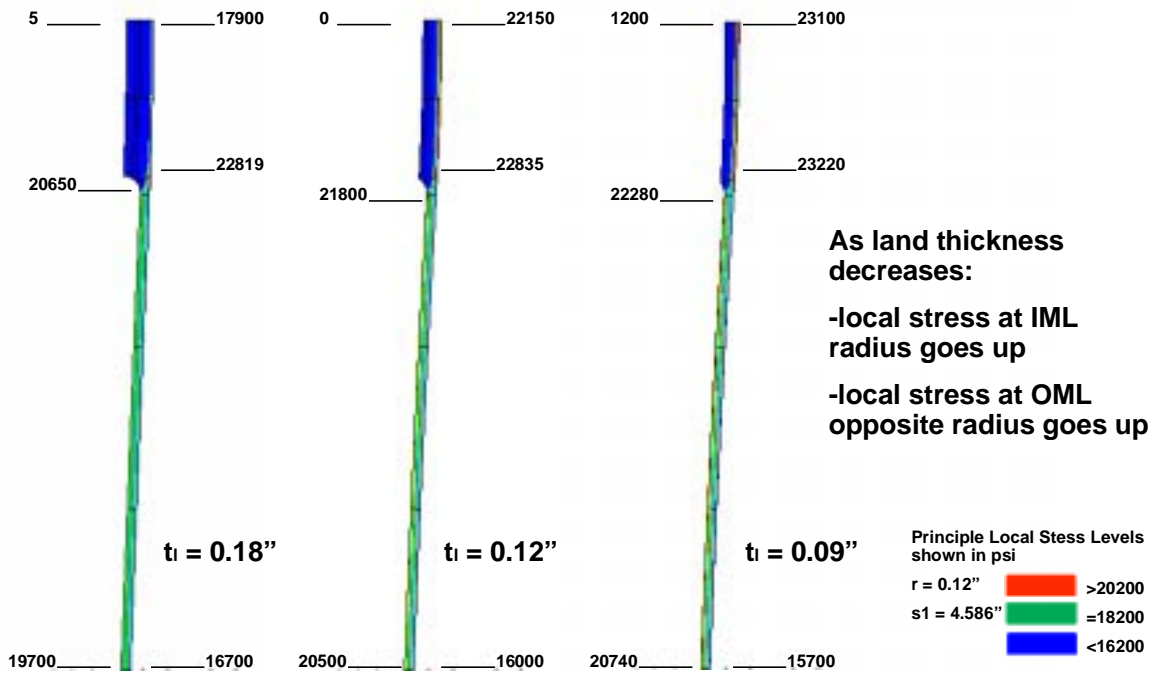
Effects of Stringer Spacing



7 IAS / 04-29-98

As the stringer spacing becomes smaller, the local stress at the IML becomes more critical, going up to 26.261 ksi ($K_t = 1.44$) for a half spacing of 2.306 inches. For a larger stringer spacing the local stress on the OML gets higher, going up to 23.229 ksi ($K_t = 1.28$).

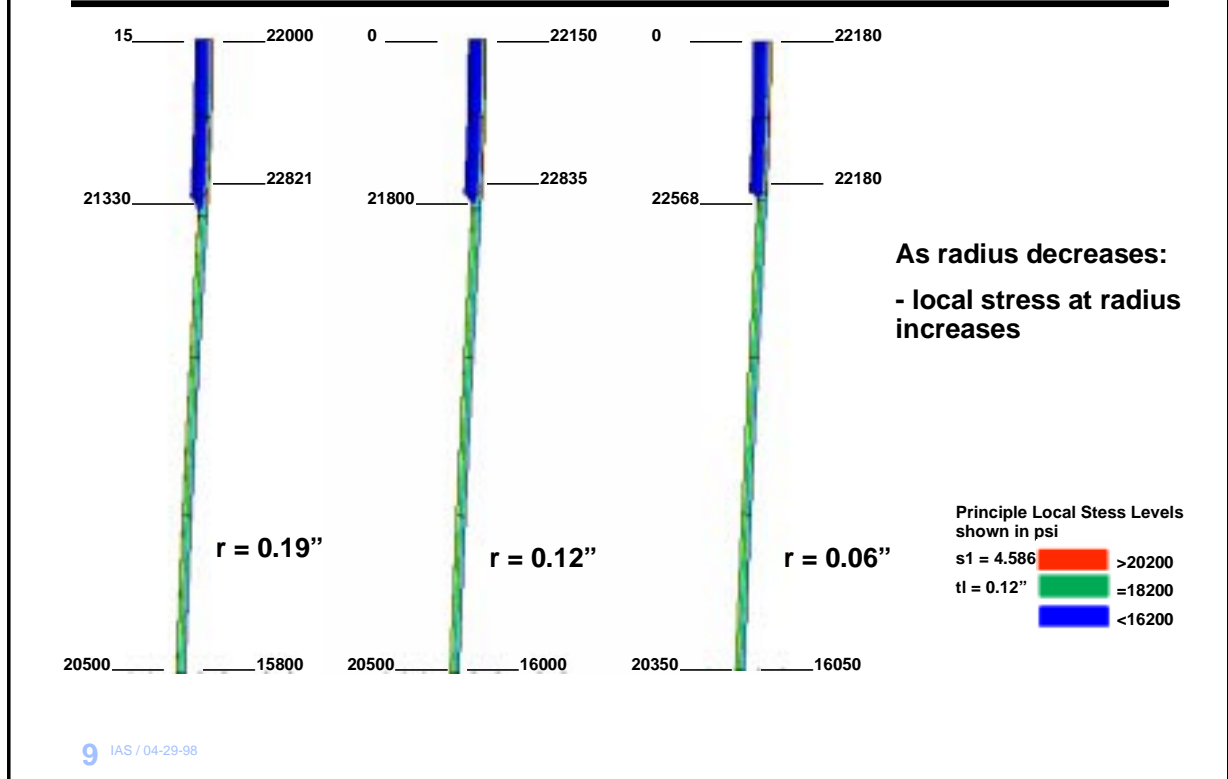
Effects of Land Thickness



8 IAS / 04-29-98

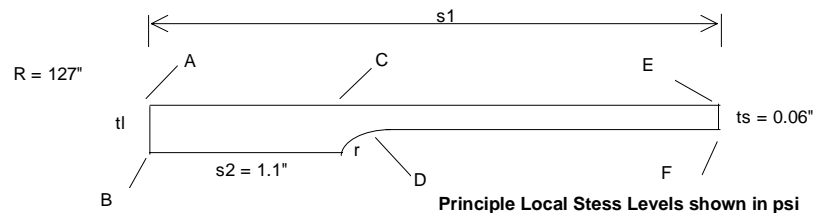
Decreasing the land thickness causes the local stress at both the IML and OML to go up slightly. Increasing the land thickness seems to have little effect.

Effects of Radius



For smaller machined land radii the local stress at the radius goes up slightly. It goes down slightly for a larger radius, as expected.

Raw Data from Two Dimensional Analysis



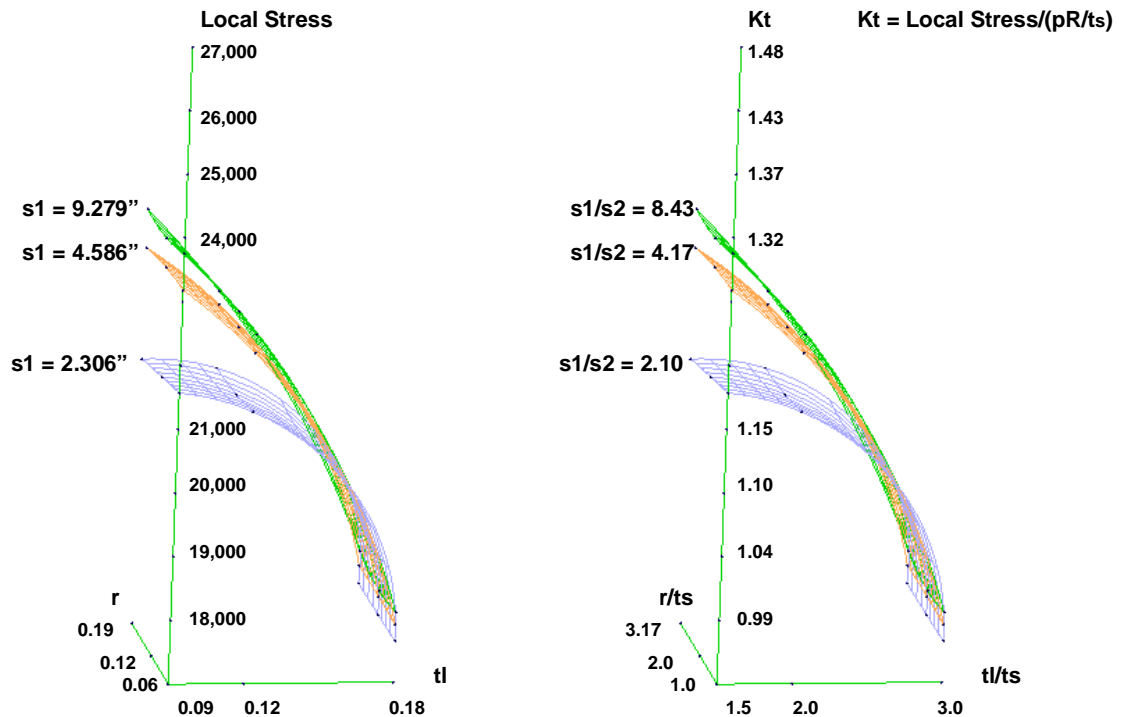
Principle Local Stress Levels shown in psi

R	s2	ts	r	s1	tl	A	B	C	D	E	F	model
127	1.1	0.06	0.19	9.279	0.18	18110	20	23227	19420	17540	18800	a11
					0.12	22200	15	23315	19750	17260	19150	a12
					0.09	23500	500	23818	20200	17060	19300	a13
				4.586	0.18	17880	20	22900	20430	16600	18800	a21
					0.12	22000	15	22821	21330	15800	20500	a22
					0.09	22900	1300	23135	21720	15600	20800	a23
				2.306	0.18	17600	20	21680	23630	13560	22860	a31
					0.12	21000	10	21220	25889	11500	24850	a32
					0.09	21150	3200	21310	25984	11500	24900	a33
			0.12	9.279	0.18	18000	5	23218	19760	17600	18800	b11
					0.12	22400	0	23229	20440	17230	19180	b12
					0.09	23550	500	23840	20780	17100	19330	b13
				4.586	0.18	17900	5	22819	20650	16700	19700	b21
					0.12	22150	0	22835	21800	16000	20500	b22
					0.09	23100	1200	23220	22280	15700	20740	b23
				2.306	0.18	17620	5	21680	23878	13900	22500	b31
					0.12	21100	10	21430	26261	11950	24450	b32
					0.09	21380	2900	21500	26430	11780	24600	b33
			0.06	9.279	0.18	18100	5	23085	21290	17600	18800	c11
					0.12	22480	0	22771	21250	17270	19140	c12
					0.09	23750	450	23850	21720	17130	19280	c13
				4.586	0.18	17900	5	22548	21760	16830	19600	c21
					0.12	22180	0	22180	22568	16050	20350	c22
					0.09	23180	1000	23251	22800	15800	20600	c23
				2.306	0.18	17650	-20	21260	24537	14300	22120	c31
					0.12	21260	0	21310	26587	12440	23940	c32
					0.09	21570	2740	21610	26794	12220	24160	c33

10 IAS / 04-29-98

The results of the sensitivity studies done with mechanics are shown in the Table. Local stress was determined at various points in the model for variations in machined land radius, stringer spacing and land thickness. Enough runs were made to produce carpet plots. For instance, look at point A, a location on the OML at the center of the land.

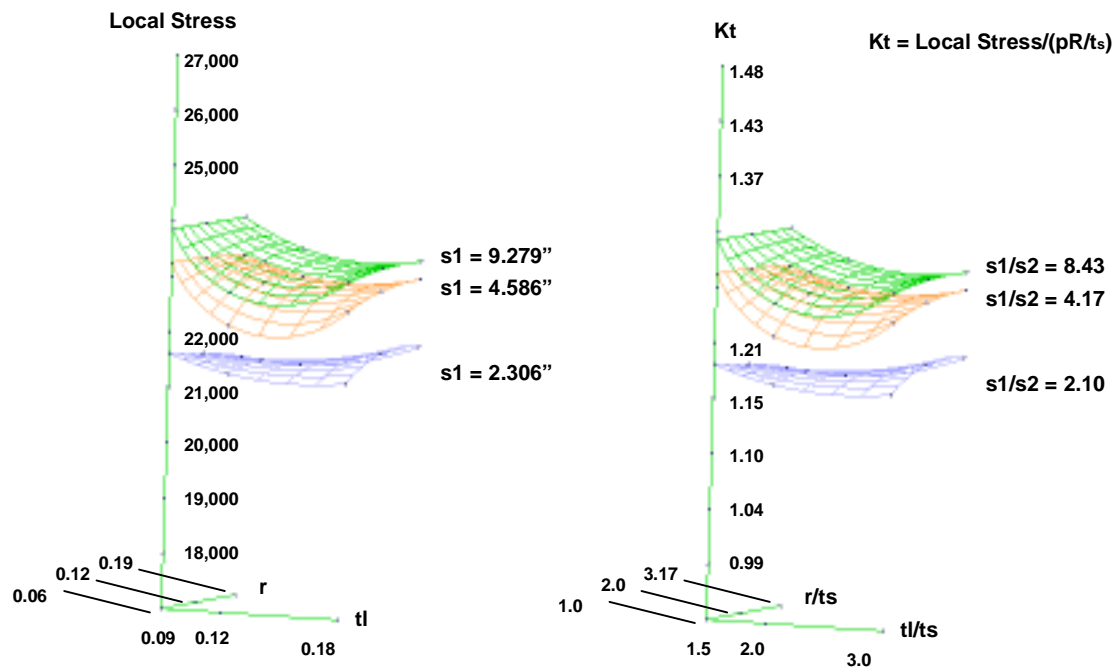
Carpet Plot of "Point A"



11 IAS / 04-29-98

Focus on the left graph in the Figure . One axis is for land thickness and the other is for machined land radius. The vertical axis is local stress. The three carpet plots represent different stringer spacing. If the local stress is divided by the reference hoop stress in the skin of 18.200 ksi, an effective Kt is obtained. The radius and land thickness can be normalized to the skin thickness (which is 0.06 inches) and the stringer spacing can be normalized to the land width (which in this case is 2.2 inches). This is plotted on the graph to the right in the Figure. In this manner, the Kt can be obtained for practically any geometry.

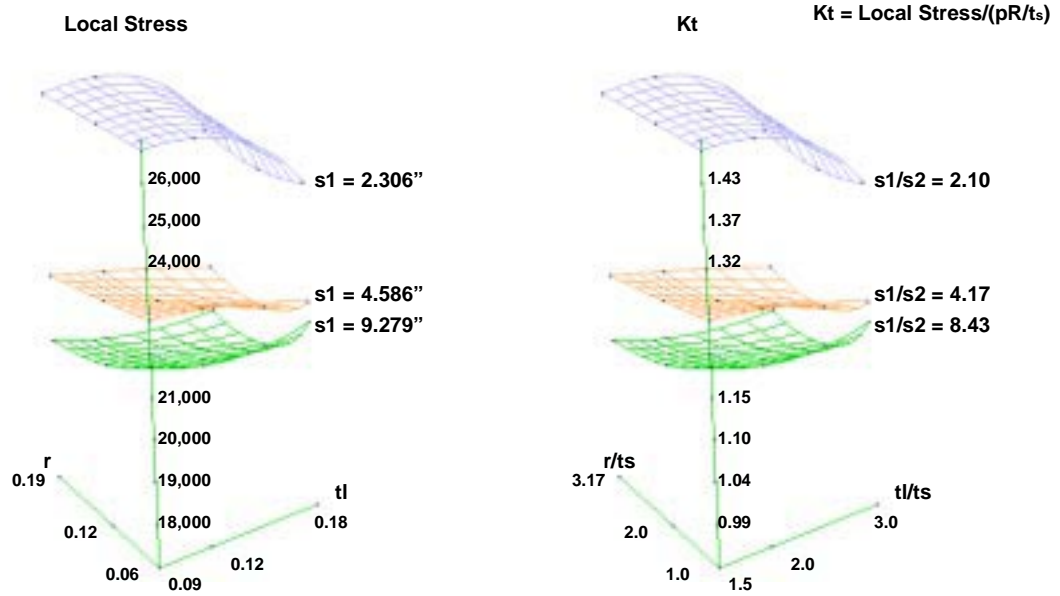
Carpet Plot of "Point C"



12 IAS / 04-29-98

This can be done for any point. "Point C" is shown in the Figure above.

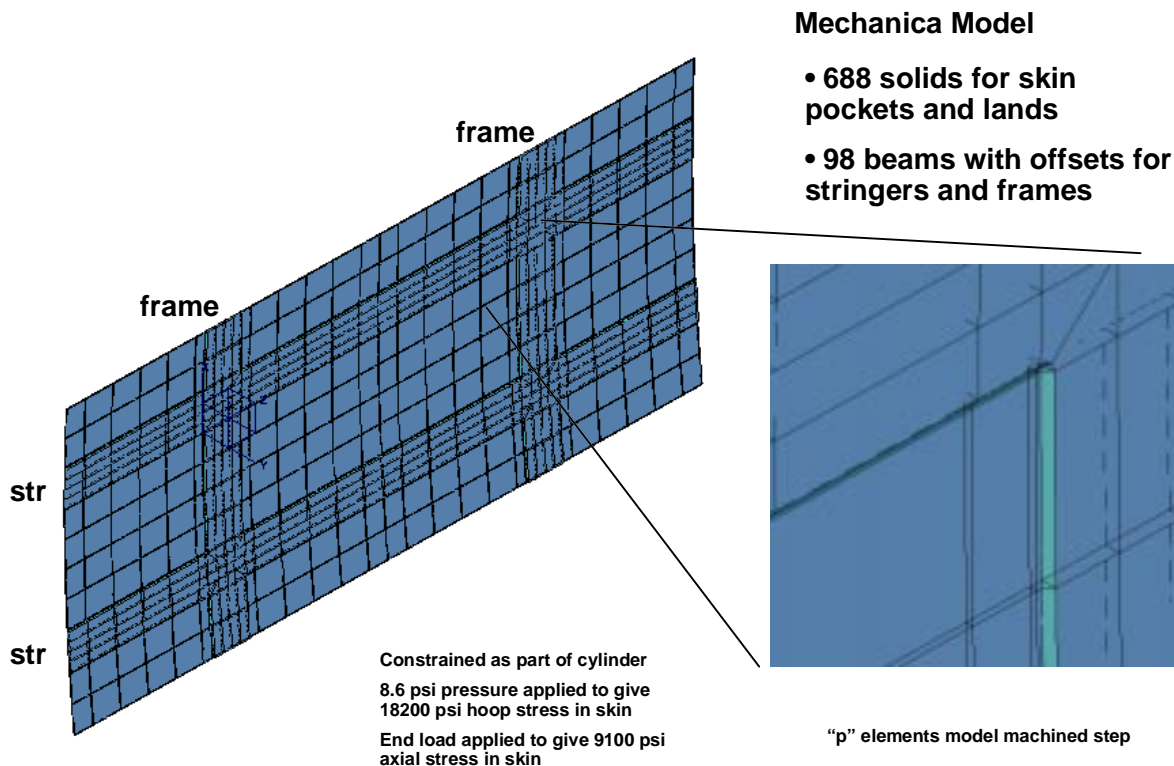
Carpet Plot of "Point D"



13 IAS / 04-29-98

Point D as shown here.

Three Dimensional Analysis

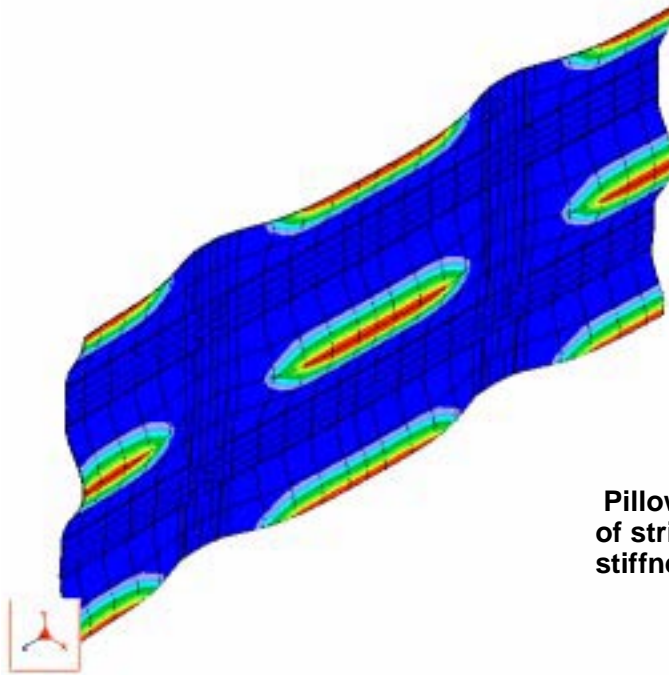


14 IAS / 04-29-98

At this point two questions arose. In the two dimensional analysis, the skin was pillowing inward toward the center of the fuselage, not outward as expected. Also, what would be the effect of including the stiffness of the stringers and frames? This led to the development of a three dimensional model.

A mechanica model and its "p element" capability was built for the baseline configuration. A panel with 2 stringers and 2 frames was created. This would allow an entire bay to be represented with the critical locations at least one half bay away from boundary constraints. 688 solids were used to model the skin and lands. The radius at the lands were modeled exactly. 98 beams, with offsets, were used to model the stringers and frames. The panel was constrained as part of a cylinder. An 8.6 psi pressure was defined to give a "pR/t" hoop stress and a longitudinal load was defined to give a "pR/2t" axial stress. These loads could be applied one at a time or simultaneously.

Hoop Stress Only (only pressure applied)



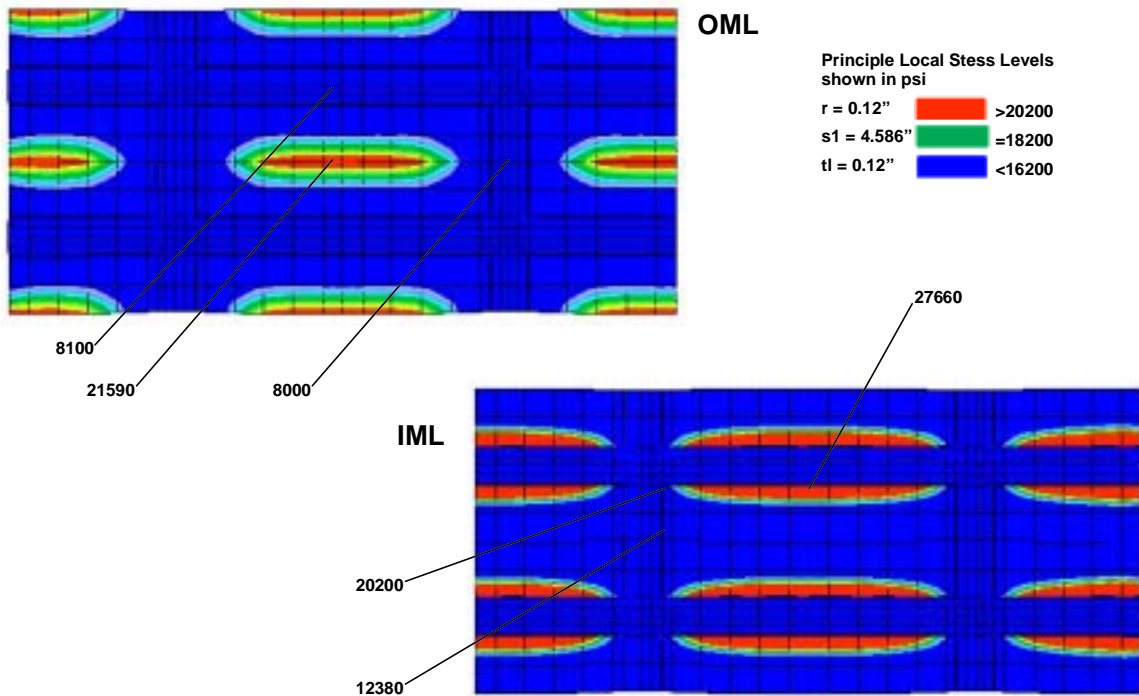
- Deformed shape
- View showing OML

**Pillows outward because
of stringer and frame
stiffness**

15 IAS / 04-29-98

If only pressure is applied (no stress due to axial loading) we get a pillowing outward, as expected, due to the rigidity of the frames and stringers.

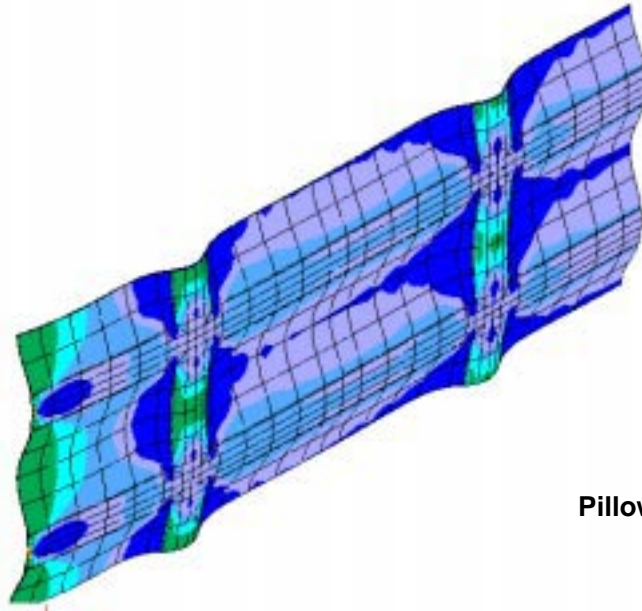
Hoop Stress Only (only pressure applied)



16 IAS / 04-29-98

Since the deflected shape is different, the local stresses (and stress concentrations) changed dramatically. The peak stress of 27.660 ksi from hoop loading only, occurs at the IML at the machined radius half way between frames. The effective K_t is $(27.660/18.200 =)$ 1.5.

Longitudinal Stress Only (only axial load applied)



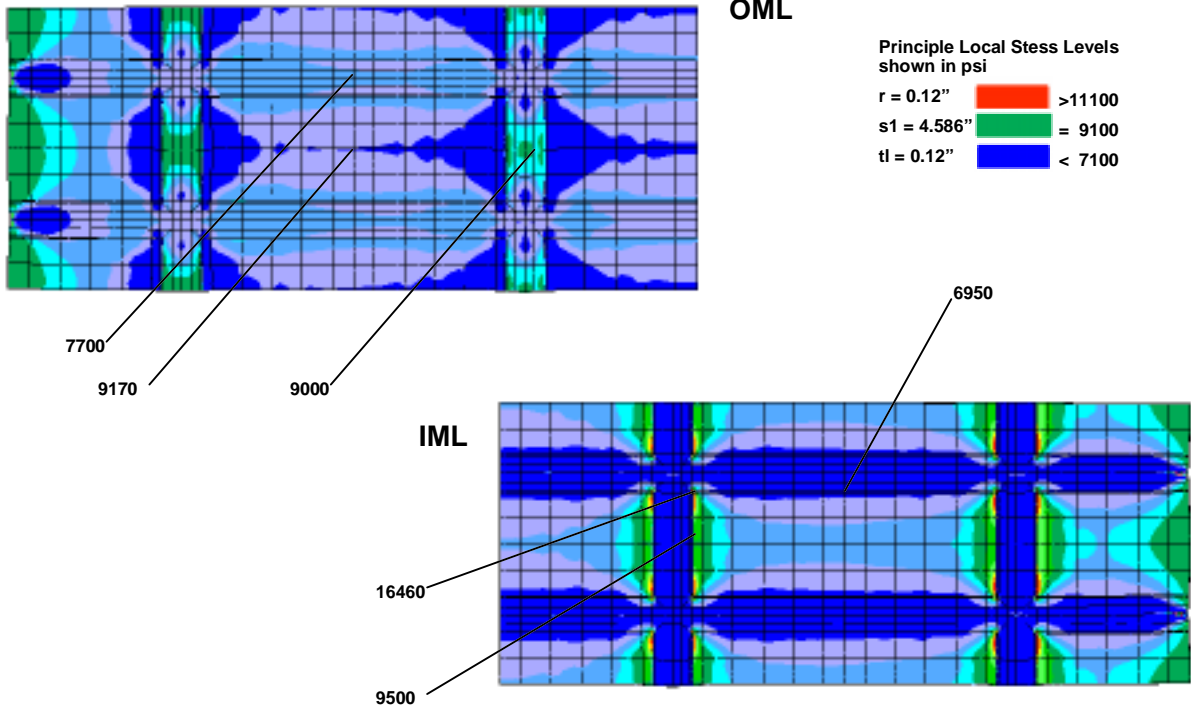
- Deformed shape
- View showing OML

Pillows inward

17 IAS / 04-29-98

For longitudinal loading only, the pillowing is inward.

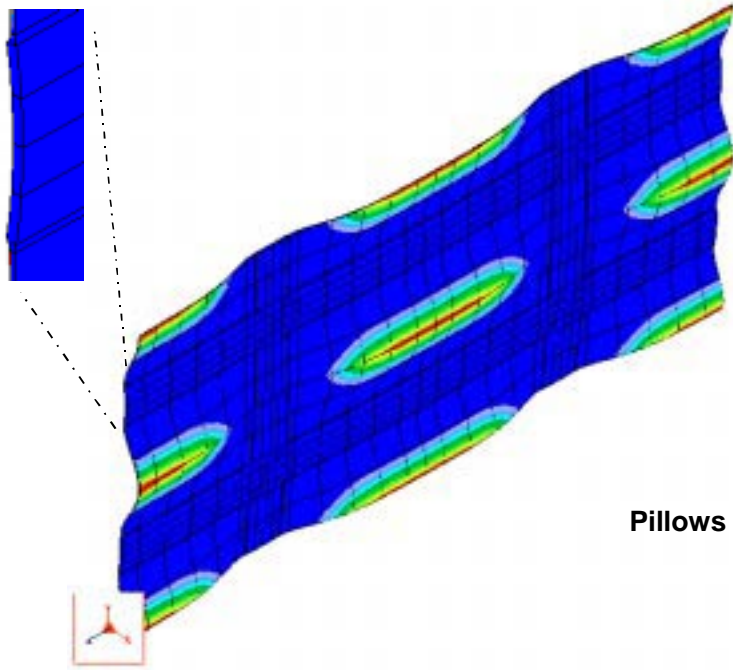
Longitudinal Stress Only (only axial load applied)



18 IAS / 04-29-98

The peak stress of 16.460 ksi occurs at the IML in the machined radius of the frame land, close to the corner of the frame/stringer lands.

Hoop + Longitudinal Stress (pressure & axial load applied)



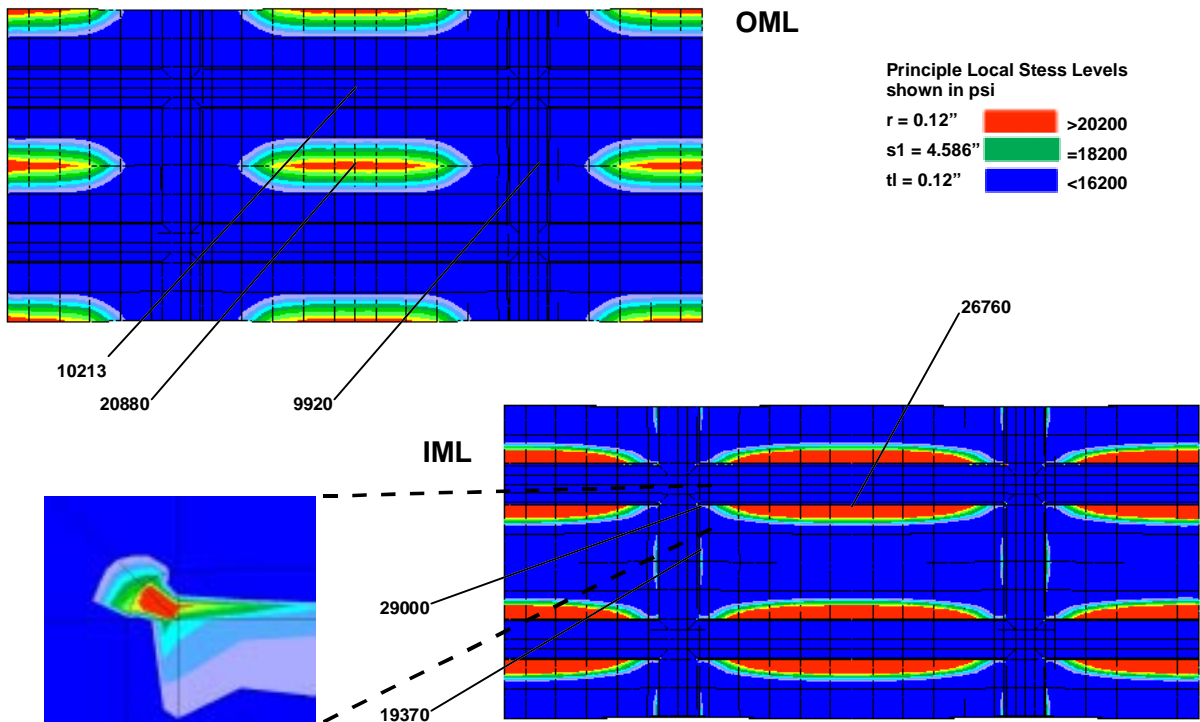
- Deformed shape
- View showing OML

Pillows outward

19 IAS / 04-29-98

For combined loading, the pillowing is outward.

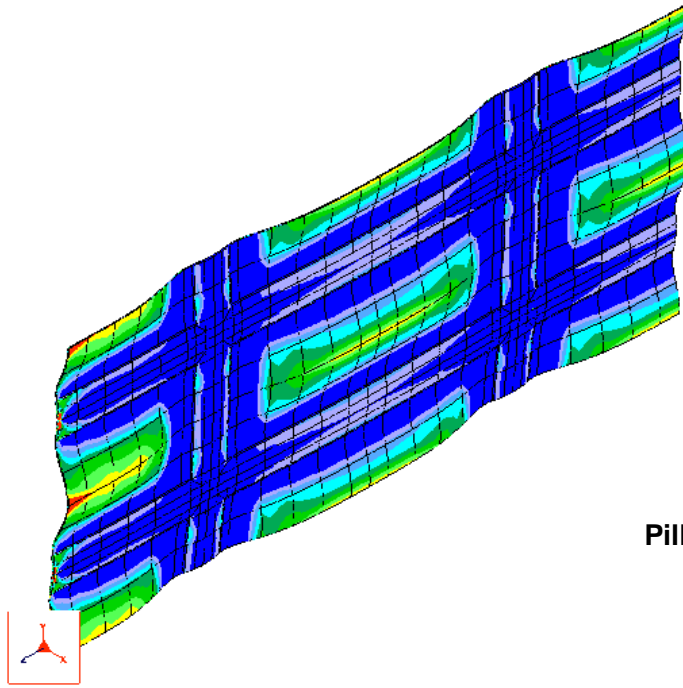
Hoop + Longitudinal Stress (pressure & axial load applied)



20 IAS / 04-29-98

The peak local stress of 29.000 ksi occurs at the IML at the machined radius at the corner of the frame and stringer lands. The effective K_t is $(29.000/18.200 =)$ 1.6.

Hoop + 2 x Longitudinal Stress (pres. + 2 x axial load appl.)



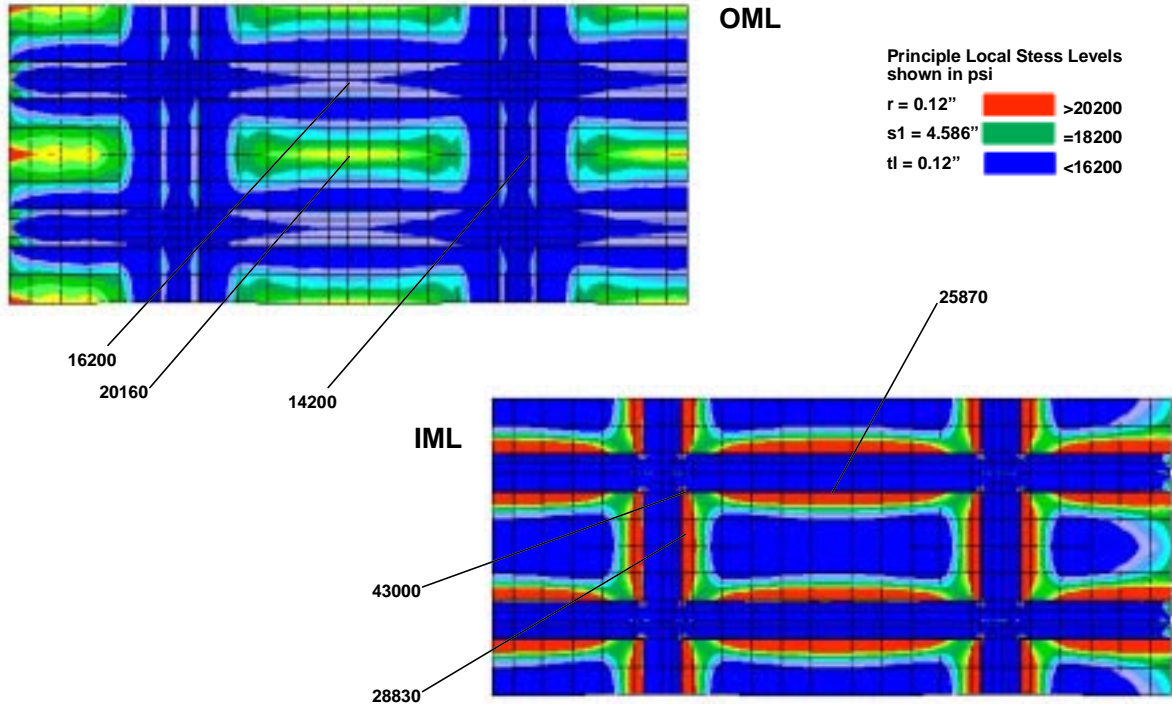
- Deformed shape
- View showing OML

Pillows outward

21 IAS / 04-29-98

To estimate the local stress for a condition of a crown panel with some fuselage bending, the longitudinal load was increased by a factor of 2 and superimposed with the pressure loading. This too, pillowed outward.

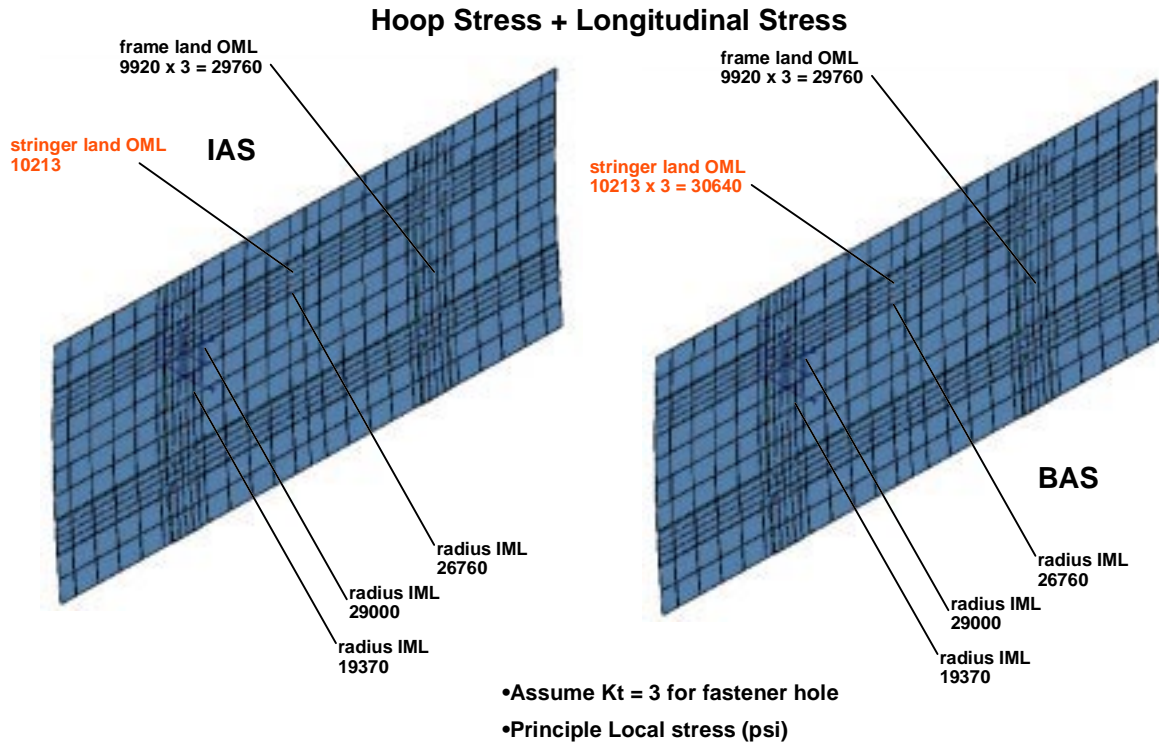
Hoop + 2 x Longitudinal Stress (pres. + 2 x axial load appl.)



22 IAS / 04-29-98

The peak stress increased to 43.000 ksi.

Durability of IAS vs BAS



23 IAS / 04-29-98

The final step in the three dimensional analysis was to compare local stresses for IAS and BAS. To account for increase in local stress for fastener holes that attach frames and/or stringers, the field stress in the center of the lands were multiplied by 3. The highest local stress lies in the BAS at the stringer attach holes (30.640 ksi for baseline geometry and loading). However, this is only slightly higher than either panel at the bay corners (29.760 ksi). For all practical purposes, the peak local stress (and therefore durability life) is the same for both structures.

Summary

- **2 Dimensional Analysis**

- modeling lands w/o offset does not account for thru-thickness changes in stress (may or may not be important)
- w/o stiffness of stringers and frames, skin at midbay pillows inward toward fuselage center
- for small ratios of stringer spacing to land width, higher local stress in radius in IML, for larger ratios, higher local stress in OML opposite radius
- small land thickness to skin thickness ratios give higher local stress at OML at center of stringer land (where fasteners are for BAS)
- as the machined radius decreases, the Kt goes up

24 IAS / 04-29-98

In summary, both two and three dimensional modeling were performed using the mechanical finite element program to address stress concentrations and durability of IAS.

In the two dimensional analyses (which ignores the stiffness of the stringers and frames), we determined stress concentrations for changes in stringer spacing, land thickness and machined radius at the land. These were normalized so that for any stringer spacing to land width ratio, any land thickness to skin thickness ratio and any machined radius to skin thickness ratio, the Kt could be obtained. We also learned that ignoring the effects of stringer and frame stiffness caused the skin to pillow inward toward the center of the fuselage instead of outward.

Summary (continued)

- **3 Dimensional Analysis**

- with stiffness of stringers and frames, skin at midbay pillows outward away from fuselage center
- hoop stress gives higher Kt at stringer radius
- longitudinal stress gives higher Kt at frame radius
- combined Kt from bi-axial loading occurs at the frame/stringer machined corners
- peak local stresses are about 30-40 ksi for combined bi-axial loading due to pressure

25 IAS / 04-29-98

In the three dimensional analyses we learned that including the stiffness of the stringers and frames does cause outward pillowing of the skin. It also dramatically changes stress concentrations. We also learned that hoop stress gives higher stress concentrations at the stringer land radius and longitudinal stress give higher stress concentrations at the frame land radius. For combined loading the highest local stress occurred at the frame/stringer land machined corner, with a Kt of about 1.6 based on “pR/t” reference hoop stress.

Conclusions and Recommendations

Conclusions

- **Less holes in IAS for cracks to start, but must assume fastener holes for repairs, doors, cut-outs, etc.**
- **Virtually no difference in local stress between IAS and BAS**
- **Durability between IAS and BAS will depend on material fatigue properties (7000 series thick plate vs 2000 series sheet)**

Recommendations

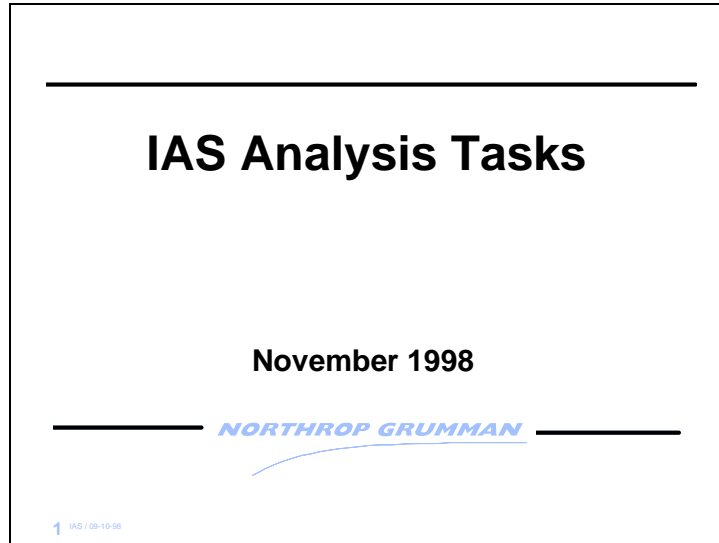
- **Evaluate durability w.r.t. material fatigue properties, especially repairs involving fastener holes**

26 IAS / 04-29-98

In conclusion, the use of the mechanica modeling system worked very well as a quick and efficient tool and provided valuable information to the insight of IAS. There is virtually no difference in local stress between IAS and BAS; however, there are considerably less holes in IAS for cracks to start since the stringers are integral and not mechanically attached. The durability between IAS and BAS will depend on material fatigue properties (7000 series thick plate vs 2000 series sheet).

It is recommended that durability of IAS be evaluated with respect to material fatigue properties, especially for repairs involving fastener holes.

X.X Northrop Grumman Analytical Task 2



Northrop Grumman had two IAS analytical tasks for 1998 which used the finite element program called “Mechanica”:

- 1) evaluate stress concentrations in IAS
- 2) evaluate stress intensity in IAS for longitudinal cracking.

This section documents the results of task 2, which was presented at the IAS meeting held in Norfolk in November, 1998.

Purpose

- **Mechanica can be a quick and effective way to help size structure in a production design environment (D&DT).**
Northrop-Grumman has two Mechanica modeling tasks:
 - Task 1 addressed Durability
 - Determined stress concentration factors in 2 and 3 dimensional analysis
 - Was presented in April 1998
 - Task 2 addresses Damage Tolerance
 - Sensitivity of Stress Intensity to changes in geometry
 - Define best configuration to meet Damage Tolerance criteria

2 IAS / 09-10-98

In the aircraft industry, engineers are particularly interested in tools that can be used in a design effort. In that environment you need programs that are quick and efficient so that a D&DT analyst can help size the structure in a timeframe that will meet aggressive milestones. Mechanica is good for that because of its use of the “p element”, a high order element that contains curved lines and surfaces. This allows the analyst to model complex geometry quickly and accurately with few elements. It’s still a linear approach, but it’s evolving to do both large deflection and non-linear material property analyses.

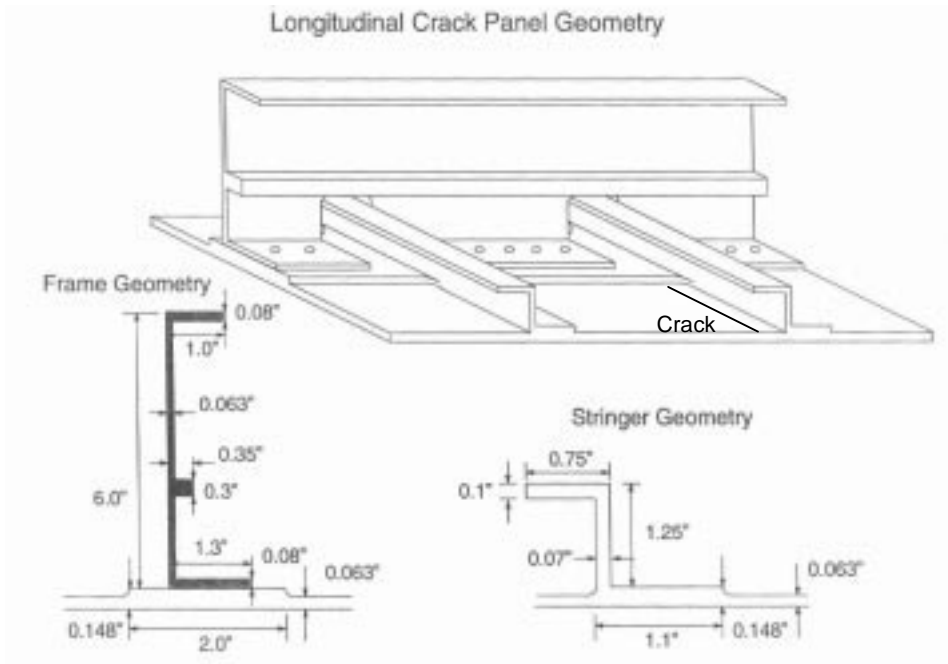
Outline

- **Configuration**
- **FEM**
 - ABAQUS
 - MECHANICA
- **Stress Intensity Predictions**
- **Load Redistribution**
- **Sensitivity Studies**
- **Improved Configuration**
- **Summary**
- **Conclusions & Recommendations**

3 IAS / 09-10-98

In this task we used Mechanica to address stress intensity of a two bay crack in the IAS panel. First, a simplified baseline model was created and compared to the ABAQUS model. Then, variations in several geometric parameters were made to determine how load was redistributed and how sensitive the stress intensity at the two bay crack tip was to these changes. After this study, a best configuration was defined and modeled. Lastly, conclusions and recommendations were drawn.

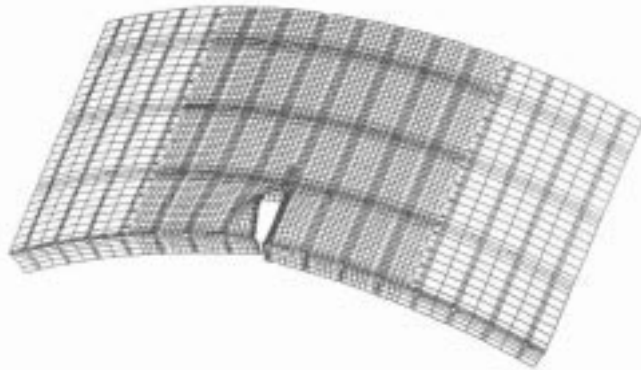
IAS Configuration



4 IAS / 09-10-98

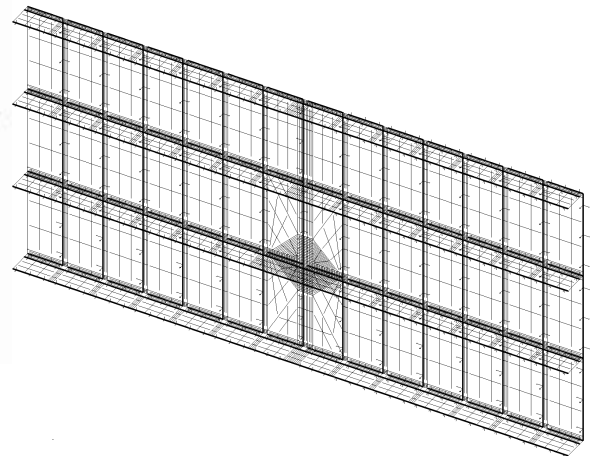
The IAS configuration is shown in the Figure above. It consists of integral “z” stringers and mechanically attached frames. Machined pockets provide lands at both the stringer and frame locations.

FEM Models



ABAQUS - curved model

- baseline model
- pressure load applied
- longitudinal load applied



Mechanica - flat model

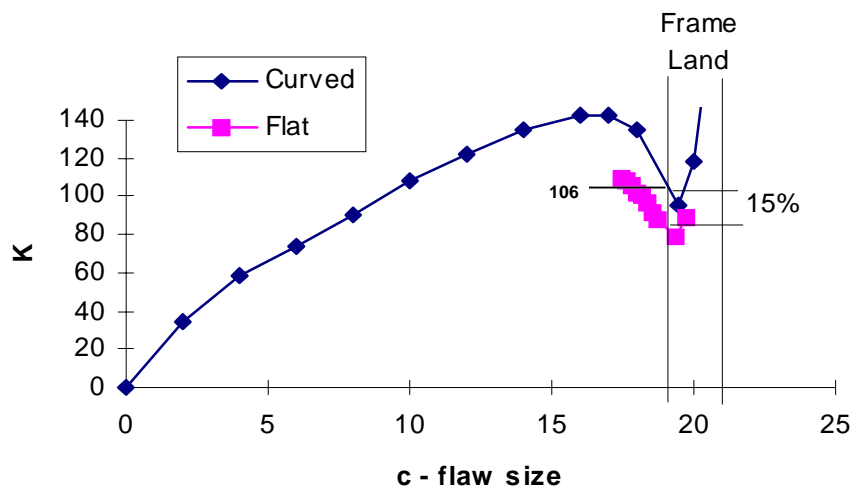
- sensitivity model
- hoop load applied
- longitudinal load applied

5 IAS / 09-10-98

The ABAQUS model (built at Boeing) is curved to match the test panel. It is a half model with a center broken frame and two bay crack. It is constrained cylindrically and loaded by pressure which supplies the hoop stress (pR/t). Also, longitudinal load is applied to supply the axial stress ($pR/2t$). This model accurately matches the pillowing effect, bulging along the crack line, stress intensity at the crack tip, fastener loads and internal load distribution, but it is a complex model and takes time and effort to create and run. This is the baseline model which was used to establish accuracy.

The Mechanica model was made flat to greatly simplify the task. It is a half model with a center broken frame and two bay crack. It is constrained along the line of symmetry and loaded bi-axially to simulate pressure loading. Consequently, there is no pillowing of the skin or bulging along the crack line. This is the sensitivity model which was used to quickly and efficiently predict changes in stress intensity, fastener loads and internal load distribution, due to variations in geometry and stiffness.

Stress Intensity Predictions



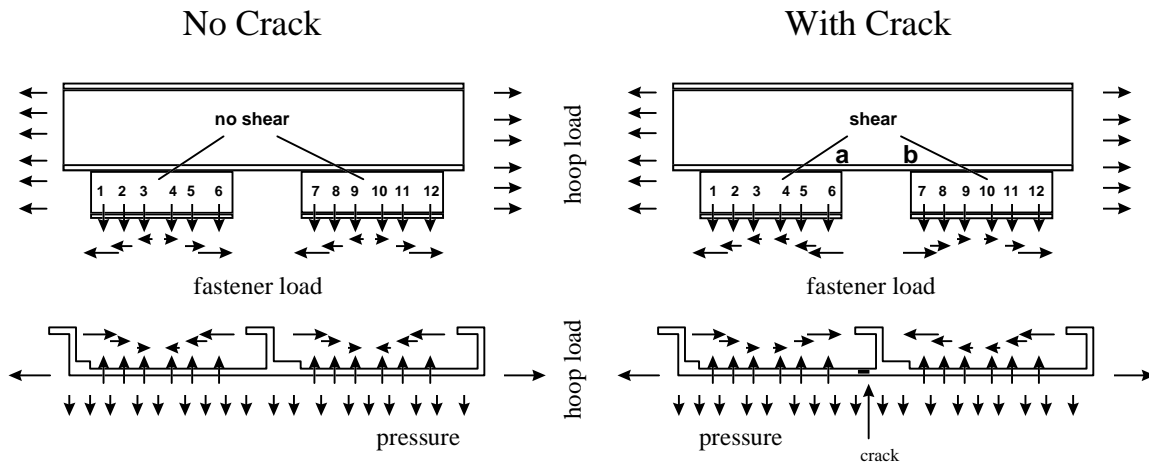
- Flat model gives lower K; Assume $K_{\text{curved}} = K_{\text{flat}} \times 1.15$
- As crack grows through land, K gets large
- Crack growth must be arrested as crack reaches frame land

6 IAS / 09-10-98

The stress intensity versus half crack length is shown above. The diamond curve is the ABAQUS prediction for the baseline configuration. As the crack grows, the stress intensity increases until just before the tip reaches the adjacent frame land. Then, as load begins to redistribute more effectively, the stress intensity goes down to reach a minimum right as the tip reach the land. As the crack grows through the land, the stress intensity increases rapidly. This demonstrates the need to arrest the flaw as it reaches the frame land.

The stress intensity predicted by the simplified Mechanics model is shown by the box curve. The stress intensity is about 15% less than that predicted by ABAQUS. This is most likely due to curvature effects and pressure loads not accounted for by the simplified model. To predict curved model stress intensity for the sensitivity studies, we will increase the flat model predictions by 15%.

Load Redistribution



- With no crack, there is no shear in the shear ties to increase load in frame
- With crack, load in fasteners 4-9 will change direction, and shear from skin will load up frame and increase tension, especially at points "a" and "b"

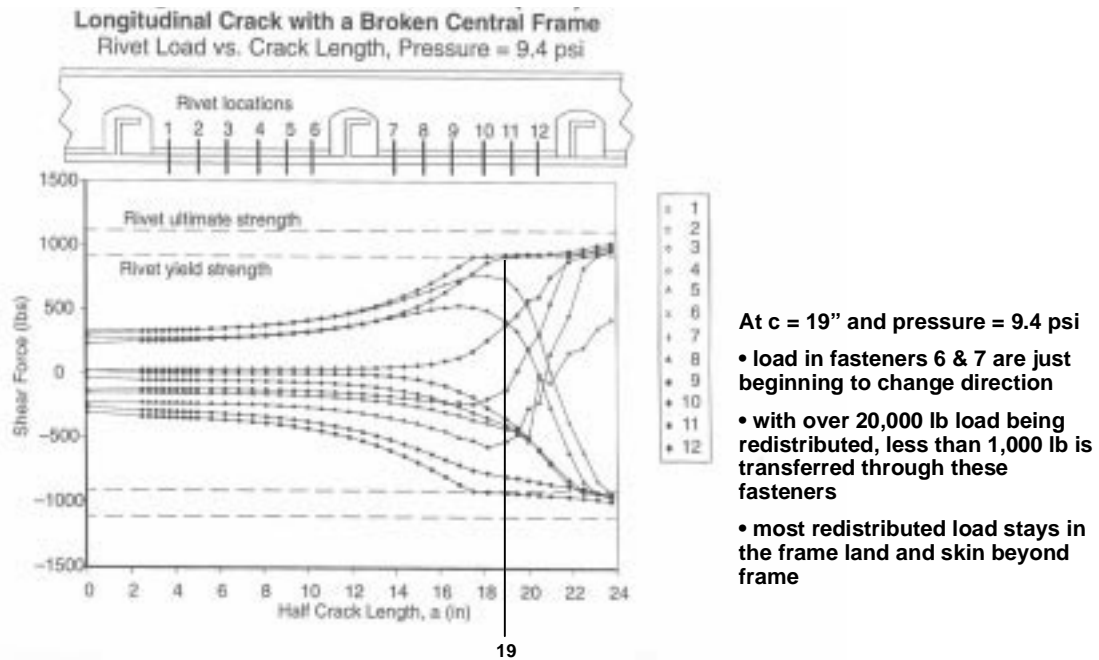
7 IAS / 09-10-98

The load distribution between the skin and frames with no crack is shown on the left in the Figure above. Look at the left shear tie. As pressure is applied and hoop loads build up, the skin stretches and pulls the attach flange of the shear tie along with it. Load goes into the flange through fasteners 1, 2 and 3 and goes out of the flange through fasteners 4, 5 and 6. No load is sheared into the frame. Tension in the frames is produced by the outward radial tension load in the fasteners.

With a crack grown through the frame land, there is no longer a load path across the land in the hoop direction. The load in fasteners 4, 5 and 6 change sign and all six fastener loads are transferred up through the shear tie and into the frame. The same happens in the shear tie across the crack, but in the opposite direction, causing an increase in frame tension across the crack.

As the two bay crack grows, potentially critical failure points would be fastener failure or tension failure of the frame, especially at hot spots "a" and "b".

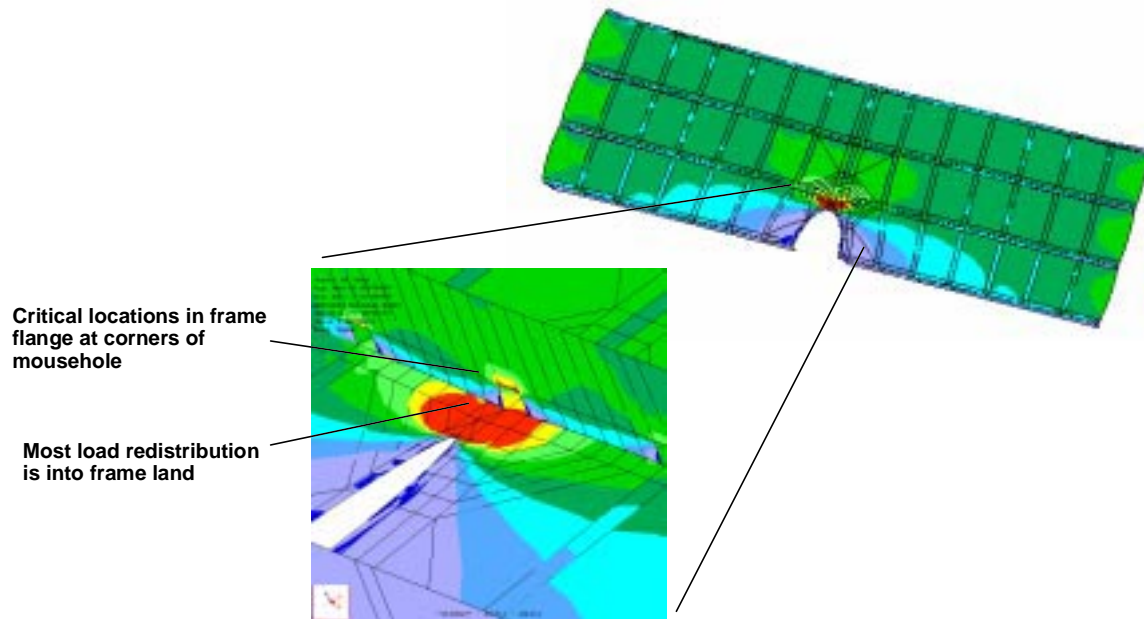
Load Redistribution



8 IAS / 09-10-98

This Figure shows the fastener load predictions (under a 9.4 psi pressure) for the baseline configuration as the crack propagates. With a 19 inch crack (right at the land), fastener 6 and 7 are only beginning to change direction. With an estimated 20,000 lbs of load being redistributed for this crack length, less than 1000 lbs is being redistributed into the frame through these fasteners. Most of the redistributed load is staying in the skin. The shear ties with the big mouse holes are not very stiff load paths to redistribute load.

Load Redistribution



9 IAS / 09-10-98

The Mechanics model also shows the same thing. There is a high load in the frame land, especially at the crack tip, and there is an increased load in the skin beyond the frame. Even though the shear ties are an unstiff load path, large deflections in the tie causes a hot spot at each corner of the mousehole.

Sensitivity Studies

Model	s	f	tl_str	tl_fr	ts	Astr	Afr_main	Afr_mh	fast	Weight/bay	Weight/in ²	Kcurved	Kadj
baseline	9	20	0.148	0.148	0.063	0.1555	0.638	0.457	3/16 al	2.3670	0.01315	106.0	106.0
a	9	20	0.148	0.148	0.08	0.1555	0.638	0.457	3/16 al	2.6136	0.01452	92.1	101.7
b	9	20	0.148	0.148	0.04	0.1555	0.638	0.457	3/16 al	2.0334	0.01130	139.5	119.8
c	9	20	0.148	0.148	0.105	0.1555	0.638	0.457	3/16 al	2.9762	0.01653	78.6	98.8
d	9	20	0.148	0.148	0.0925	0.1555	0.638	0.457	3/16 al	2.7949	0.01553	85.2	100.6
e	9	20	0.148	0.222	0.063	0.1555	0.638	0.457	3/16 al	2.4863	0.01381	101.5	106.6
f	9	20	0.148	0.075	0.063	0.1555	0.638	0.457	3/16 al	2.2494	0.01250	118.5	112.6
g	9	20	0.148	0.148	0.063	0.311	0.638	0.457	3/16 al	2.6842	0.01491	104.0	117.9
h	9	20	0.148	0.148	0.063	0.07775	0.638	0.457	3/16 al	2.2084	0.01227	106.5	99.4
i	9	20	0.148	0.148	0.063	0.1555	1.276	0.914	3/16 al	2.9324	0.01629	91.8	113.7
j	9	20	0.148	0.148	0.063	0.1555	0.319	0.2285	3/16 al	2.0843	0.01158	119.4	105.1
k	9	20	0.148	0.148	0.063	0.1555	0.638	0.457	1/4 ti	2.3670	0.01315	105.0	105.0
l	9	20	0.148	0.148	0.063	0.1555	0.638	0.457	5/32 al	2.3670	0.01315	107.0	107.0
m	6	20	0.148	0.148	0.063	0.1555	0.638	0.457	3/16 al	1.7342	0.01445	105.5	115.9
n	12	20	0.148	0.148	0.063	0.1555	0.638	0.457	3/16 al	2.9998	0.01250	105.5	100.3
o	9	25	0.148	0.148	0.063	0.1555	0.638	0.457	3/16 al	2.7832	0.01237	130.7	122.9
p	9	15	0.148	0.148	0.063	0.1555	0.638	0.457	3/16 al	1.9508	0.01445	85.0	93.4
q	9	15	0.148	0.148	0.08	0.1555	0.638	0.457	3/16 al	2.1289	0.01577	71.6	85.9
r	9	15	0.148	0.148	0.125	0.1555	0.638	0.457	3/16 al	2.6003	0.01926	55.1	80.7
s	9	15	0.101	0.101	0.085	0.106	0.436	0.312	3/16 al	1.7753	0.01315	80.9	80.9

Kcurved = Kflat x 1.15 for crack up to frame land

Kadi = Kcurved x (Weight per in² surface area for confia / Weight per in² surface area for baseline)

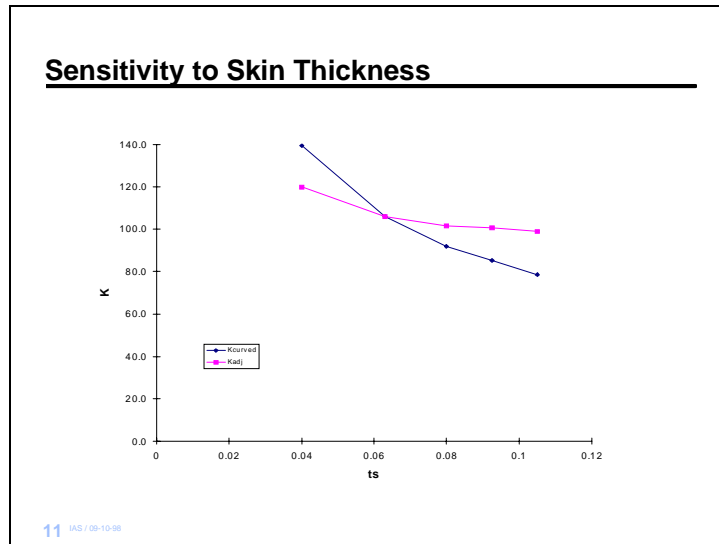
s - stringer spacing f - frame spacing tl_str - land thickness at str tl_fr - land thickness at frame ts - skin thickness
Astr - stringer area Afr_main - area in main part of frame Afr_mh - area in frame at mouse hole fast - fastener dia & mat'l

Using the Mechanics model as a sensitivity tool, runs were made with variations in stringer spacing, frame spacing, land thickness at the stringer, land thickness at the frame, skin thickness, stringer area, frame area (both between the stringers and at the mouseholes), and fastener diameter.

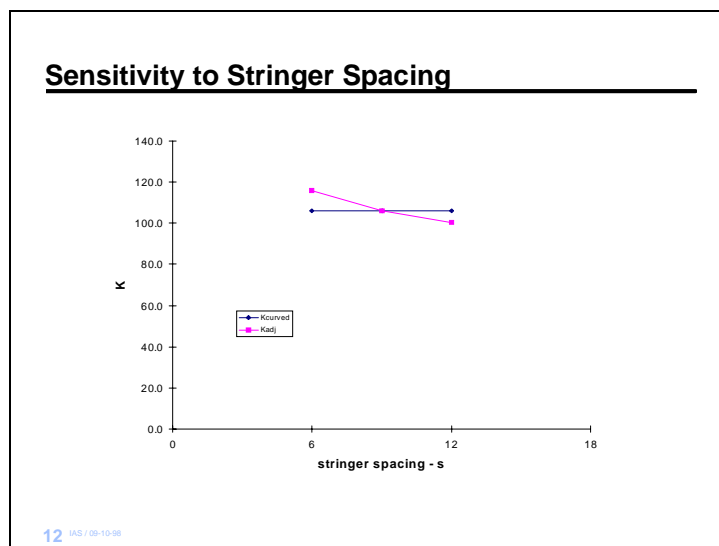
For each configuration, the weight of one bay was calculated (from the center of one stringer to the center of the adjacent stringer and from the center of one frame to the center of the adjacent frame, plus the skin in-between). Then the weight per square inch of surface area was calculated.

The stress intensity for a crack just as it reached the frame land (two bay crack) was predicted for the curved panel by taking the Mechanics stress intensity and ratioing it up by 15% (learned through baseline comparison with ABAQUS).

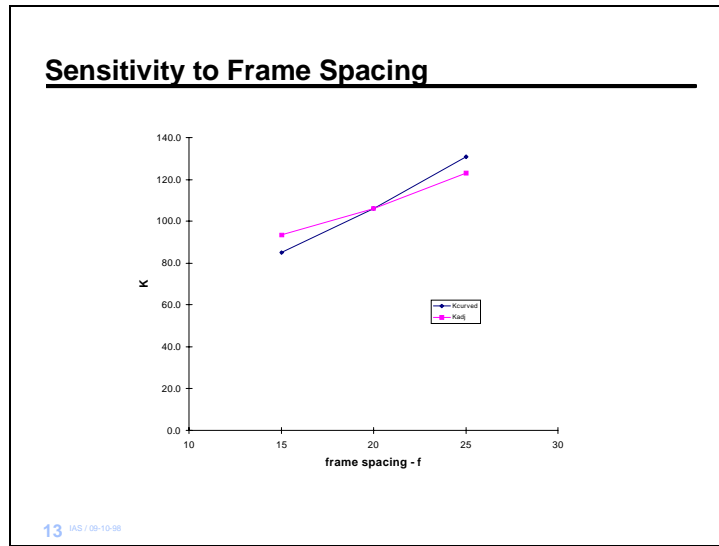
Finally, this stress intensity was adjusted for weight. For instance, assume the weight of a new configuration increased by 10%. To get to the same weight as the baseline, 10% of the volume must be removed uniformly, thereby raising the stress, and therefore stress intensity by 10%. This allowed for a fair comparison from one configuration to another.



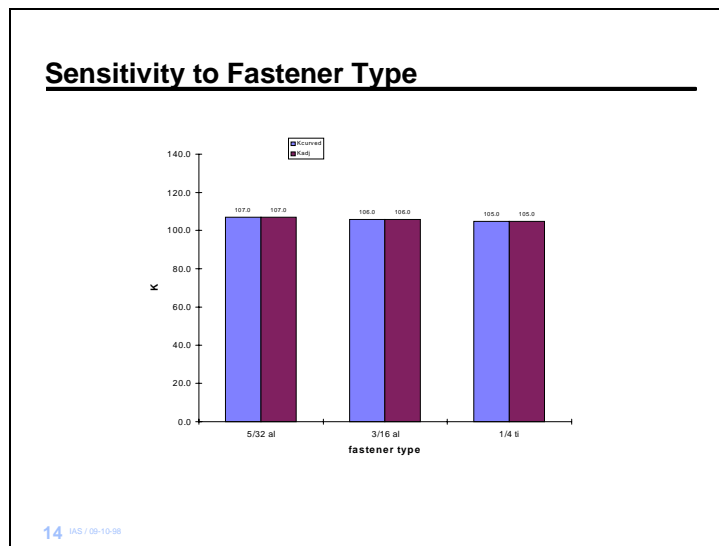
Increasing the skin thickness decreases the stress intensity, but the weight goes up accordingly.



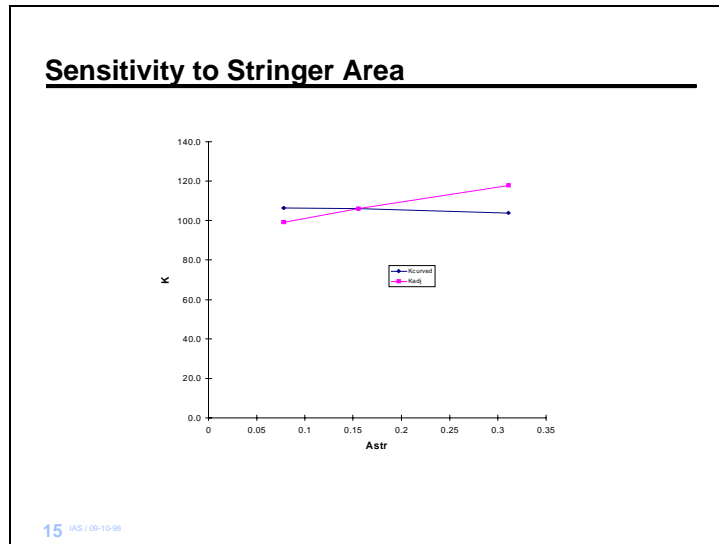
Stringer spacing seems to have no effect on the stress intensity (discounting any pillowing effects), but closer spacing increases weight.



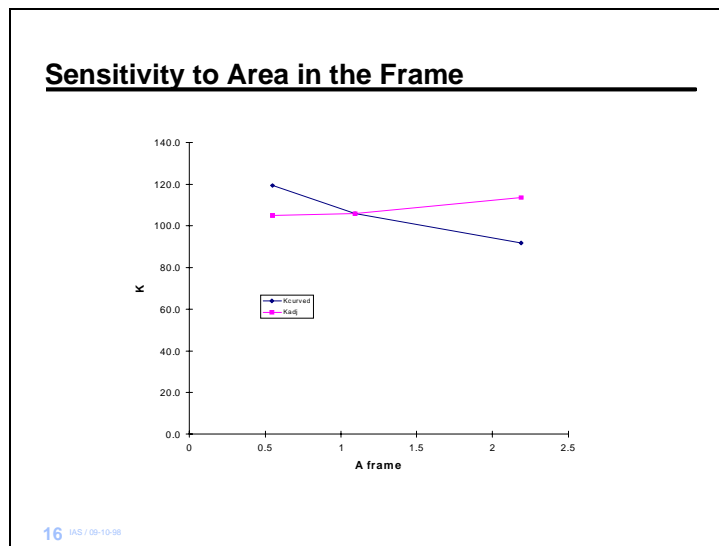
Decreasing the frame spacing significantly decreases the stress intensity, primarily because the two bay crack becomes shorter.



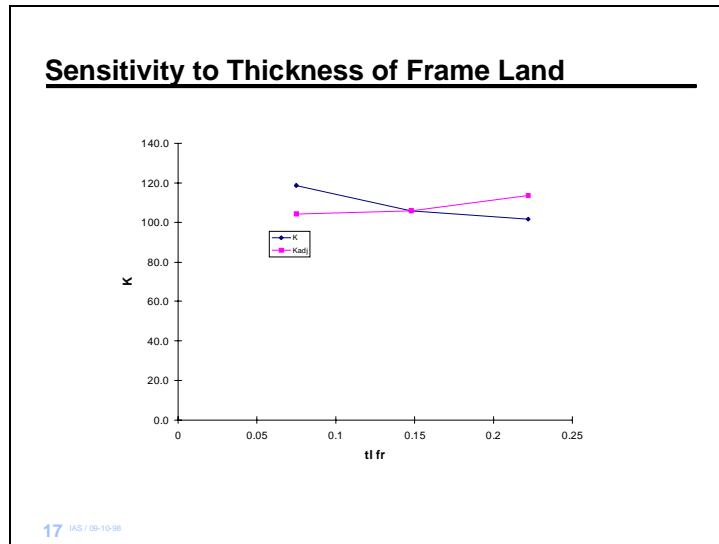
Fastener size and material has virtually no effect on changing the stress intensity.



Increasing the stringer area has little effect other than increasing the weight.



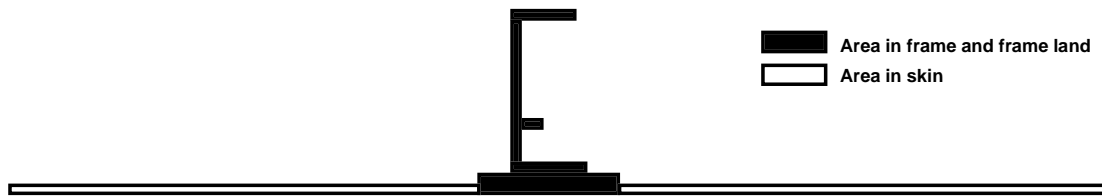
Increasing the frame area decreases the stress intensity, but after accounting for weight, it is detrimental.



Increasing the frame land thickness decreases the stress intensity, but after accounting for weight, it is also detrimental.

Sensitivity to Area Distribution

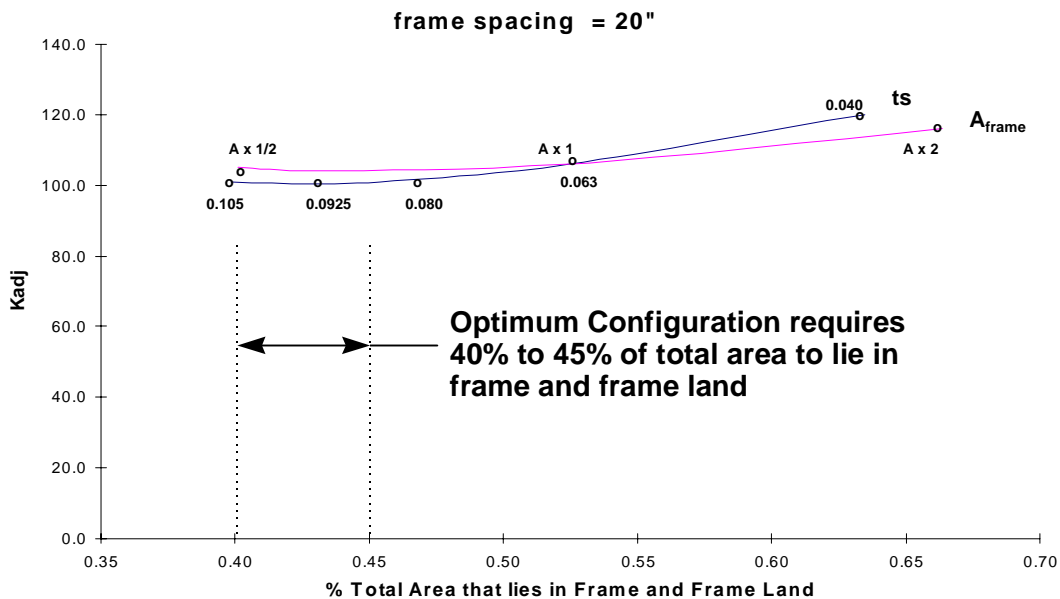
Model#	s	f	tl_str	tl_fr	ts	Astr	Afr_main	Afr_mh	fast	Kadj	Askin	Aframe	Atot	%Atot(fr)
baseline	9	20	0.148	0.148	0.063	0.1555	0.638	0.457	3/16 al	106.0	1.260	1.391	2.651	0.52
a	9	20	0.148	0.148	0.08	0.1555	0.638	0.457	3/16 al	101.7	1.600	1.391	2.991	0.47
b	9	20	0.148	0.148	0.04	0.1555	0.638	0.457	3/16 al	119.8	0.800	1.391	2.191	0.63
c	9	20	0.148	0.148	0.105	0.1555	0.638	0.457	3/16 al	98.8	2.100	1.391	3.491	0.40
d	9	20	0.148	0.148	0.0925	0.1555	0.638	0.457	3/16 al	100.6	1.850	1.391	3.241	0.43
e	9	20	0.148	0.222	0.063	0.1555	0.638	0.457	3/16 al	106.6	1.260	1.539	2.799	0.55
f	9	20	0.148	0.075	0.063	0.1555	0.638	0.457	3/16 al	112.6	1.260	1.245	2.505	0.50
g	9	20	0.148	0.148	0.063	0.311	0.638	0.457	3/16 al	117.9	1.260	1.391	2.651	0.52
h	9	20	0.148	0.148	0.063	0.07775	0.638	0.457	3/16 al	99.4	1.260	1.391	2.651	0.52
i	9	20	0.148	0.148	0.063	0.1555	1.276	0.914	3/16 al	113.7	1.260	2.486	3.746	0.66
j	9	20	0.148	0.148	0.063	0.1555	0.319	0.2285	3/16 al	105.1	1.260	0.844	2.104	0.40
k	9	20	0.148	0.148	0.063	0.1555	0.638	0.457	1/4 ti	105.0	1.260	1.391	2.651	0.52
l	9	20	0.148	0.148	0.063	0.1555	0.638	0.457	5/32 al	107.0	1.260	1.391	2.651	0.52
m	6	20	0.148	0.148	0.063	0.1555	0.638	0.457	3/16 al	115.9	1.260	1.391	2.651	0.52
n	12	20	0.148	0.148	0.063	0.1555	0.638	0.457	3/16 al	100.3	1.260	1.391	2.651	0.52
o	9	25	0.148	0.148	0.063	0.1555	0.638	0.457	3/16 al	122.9	1.575	1.391	2.966	0.47
p	9	15	0.148	0.148	0.063	0.1555	0.638	0.457	3/16 al	93.4	0.945	1.391	2.336	0.60
q	9	15	0.148	0.148	0.08	0.1555	0.638	0.457	3/16 al	85.9	1.200	1.391	2.591	0.54
r	9	15	0.148	0.148	0.125	0.1555	0.638	0.457	3/16 al	80.7	1.875	1.391	3.266	0.43
s	9	15	0.101	0.101	0.085	0.106	0.436	0.312	3/16 al	80.9	1.280	0.950	2.230	0.43



18 IAS / 09-10-98

The results of all the sensitivity runs is shown in the Table. Also shown is the total cross-sectional area from the center of one bay, across the frame and frame land, to the center of the adjacent bay. The last column in the table shows what percent of this total area lies in the frame and frame land.

Sensitivity to Area Distribution

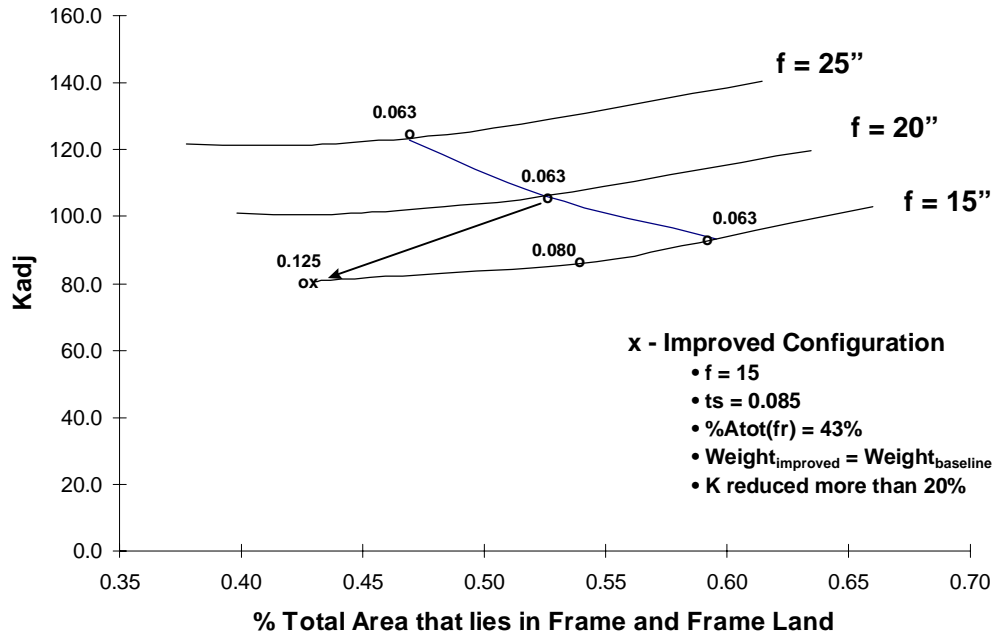


19 IAS / 09-10-98

Look at the data for a 20 inch frame spacing. Plotting the percent of total area that lies in the frame and frame land versus adjusted stress intensity, we notice that a minimum lies in the range from 40% to 45%. This means that to obtain a load distribution giving the lowest stress intensity for a two bay crack for the same weight, we need to have about 40% to 45% of the total cross-sectional area to lie in the frame and frame land.

Consider this. If the skin is thin, the percent of load carried by the frames and frame lands is higher than if the skin was thick. The amount of load the center, broken frame and frame land was carrying has to be redistributed to the adjacent frames and frame lands. If this load is too high the stress intensity for a two bay crack becomes too big. Conversely, if the skin is too thick (the frames and frame lands are smaller for this configuration), then the adjacent frames and frame lands are too small to lower the stress intensity enough as the crack approaches a two bay crack length. It's a matter of area distribution. Somewhere between a too thick skin and a too thin skin is an optimum thickness.

Improved Configuration



20 IAS / 09-10-98

Now, if we look at the same curve for different frame spacing, we notice that a significant decrease in stress intensity can be obtained for a 15 inch frame spacing, for the same weight. The primary reason for this is that a two bay crack length for this configuration is much shorter. What is interesting is that for the same weight (essentially taking weight out of the frames and putting it into the skin, then moving the frames closer) we can reduce the stress intensity by 20%. Of course, this would have to be verified with an ABAQUS model, as the last step in this process.

Summary

- **ABAQUS used for Baseline - Mechanica used for sensitivity**
- **Flat model yielded lower K, approx. 15%**
- **Crack growth must be arrested as tip reaches frame land**
- **Not sensitive to fastener size/material**
- **Little load redistribution through fasteners until crack grows through frame land**
- **Stringer spacing has little effect on longitudinal cracking**
- **Optimum configuration requires 40-45% of total cross-sectional area (area carrying hoop load) to lie in frame and frame land**
- **Optimum frame spacing is 15 inches**

21 IAS / 09-10-98

In summary, we defined an ABAQUS model to establish accuracy for a baseline configuration. Then we made some simplifying assumptions to reduce the complexity of the model, used Mechanica (a quick and easy to use method) to do a large number of sensitivity studies to define an optimum configuration. A final step would be to verify this with ABAQUS.

Along the way we realized:

- 1) simplification to the model reduced the accuracy, as expected,
- 2) two bay crack growth for IAS must be arrested as the tip reaches the frame land,
- 3) redistribution of load as the crack grows is not very sensitive to fastener size or material; there is relatively little load sheared into the frame through the fasteners as the flaw grows,
- 4) stringer spacing has little effect on longitudinal cracking (not counting the pillowing effect ignored by mechanica; stringer spacing should be determined with static compression analysis or lateral 2 bay cracking with broken stringer),
- 5) the optimum configuration requires that 40-45% of total cross-sectional area (area carrying hoop load) should lie in the frame and frame land,
- 6) the optimum frame spacing is about 15 inches.

Conclusions and Recommendations

For production design

- use non-linear model for baseline to establish accuracy
- use quick linear model, verified against BL, for sensitivity studies

Design panel to arrest crack as tip reaches frame land

Choose configuration wisely

- Let 40-45% of total cross-sectional area lie in frame and frame land
- Set frame spacing at 15 inches
- Size stringer spacing with static compression analysis or lateral 2 bay cracking with broken stringer

Use non-linear model for verification of best configuration

Establish Fatigue and Damage Tolerance Criteria for IAS

22 IAS / 09-10-98

In conclusion:

- 1) Using a non-linear model (such as ABAQUS) to establish accuracy for a baseline configuration and a quick, simplified, linear model (such as Mechanica), verified against BL, for sensitivity studies worked very well and could be used in a production design.
- 2) Based on the sensitivity studies, an optimum configuration can be defined.
- 3) Using the non-linear model, this optimum configuration should be verified.

It is recommended that for a new design, this approach should be considered. In addition, after the IAS panel test has been completed, Fatigue and Damage Tolerance Design Criteria should be established for IAS. Lastly, the optimum configuration defined in this study should be verified by ABAQUS. This improved configuration could significantly decrease weight for IAS or reduce risk of two bay crack failure.

Appendix H

Integral Tear Strap Crack Arrest Evaluation

Following is the Boeing Long Beach report “Integral Tear Strap Crack Arrest Evaluation,” dated October 1998.

Copy Number:

Report Number: MDC 98K0503

Integral Tear Strap Crack Arrest Evaluation

Revision Date:

Revision Letter: Original

Issue Date: October 1998

Contract Number: Seattle IDWA
#B50105

Prepared by

R. G. Pettit

J.J. Wang

Chin Toh

Approved by

Trent Logan
Senior Manager
Advanced Design & Technology

MCDONNELL DOUGLAS

FOREWORD

This report documents work performed by the Boeing Long Beach Advanced Transport Aircraft Development organization in fulfillment of the Boeing Seattle IDWA #B50105 (under Seattle NASA contract NAS1-20267, Task 18). Cognizant representatives for this work are John Munroe, Boeing Commercial Airplane Group, and Trent Logan, Director, Prototype Center, Advanced Transport Aircraft Development (Long Beach, CA), Boeing Phantom Works.

ABSTRACT

Crack arrest for straight-growing cracks was studied in statically loaded 7050-T7451 panels with integral tear straps. Failure loads were compared to predictions based on linear elastic fracture mechanics, and good correlation was obtained.

Keywords:

Integral Structures

Damage Tolerance

TABLE OF CONTENTS

SECTION	TITLE PAGE
1.0 INTRODUCTION	H-8
2.0 THICKNESS INTERFACE TESTS	H-8
3.0 CONCLUSIONS AND RECOMMENDATIONS	H-21
4.0 REFERENCES	H-22

LIST OF FIGURES

1	<i>Thickness Interface Specimen Concept</i>	H-10
2	<i>FRANC2D Model of Thickness Interface Specimen</i>	H-11
3	<i>Close-up of FRANC2D Crack Tip Mesh at Tear Strap Interface (a=F)</i>	H-12
4	<i>Normalized Stress Intensity Plot for Thickness Interface Specimen Based on FRANC2D Model</i>	H-13
5	<i>Plots of Load vs. Crack Opening Displacement for 23.80 Inch Wide Specimens</i>	H-16
6	<i>Plots of Load vs. Crack Opening Displacement for 15.86 Inch Wide Specimens</i>	H-17
7	<i>Plots of Load vs. Crack Opening Displacement for 11.90 Inch Wide Specimens</i>	H-17
8	<i>Load/Crack Length Plots for all Specimens</i>	H-20
9	<i>Photograph of Test Setup</i>	H-20
10	<i>Correlation of Thickness Interface Specimen Data with Linear Elastic Analysis</i>	H-21

LIST OF TABLES

1	<i>Average Lot Release Data for 7050-T7451 Plate Material</i>	H-9
2	<i>Thickness Interface Specimen Test Matrix</i>	H-9
3	<i>Tabulated Thickness Interface Specimen Measurements</i>	H-18
4	<i>Tabulated Thickness Interface Test Results</i>	H-19

1.0 INTRODUCTION

This report documents testing performed as part of the NASA Integral Aircraft Structures (IAS) program to evaluate the feasibility of integral metallic fuselage structures [1]. The overall program objective is to obtain equal or better structural performance for lower cost, with the anticipation that the low part count nature of properly designed integral structure can enable significant cost savings.

A significant technical challenge to this class of structures is damage tolerance and fail safety [2]. With regard to fail safety, such as in the arrest of a two-bay crack, there is little available data in the literature with regard to the current ability of fracture mechanics to predict the arrest of a statically propagating cracks in integrally stiffened structure. Various investigators have provided test data for fatigue cracking [3,4], and in one case there was mention of substantial static crack arrest capability, but no data was given [4]. This study provides test data and analyses to evaluate the ability of integral tear straps to arrest a straight, statically propagating skin crack. The data presented has direct application to the prediction of failure loads for larger panels presently undergoing test at NASA Langley Research Center and Boeing Seattle as part of the IAS program.

2.0 THICKNESS INTERFACE TESTS

2.1 Test Specimens

All specimens were machined out of a single lot of 1.5x48x144 inch 7050-T7451 aluminum alloy plate procured jointly for the IAS program by Boeing Seattle and Boeing Long Beach. Average lot release data for that lot of material are given in Table 1.

Numerous additional material coupons were supplied under the Boeing Seattle contract for testing at NASA from this same lot, including 24 inch wide center-cracked panels for R-curve testing in both T-L and L-T orientations in machined thicknesses of 0.060 and 0.012 inches. In addition, Boeing Long Beach derived L-T R-curves from Double Cantilever Beam (DCB) specimens of 0.090 inch thickness, also from the same lot. The NASA center cracked panels [5] produced maximum L-T and T-L fracture toughnesses of 108 and 76 ksi-in^{1/2} respectively¹. From the Boeing Long Beach DCB specimens [1], several more complete T-L R-curves were obtained, giving a typical maximum value of about 83 ksi-in^{1/2}. Because the DCB R-curves were more complete, the T-L value of 83 ksi-in^{1/2} will be employed for failure analysis of specimens of that orientation.

¹The NASA data was presented as work in progress, and toughness was based on physical crack length measurements. The DCB specimens were reduced using effective crack length.

Table 1. Average Lot Release Data for 7050-T7451 Plate Material

Stock Size (inches)	Manufacturer (Lot No.)	Property	L (Sample count)	LT (Sample count)
48.5x144x1.5	Pechiney (75394/011)	TUS, ksi	77.4 (1)	76.9 (1)
		TYS, ksi	68.0 (1)	68.3 (1)

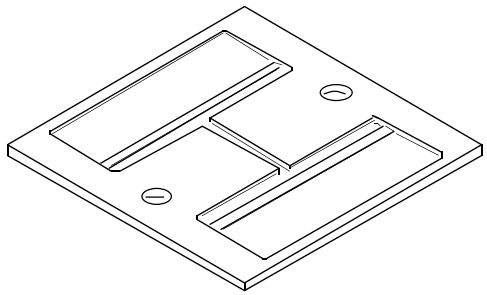
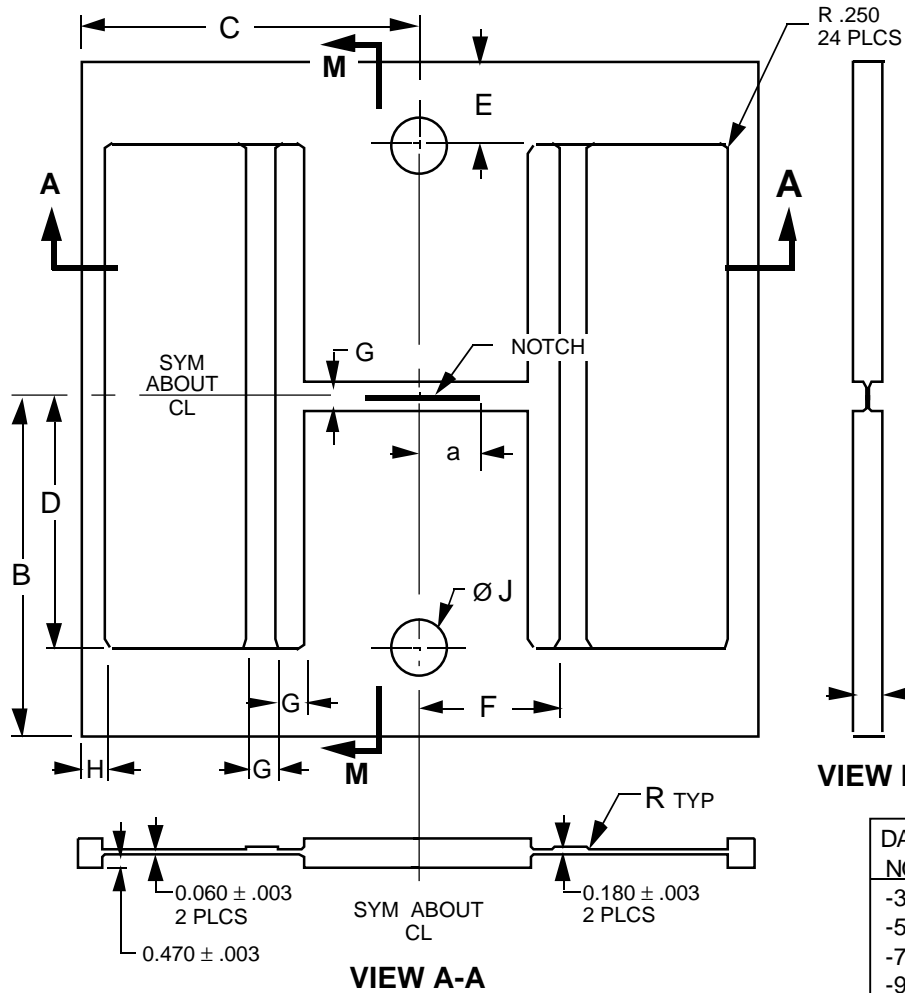
A total of twelve thickness interface specimens were manufactured as part of the Boeing Long Beach IAS contract [1], and were divided for testing among Boeing Seattle and Long Beach contracts². Also, one specimen was sent to NASA Langley Research Center for testing, as indicated in Table 2.

Table 2. Thickness Interface Specimen Test Matrix

Specimen No	Configuration (Orientation)	Panel Width (inches)	Fillet Radius	Test Responsibility
THIF-3L	-3 (L-T)	23.80	.063	Boeing Seattle
THIF-5L	-5 (L-T)	23.80	.188	Boeing Seattle
THIF-9L#1	-9 (L-T)	15.86	.188	Boeing Seattle
THIF-9L#2	-9 (L-T)	15.86	.188	Boeing Seattle
THIF-11L	-11 (L-T)	11.90	.063	Boeing Long Beach
THIF-13L	-13 (L-T)	11.90	.188	Boeing Long Beach
THIF-3T	-3 (T-L)	23.80	.063	Boeing Seattle
THIF-5T	-5 (T-L)	23.80	.188	Boeing Seattle
THIF-9T#1	-9 (T-L)	15.86	.188	Boeing Seattle
THIF-9T#2	-9 (T-L)	15.86	.188	Boeing Seattle
THIF-11T	-11 (T-L)	11.90	.063	Boeing Long Beach
THIF-13T	-13 (T-L)	11.90	.188	NASA LaRC

The specimen configuration refers to the test geometry given in Figure 1. The basic skin thickness is nominally 0.060 inches, with two integral tear straps of 0.018 inch nominal thickness. The bulky region in the center of the specimen was intended to stabilize the specimen from out of plane movement, and increases the load transfer at the center of the specimen, thus increasing the stress intensity factor without widening the panel (in order to produce failure at loads well below net section yielding). All specimens were designed to be geometrically similar with regard to all in-plane dimensions with the exception of the fillet radii and the loading hole diameters. The thickness of each feature of the specimen was the same for all specimens; however, panels were configured with two different fillet radii as indicated in the test matrix to investigate the effect of fillet radius on crack arrest capability.

²Boeing Seattle subcontracted work to Long Beach, thus all panels reported herein were tested in the Engineering Labs at the Boeing Long Beach Facility.



ISOMETRIC VIEW

GENERAL NOTES:

1. ALL DIMENSIONS IN INCHES.
2. DEFAULT TOLERANCES ARE AS FOLLOWS:
 .XX (2 DECIMAL PLACES, ±0.03)
 .XXX (3 DECIMAL PLACES, ±0.015)
3. SURFACE FINISH 63√ PER ANSI B46-1978.
4. SPECIMEN SURFACES SHALL BE FREE OF NICKS AND GROOVES.
5. MATERIAL, GRAIN ORIENTATION, AND NOTCH DIMENSIONS TO BE SPECIFIED BY ENGINEER.

VIEW M-M

DASH NO	B	C	D	E	F	G	H	J	R
-3	11.90	11.90	8.90	3.00	5.00	1.00	0.90	2.005	0.063
-5	11.90	11.90	8.90	3.00	5.00	1.00	0.90	2.005	0.188
-7	7.93	7.93	5.93	2.00	3.33	0.67	0.60	1.505	0.063
-9	7.93	7.93	5.93	2.00	3.33	0.67	0.60	1.505	0.188
-11	5.95	5.95	4.45	1.50	2.50	0.50	0.45	1.005	0.063
-13	5.95	5.95	4.45	1.50	2.50	0.50	0.45	1.005	0.188

Figure 1. Thickness Interface Specimen Concept

2.2 FRANC2D Analyses

Since the specimens were flat, well stiffened, and nearly symmetric through the thickness (with the exception of the integral tear strap, which was on one side only) they were analyzed in two dimensions using FRANC2D, a finite element based fracture code¹ developed at Cornell University [6]. Because they were all geometrically similar, a single model² was used for all specimens. A snapshot of the model is shown in Figure 2, with a close up of the crack tip in Figure 3. Fillet material was neglected in the finite element analysis.

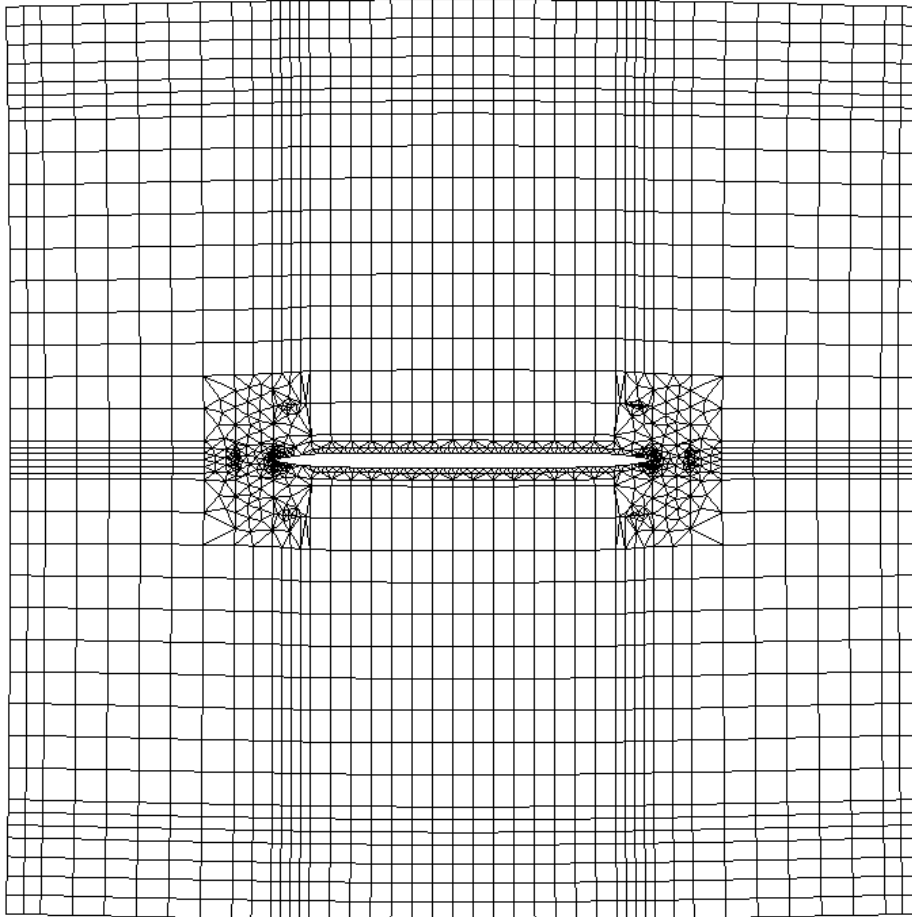


Figure 2. FRANC2D Model of Thickness Interface Specimen

¹ FRANC2D and supporting documentation can be downloaded free of charge from the Cornell Fracture Group web site at www.cfg.cornell.edu.

² Model provided under Boeing Long Beach Contract

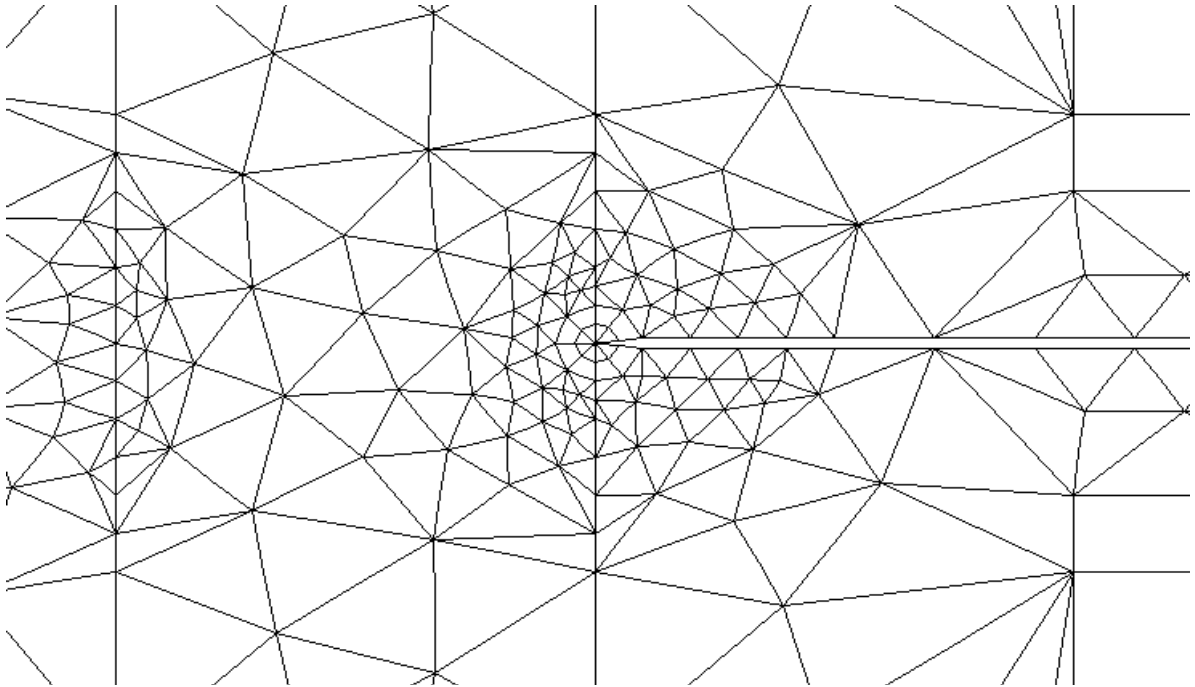


Figure 3. Close-up of FRANC2D Crack Tip Mesh at Tear Strap Interface ($a=F$)

A stress intensity plot for the specimen geometry is presented in normalized format in Figure 4. In FRANC2D, stress intensity factors given are determined from a J integral evaluated along the outside contour of a circular rosette of singular 6-node elements at the crack tip (as shown in Figure 3). The stress intensity factor is then determined by the well-known relation (for plane stress)

$$K = \sqrt{JE} \quad (1)$$

or in normalized form

$$\beta = \frac{K}{\sqrt{\pi a}} = \sqrt{\frac{JE}{\pi a}} \quad (2)$$

Where E is Young's modulus, and J represents the strain energy release rate determined by the contour integral. This method is generally very accurate, typically giving stress intensity factors within one or two percent even with moderately abusive meshes. Assuming linear elastic fracture mechanics applies, the crack propagates at a gross stress given by

$$\sigma_{\text{crit}} = \frac{K_c}{\beta\sqrt{\pi a}} \quad (3)$$

Where the fracture toughness, K_c is 108 ksi-in^{1/2} in the L-T orientation and 83 ksi-in^{1/2} in the T-L orientation as described above. Actually these values are only valid after the crack has already torn at least an inch to fully develop the maximum R-curve toughness of the material. Thus specimens are precracked to within nominally 1.5 inches of the edge of the integral tear strap, so that the full fracture toughness is developed by the time the crack reaches the interface, which is believed to be the point of maximum load capacity.

However, when the crack tip lies precisely at a thickness interface, K is theoretically undefined, or at least differs in mathematical nature from the familiar stress intensity factor. Nevertheless, theoretically valid stress intensity factors can be evaluated on either side of the interface. However, as shown in Figure 4, the points evaluated show a sharp dip just as the crack begins to enter into the integral tear strap. The dip is so sharp and deep that intuitively, as the width of the cusp becomes smaller than the plastic zone (not to mention three-dimensional effects), one would doubt that the load required to tear through the interface would follow the extreme trend indicated by its lowermost point. In fact, this lower bound seems almost arbitrarily low depending how close to the interface one analyzes it.

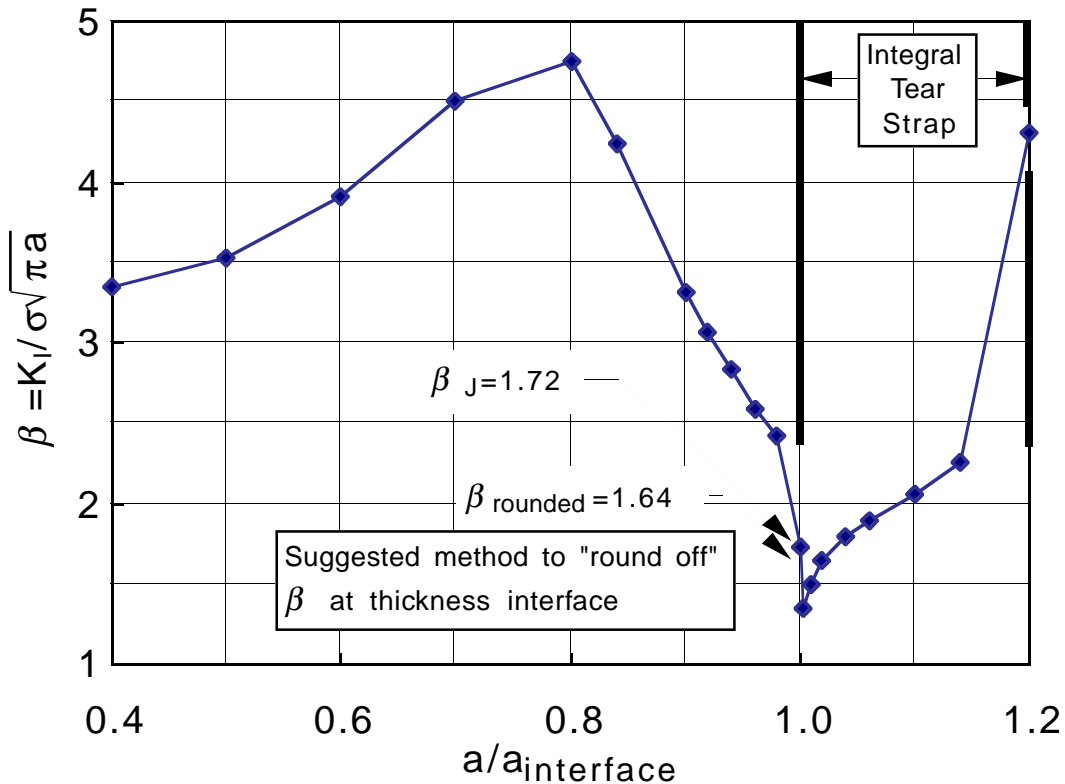


Figure 4. Normalized Stress Intensity Plot for Thickness Interface Specimen Based on FRANC2D Model

One estimate of an appropriate value of β for the interface might be obtained by rounding off the cusp in some way, such as that shown in Figure 4. The slope of the curve is extrapolated from the point of inflection within the tear strap back to the thickness interface, intersecting at a value of 1.64. Otherwise, despite the theoretical shortcomings, one might be tempted to use the value of β calculated directly from the J integral given by FRANC2D at the interface, which was calculated as 1.72 for the mesh shown in Figure 3.

A closer look at the calculation of the interface β value in FRANC2D revealed that it is not a clear-cut value. The value of 1.72 given above was determined with the rosette subdivided once by a factor of 0.5 as shown in Figure 3. This resulted in an inner rosette diameter (and thus integration path radius) equal to about 1/24th of the tear strap width. Whereas generally the J integral and resulting stress intensity factors given by FRANC2D are fairly insensitive to mesh size and integration paths, it was found that each such subdivision of the rosette (and corresponding halving of the integration path) reduced the β factor by about 7 percent. After refining the rosette mesh to a radius of integration equal to about 1/200th of the integral tear strap, the predicted β had dropped to 1.39, and was still dropping about 7 percent per subdivision. To further cloud the issue, alternative stress intensity values calculated at the interface using the modified crack closure technique were about 30 percent higher than the J-integral at each level of mesh refinement (normally the two methods should agree within a few percent).

Because of the difficulty in determining a unique β value at the interface, it was decided to use the value obtained from the round off method proposed earlier. Thus, the failure stress was predicted using Equation (3) with $\beta = 1.64$, and compared with test results. We thus have for the L-T configuration

$$\sigma_{\text{crit}} = \frac{108}{1.64\sqrt{\pi a_{\text{interface}}}} \quad (\text{ksi}) \quad (4)$$

and in the T-L configuration

$$\sigma_{\text{crit}} = \frac{83}{1.64\sqrt{\pi a_{\text{interface}}}} \quad (\text{ksi}) \quad (5)$$

where the half-crack length at the thickness interface is given in inches.

2.3 Test Procedure

The test plan for the thickness transition specimens was as follows:

1. Measure specimen dimensions across center of specimen.
2. Polish as required in vicinity of crack path and stiffener for crack observation.
3. Cut center notch to within 1.55 inches of the edge of the integral tear strap on each side.
4. Load into test machine and precrack at indicated loads to within 1.50 inches of the integral tear strap. Precrack should proceed at approximately $1\text{E-}6$ to $1\text{E-}5$ inches/cycle. Sawcut and precrack dimensions should conform to ASTM guidelines.
5. Measure final precrack length on both sides of both crack tips.
6. Mount clip gage/extensometer at center of specimen to measure crack opening displacement (COD).
7. Pull to ultimate failure at 0.02 inches/minute. Take load, head deflection, and COD measurements at 1 Hz. Pause occasionally (with load held constant) to measure physical crack length on both sides of specimen, both crack tips.
8. Record maximum load as crack tears through 0.18 inch thick integral tear straps.

2.4 Results

Tabulated specimen measurements are presented in Table 3 for all specimens, except THIF-IIT which suffered a serious test machine malfunction, and THIF-13T, which at this writing still awaited testing at NASA. A tabulation of failure loads and other data of interest is presented in Table 4. Note that the gross failure stress reported does include the nominal fillet area, but that otherwise the effect of the fillet radius on the failure load appears to be negligible for the radii tested.

Load/deflection curves for all specimens are plotted in Figures 5-7, and Load/crack growth curves for all specimens are given in Figure 8. In all specimens, the initial crack growth arrested at the transition at the integral tear strap. The load was subsequently increased, until the specimen rapidly failed through the tear strap. The strap tear through load was taken as the failure load.

Specimen photographs are presented in Figure 9. Note that the observed out of plane deflection took place after failure of the integral tear strap. The out of plane deflection prior to strap failure was very slight, though observable in the reflective surface immediately around the crack tip.

Gross failure stress is plotted as a function of the half crack length at which the crack reaches the interface in Figure 10. Equations (4) and (5) are plotted for comparison. Apparently, use of a stress intensity factor determined by the proposed round off method yields a very good approximation of the residual strength, at least for the geometry and material tested. It was noted, however, that the predictions were slightly non-conservative at the higher stress levels (smallest specimens, L-T orientation).

It should be noted that the nominal net-to-gross area ratio with the crack advanced to the thickness transition is 0.82 for all specimens, resulting in net section failure stresses ranging from 15 to 28 ksi, compared to the material tensile yield strength of 68 ksi. Thus, all specimens were well away from net section yield when failure occurred. However, based on the linear elastic analysis performed, the stresses in the integral tear strap were approximately sufficient to yield the integral tear strap almost completely through its cross-section in the smaller L-T specimens, and may account for the slightly lower than predicted loads. The question remains as to whether a more grossly yielded strap would result in further reduction in strength. Perhaps an elastic plastic Crack Tip Opening Displacement (CTOD) of analysis might shed light on this in future work.

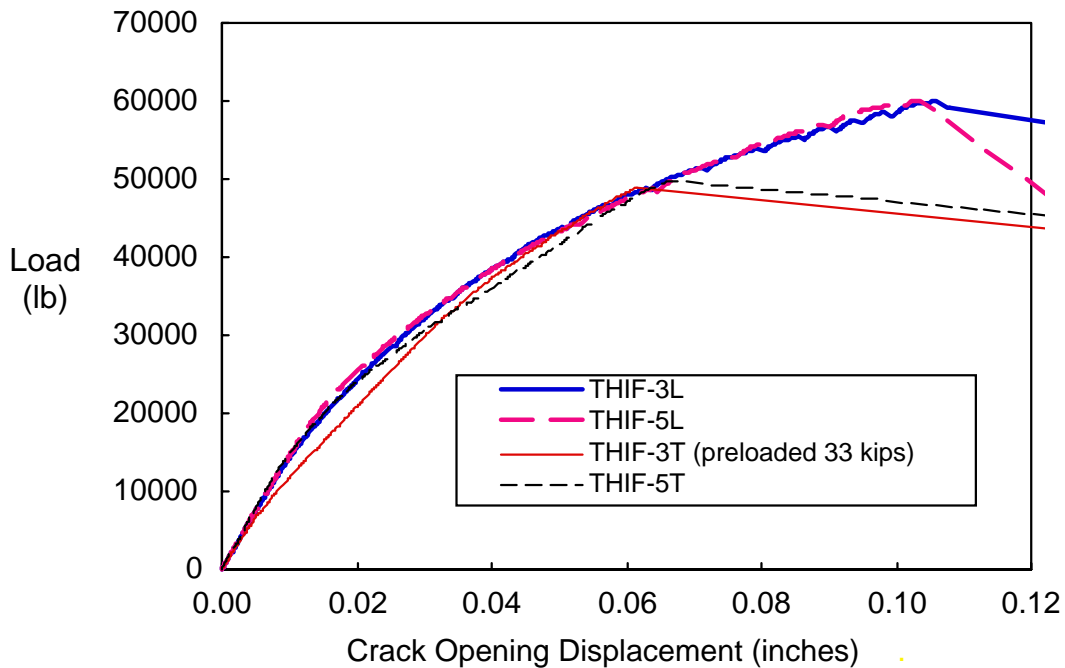


Figure 5. Plots of Load vs. Crack Opening Displacement for 23.80 Inch Wide Specimens

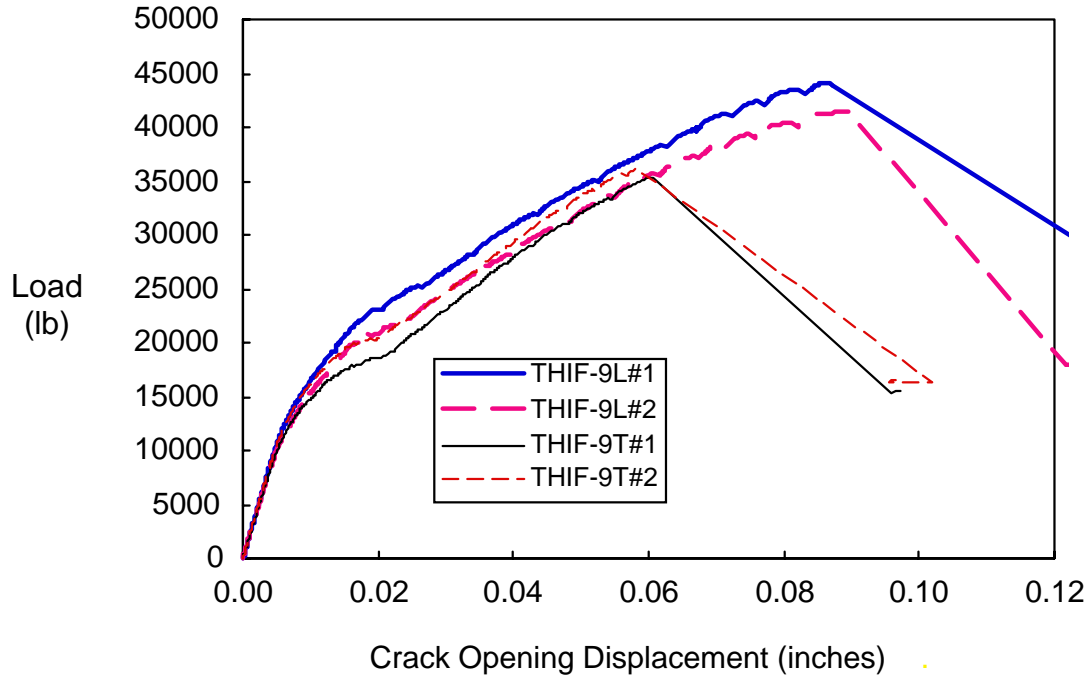


Figure 6. Plots of Load vs. Crack Opening Displacement for 15.86 Inch Wide Specimens

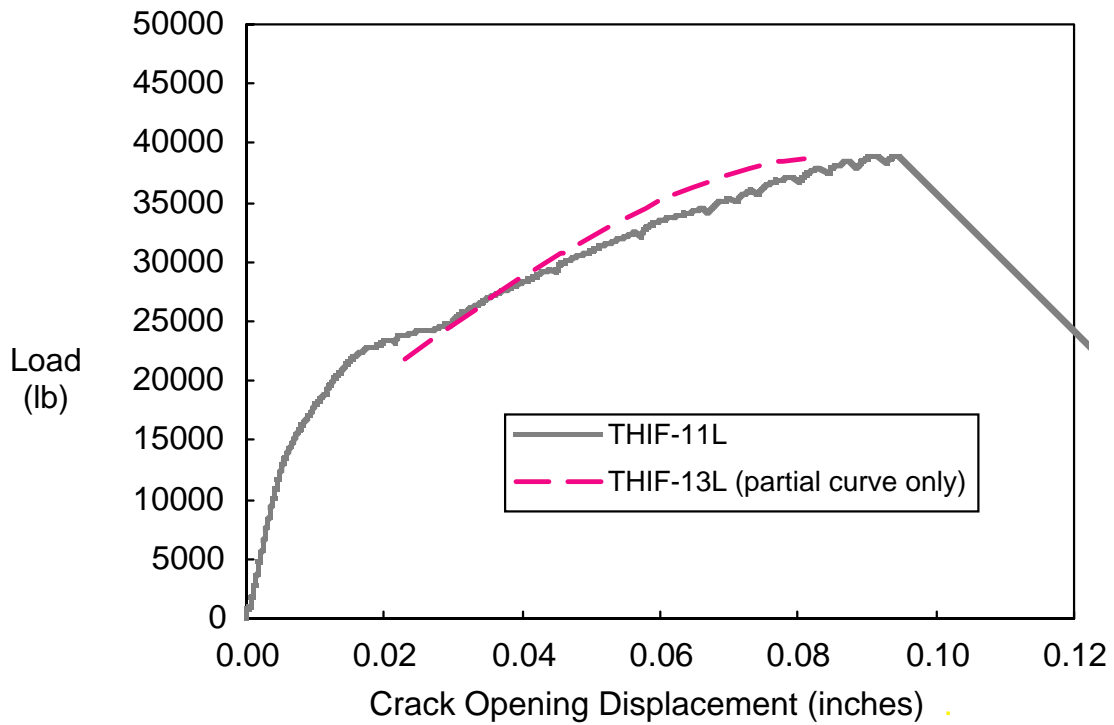


Figure 7. Plots of Load vs. Crack Opening Displacement for 11.90 Inch Wide Specimens

Table 3. Tabulated Thickness Interface Specimen Measurements

L-T Specimens	Segment*	1	2	3	4	w5 (t4+t6)/2	6	7	8	9	10	11	Nominal Fillet Area	Total Area
	THIF-3 L	w	0.9035	4.9975	0.9965	0.9995	8.0000	0.9990	1.0010	4.9980	0.9020	23.7955	23.7905	
	t	0.9889	0.0746	0.1940	0.0701	0.0698	0.0695	0.1894	0.0695	0.9910	n/a	n/a		
	area	0.8935	0.3728	0.1933	0.0701	0.5584	0.0694	0.1896	0.3474	0.8939	n/a	n/a	0.0062	3.5945
THIF-5 L	w	0.8995	4.9820	1.0260	0.9890	7.9990	0.9860	1.0175	4.9855	0.8970	23.7950	23.7910		
	t	0.9899	0.0683	0.1869	0.0692	0.0659	0.0626	0.1897	0.0709	0.9873	n/a	n/a		
	area	0.8904	0.3403	0.1918	0.0684	0.5271	0.0617	0.1930	0.3535	0.8856	n/a	n/a	0.0534	3.5653
THIF-9#1 L	w	0.6015	3.3030	0.7130	0.6470	5.3140	0.6420	0.7050	3.3090	0.6017	15.8795	15.8775		
	t	1.0043	0.0629	0.1788	0.0619	0.0607	0.0595	0.1780	0.0621	1.0018	n/a	n/a		
	area	0.6041	0.2078	0.1275	0.0400	0.3226	0.0382	0.1255	0.2055	0.6028	n/a	n/a	0.0534	2.3273
THIF-9#2 L	w	0.6035	3.3050	0.6970	0.6500	5.3100	0.6590	0.6970	3.3050	0.6050	15.8720	15.8875		
	t	1.0052	0.0562	0.1756	0.0577	0.0579	0.0580	0.1754	0.0566	1.0052	n/a	n/a		
	area	0.6066	0.1857	0.1224	0.0375	0.3072	0.0382	0.1223	0.1871	0.6081	n/a	n/a	0.0534	2.2686
THIF-11 L	w	0.4525	2.5015	0.5005	0.4995	3.9995	0.4995	0.5005	2.4995	0.4490	11.8990	11.8990		
	t	1.0050	0.0630	0.1829	0.0617	0.0619	0.0620	0.1825	0.0622	1.0050	n/a	n/a		
	area	0.4548	0.1576	0.0915	0.0308	0.2474	0.0310	0.0913	0.1555	0.4512	n/a	n/a	0.0062	1.7173
THIF-13 L	w	0.4470	2.4855	0.5165	0.4880	3.9955	0.4860	0.5195	2.5160	0.4450	11.8990	11.8985		
	t	1.0085	0.0632	0.1821	0.0626	0.0629	0.0632	0.1827	0.0618	1.0095	n/a	n/a		
	area	0.4508	0.1571	0.0941	0.0305	0.2513	0.0307	0.0949	0.1555	0.4492	n/a	n/a	0.0534	1.7676
T-L Specimens														
THIF-3 T	w	0.9110	4.9970	0.9935	1.0010	7.9940	0.9960	1.0000	4.9975	0.9040	23.7935	23.7960		
	t	0.9930	0.0837	0.1993	0.0803	0.0781	0.0758	0.1984	0.0765	0.9934	n/a	n/a		
	area	0.9046	0.4182	0.1980	0.0804	0.6239	0.0755	0.1984	0.3823	0.8980	n/a	n/a	0.0062	3.7856
THIF-5 T	w	0.8985	4.9815	1.0370	0.9730	7.9960	0.9845	1.0200	4.9795	0.9010	23.7940	23.7925		
	t	0.9914	0.0818	0.1980	0.0781	0.0775	0.0769	0.1968	0.0797	0.9982	n/a	n/a		
	area	0.8908	0.4075	0.2053	0.0760	0.6197	0.0757	0.2007	0.3969	0.8994	n/a	n/a	0.0534	3.8254
THIF-9#1 T	w	0.5980	3.3210	0.6690	0.6640	5.3110	0.6690	0.6900	3.3280	0.5980	15.8790	15.8835		
	t	1.0126	0.0528	0.1783	0.0535	0.0582	0.0628	0.1806	0.0596	1.0079	n/a	n/a		
	area	0.6055	0.1753	0.1193	0.0355	0.3088	0.0420	0.1246	0.1983	0.6027	n/a	n/a	0.0534	2.2657
THIF-9#2 T	w	0.5980	3.3070	0.6810	0.6560	5.3100	0.6560	0.7040	3.3070	0.6000	15.8790	15.8800		
	t	0.9963	0.0601	0.1783	0.0595	0.0613	0.0631	0.1826	0.0643	0.9869	n/a	n/a		
	area	0.5958	0.1988	0.1214	0.0390	0.3255	0.0414	0.1286	0.2126	0.5921	n/a	n/a	0.0534	2.3087

Note: Segments denote constant thickness regions as one measures thickness from left to right across the center of the panel

Table 4. Tabulated Thickness Interface Test Results

	$a_{precrack}$ (avg) (in)	a_{arrest}^* (in)			Δa_{arrest} (avg) (in)	Measured Specimen Gross Area (sq in)	Nominal Fillet Radius (in)	Maximum Load (kips)	COD at Max Load (in)	Gross Failure Stress (ksi)	Predicted Failure Stress (ksi)
		Flush side	Stiffened side	Average of both sides							
L-T Specimens											
THIF-3 L	3.511	5.088	4.983	5.035	1.525	3.5945	0.063	59.98	0.1059	16.69	16.62
THIF-5 L	3.500	4.971	4.922	4.946	1.446	3.5653	0.188	60.02	0.1027	16.83	16.62
THIF-9#1 L	1.833	3.297	3.255	3.276	1.444	2.3273	0.188	44.06	0.0858	18.93	20.36
THIF-9#2 L	1.834	3.294	3.240	3.267	1.433	2.2686	0.188	41.43	0.0890	18.26	20.36
THIF-11 L	1.028	2.565	2.489	2.527	1.500	1.7173	0.063	38.90	0.0942	22.65	23.50
THIF-13 L	1.033	2.596	2.466	2.531	1.498	1.7676	0.188	38.86	0.0808	21.99	23.50
T-L Specimens											
THIF-3 T	3.553	5.002	4.970	4.986	1.433	3.7856	0.063	48.89	0.0616**	12.92	12.77
THIF-5 T	3.525	4.896	4.865	4.881	1.356	3.8254	0.188	49.83	0.0671	13.03	12.77
THIF-9#1 T	1.834	3.247	3.168	3.207	1.374	2.2657	0.188	35.38	0.0608	15.61	15.65
THIF-9#2 T	1.831	3.330	3.253	3.291	1.460	2.3087	0.188	36.19	0.0584	15.67	15.65
THIF-11 T	Test machine malfunction, no data										
THIF-13 T	Specimen awaits testing at NASA LaRC										

* a_{arrest} is based on the last physical crack measurement prior to maximum load, which was always in the fillet adjacent to the tear strap, but which may differ slightly from the crack length at maximum load. Flush side and stiffened side measurements are average of left and right half crack values; an overall average is also given.

** Specimen inadvertently overloaded to approx. 33 kips after precracking, but prior to test. Overload undoubtedly effected subsequent COD measurements, but should not have affected max load.

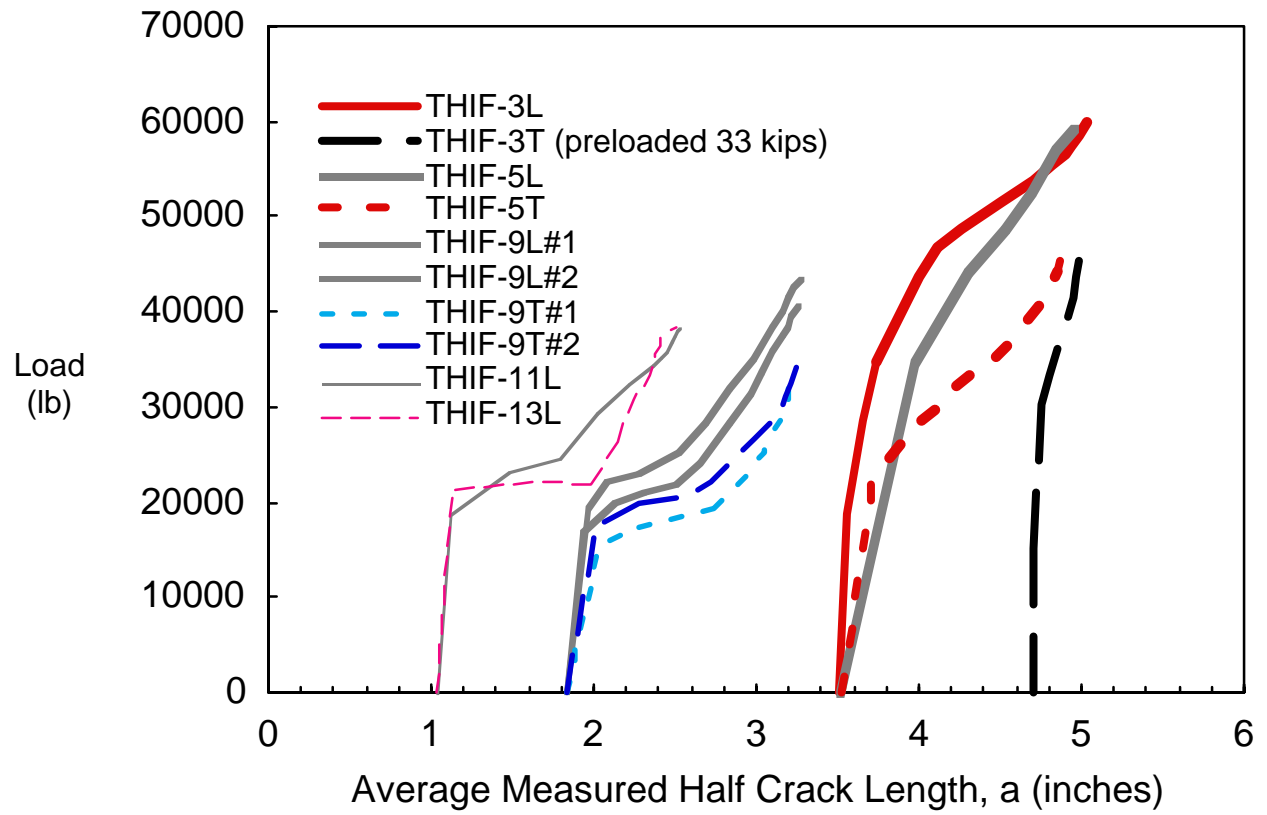


Figure 8. Load/Crack Length Plots for all Specimens

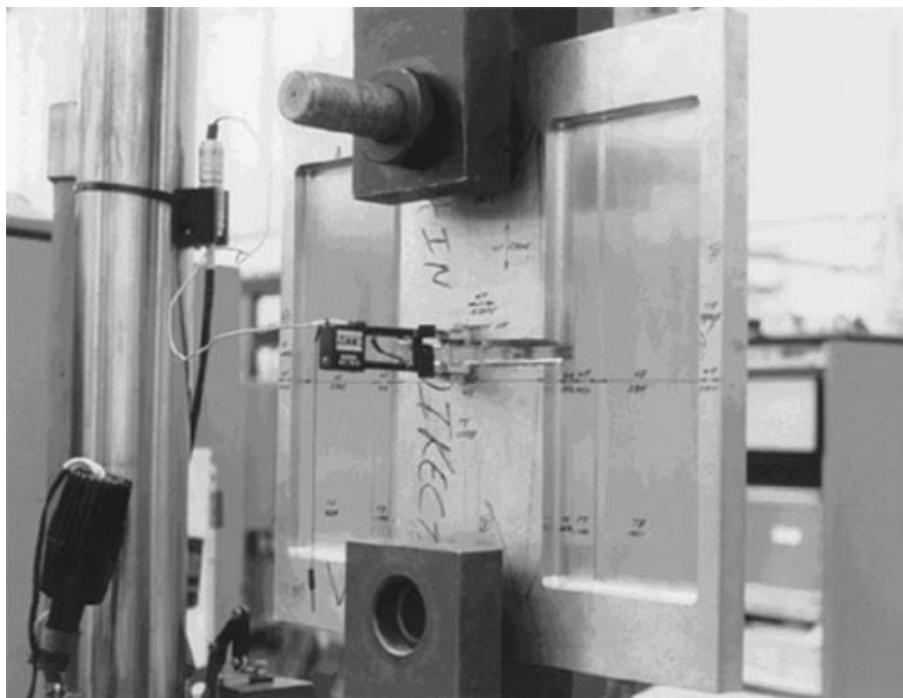


Figure 9. Photograph of Test Setup

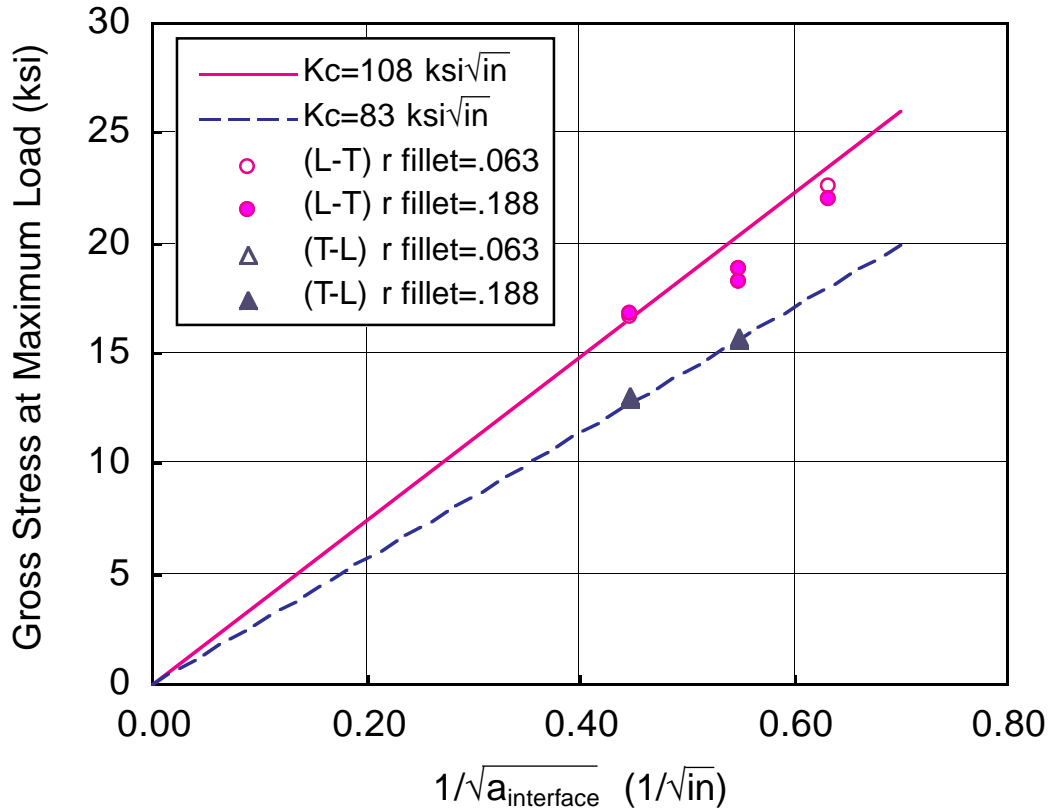


Figure 10. Correlation of Thickness Interface Specimen Data with Linear Elastic Analysis

3.0 CONCLUSIONS AND RECOMMENDATIONS

Based on the results of the thickness interface specimens, it appears that the crack stopping potential of integral tear straps is quite substantial. The load required for a straight crack to tear through an integral tear strap can be well approximated with linear elastic fracture mechanics if the stress intensity at the thickness transition is approximated by the round off method described. However, caution should be exercised if the region of plasticity extends beyond the integral stiffener, which is arresting the crack.

4.0 REFERENCES

1. R.G. Pettit, J.J. Wang, C. Toh, *Integral Airframe Structures (IAS)--Validated Feasibility Study of Integrally Stiffened Metallic Fuselage Panels for Reducing Manufacturing Costs*, Final Report, NASA Contract NAS1-20014, Task 34, The Boeing Phantom Works (Long Beach), November 1998.
2. T. Swift, "Application of Damage Tolerance Technology to Type Certification", SAE Paper #811062, Aerospace Congress and Exp., Anaheim, CA October 1981.
3. C. C. Poe, "Crack Propagation in Stiffened Panels", ASTM STP 486, 1971.
4. H. F. Hardrath et al, NACA Tech Note #3856, 1956.
5. M. S. Domack, *Fatigue Crack Growth Rate and Fracture Toughness Testing at NASA Langley Research Center*, IAS Workshop, NASA LaRC, April 29-30, 1998.
6. T. J. Boone, P. A. Wawrzynek, and A. R. Ingraffea, *Engineering Fracture Mech.*, Vol. 26, No. 2, pp. 185-201, 1987.

